AUTOMATING ELECTRIC UTILITY DISTRIBUTION SYSTEMS:

THE ATHENS AUTOMATION AND CONTROL EXPERIMENT

Edited and compiled by

P. A. Gnadt and J. S. Lawler

Technical Editor

E. W. Whitfield

Prentice Hall, Englewood Cliffs, N.J. 07632

Prentice Hall Advanced Reference Series

Engineering

DENNO *Power System Design and Applications for Alternative Energy Sources*

ESOGBUE, ED. *Dynamic Programming for Optimal Water Resources Systems Analysis*

FERRY, AKERS, AND GREENEICH *Ultra Large Scale Integrated Microelectronics*

GNADT, LAWLER, EDS. *Automating Electric Utility Distribution Systems: The Athens Automation and Control Experiment*

HAYKIN, ED. *Advances in Spectrum Analysis and Array Processing Vol. I*

HAYKIN, ED. *Advances in Spectrum Analysis and Array Processing Vol. II*

HAYKIN, ED. *Selected Topics in Signal Processing*

JOHNSON *Lectures on Adaptive Parameter Estimation*

MILUTINOVIĆ, ED. *Microprocessor Design for GaAs Technology*

QUACKENBUSH, BARNWELL III, AND CLEMENTS *Objective Measures of Speech Quality*

ROFFEL, VERMEER, AND CHIN *Simulation and Implementation of Self-Tuning Controllers*

SASTRY AND BODSON *Adaptive Control: Stability, Convergence, and Robustness*

AUTOMATING ELECTRIC UTILITY DISTRIBUTION SYSTEMS:

THE ATHENS AUTOMATION AND CONTROL EXPERIMENT

Edited and compiled by

P. A. Gnadt and J. S. Lawler

Technical Editor

E. W. Whitfield

Prentice Hall, Englewood Cliffs, N.J. 07632

Library of Congress Cataloging-in-Publication Data

Automating electric utility distribution systems : the Athens
Automation and Control Experiment / edited and compiled by P.A.
Gnadt and J.S. Lawler : technical editor, E.W. Whitfield.
p. cm.
Includes bibliographical references.
ISBN 0-13-053737-3
1. Electric power distribution--Tennessee--Athens--Automation.
2. Electric power distribution--Automation--Economic aspects-
-Tennessee--Athens. I. Gnadt, P. A. II. Lawler, J. S.
III. Whitfield, E. W.
TK3091.A78 1990
621.319--dc20 89-48286
CIP

Editorial/production supervision: *Brendan M. Stewart*
Cover design: *Karen Stephens*
Manufacturing buyer: *Denise Duggan*

A Division of Simon & Schuster
Englewood Cliffs, New Jersey 07632

This book can be made available to businesses and organizations at a special discount when ordered in large quantities. For more information contact:

Prentice-Hall, Inc.
Special Sales and Markets
College Division
Englewood Cliffs, N.J. 07632

Prepared by the Oak Ridge National Laboratory, Oak Ridge, Tennessee 37831, operated by Martin Marietta Energy Systems, Inc. for the U.S. Department of Energy under Contract No. DE-AC05-840R21400.

Printed in the United States of America
10 9 8 7 6 5 4 3 2 1

ISBN 0-13-053737-3

Prentice-Hall International (UK) Limited, *London*
Prentice-Hall of Australia Pty. Limited, *Sydney*
Prentice-Hall Canada Inc., *Toronto*
Prentice-Hall Hispanoamericana, S.A., *Mexico*
Prentice-Hall of India Private Limited, *New Delhi*
Prentice-Hall of Japan, Inc., *Tokyo*
Simon & Schuster Asia Pte. Ltd., *Singapore*
Editora Prentice-Hall do Brasil, Ltda., *Rio de Janeiro*

CONTENTS

FOREWORD

G. H. Usry

The culmination of the Athens Automation and Control Experiment is not only a technical success but also a demonstration of what is truly right with this great country of ours. The project demonstrates what cooperation of the federal government, private enterprise, universities, local government, and—most important—the people of grass-roots mid-America can accomplish.

We began this project with the goal of installing a completely integrated automation and load control electronic system on an urban/rural electric distribution system typical of those that exist throughout the United States. The idea was to begin with the major substation equipment and follow each system component down to individual residential appliances by installing computer-controlled and -integrated hardware and software to monitor, evaluate, and ultimately control every aspect of an electric distribution system. This objective had never been accomplished before; to my knowledge, we are very much ahead of others who are now working toward the same goal.

During the energy crisis of the mid to late 1970s, doomsayers projected that many of our natural energy resources would be in short to zero supply by the early 1990s. It was determined that if local control of load dispatch could become a reality at a reasonable cost, then the electric utility industry could begin to contain several of the most costly aspects of providing the vital electric needs of the ultimate customer. Although the crisis of short supply has subsided, the issue of economics has not.

Why an integrated distribution automation system would be of benefit to the ultimate customer is a natural question. Economics is a major benefit.

First, an automation system would give us more control over the most costly kilowatts sold—the hourly demand for electricity during peak periods. The demand component of the Athens Utilities Board (AUB) rate structure more than doubled in cost during the course of the project. The value of being in control of a part of this component of our cost has increased proportionally.

A second and equally important benefit is that specific knowledge of the use patterns on the system would allow proper economic decisions to be made concerning the construction of new generating capacity. History has now proven that the lack of this specific knowledge has cost the rate payers throughout the United States billions of dollars—on both sides of the demand line. Some utilities have too little capacity, and others may have too much. It costs both of them to be in their respective position. Widespread use of the type of system demonstrated at Athens can supply the much needed hard data to support such monumental decisions. It is amazing how well this country has prospered on rule-of-thumb, flip-a-coin, and gut-feeling decision making during the 20th century. We will not be allowed this luxury in the 21st century.

Third, the simple principle of economics, improved efficiency means lower costs. I can attest to the improved efficiency of the AUB system as a result of the automation of our system.

How have we measured the success of the project? First is the fact that AUB employees—not contractors—installed, maintained, and are operating the system, which proves that the typical utility can, without fear of oversophistication, accomplish and accept such a system for routine daily use.

A second measure of success of the project is the acceptance by our customers of the load control equipment on their appliances without subsidies. Many utilities pay a fixed price for installing load control equipment. Many critics cannot believe that our customers have accepted this program on the basis of what is good for one will ultimately be good for all. The typical reaction of our customers has been that if this will help maintain a stable rate situation, they will support the program.

Third, the interest in this project by other utilities and engineering institutions throughout the United States—and indeed the world—has been overwhelming. AUB has had visitors from such faraway places as Sweden, Switzerland, Germany, Japan, Africa, Canada, Brazil, and Mexico. The long list of our visitors from the major utilities in the United States includes representatives from both the largest investor-owned utilities and some of the smallest cooperatives.

A fourth important success measure is that members of this project team have been invited to present papers and seminars to many utility conferences in the United States and in foreign countries. Presentations have been made at the Institute of Electrical and Electronics Engineers (IEEE) Power Engineering Societies (PES) 1987 and 1988 Winter and Summer meetings, the IEEE PES 1987 Transmission and Distribution Conference, the IEEE PES 1987 and 1988 Distribution Energy Exposition, the IEEE PES 1989 Winter Meeting, and the IEEE 1989 Transmission and Distribution Conference. Additionally, presentations have been made at the International Seminar on Electric Power held in Sao Paulo, Brazil, in 1987; the jointly sponsored CIRED-UPDEA International Conference on Electricity Distribution in the Developing Countries held in 1988 in the Ivory Coast, Africa; and the Middle East Power Conference held in 1989 in Egypt.

What are we looking forward to in the future? First, AUB will continue to operate the system as a real-time utility tool to take advantage of experimental data that have been generated. Second, the AUB staff and board are dedicated to maintaining the most modern distribution system that benefits our customers. There are many opportunities for building on this system because the foundation equipment is in place. As the experimental mode ends, the efficiency mode begins. We believe that we have the base on which to build and operate the most efficient system to be found anywhere. Improved efficiency can only mean lower cost to our customers.

AUB personnel hope that the compilation of the results of the Athens Automation and Control Experiment in this book will be as important to other utilities in serving their customers as the experiment has been to AUB.

George H. Usry, General Manager
Athens Utilities Board
Athens, Tennessee

PREFACE

Researchers at the Oak Ridge National Laboratory (ORNL) have successfully completed the Athens Automation and Control Experiment (AACE) at the Athens (Tennessee) Utilities Board (AUB). The AACE provided the research and development required for integrating automated electric power distribution equipment such as disconnect switches, transformer load-tap changes, capacitors, and appliance controllers with computer-assisted controls and monitoring devices. The AACE is the first fully integrated distribution automation system in the United States.

The experiment was jointly sponsored by the AUB and the U.S. Department of Energy's (DOE's) Office of Energy Storage and Distribution and was conducted in cooperation with the Tennessee Valley Authority (TVA), the Electric Power Research Institute (EPRI), the Tennessee Valley Public Power Association (TVPPA), and the Baltimore Gas and Electric Company. Experts from the utility industry provided advice and guidance for the project.

The purpose of the AACE was to develop and test various load control options, voltage and reactive power (var) control options, and distribution system reconfiguration capabilities on an electric distribution system from the transmission substation transformer to individual residential appliances. The resulting technology would be transferred to the electric utility industry for large-scale implementation.

The AUB reports that the AACE system has improved the reliability of service; facilitated maintenance and lowered the maintenance cost of the system; improved the power factor, which has resulted in reduced power delivery costs; improved customer relationships; and improved system planning and capacity utilization.

Load control experiments have shown that it is possible to (1) accurately measure changes in load resulting from control actions, (2) determine the controllable load prior to control actions, and (3) use high-speed data acquisition at the feeder level as an alternative to expensive monitoring equipment located at each customer home under control.

System reconfiguration experiments show that load can now be transferred more quickly and more economically than before the system was automated. The experiments also show that load transfers do not result in the loss reduction normally expected because of the sensitivity of customer load to voltage.

Volt/var experiments indicate that customer load is sensitive to the voltage profile of the system and that the load must be modeled accurately to quantify loss reduction. An improvement in voltage profile due to the switching in of capacitors can result in an increase in load that exceeds the loss reduction. Some load models conventionally used by utilities do not accurately model changes to the system resulting from capacitor switching.

Measurement of system parameters in real time allows control action results to be studied, and new measurement techniques allow more accurate analysis of system response to control actions.

Computer programs have been developed to control and analyze distribution automation functions and enable (1) estimation of the effects of planned control actions on the distribution system prior to taking action, (2) automatic control of feeder capacitors to improve the power factor and to reduce losses and power delivery costs, and (3) calculation of losses on the system.

A briefing on the project given in Athens on November 21, 1987, was attended by more than 50 guests, including Congressman John J. Duncan; Nancy Jeffery, Staff of the House of Representatives Committee on Science, Space, and Technology; TVA staff; TVPPA staff; American Public Power Association members; DOE managers; local government officials; and news media representatives.

We at ORNL believe that one way to transfer to the electric utility industry the technology developed during the Athens experiment is to assemble the results of the experiments and to describe the experiences of the project. With this in mind, we have assembled the information into this book.

Presented are design philosophy, detailed design information, information from technical papers delivered during the experimental phase of the project, and descriptions of software developed during the course of the project.

ACKNOWLEDGMENTS

This book is a result of the efforts of many contributors. The authors are acknowledged in the individual chapters. Their cooperation in preparing manuscripts, changing existing manuscripts to adhere to the style of the book, and reviewing materials is greatly appreciated.

Enough cannot be said about the contributions of the Athens Utilities Board (AUB), particularly George H. Usry, general manager, and the residents of Athens. Without their support and absolute cooperation, the Athens Automation and Control Experiment (AACE) could not have been completed. The citizens of Athens and the AUB staff allowed the research staff of Oak Ridge National Laboratory's Power Systems Technology Program to experiment with their electrical distribution system, sometimes affecting lifestyles and personal habits. The participation of the customers of AUB—*without incentives*—has attracted favorable attention throughout the electric utility industry. Other utilities were unable to attract a sufficient number of participants—*even with incentives of billing reductions or outright payments.* It is a tribute to the personnel at AUB that they were able to create such an atmosphere of cooperation. AUB's customers were patient and showed great interest during the project.

Without the funding of the U.S. Department of Energy's (DOE's) Office of Energy Storage and Distribution (OESD), the AACE could not have been conducted. Kenneth W. Klein, director of OESD, and his staff members, Deitrich J. Roesler and Russell Eaton III, showed great patience over the course of the experiment. George Manthey, Jr., branch chief of the DOE

Oak Ridge Operations Office, was very supportive of the project and furnished administrative guidance.

This experiment was an uncharacteristic one for the Oak Ridge National Laboratory (ORNL). Conducting such an experiment on an operating industrial system is indeed unique. The support of Murray W. Rosenthal, ORNL associate director of Advanced Energy Systems; William Fulkerson, director of the ORNL Energy Division; and Roger S. Carlsmith, director of the ORNL Conservation and Renewable Energy Program, during the planning, construction, and experimental phases of the project was invaluable.

The advice and guidance of the utility advisors to the project team is greatly appreciated. A list of these advisors is included in Appendix A.

Others who contributed to the technical progress of the AACE are Ben W. McConnell, the project manager in the conceptual design phase; Steven L. Purucker, the project manager during the construction phase; Hugh M. Long and Thomas W. Reddoch, program managers of the Power Systems Technology Program during different stages of the project; Kevin E. McKinley of the Baltimore Gas and Electric Company, who was assigned to the project for two years; Howard Fox of the Tennessee Valley Authority, who was assigned to the project for a year in the conceptual design phase; Robert A. Stevens of ORNL, who was assigned to the project for a short period of time; Patricia S. Hu and Teresa A. Vineyard of ORNL, who assisted with data analysis and data handling; Raymond D. Dunlop, who served as DOE office director (Electric Energy Systems Program) during part of the project; Robert L. Sullivan of the University of Florida, who contributed technical expertise and advice throughout the course of the project; Julia M. MacIntyre, who worked on the project while an employee at ORNL and who continued to consult on the project after leaving ORNL; and Lawrence C. Markel of Electrotek Concepts, who acted as support contractor to the DOE OESD in the latter stages of the project. The technical support and guidance of these individuals contributed to the success of the project.

The authors also wish to acknowledge Charles T. Huddleston, Asif H. Khan, Ashok A. Oka, Jeffry C. Thompson, Gurvinder S. Ahuja, and Hamidreza Maghdan-Dezfooly, graduate students at Tennessee Technological University, who assisted with the analyses of the voluminous amount of data associated with this project.

The technical reviewers and authors are indebted to the editors, makeup personnel, and compositors in the Publications Division offices at ORNL. Their hard work and dedication were invaluable to the completion of the book.

The Authors

ABBREVIATIONS, ACRONYMS, AND INITIALISMS

AACE	Athens Automation and Control Experiment
AACETS	Athens Automation and Control Experiment Test System
ACSR	aluminum cable steel reinforced
ARM	appliance research meter
ARMS	appliance research metering system
AUB	Athens Utilities Board
BBC	Brown-Boveri Control Systems, Inc.
CCC	central control center
CRT	cathode-ray tube
DAC	distribution automation and control
DBMS	data base management system
DCR	distribution control receiver
DLC	direct load control
DOE	U.S. Department of Energy
DRTU	distribution remote terminal unit
EDP	electronic data point
EMS	energy management system
EPRI	Electric Power Research Institute
IDCS	Integrated Distribution Control System
IEEE	Institute of Electrical and Electronics Engineers, Inc.
LCR	load control receiver
LTC	load-tap changing
MOV	metal oxide varistor
OESD	Office of Energy Storage and Distribution
ORNL	Oak Ridge National Laboratory
PG&E	Pacific Gas and Electric Company
PRAM	Predictive Reliability Assessment Model
PTU	pole-top unit
RTU	remote terminal unit
SCADA	Supervisory Control and Data Acquisition
SIU	signal injection unit
SM	smart meter
SRTU	substation remote terminal unit
SYSRAP	System Reconfiguration and Analysis Program
TVA	Tennessee Valley Authority
TVPPA	Tennessee Valley Public Power Association

1

INTRODUCTION

P. A. Gnadt and J. P. Stovall

In an effort to provide electricity at a minimum cost, the electric utility industry continues to examine methods to operate generating plants, transmission lines, distribution equipment, and customer appliances more efficiently. The Athens Automation and Control Experiment (AACE) was conceived and implemented to address these needs in the context of electric distribution systems.

Located on the Athens Utilities Board (AUB) system in Athens, Tennessee, AACE is a highly instrumented system designed as a test for distribution automation and load control experiments. AACE was created to obtain more information about the electric power distribution system and its customers than is practical during an electric utility's normal operations. The result is a "test bed," an environment in which controlled experiments, control strategies, and operating procedures can be carried out. Observation of the results help to show which controls are worthwhile, what data and instrumentation are needed, and which monitoring and control functions for distribution systems are justified.

The experiment was sponsored by the U.S. Department of Energy's Office of Energy Storage and Distribution and the AUB, and it was managed through the Power Systems Technology Program of the Oak Ridge National Laboratory (ORNL). The Electric Power Research Institute provided some equipment for monitoring load profiles. The experiments were conducted by ORNL personnel with AUB assistance. An advisory committee composed of ten distribution system experts from electric utilities provided guidance to the project team (see Appendix A). Appendix B lists publications used in compiling the manuscript.

The AUB purchases power from the Tennessee Valley Authority (TVA) and serves approximately 10,500 customers. The annual peak load is 90 MW. Testing of the new automated system began in the fall of 1985, and the results will be useful for the design and operation of future electric power systems. The computer control and communications systems can control the electric energy consumption of AUB's customers, optimize the efficiency of power distribution circuits, and maintain high-quality service by automated voltage and reactive power control, reconfiguration of the system, and control of load. The project is an example of close cooperation between the U.S. government and the private sector to undertake the research and development necessary to ensure efficient and reliable power systems in the future. As a result of these experiments, AUB has become one of the most technologically advanced electric distribution systems in the United States.

Centralized control and dispatch of generating plants (called energy management systems), remote monitoring and control of transmission and subtransmission lines [called supervisory control and data acquisition (SCADA)], remote monitoring and control of distribution equipment [(called distribution automation and control (DAC)], and control of customer appliances such as air conditioners and water heaters (called load control or load management) are methods used by the utility industry in recent years to provide electricity at minimum cost. In general, each of these automated methods has been developed as an independent subsystem and, before AACE, was not integrated into an overall control system. However, AACE has integrated these automated methods into a single control system, is developing and testing control strategies for the efficient delivery of electricity, and will be evaluating the benefits of this integrated system. The integrated automation system combines the three subsystems of SCADA, DAC, and load control. The automation system design uses existing technology in computer systems, communication systems, and control systems and integrates them with the existing power system. Figure 1-1 depicts the various equipment that is monitored and controlled at the AUB Control Center.

Load-tap-changing transformers, voltage regulators, capacitor banks, remotely operated disconnect and load break switches, remotely operated reclosers and circuit breakers, fault detectors, current transformers, and voltage transformers were added to the AUB distribution system. Special residential metering, capable of recording and transmitting load usage to the control center, was installed in some homes. Appliance load control switches, which can be operated from the AUB control rooms were installed in approximately 1600 homes. These appliance switches were connected to air conditioners, heat pumps, space heaters, and water heaters. During the experiments, computer programs turned these appliances off and on at

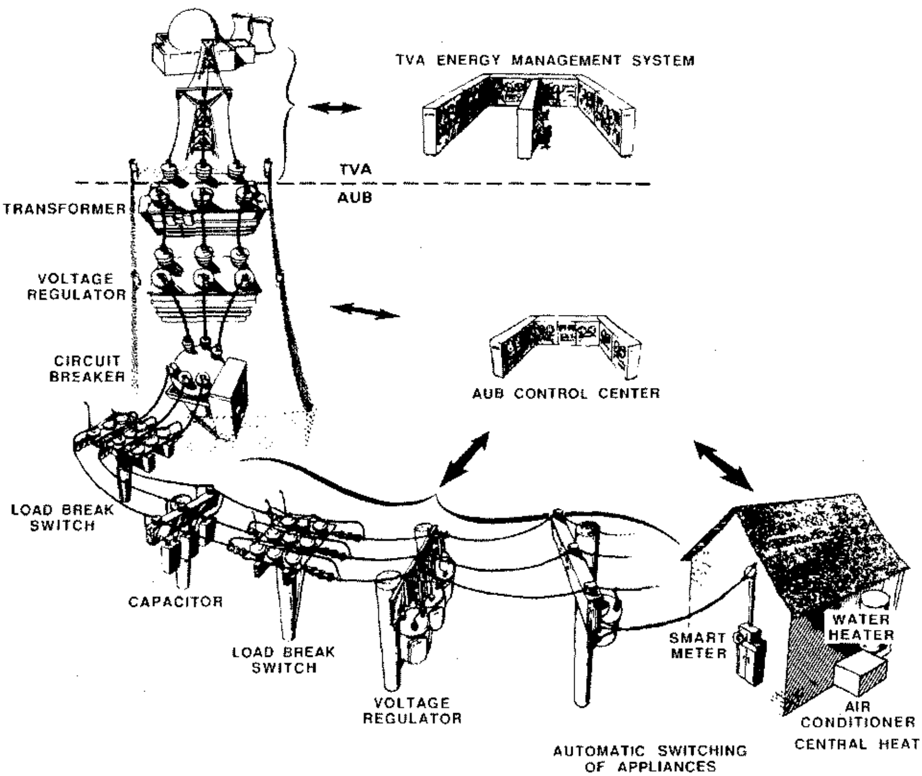

Figure 1-1 Automated equipment for the Athens Automation and Control Experiment.

predetermined intervals. The three principal areas of experimentation were (1) voltage control, (2) reactive power control, (3) system reconfiguration, and (4) load control.

Load control offers the potential of delaying or deferring the construction of new generating plants or reducing the use of power plants that use expensive fuel and are required or used only for peaking purposes. Figure 1-2 graphically shows how reducing the load at peak times can save new capital costs and reduce the use of high-priced fuel.

The use of voltage control to reduce peaks and to conserve energy is shown in Figure 1-3. The reduction of losses by capacitor switching is an effective means to reduce energy losses; however, as discussed in Chapter 5, capacitor switching without a corresponding decrease in voltage may increase energy use. This effect is shown graphically in Figure 1-4.

System reconfiguration techniques (the transferring of load from a heavily loaded feeder section to a more lightly loaded feeder section) has the potential for reducing losses by decreasing line losses and deferring the need for additional substation capacity. Reduction of outage duration in the event of faults and/or switching can be accomplished if automatic switching equipment is available. Restoring load by a feeder section using the

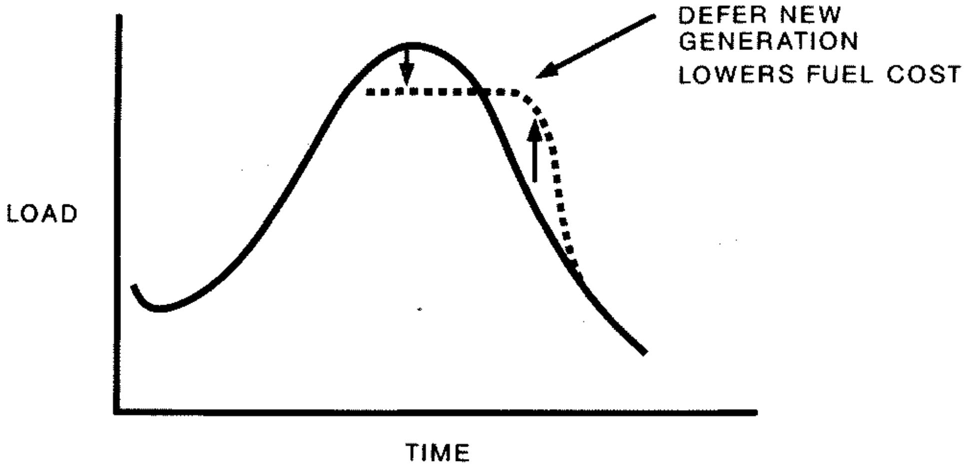

Figure 1-2 Reduction of load peaks can defer installation of new generating plants or can eliminate the use of peaking plants with high fuel costs.

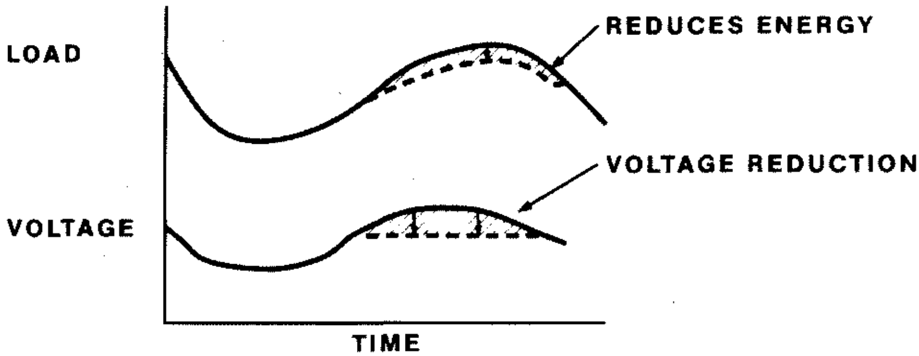

Figure 1-3 Reducing voltage can reduce peak loads or can conserve energy.

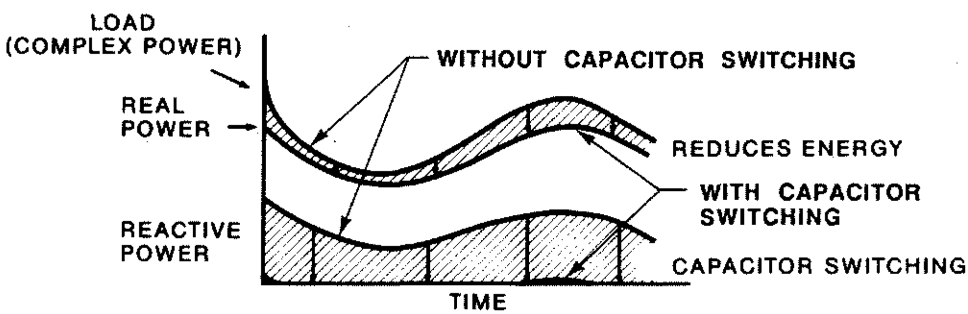

Figure 1-4 Electrical losses can be reduced by improving the power factor on the feeders.

automated equipment can also reduce line surges during the restoration process (see Figure 1-5). Fault location signals sent to the central control room help the operator to determine the location of the faulted line. Remotely operated isolation switches allow the restoration of load to all but the faulted section of the feeder.

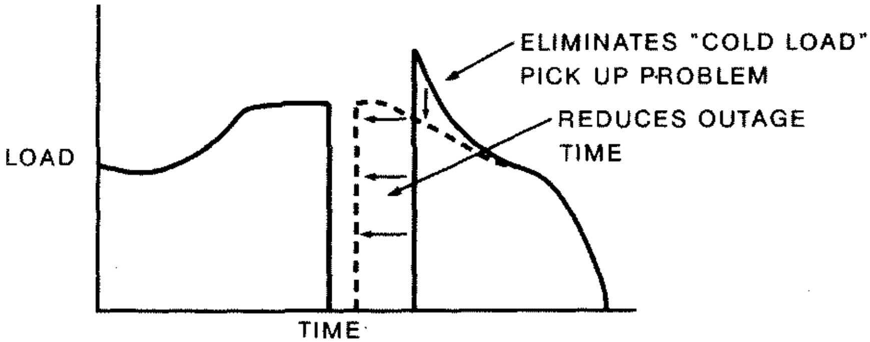

Figure 1-5 Restoring load by feeder section can reduce line surges during the restoration process. Fault location signals and centralized control can reduce outage time.

SUMMARY OF THE EXPERIMENTS

Data Acquisition System

A unique method of measuring the impacts of control on the distribution system in the three experimental areas has been developed. A high-speed data acquisition system capable of recording ten analog data channels at an aggregate rate of 10,000 samples per second was used. The system uses a minicomputer and can be installed in a substation to monitor real power, reactive power, and voltage on each phase of a feeder. This high-speed data acquisition system (data logger) allows the monitoring of impacts from a control action on a millisecond-time-frame basis. As a result, the effects of capacitor switching, load-tap-changing, load transfers by automated switching, and load control have been delineated. This equipment is fully described in Chapter 3. Because of the large and relatively fast natural variation in the feeder loads, changes resulting from control actions are not easily detectable by the slower data acquisition systems being used at Athens or by the equipment normally used on other utility systems.

Voltage and Reactive Power Control

The voltage and reactive power control experiment concentrated on determining the system response to voltage control using the substation load-tap-changing transformers and to reactive power control using automated feeder capacitor banks. These results are described in Chapter 5. The change in real power flow has been found to be quite sensitive to changes in voltage that result from capacitor switching. In general, the real power increased (decreased) with capacitor switching in (out), which is contrary to the results from some simulation models used by the industry. The results of switching capacitors is shown in Figure 1-6. Conventionally, the utility industry uses a constant power load model that is not sensitive to voltage to simulate the response of the distribution system to capacitor control and other

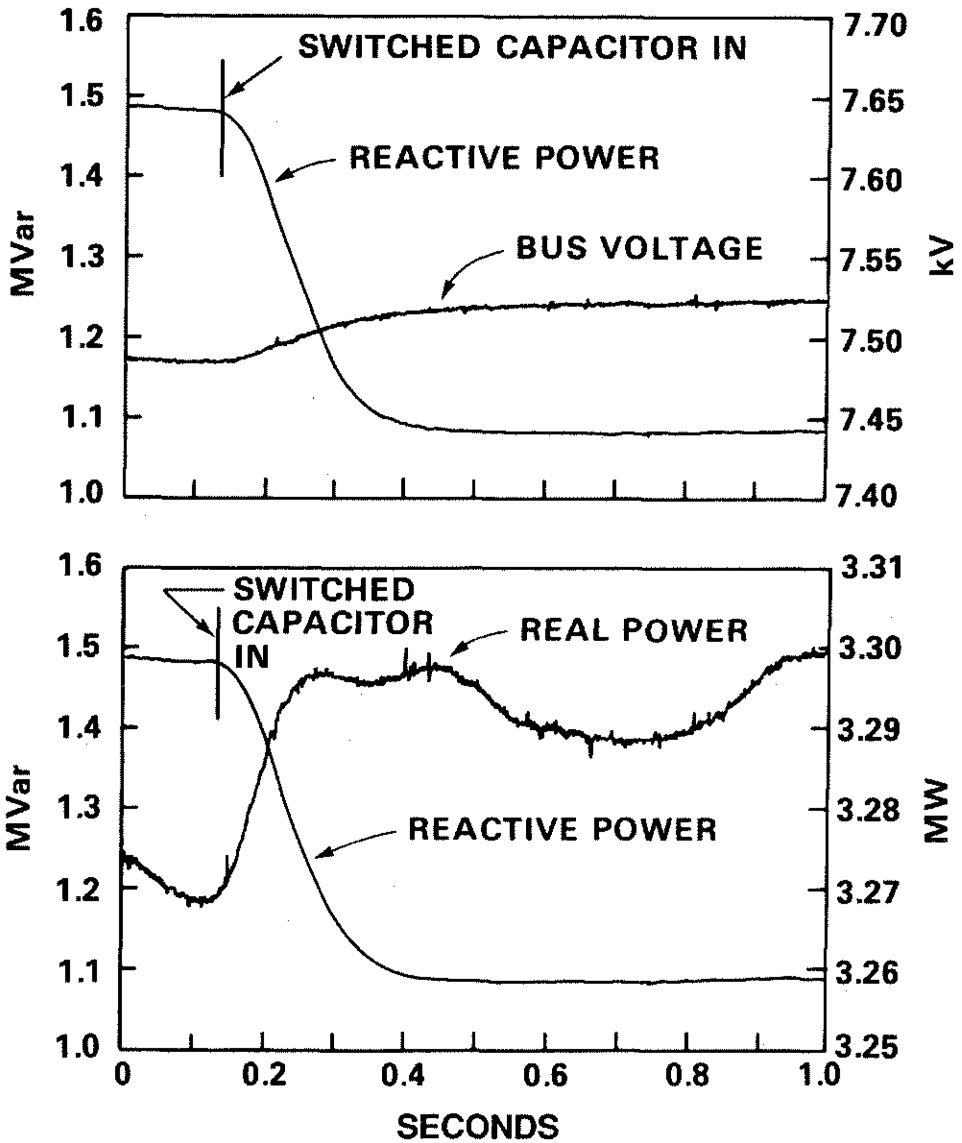

Figure 1-6 High-speed data taken during capacitor switching tests. The data show that as the capacitors are switched in, a voltage increase is observed and the actual load increases.

perturbations. Load-tap-changing transformer control tests have further confirmed the sensitivity of the customer loads to voltage (see Figure 1-7).

A procedure has been developed for automating the control of distribution feeder capacitors using the substation and feeder monitoring and control hardware system installed on the AUB distribution system. The purpose of the procedure is to automatically switch capacitors to control the power factor. A computer program implementing the procedure has been written and is being used on the AUB system. The use of this procedure lowers the cost of power purchased from TVA by the AUB system because a price penalty is invoked if the AUB power factor is not kept within specified limits.

System Reconfiguration

The system reconfiguration experiments have concentrated on determining the impact of transferring load from an overloaded or faulted feeder to a feeder capable of supporting the loads. These experiments are described in Chapter 4. The analysis has determined that load sensitivity to voltage has a major impact on the AUB system response to "large" load transfers. Load transfers of 1.5 and 4.0 MW between substations have been made. Reconfiguration alters the distribution of the load between two feeders and alters the feeder voltage profiles. When the loads are voltage sensitive, the demands will increase (decrease) if the transfer shifts loads to a higher (lower) voltage level. The results of one such switching experiment are shown in Figure 1-8. A personal computer analysis tool called the System Reconfiguration and Analysis Program (SYSRAP) has been developed to simulate load transfers, capacitor switching, and voltage control. SYSRAP (see Chapter 8) combines the features of power flow analysis, voltage-sensitive load models, and data base manipulation. The program allows the use of different load models that have increasing order of sensitivity to voltage. SYSRAP has been able to accurately simulate feeder responses, capacitor switching and voltage control, and load transfers when conventional programs have been inadequate.

Load Control

The load control experiments have produced a reliable data set by cycling appliances in residential homes over a range of outdoor temperatures and durations of appliance off times (duty cycle). These experiments are described in Chapter 6. The load control experiments began during the summer of 1986 with the cycling of air conditioners. Water heater control and space heater control began in the fall of 1986. The data were used to determine the impact of load control on the distribution system. The impact of cycling air conditioners on a feeder was directly measured using the high-speed data acquisition system (see Figures 1-9 and 1-10).

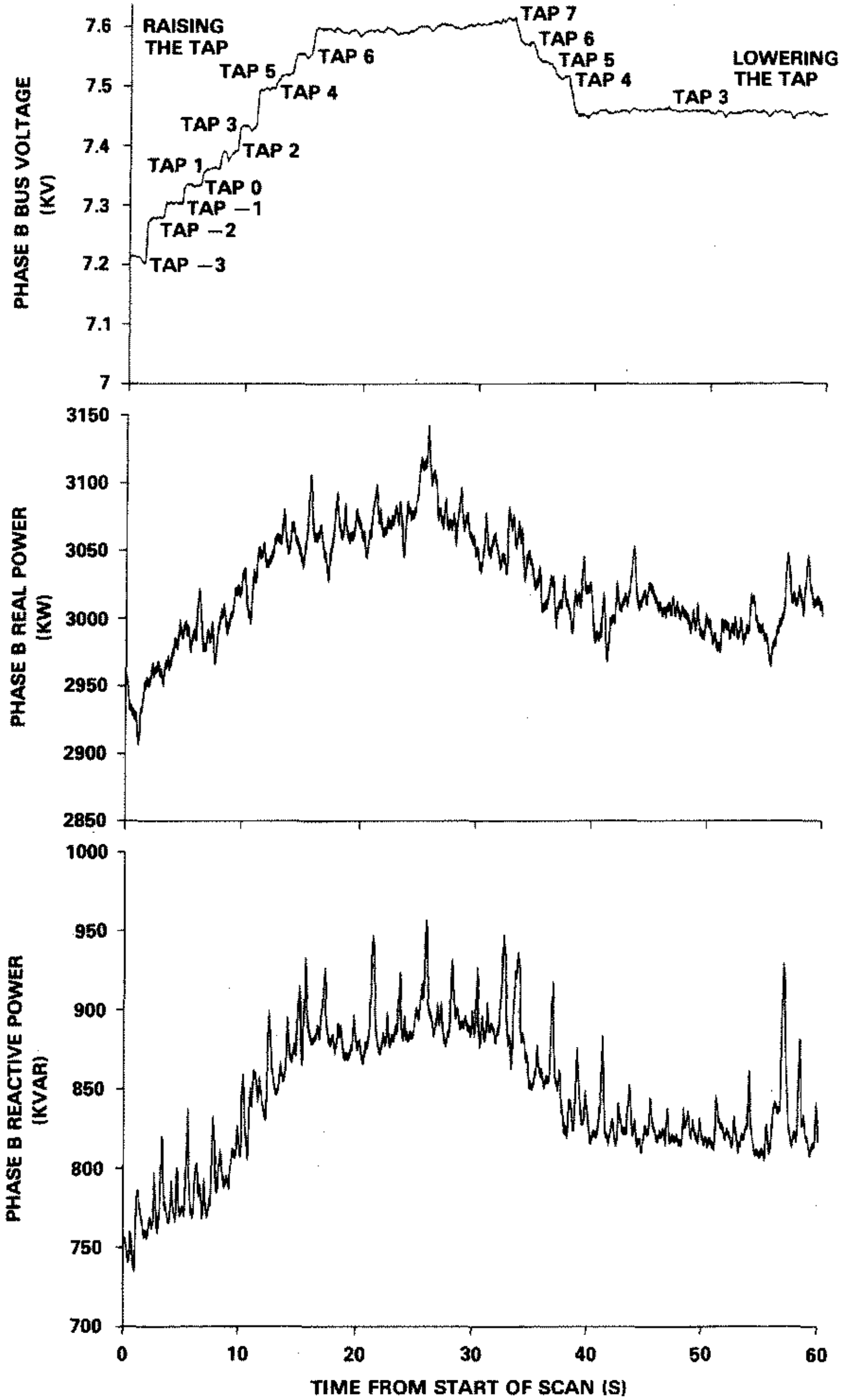

Figure 1-7 High-speed data taken during load-tap-changer control tests show the sensitivity of customer loads to voltage changes.

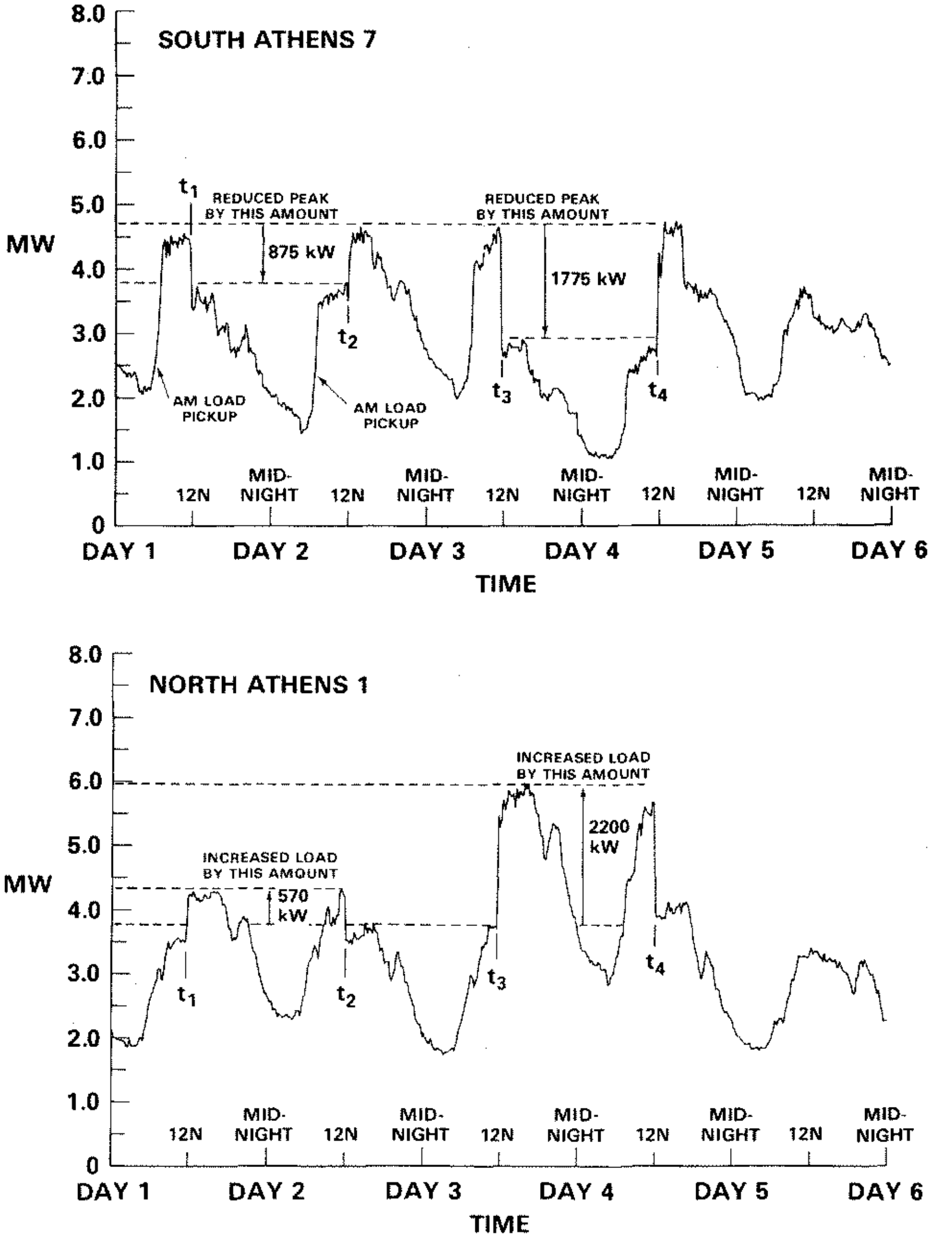

Figure 1-8 Load transfer from Athens Utilities Board South Athens 7 feeder to North Athens 1. Note that amount of loads transferred from one feeder to another is not the same.

Residential-level and feeder-level data for water heater and heat pump cycling experiments have been collected by Metretek smart meters, the Brown Boveri Control Systems, Inc., automation system, and the high-speed data acquisition system. A data base for load data collected since October

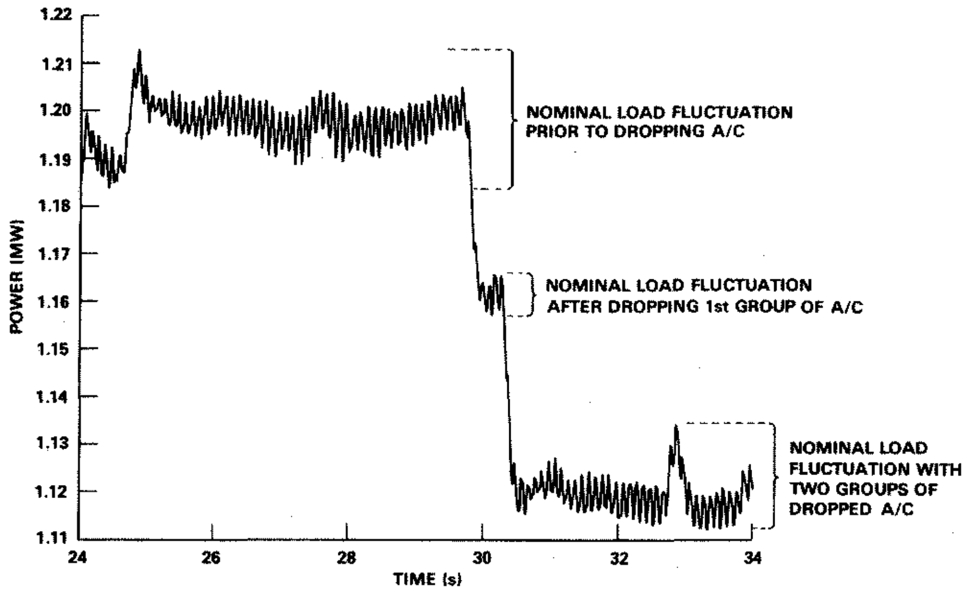

Figure 1-9 High-speed data taken during air-conditioning cycling tests show that load reduction can be readily seen at the feeder level.

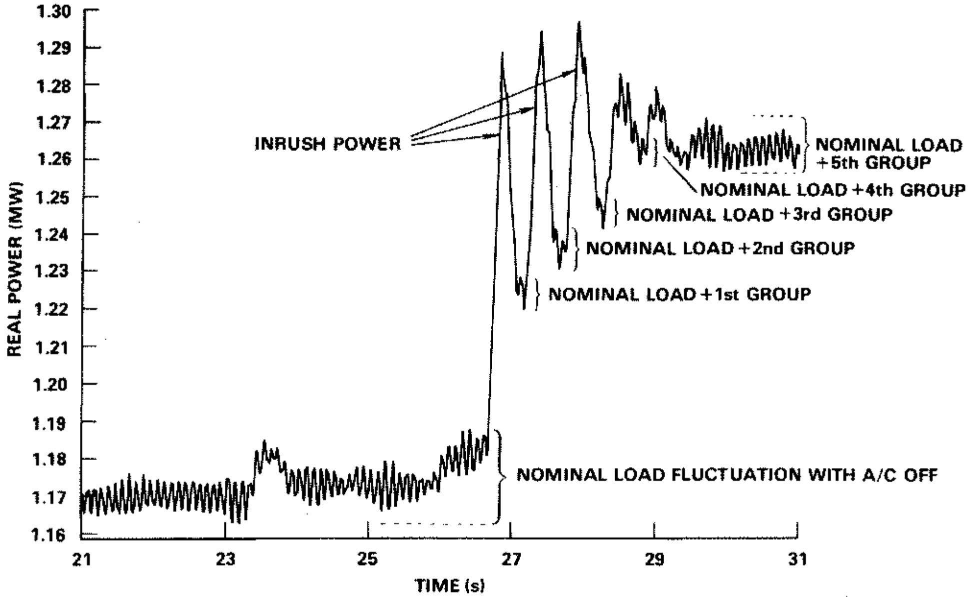

Figure 1-10 High-speed data taken during air-conditioning cycling tests show air conditioners being switched on in groups after they had been controlled to the off position for the experiments.

1985 has been developed. The results of the load control experiments are discussed in Chapter 6.

An operations data base consisting of voltages, power flow, system conditions, and operator interaction is being collected for AUB. The data are taken and stored every 15 minutes. Weather data are being collected by weather stations at each of the AUB substations. The new data base will allow the correlation of weather with customer energy use and the correlations of feeder load flow with customer energy use and weather.

2

THE AUTOMATED SYSTEM*

P. A. Gnadt and J. S. Lawler

Before the AACE began, an extensive review was made of distribution systems that would be likely candidates as the host TVA electrical distributor for the project. During this review, consideration was given to the following factors: daily, monthly, and seasonal load patterns; the capability and configuration of the power distribution system; the mixture of residential, commercial, and industrial loads; the seasonal weather pattern; and the attitude of the populace in accepting load control.

The results of the review indicated that several distribution systems in the TVA territory were likely candidates as the host distributor. The primary reason for selecting AUB was that its load profile was very similar to that of the total TVA system. This chapter presents a description of the equipment installed to automate the AUB system.

INTEGRATED DISTRIBUTION CONTROL SYSTEM

The overall control system installed on the AUB distribution system was originally called the Integrated Distribution Control System (IDCS).[1–5]

The IDCS hardware arrangement, shown in Figure 2-1, consists of three subsystems: substation automation and monitoring, distribution feeder

*This chapter includes excerpts from S. L. Purucker et al., *Athens Automation and Control Experiment: Substation and Distribution System Automation Designs and Costs*, ORNL/TM-9596, Oak Ridge National Laboratory, June 1986.

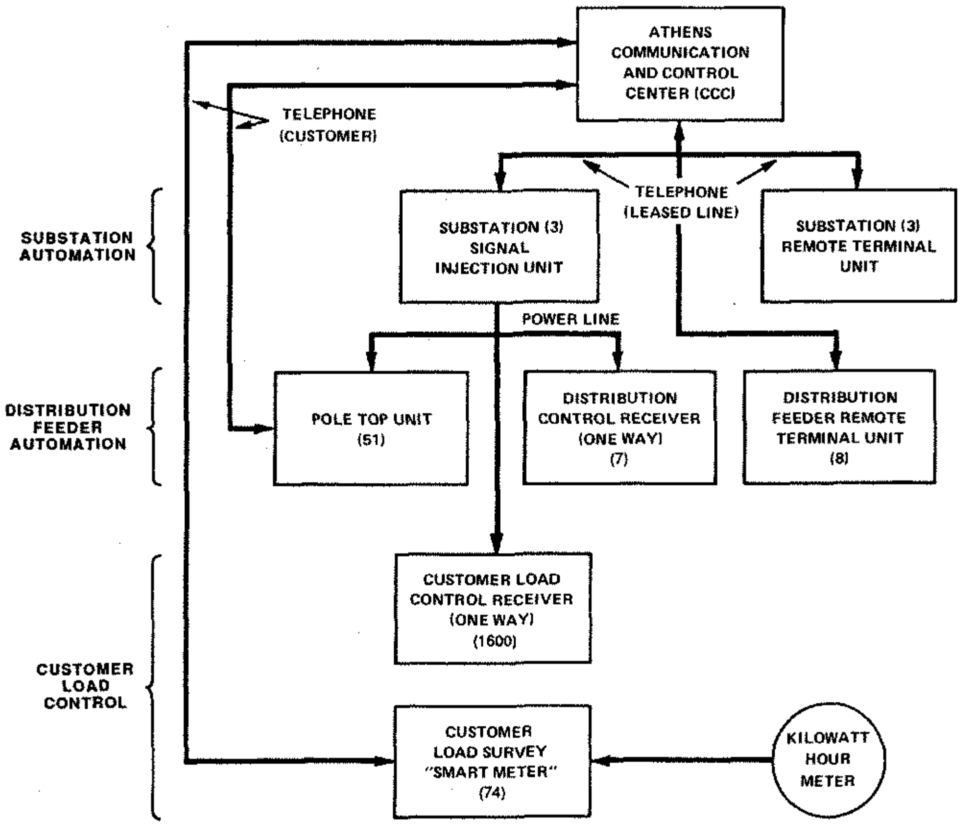

Figure 2-1 Integrated Distribution Control System.

automation, and customer load control. The Communication and Control Center (CCC) is the integrating link for the three subsystems and provides the intelligence required for operation of the IDCS.

The CCC consists of two Digital Equipment Corporation PDP-11/44 computers and associated peripheral equipment. These computers are shown in Figure 2-2, and the control room equipment is shown in Figures 2-3 and 2-4. The man–machine interface uses dual Aydin color graphic displays; modems, printers, and data loggers complete the CCC hardware configuration. The "MODSCAN" data acquisition and control software, furnished by Brown-Boveri Control Systems, Inc. (BBC), monitors and controls all field devices. Application software developed by ORNL supports the control effort.

The substation automation subsystem is provided by the remote terminal units located in each of the three substations. These units monitor real power, reactive power, voltage, transformer tap position, air temperature, humidity, breaker position, relay status, and capacitor switch status. The remote

Figure 2-2 Dual PDP-11/44 computers used on Athens Automation and Control Experiment.

terminal unit also initiates control actions as directed by the CCC to control breakers, transformer taps, and capacitors in the substation.

The load control subsystem of the IDCS consists of the signal injection units, the load control receivers, and the customer-load-survey smart meters, which communicate with the CCC. The signal injection unit modulates the power system voltage signal by injecting a 340-Hz voltage waveform onto the 60-Hz voltage wave. This "ripple" signal is detected by the various control devices downstream of the injection location. The load control receiver, located in the customer's home, decodes the ripple signal into a control

Figure 2-3 Athens Utilities Board control room after the system was automated.

message. The load control receiver has three internal relays that can be used to control loads such as the water heater, central heating unit, or central air-conditioning unit.

A smart meter installed in a customer's home integrates a standard kilowatt-hour meter with an electronics package and counts the revolutions of the electric meter disk. The revolution counts are stored in the smart meter's memory and are transferred to the CCC via the customer's telephone line. Once the smart meter has established contact with the CCC, it conveys the meter count to the CCC, which also logs the time of the call. The CCC then communicates a callback time to the smart meter for its next return call.

The distribution feeder automation subsystem consists of the distribution remote terminal units, the pole-top units, and the distribution control receivers. The distribution remote terminal unit, a smaller version of the substation remote terminal unit, is capable of monitoring local three-phase real power, reactive power, and voltage and can detect the status of relays and fault sensors on distribution feeders. The distribution remote terminal unit, which is connected to the CCC via a 1200-baud leased telephone line, can control several switches or voltage regulators at each distribution location.

The pole-top unit is similar to the distribution remote terminal unit except that it communicates differently and has fewer control and monitoring

Figure 2-4 Computer terminal and graphic display, Athens Automation and Control Experiment.

connections. The pole-top unit receives its control signal from the signal injection unit and conveys information to the CCC via a 300-baud customer-grade telephone line. Because the pole-top unit initiates both routine and random telephone calls to the CCC, communication throughput may be decreased as a result of potential communication collisions with other pole-top units. If the computer telephone lines are busy, the pole-top unit will reinitiate a call later. The pole-top unit has backup telephone communications capability. In the event of a power outage, where the signal injection unit cannot communicate with the pole-top unit, the CCC can send a control signal to the pole-top unit via the telephone line.

The distribution control receiver is a one-way control device that is installed at some distribution feeder capacitor positions. The distribution control receiver receives its control signal from the signal injection unit and switches a capacitor bank. Control verification is received by the CCC indirectly because the change in reactive power flow is observed by the substation remote terminal unit and reported to the CCC. The common links among the distribution remote terminal unit, pole-top unit, and distribution control receiver are that they control distribution feeder equipment and, with the exception of the distribution control receiver, monitor distribution feeder power, voltage, and equipment status. The various devices (remote terminal unit, signal injection unit, load control receiver, smart meter, distribution remote terminal unit, pole-top unit, and distribution control receiver) used are shown in Figure 2-1.

Supporting the IDCS are two types of control software: (1) the real-time data acquisition and control software and (2) the ORNL-developed applications software. The "MODSCAN" real-time software package, supplied by BBC, is primarily a data base management system using a hierarchical data base. Supporting elements include a man–machine interface package, a remote terminal unit scan package, a telephone receiver package (associated with the pole-top unit and smart meter), a control package (for issuing control signals), various main memory and disk-handling packages, and provisions for access to the data base by applications software. The software developed by ORNL controls the load, voltage, reactive power (var), and system reconfiguration equipment to conduct experiments and to improve the efficiency and operability of the power system.

MONITORING AND CONTROL REQUIREMENTS

Substation and feeder installations require three different types of equipment: standard distribution equipment; automation equipment; and interface equipment (i.e., transducers, interposing relays, potential transformers, and current transformers), which links the automation equipment to the standard distribution equipment. The various types of substation and feeder distribution equipment, customer-monitoring and -control installations, and the quantities of each on the AUB distribution system are as follows:

- Substation equipment (3 substations)
  - — 2 load-tap changing (LTC) transformers
  - — 1 three-phase regulator
  - — 11 substation feeder breakers
  - — 5 substation capacitor banks
  - — 3 weather stations

- Feeder distribution equipment (12 feeders)
  - 45 feeder load monitoring locations
  - 35 load-break switches
  - 12 power reclosers
  - 5 voltage regulator banks
  - 29 capacitor banks
- Customer installations
  - 200 smart meters (whole-household monitoring)
  - 1600 load control receivers (residential appliance load control)*
  - 74 Electric Appliance Research Metering (ARM)† devices (appliance load monitoring)

The relatively large amount of instrumentation in the substations and on the distribution feeder was intended to create an overinstrumented, flexible monitoring and control system so that experiments could be conducted to define the appropriate level of instrumentation required to support control strategies for specific system benefits. The Electric ARM appliance monitoring system was furnished by EPRI for load control studies. The Electric ARM equipment is not part of the IDCS; the data collected by this equipment were input into a computer system different from that associated with the IDCS.

BASIC MONITORING AND CONTROL SYSTEM

A block diagram showing how the three types of IDCS equipment interact is given in Figure 2-5.

The communication and control system equipment consists of

- computers,
- communications equipment,
- substation remote terminal units,
- distribution feeder remote terminal units, and
- pole-top remote terminal units.

*Although 2000 load control receivers were planned, only 1600 were installed for the experiments.

†The Electric ARM is a trademark of Robinton Products, Inc. Although 200 of these units were provided by EPRI, only 74 were installed.

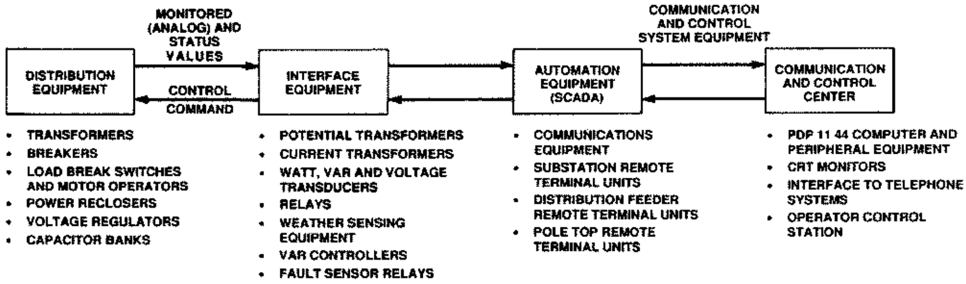

Figure 2-5 Block diagram showing interconnections of distribution equipment, control equipment, and communications at Athens Utilities Board.

The interface equipment that is required to link the communications and control system to the distribution system typically consists of

- potential transformers,
- current transformers,
- watt/var and voltage transducers,
- various control relays, and
- weather-sensing equipment.

The three types of remote terminal units mentioned above (substation, distribution feeder, and pole-top) are very similar. The substation and distribution feeder remote terminal units are both universal, asynchronous receiver/transmitter units that essentially differ only in the number of input/output points that can be accommodated, with the substation unit having the greater capacity. The pole-top remote terminal unit is also equipped with a special circuit that provides initiation of telephone communications back to the CCC for "off-normal" conditions. BBC manufactured all three types of remote control and monitoring units and designed them to interface with the CCC. These units were intended primarily for data acquisition and control applications. The heart of the remote terminal units is the microprocessor, memory, and signal-decoding circuitry for standard communications interface logic.

Two types of monitoring are included in the IDCS: analog and status point. Analog monitoring is the sensing of values such as voltage and real and reactive power to yield numeric values; status monitoring is the determination of relay position or switch position (i.e., open or closed).

Analog Monitoring

Analog monitoring for the IDCS originates from potential and/or current transformers. Output signals (voltage and/or current) that are proportional to the phase voltage and/or current are sent to the transducer. The transducer produces a dc output representative of the watt, var, or voltage values that exist in the distribution system circuits being monitored. The analog signal is fed into an analog card within the remote terminal unit and then into an analog-to-digital converter, which converts the dc signal into a digital signal. Also, analog signals from the weather station equipment are processed by the remote terminal unit for subsequent conversion to digital signals. When the remote terminal unit is polled by the CCC, the digital signals are sequentially transmitted via a modem to the CCC computer. Communication occurs over the dedicated telephone circuit for the remote terminal units or, in the case of the pole-top units, via a multiparty telephone line. The digital information is received by another modem on the computer side of the telephone lines. The digital signal is, in turn, presented to a data buffer unit, which preprocesses the digital data for input to the CCC computer real-time data base.

Status Monitoring

Status monitoring is very similar to analog monitoring except that the signal originates at a relay contact that represents the status of the switch or device (i.e., open or closed). This status signal is then fed to a status card within the remote terminal unit and converted to a digital signal; then, upon polling by the CCC, the status condition is transmitted back to the CCC into a real-time data base.

Control

Control commands can be initiated at the CCC in two ways: by the operator or, in some instances, by real-time control software. When control action is implemented directly by the operator, it is referred to as "open-loop control." The operator interacts with the real-time data base through two color cathode-ray tube screens. The operator can access analysis programs and then make and implement control decisions. When a control action is implemented by the real-time control software without operator intervention, it is referred to as "closed-loop control." When closed-loop control is used, data are extracted from the real-time data base and are processed by control software, which makes and then implements a control decision.

After a control decision has been made by either the open- or closed-loop control technique, the control decision is transmitted to the real-time data base. Another data buffer unit processes and formats the digital control command for presentation to the computer modem, which, in turn, transmits the control signal to a remote terminal unit. The remote terminal unit takes the digital control information from its modem and transmits it to a control card, which contains low-current relays. A low-current relay responds to the control signal and activates a higher current interposing relay. This interposing relay then drives the motor that operates substation equipment or one of the four feeder automation devices: the load-break switch, the voltage regulator, the power recloser, or the capacitor bank.

SUBSTATION INSTALLATIONS

The monitoring and controlling functions for the substation are the traditional supervisory control and data acquisition functions. The instrumentation described below represents the equipment and parameters that are normally monitored and controlled in a comprehensive substation control system. Both real and reactive power are monitored for each phase of each feeder. Single-phase voltages are also monitored, as well as switch status and the position of various station and breaker relays. Substation breakers, capacitors, and regulating transformers are controlled, and temperature and humidity levels at the substations are monitored. In one AUB substation, a weather station is installed to monitor wind velocity and direction, barometric pressure, humidity, temperature, and solar radiation.

FEEDER AUTOMATION INSTALLATIONS

Four types of devices on the distribution feeders are monitored and controlled: load-break switches, power reclosers, voltage regulators, and capacitor banks. *Load-break switches* isolate faulted overhead lines and transfer loads while the circuit is energized. Load-break switches are also used at "tie switch" points where two feeders can be connected so that one feeder can become the alternate supply to the other feeder. *Power reclosers* transfer load and clear electrical faults (in coordination with the substation breaker). Reclosers automatically reclose on the line for continuity of service and reopen if the fault persists. *Voltage regulators* are usually a transformer-type device with underload tap-changing capability to increase or decrease the load-side voltage. *Capacitor banks* are installed on the distribution feeders to provide reactive power correction, thus minimizing the current in the feeder and reducing feeder power losses.

The existing AUB distribution equipment, which consisted of different manufacturers' equipment, was adapted as necessary for use in the AACE. Supplemental control equipment was added to some capacitors to enhance the versatility and reactive control capability of the system. Also, some installations are equipped with single-phase (vs three-phase) monitoring equipment because full metering is not required at every feeder point.

Load-Break Switch

The load-break switch installation consists of a three-phase, group-operated load-break switch and electric motor operator; in some cases, a battery backup for both the motor operator and the pole-top remote terminal unit; metal-oxide-varistor surge arresters; a fault-detection relay; and combination potential-metering/current-metering transformers with bypass switches. Transducers in weatherproof cabinets are mounted at the base of the power poles. A pole-top remote terminal unit is mounted under the transducer cabinet. A photograph of an actual three-phase installation is shown in Figure 2-6, and a pictorial diagram taken from the design drawings[5]

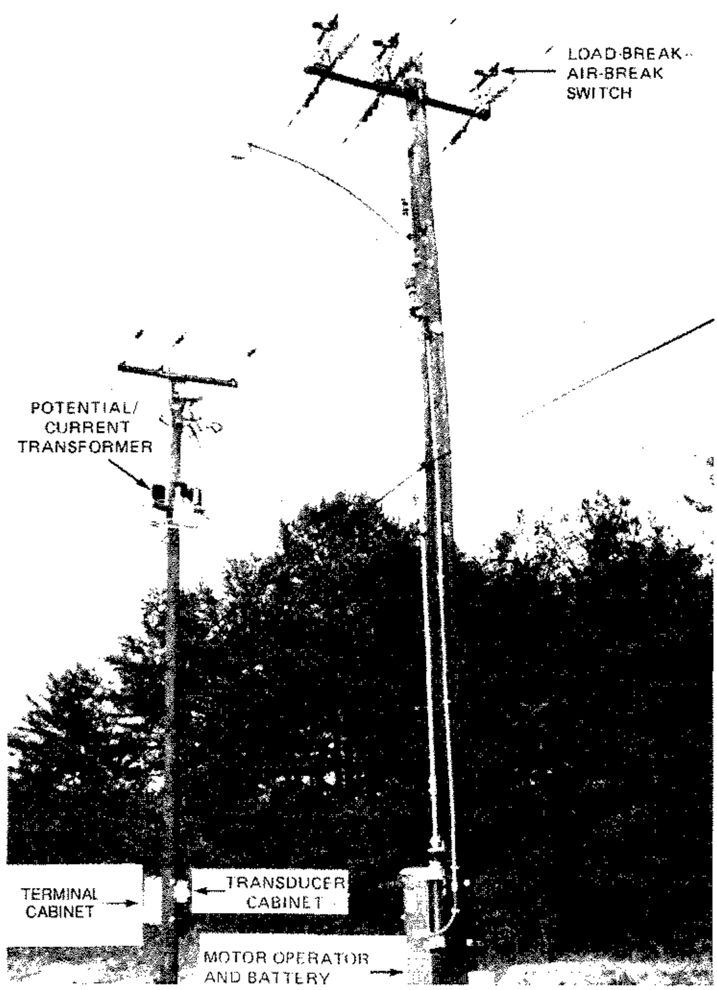

Figure 2-6 Automated three-phase load-break switch and feeder monitoring equipment.

is shown in Figure 2-7. Note the differences between the actual installation in Figure 2-6 and the standard design drawing shown in Figure 2-7. The standard design established the electrical design. Modifications were required at most field locations to accommodate existing distribution pole and equipment configurations.

Table 2-1 lists the monitoring and control points associated with the load-break switch.

Power Recloser

The power recloser installation consists of a Westinghouse type "PR" recloser, a normally open air-break bypass switch with six isolation disconnect switches, a pole-top remote terminal unit, and a transducer cabinet. Generally, a group-operated, three-phase air-break switch is used to bypass

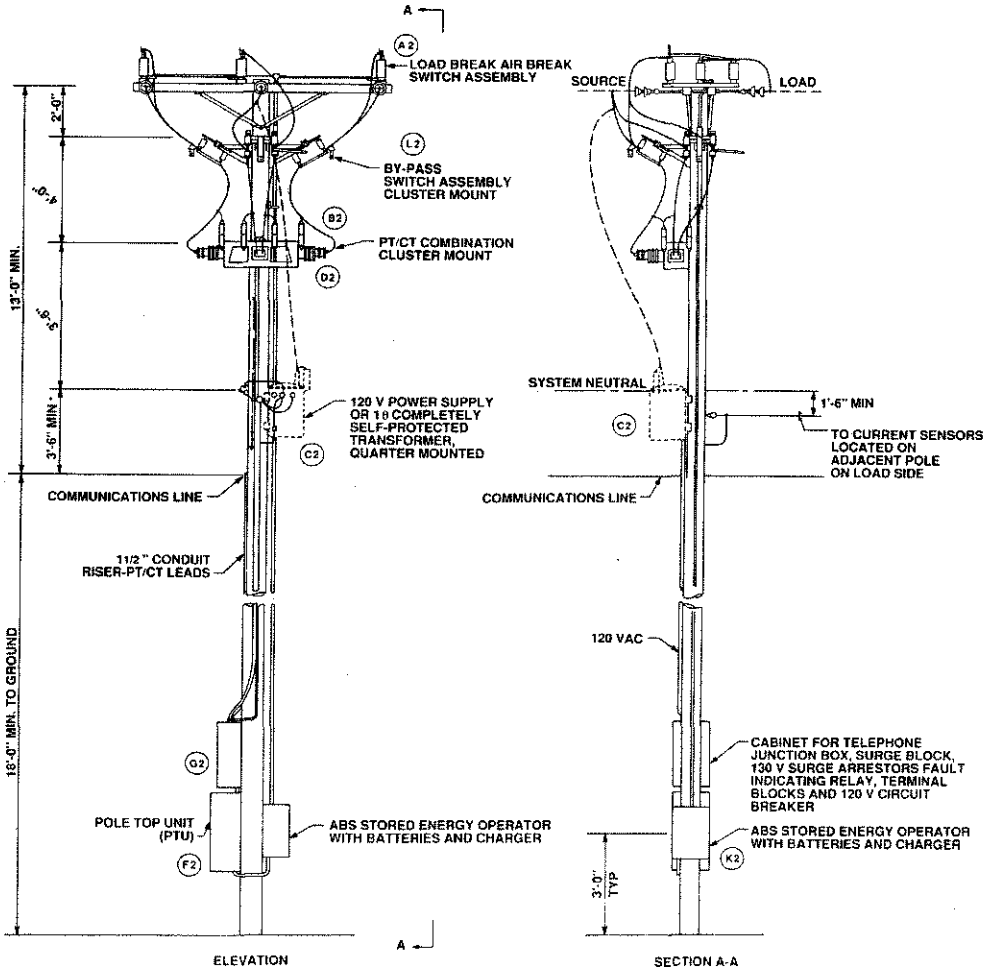

Figure 2-7 Architectural drawing of load-break switch and feeder monitoring equipment.

TABLE 2-1 Load-break switch monitoring and control points

Analog

- Real power (three 1ϕ)
- Reactive power (three 1ϕ)
- Voltage (three 1ϕ)

Status

- Switch status
- Local/remote control switch status
- Fault indicator

Control

- Switch open/close control

the recloser and other equipment on the pole. The transducer cabinet contains the transducers required for monitoring at the recloser.

The power recloser installations are similar to the load-break switch installations; however, the recloser does not have a motor operator or a battery backup power supply. Figure 2-8 is a photograph of a power recloser installation. Table 2-2 gives a listing of the monitoring and control points associated with the power recloser.

Voltage Regulator

The voltage regulator installations, located on selected 13.2-kV distribution feeders, consist of three single-phase regulators. The distribution feeder remote terminal unit is mounted at the bottom of a pole assembly, and the transducer terminal cabinet is mounted above it. Figure 2-9 is a photograph of one of the three-phase regulator installations.

The voltage regulator remote terminal unit installation provides remote voltage regulator control and monitors the system voltage and power flows at that particular location. When computer-directed voltage control is required, interposing relays are used to bypass the local regulator control, and additional relays are used to remotely operate the voltage regulator tap changer. By controlling the distribution feeder voltage with the voltage regulator, the system peak demand can be reduced by lowering the feeder voltage at critical peak periods. Also, adjustment of the feeder voltage will affect the var requirements when a static capacitor bank is located on the load side of the voltage regulator.

For proper power system operation, the position of the tap-changer controller of the voltage regulator must be known. A method to directly convert the mechanical position of the tap changer into an electrical position signal was not available for the existing regulators. Therefore, potential

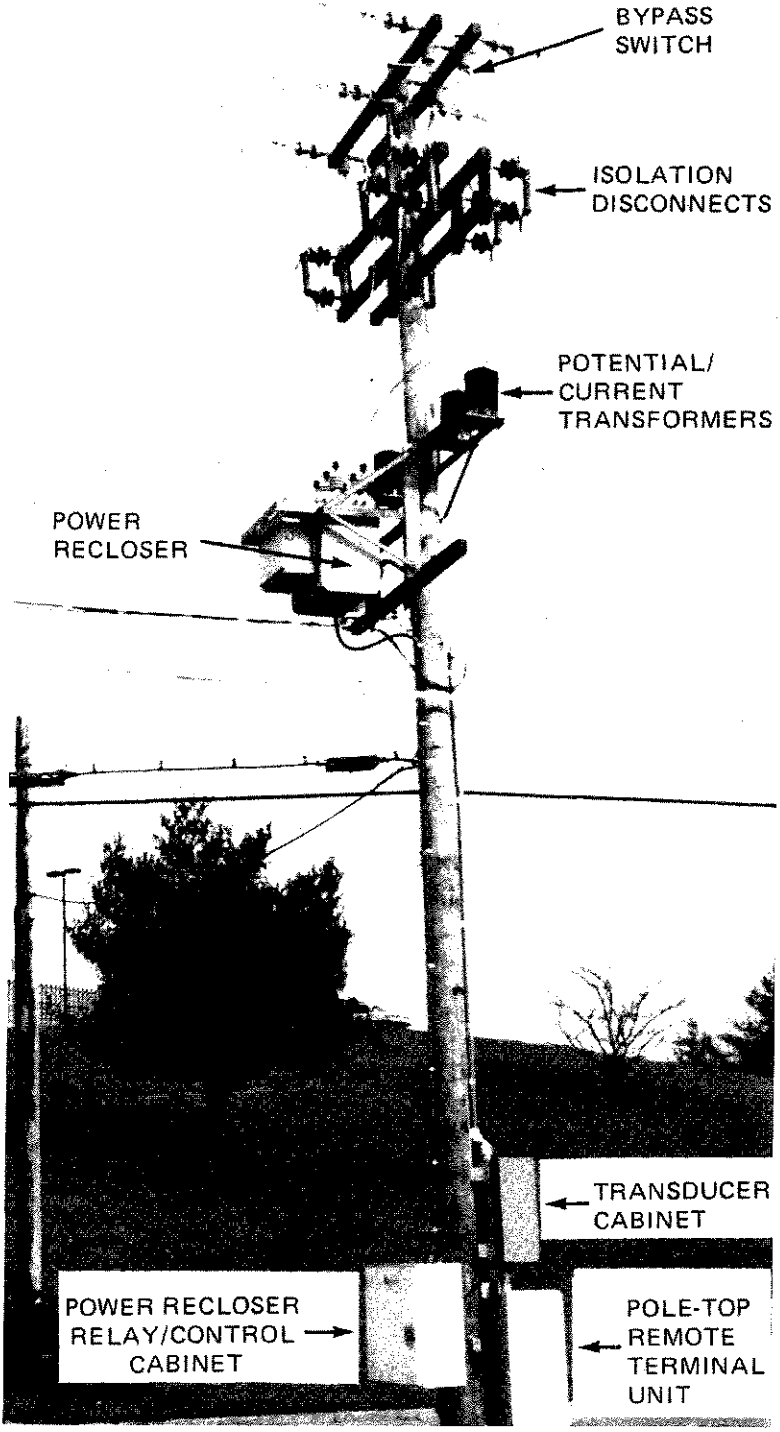

Figure 2-8 Typical Athens Utilities Board three-phase power recloser amd monitoring equipment installation.

TABLE 2-2 Power recloser monitoring and control points

Analog
• Real power (three 1ϕ)
• Reactive power (three 1ϕ)
• Voltage (three 1ϕ)
Status
• Switch status
• Reclosing relay cutout switch status ("A" switch)
• Manual remote control enable/disable switch status
• High-set ground instantaneous overcurrent target status (one)
• Low-set ground instantaneous overcurrent target status (one)
• Low-set ground time overcurrent target status (one)
• Phase time overcurrent target status (three)
• Phase instantaneous overcurrent target status (three)
Control
• Recloser open/close control
• Reclosing relay "A" switch

metering transformers were installed on the line side to supplement the potential transformers on the load side of the regulator. By transmitting the voltages to the CCC and programming the computer to calculate and divide the voltage drop across the regulator by the voltage/tap constant, the tap position is determined.

Table 2-3 lists the monitoring and control points associated with the voltage regulator.

Capacitor Banks

Three different types of control schemes are used to control the capacitor bank installations: (1) a distribution control receiver for one-way control; (2) a locally mounted var controller operating through a pole-top remote terminal unit; and (3) a pole-top remote terminal unit to actuate the capacitor oil switches from the CCC. The latter two schemes can be used in conjunction with metering of the distribution system power and voltage parameters.

The capacitor bank installation consists of one potential transformer/current transformer combination unit with isolation switches; metal-oxide-varistor (MOV) surge arresters; a bank of capacitors with MOV surge arresters; and, depending on the control scheme, a pole-top remote terminal unit and a var controller with a neutral current relay. A typical var controller and pole-top unit with single-phase metering are illustrated in Figure 2-10.

The capacitor banks can be controlled either locally or remotely. In the local control option, the output of the potential transformer/current

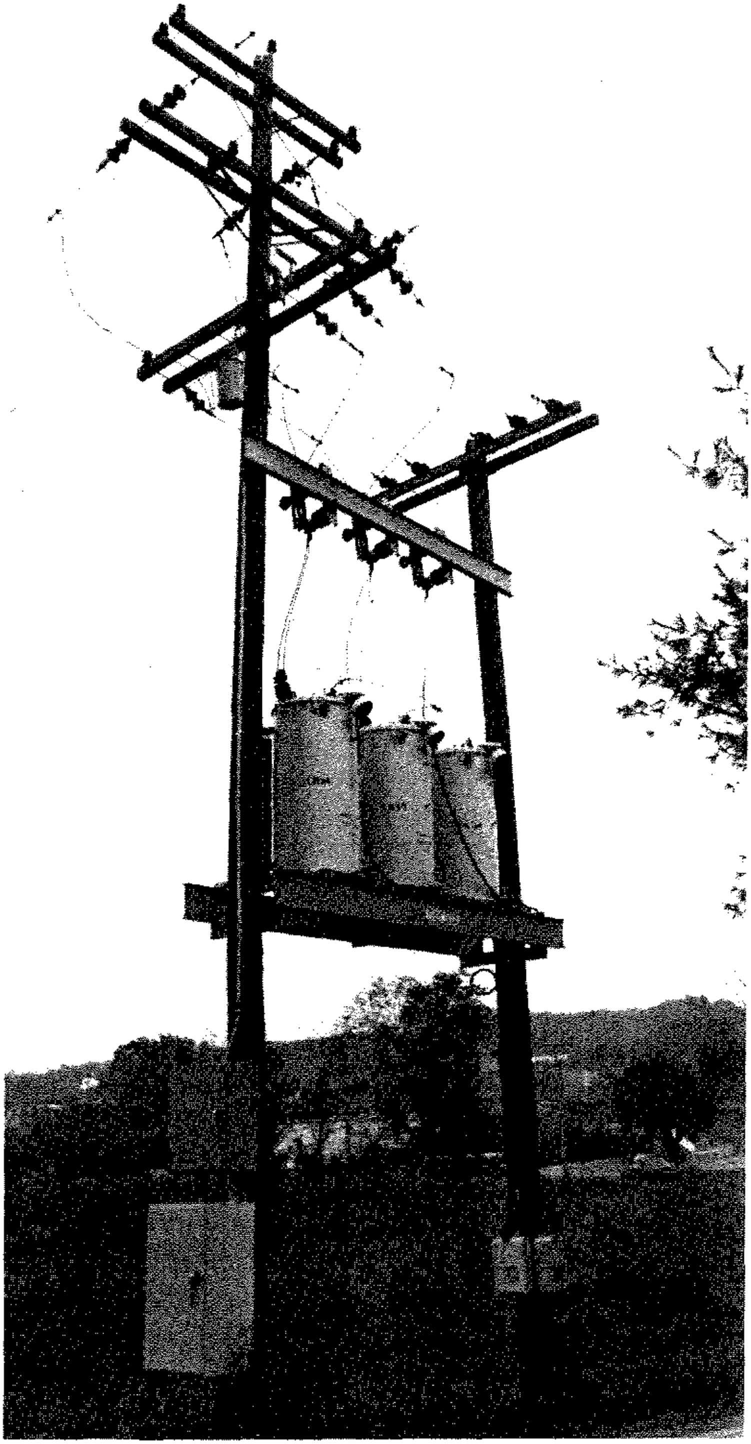

Figure 2-9 Typical three-phase regulator bank on Athens Utilities Board system.

TABLE 2-3 Voltage regulator monitoring and control points

Analog
• Real power (three 1ϕ)
• Reactive power (three 1ϕ)
• Voltage (three 1ϕ—source side)
• Voltage (three 1ϕ—load side)
• Tap position (computed from voltages)
Status
• Neutral tap position status
• Local/remote relay status
• Manual remote control enable/disable switch
Control
• Local/remote relay control
• Raise or lower regulator tap (remote mode only)

transformer combination unit (or post insulator current sensor and potential transformer) is used to operate the var controller, which controls the capacitor bank. In the remote control option, the CCC is used to monitor voltages and reactive power and to switch the capacitors according to the criteria programmed into the CCC. Computer control of the capacitors allows greater flexibility with regard to developing control algorithms. A software change is all that is required to change the type of local control. For example, voltage, time-clock, and reactive local control can be simulated with field values and the computer's clock. Remote control does not require that a var controller be included in each installation. In addition, a neutral current relay opens the capacitor bank switches if the capacitors on any phase malfunction and cause zero-sequence current to flow.

Table 2-4 lists the monitoring and control points associated with the capacitor.

Customer Installations

Originally, instrumentation to be installed in customers' homes included 2000 load control receivers to control customer loads, 200 smart meters to record the kilowatt-hours used and to communicate these data to the CCC, and 200 Electric ARMs. The load-control receiver controls customer appliances such as the water heater, central air-conditioning unit, or central heating unit. Two hundred load-control receivers were to be installed at smart meter locations, and an additional 200 were to be installed in the homes with the Electric ARMs. However, the installation of monitoring equipment in customers' homes proved to be more time consuming than was anticipated;

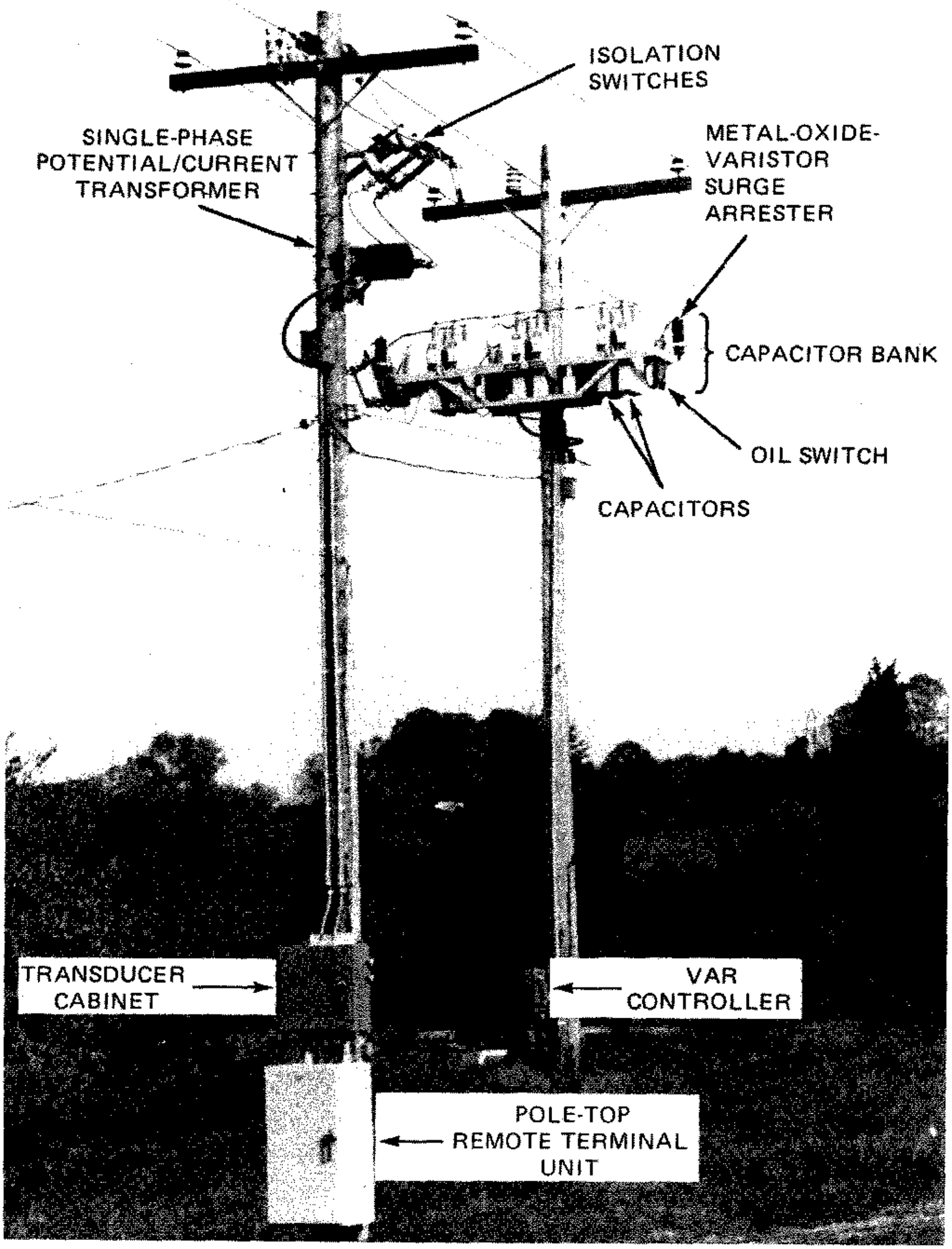

Figure 2-10 Typical three-phase capacitor and var controller installation on Athens Utilities Board system.

TABLE 2-4 Capacitor monitoring and control points

Analog

- Real power (one 1ϕ)
- Reactive power (one 1ϕ)
- Voltage (one 1ϕ)

Status

- Capacitor bank status
- Local/remote switch status
- Manual remote control enable/disable switch status
- Neutral current relay status

Control

- Local/remote relay control
- Capacitor open/close control (remote mode only)

and installations of load-control receivers and Electric ARMs were reduced to 1000 and 74 units, respectively.

The smart meter monitors the whole-household load by reading the customer's kilowatt-hour meter. These whole-household customer load data are periodically transmitted back to the CCC via the customer's telephone. The smart meters are connected to the IDCS real-time control system, and this data feedback serves as input for the load-control operating models. Figure 2-11 is a photograph of a smart meter and Figure 2-12 shows the installation of a smart meter in an Athens residence.

The third device, the Electric ARM, was installed to monitor the electricity usage of water heaters, the central heating unit, and the central air conditioning unit in 5-minute intervals; the device also measures the whole-household power usage and the inside-house ambient air temperature. The Electric ARM devices were installed to acquire basic appliance load data, which will be used to calibrate and develop planning and operating models. EPRI is investigating the transferability of data and load control planning models to other utilities. Figure 2-13 is a photograph of the ARM devices and the load-control unit.

Surge Protection

Extensive surge protection was applied in the IDCS design to protect the electronic equipment installed on the system. The feeders are equipped with 10-kV metal oxide varistor surge arresters, and the secondary circuits of the potential transformers are protected by low-voltage metal oxide varistors. Also, the 120-V power circuits from the distribution transformers have shunt-installed metal oxide varistors before the point where the power passes through low-pass electromagnetic interference filters. This electromagnetic

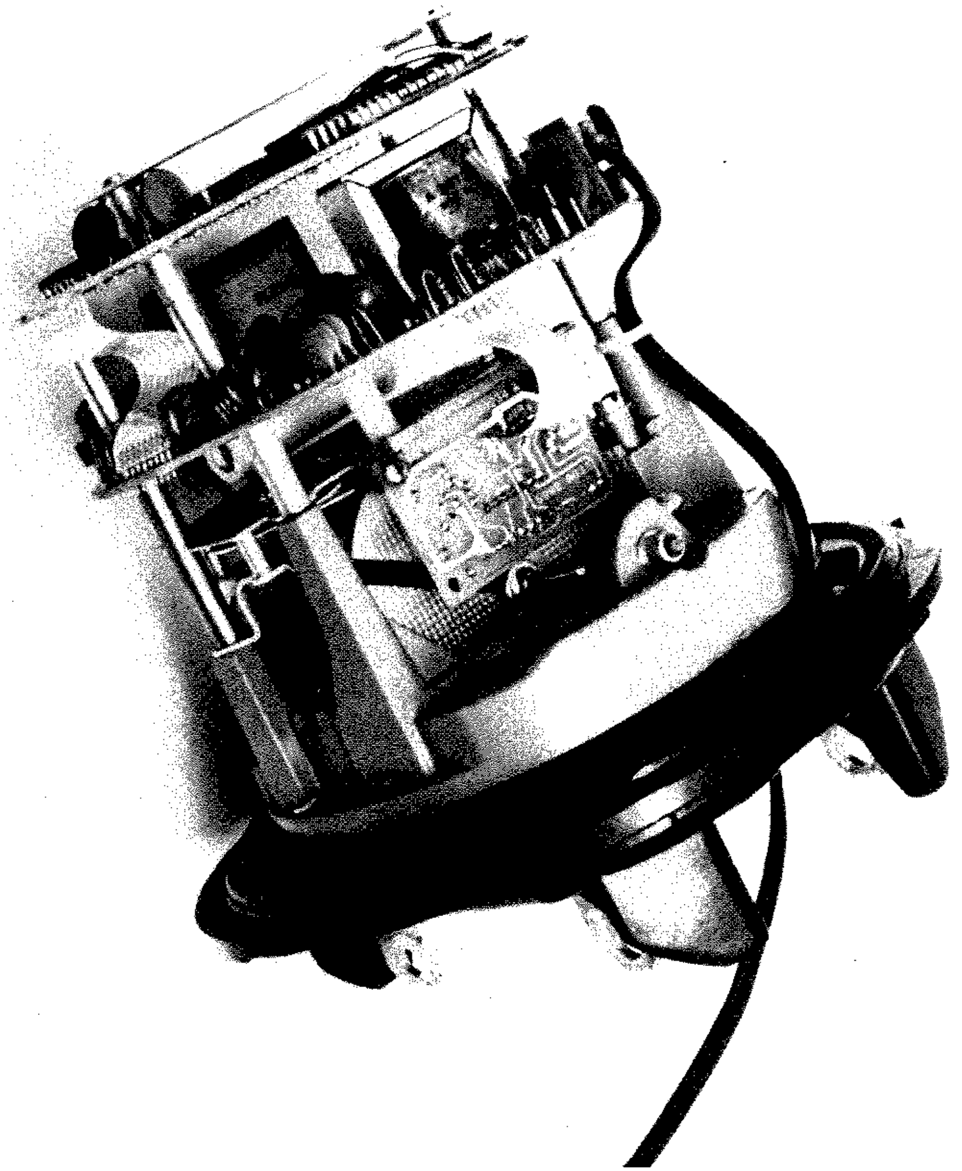

Figure 2-11 Photograph of a smart meter used to measure household load and transmit the results to the Athens Utilities Board central control room.

interference equipment was applied to minimize the damage of customer inductive equipment and/or close-proximity lightning strikes to the input circuits of the transducers and the remote terminal units and pole-top units. Operating experience with these units indicated that the surge-control equipment might not be adequate.

Figure 2-12 Typical smart meter installation in Athens Utilities Board customer home.

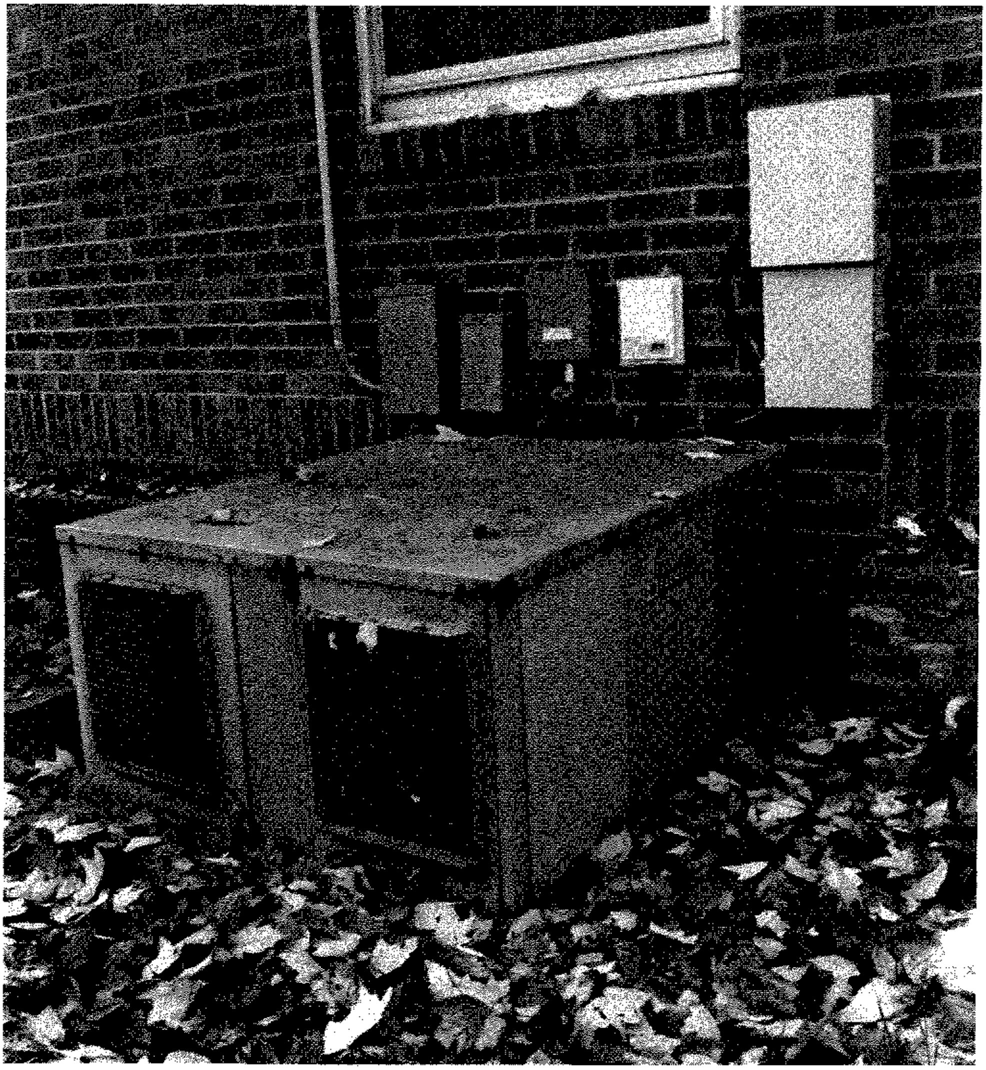

Figure 2-13 Typical appliance research meter and load controller installation in Athens Utilities Board customer home. The large unit in the foreground is the customer's air-conditioning unit.

Equipment failures and maintenance associated with the equipment are discussed in Chapter 9. In general, the project staff believes that additional surge protection was needed for most of the applications, particularly those with electronic circuits.

INSTALLATION DESIGN

The designs for automating the equipment were developed in three phases: conceptual design, preliminary design, and final design. The conceptual design included establishing the design objectives and design criteria. The preliminary design defined in detail the power system metering equipment, status-of-equipment monitoring, and system device control requirements at each control point; determined the amount of equipment required; provided cost estimates; and developed the installation drawings. The final design provided the specifications for equipment procurement and drawings for the installations. Appendices A through E of reference 5 document the designs, specifications for the equipment, the quantity and functions of the equipment, and installation costs.

Conceptual Design Phase

A major objective of the AACE was to determine the benefits obtained for various installations of automation and control. Therefore, the conceptual design included more instrumentation than was initially considered necessary. The goals for the AACE included investigating the economic and technical feasibility of the systems.

Designs were provided to

- monitor the basic power system values (voltage and real and reactive power) on all three phases of each feeder;
- monitor all pertinent substation equipment: breakers, transformer taps, voltage regulator taps, and capacitors;
- obtain the status of all important devices such as switch and relay positions;
- monitor weather data to aid in the correlation of load dependency with weather; and
- control breakers, regulators, and capacitors.

It was also desired that the 13.2-kV distribution feeder systems would

- have load-break switches located at key positions,
- ensure adequate service to critical loads,
- be subdivided into small feeder sections to minimize the extent of service interruptions during emergency conditions,
- be highly instrumented at each of the feeders, and
- have provisions for remote control of load-break switches, power reclosers, voltage regulators, and capacitors.

A load of 2000 kVA between monitoring points during peak load conditions was selected for the placement of monitoring and control equipment.

Figure 2-14 shows the 161/69/13.2-kV substation. Three 161-kV transmission lines from the TVA system are connected to the primary North Athens substation. This substation provides power for six main 13.2-kV distribution feeders and connects 69-kV service to the South Athens and Englewood substations, which were the other substations automated for the AACE.

In addition to the six 13.2-kV feeders emanating from the North Athens substation, three feeders emanate from both the South Athens and Englewood substations, making a total of 12 feeders to be monitored.

Preliminary design phase. After equipment locations were determined, the functions at each automation point were defined. AUB and ORNL jointly developed the functional requirements of each automation point and identified the points to be metered, monitored, and controlled.

The quantity of analog-metering points, status-monitoring points, and momentary/latching relay points determined the size of the substation remote terminal unit. For the North and South Athens substations, a BBC dual-bay type 6200 remote terminal unit was required to monitor and control the stations; at Englewood, a single-bay type 6200 remote terminal unit was sufficient.

Three types of automation equipment were installed on the distribution feeders: a distribution-control receiver for one-way capacitor control; a pole-top remote terminal unit for normal monitoring (up to 12 analog and 12

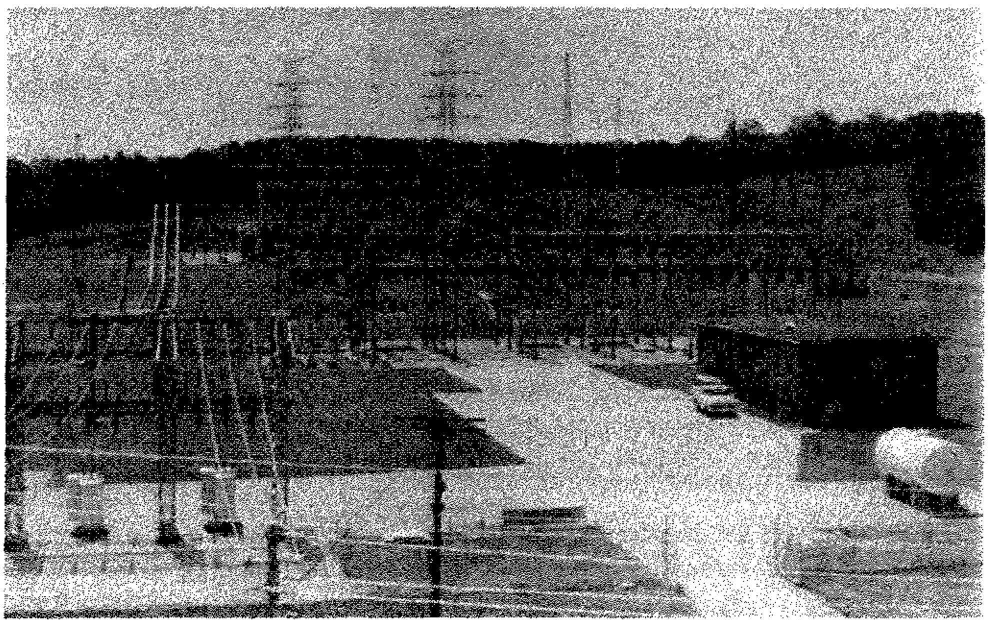

Figure 2-14 Photograph of the 161/69/13.2-kV substation, which supplies Tennessee Valley Authority power to Athens Utilities Board.

status points) and control (4 points); and the BBC type 5000 series distribution remote terminal unit for those times when the number of analog, status, or control points exceeds the capabilities of the pole-top unit. The installation of the control and monitoring equipment on the 13.2-kV distribution poles presented problems because of the quantity of equipment involved and the diversity of connections (i.e., seldom is there a "clean pole" on which a standard equipment configuration can be installed). The conceptual designs for the equipment were originally developed by ORNL and AUB project personnel; however, the preliminary design phase required more detailed drawings, and an architect–engineering company was awarded a contract to prepare a series of standard design drawings. By modifying this set of base designs, AUB then prepared sketches for each individual pole-top installation.

Power input leads from the metering potential and current transformers at the top of the pole, fault detection relays, var controllers, motor operators, voltage regulators, static capacitor oil switches, and the power recloser breakers all terminate in a transducer cabinet. The telephone line used for transmission of data to the CCC and for control signals back to the pole-top equipment is also routed through this cabinet. The telephone line is connected to the phone company's station protector and then to the phone company's network. Dial tone leads are connected to a phone connector in the pole-top unit cabinet. Figure 2-15 is a photograph of a typical installation. A portable transducer calibration unit is used to inject a given voltage and/or current at a controllable phase angle into the transducer input terminals to calibrate the transducers.

Final design phase and installation costs. The final design phase included preparation of the specifications, equipment procurement, and installation drawings of equipment.

Installation costs are summarized in Table 2-5. These costs reflect equipment procured. The equipment cost includes the cost for a motor-operated load-break switch or capacitor bank where appropriate, but it does not include the cost for regulator or recloser equipment. Single-phase or three-phase monitoring is defined to include voltage and real and reactive power unless otherwise noted. Labor time (in worker-hours) is provided in lieu of installation cost because each utility's labor rates may vary.

REFERENCES

1. S. L. Purucker et al., "The Design of an Integrated Distribution Control System," *IEEE Trans. Power Appar. Syst.* **PAS-104**(3), 745–52 (March 1985).
2. S. L. Purucker et al., "Automation and Control of a Distribution Power System," presented at the IEEE Control of Power Systems (COPS) Conference, Oklahoma City, March 20–21, 1984.

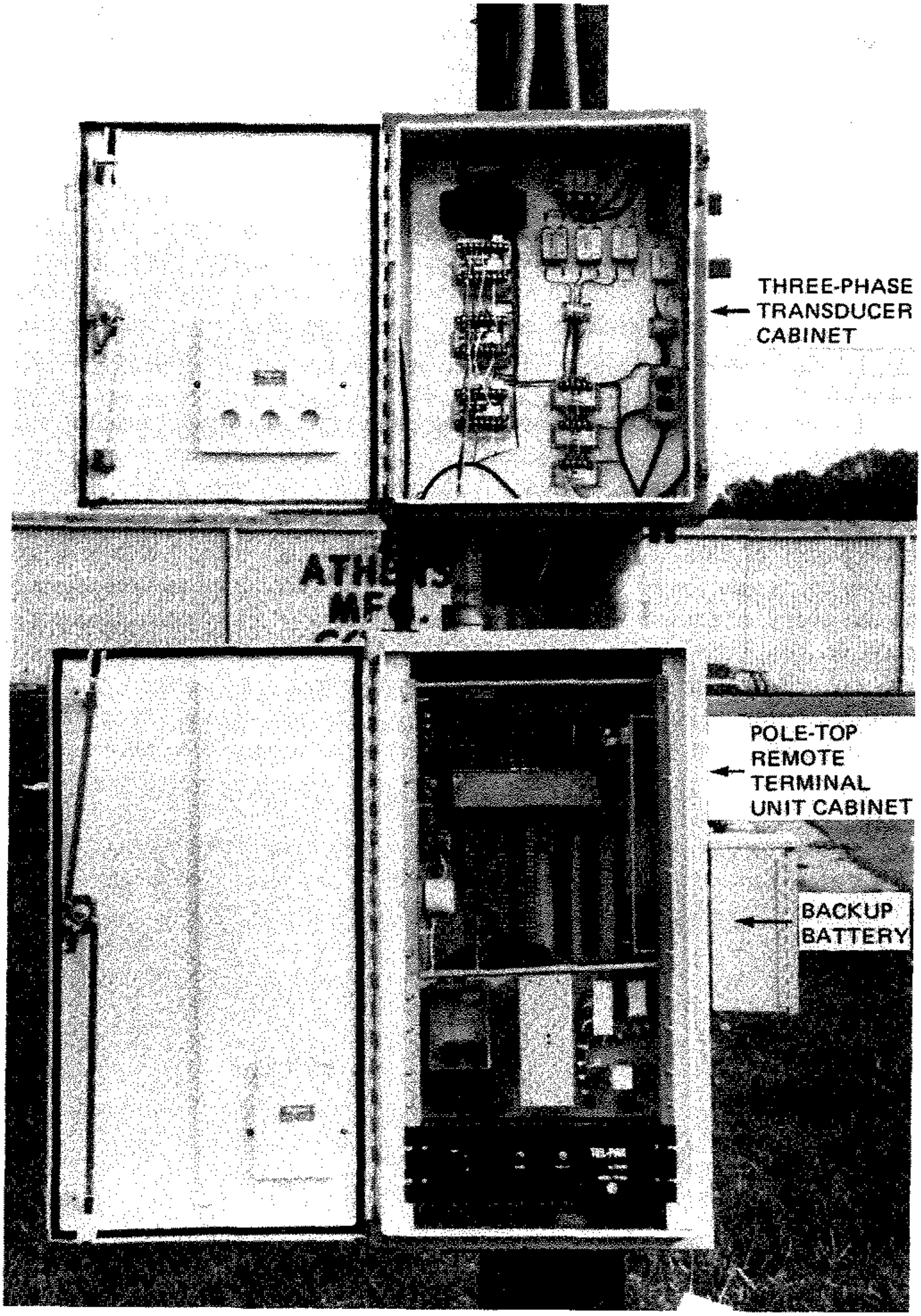

Figure 2-15 Photograph of a metering cabinet and control cabinet for pole-top unit, Athens Automation and Control Experiment.

TABLE 2-5 Athens Utilities Board automation equipment installation summary

Type of installation	Material cost (1986 dollars)[a]	Labor (worker-hours)
Substation (interface equipment only)		
6-feeder substation—North Athens	15,400	815
3-feeder substation—South Athens or Englewood	10,520	590
1 weather station—South Athens substation	13,270	30
Load-break switch		
Switching/status indication	6,500	51
Switching/status indication/1-phase monitoring	8,150	91
Switching/status indication/3-phase monitoring	11,100	153
Capacitor bank (1200 kvar with oil switches)		
One-way distribution control receiver with var controller	4,800	43
One-way distribution control receiver without var controller	3,780	34
Control with pole-top unit and var controller/ 1-phase monitoring	6,760	96
Regulator (not to include regulator)		
Tap control with 3-phase monitoring	2,900	117
Recloser (not to include recloser)		
Switching/status indication	550	46
Switching/status indication/1-phase monitoring	1,600	66
Switching/status indication/3-phase monitoring	3,750	82

[a]The cost of the Brown-Boveri Control Systems, Inc., supervisory control and data acquisition automation equipment is not included in the material costs.

3. B. W. McConnell et al., "Distribution Energy Control Center Experiment," *IEEE Trans. Power Appar. Syst.* **PAS-102**(6), 1582–89 (June 1983).
4. S. L. Purucker, R. J. Thomas, and L. D. Monteen, "Feeder Automation Designs for Installing an Integrated Distribution Control System," Paper No. 85 WM 191-2, presented at the IEEE PES Winter Meeting, New York, Feb. 3–8, 1985; published in *IEEE Trans. Power Appar. Syst.* **PAS-104**(10) (October 1985).
5. S. L. Purucker et al., *Athens Automation and Control Experiment: Substation and Distribution System Automation Designs and Costs,* ORNL/TM-9596, Oak Ridge National Laboratory, June 1986.

3

MONITORING AND CONTROL

D. T. Rizy, E. R. Broadaway, J. S. Lawler, J. H. Reed, and G. R. Wetherington

Monitoring of the distribution system operation during the Athens experiments was crucial to understanding the effects of automated control actions. This chapter describes the monitoring equipment originally installed and the innovations that were necessary during the experiments to allow the effects of the control actions to be fully understood. Also included is a discussion of the equipment that was most helpful to the AUB operators.

Traditionally, utilities have operated distribution systems with minimal monitoring. Normally, power, highest demand, voltage, current, and reactive power are monitored with strip charts or magnetic tape devices. The data normally are not available except when the distribution substation is visited. Gathering and processing of data are limited to the amounts essential for customer billing and maintenance of the system.

The monitoring system provided when the AUB system was automated had a sampling rate of one sample/20 seconds, and this was sufficient for day-to-day operations; however, it lacks sufficient data resolution to determine system changes resulting from automated capacitor control, voltage control, load transfers, and load control. Specialized higher-resolution equipment was required by the experimenters to eliminate from the data the effects of normal load variations. Sampling rates of up to 1000 samples/second were provided by a high-speed acquisition system to obtain the data required for discerning the transient response of automated control actions from the high-frequency "noise" components of the load. This ability to separate normal system dynamics from the effects of control action is important to quantify the benefits of automation, develop control strategies, and verify the effectiveness of the strategies. The higher-resolution systems allow assessment of the effects of control actions within microseconds of the actions. The high-resolution system is unsuitable for day-to-day operation because of the massive amounts of data collected. However, we predict that, in the near future, automation systems will require on-line computer support and that, with the application of artificial intelligence and expert systems, fast data acquisition systems will be used to monitor and control power systems.

Distribution system and load forecasting models offer a possibility of reducing the level of monitoring required. The loads on the AUB system are voltage sensitive and can only be modeled by higher-resolution data. A system model combined with a load forecasting model can be used to determine the suitability of planned control actions and the length of time the control actions are feasible.

MONITORING SYSTEMS USED IN ATHENS

Feeder level monitoring and end-use monitoring were used to gather data on the AUB system. Three monitoring systems were available for monitoring substation and feeder data: (1) the distribution automation and control system (see Chapter 2), (2) a slightly faster monitoring system (see Chapter 8), and (3) a high-speed portable data acquisition system. The high-speed system is described in this chapter.

Two types of end-use monitoring systems were used. The first type was the appliance research metering devices (ARMS), which gather four channels of energy and demand use data on appliances, interior household temperature, and household watt-hour usage. The second type of end use monitoring is the smart meter, which gathers total household energy use. Analog data can be monitored at the rate of 1 sample/20 seconds, and the computer screens in the control room can be updated at this rate. Monitoring and equipment control were placed at 75 locations on the 12 feeders. Communication to the 75 locations is accomplished by dedicated telephone service, powerline carrier outbound and telephone service inbound, or powerline carrier outboard. This system is fully described in Chapter 2.

A higher-speed monitoring system using hardware by Acurex® was used to gather data prior to the installation of the IDCS and was retained since it provided the capability to gather higher resolution data. The remote units are commanded to scan their input channels and to transmit data to a DEC PDP 11/44 computer every 7–10 seconds in one monitoring mode and 5–10 minutes in a slower monitoring mode. The Acurex system is described fully in Chapter 8 under the subheading Data Acquisition.

Analysis of data from the early Athens experiments indicated that the effects of the control actions on the system could not be determined with the installed monitoring systems. Effects of the control actions could not always be separated from normal system dynamics. It was determined that the SCADA systems, which had a sampling rate of one sample/second (or greater), are too slow to measure the short-term or immediate effects of control actions.

High-Speed Data Acquisition System

Control actions for power factor correction produced an increase in system load rather than the predicted decrease in load.[1] To investigate this phenomenon further and to separate the effects of control actions on the system from normal system dynamic changes, a higher-speed data acquisition system was developed. This system was used to monitor and record the system changes resulting from switching capacitors; from voltage control; from cycling of residential water heaters, space heaters and cooling equipment; and from load transfers between feeders. The data obtained by this equipment have been critical in developing a voltage sensitive load model of the AUB system. This load model can accurately predict the system response to the automated control actions. The data from the high-speed acquisition system have been invaluable in understanding the effects of control on the AUB distribution system.

The high-speed data acquisition system is a minicomputer-based system developed for another R&D project at ORNL. The system consists of a Digital Equipment Corporation PDP 11/23 minicomputer with a multiuser operating system, a 30-Mbyte fixed disk drive, a 10-channel 14-bit analog-to-digital (A/D) converter, filters to reduce bandwidth noise, an external trigger to set the sampling rate, software for data acquisition, and posttest graphic analysis and cabling (Figure 3-1). The cabling connects the system to watt, var, and voltage transducers mounted in the substation or at a remote installation on the feeder. The system is portable and features ten differential input signal channels with a data scan rate that can be set from 250 to 10,000 samples/second aggregate or 25 to 1000 samples per channel. The system is capable of recording 5 million samples (nearly 6 hours of data at the slowest sampling rate and slightly greater than 8 minutes of data at the fastest sampling rate).

After a test is completed, the data are transferred from the fixed disk directly to another minicomputer for archival storage and via magnetic tape to a mainframe computer for analysis. Graphics programs that permit multiple channels on a single plot provide field analysis capability. Typically, measurements are taken for voltage (kV), real power (kW), and reactive power (kvar) for individual phases and for all three phases simultaneously.

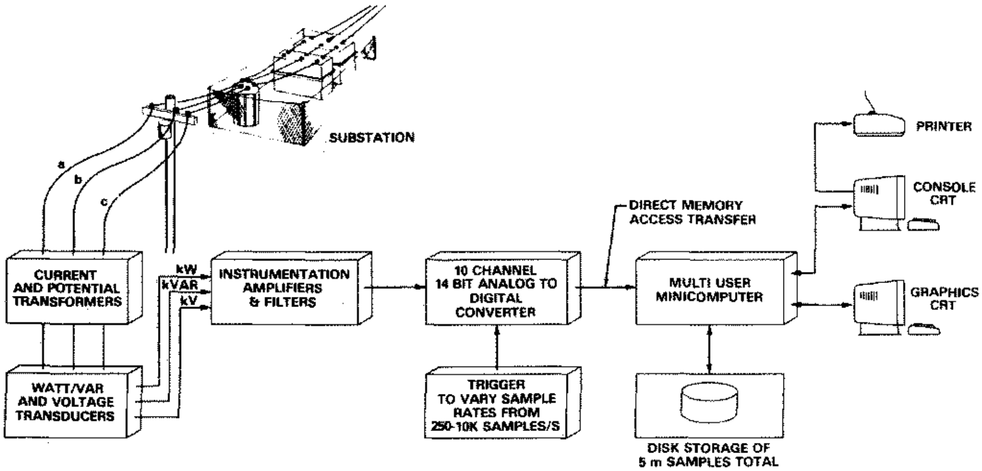

Figure 3-1 Schematic diagram of high-speed data acquisition system developed to determine the effects of control actions on the AUB system.

The system may be transported to the test site by a van or truck. Installation and wiring connections can be completed in about 1 hour. The signal inputs at the feeder are attached using quick-disconnect "clip leads," which connect to the existing voltage, watt, and var transducers at the substation circuit breakers. The monitored signals are prefiltered using 10-μF capacitors connected in parallel with the input signal from the transducers. Standard 50-Ω coaxial cables (RG 58) are used to connect the transducer cabinets to a minicomputer, and each input signal is conditioned through a low-pass filter with a 10-Hz cutoff frequency to reduce signal noise. Inputs to the filters are differential inputs, thus increasing common-mode rejection, a feature especially important in the noisy environment of an electrical power distribution substation.

The outputs from the filters are connected to the inputs of the A/D converter. The data rate is set using an external triggering device connected to the converter, and an oscilloscope is used to monitor adjustments to the trigger rate.

Data Resolution

The effect of the data resolution or sampling rate on system response to a switching action is described in detail in Chapters 4, 5, and 6. The high-speed system enabled the experimenters to easily evaluate the effects of control actions. By monitoring the switching tests with a resolution of 1000 samples/second, the natural variation in system load can be assumed to be constant. The high-speed data system also allowed the analyst to develop an accurate load control model that can be used to predict the effects of control actions. A method of detecting appliance starts within the high speed data has been developed. The real-time information may be used by the system operator to make decisions about load control actions.[2] A photograph of the high-speed data acquisition system is shown in Figure 3-2.

A large quantity of data is generated when using a high-speed data acquisition system. The Athens equipment is not designed to provide information from a high-speed system in real time. It is not practical to install permanent high-speed systems at all the Athens substations to monitor load control; the portable systems are used only to verify control actions.

A comparison of the data resolution of the three monitoring systems (slow, intermediate, and high speed) is shown in Figures 3-3, 3-4, and 3-5. The data plots in the figures were created from actual data acquired from the high-speed data acquisition system at 1000 samples/second. No control actions were taken during this 260-minute period; hence, the data plotted show normal system dynamic changes.

In Figure 3-3, only readings 20 seconds apart are plotted. As Figure 3-3 indicates, differences in real power due to a control action of less than ± 25 kW cannot be easily detected when the data at 20-second intervals are plotted. (Differences in reactive power less than ± 10 kVar and bus voltages

Figure 3-2 High-speed data acquisition system used for determining the effects of control actions on the feeders. The equipment was temporarily connected to feeder sensors in the substation to determine these effects.

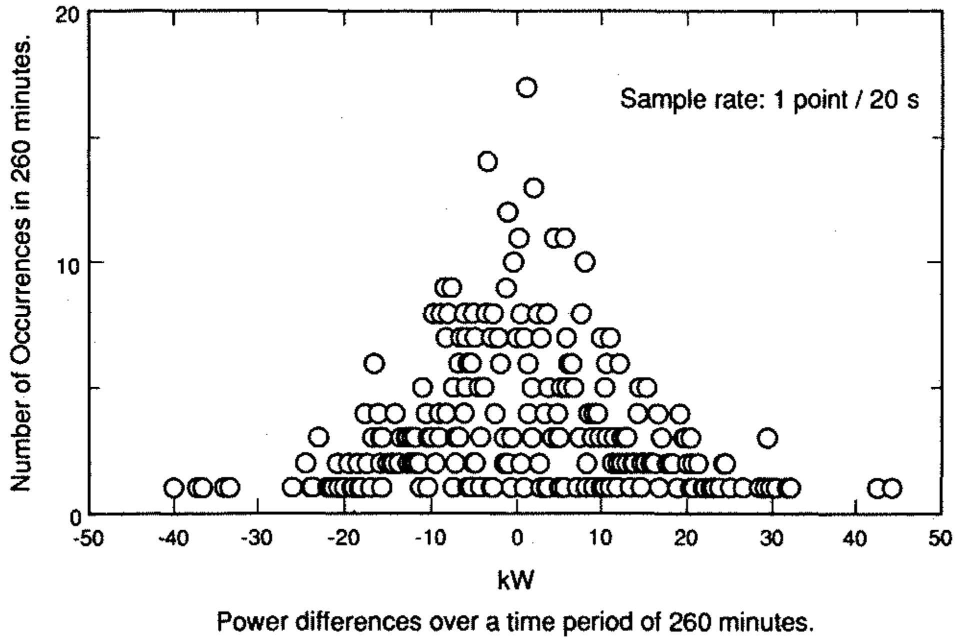

Figure 3-3 Data resolution of a monitoring system which collects data at 1 sample every 20 seconds.

less than ± 0.02 kV would also be masked.) Figure 3-4 shows the same data plotted at a higher speed of seven samples/second. The plot has slightly better resolution, and power changes that are greater than 20 kW over a 7-second time interval can be detected. This level of load change due to a control action would not be masked by the normal load fluctuations. A significant improvement in data resolution is achieved when data are plotted at a higher speed (see Figure 3-5). The resolution for data plotted at 1 sample/second, 10 samples/second and 50 samples/second are shown. The data taken at higher speeds increase the resolution from ± 10 kW for a 1-point/second sampling rate, to ± 5 kW for a 10-point/second sampling rate, and finally to ± 2.5 kW for a 50-sample/second sampling rate. In most cases, it probably is not necessary to monitor at sample rates higher than 10 samples/second to measure system perturbations. Figure 3-6 shows the level of resolution for a sampling rate of 1 point/second for reactive power measurements. Figure 3-7 indicates that the normal changes in bus voltage are on the order of ± 0.02 kV. This is the same value obtained when data were plotted at 20-second intervals and shows that little improvement is achieved for monitoring bus voltage at a sampling rate higher than 1 sample/20 seconds.

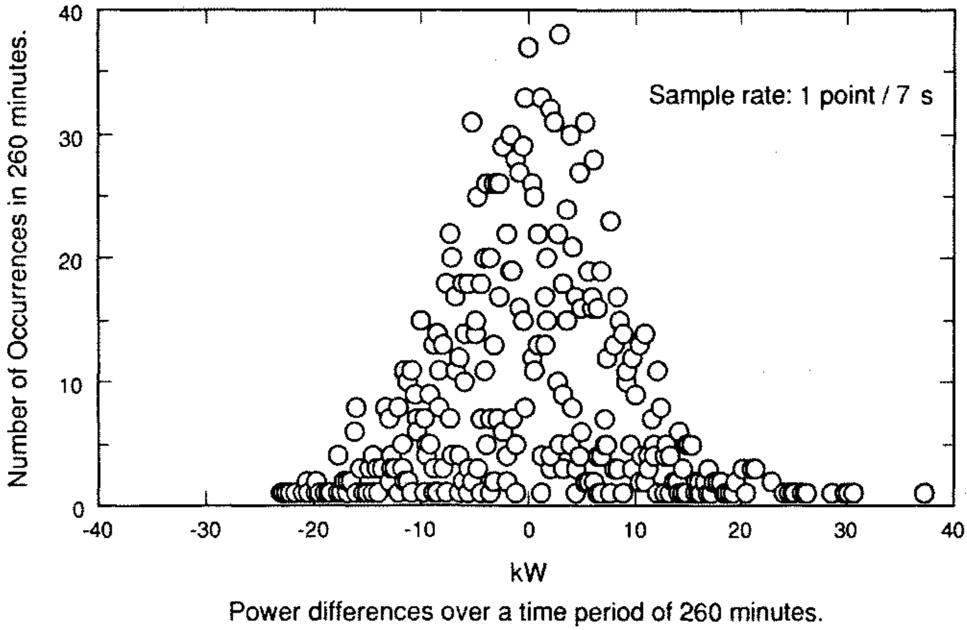

Figure 3-4 Data resolution of a monitoring system which collects data at 1 sample every 7 seconds.

AUB OPERATIONS

AUB has been operating the newly automated system since January 1985. The system was initially instrumented to give extensive substation monitoring and control, feeder monitoring and control, and fault-sensing abilities. AUB is gradually eliminating monitoring and control points not necessary for day-to-day operations. The automated system has been used by AUB personnel primarily to determine equipment failure, for capacitor dispatch, for voltage control, for fault location and isolation, for load transfers, and for load control. The system has provided some unexpected benefits as discussed below.

The objective of the originally installed monitoring system was to measure at least three system parameters at each monitoring location and to calculate the remaining parameters. AUB has found the use of three watt/var and three voltage transducers to be less costly than the use of three current, voltage, and phase angle transducers.

Before automating the system, billing information was used to determine which phase should receive new load. The effect of new loads was checked by weekly readings of substation strip charts. Now the continuous monitoring of

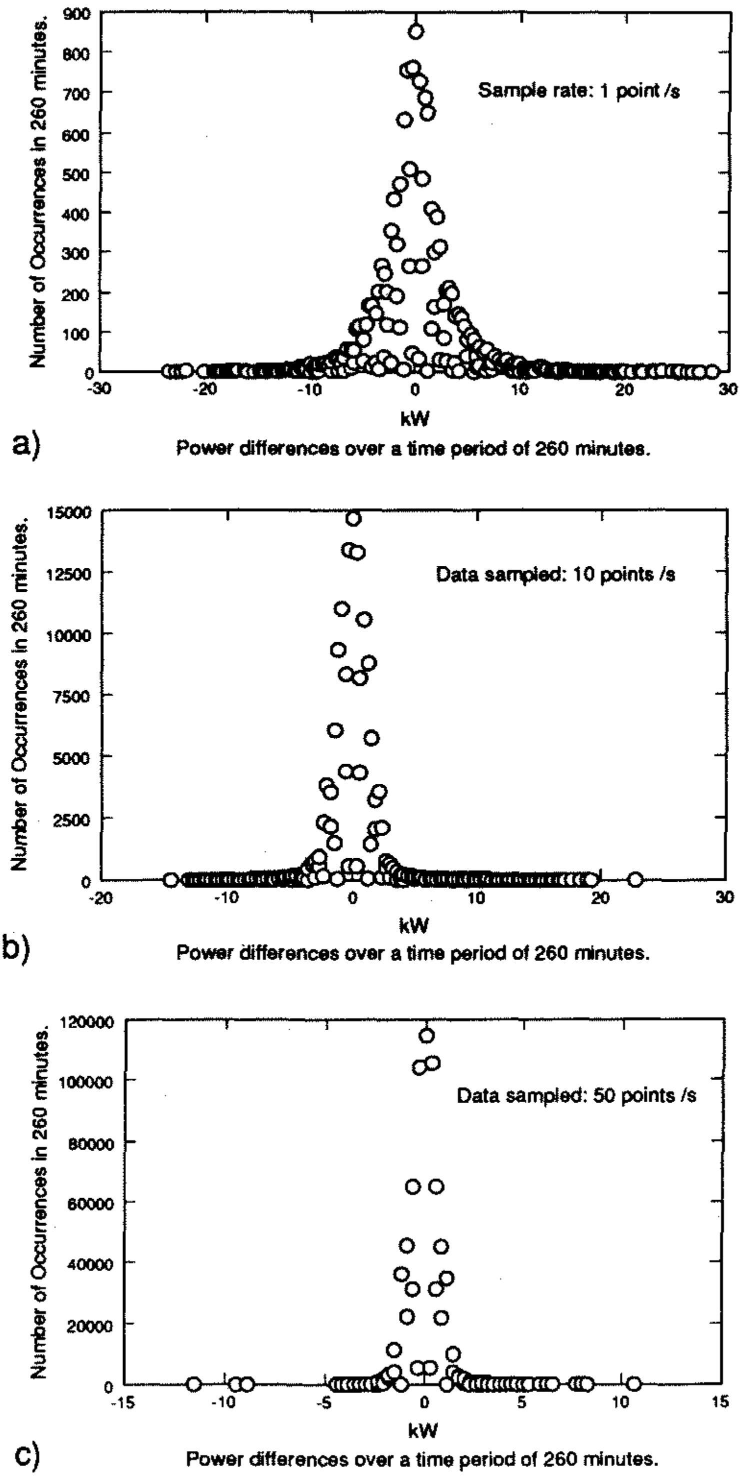

Figure 3-5 Data resolution of the Athens high-speed data acquisition system.

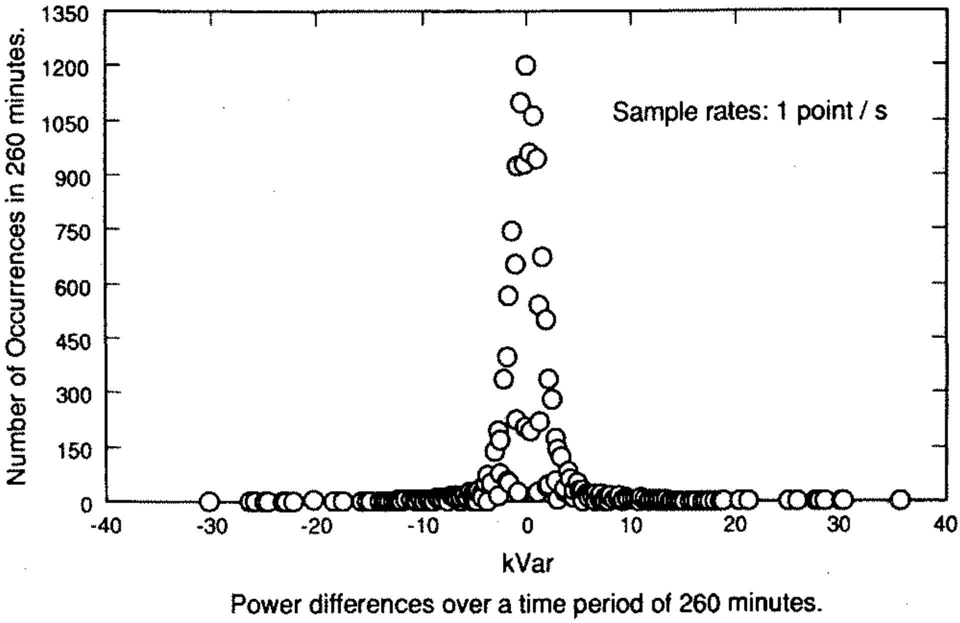

Figure 3-6 Data resolution for reactive power readings plotted at 1 sample per second.

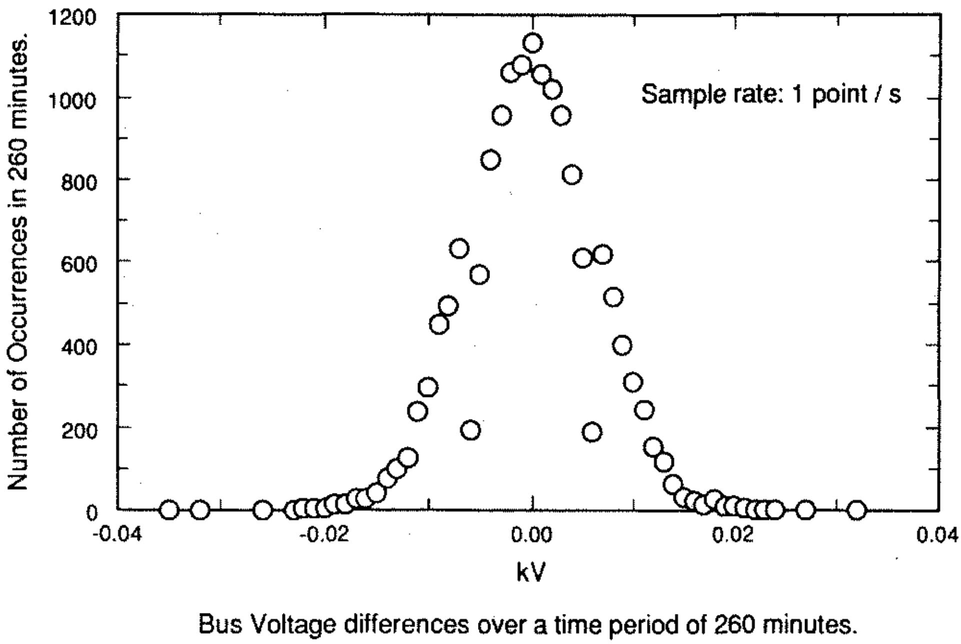

Figure 3-7 Data resolution for bus voltage readings plotted at 1 sample per second.

real and reactive power flow and voltage and the calculation of single-phase current allow a continual check on load balance of each circuit. A determination can now be made as to which phase should receive new load to maintain a balanced system.

Continuous intermediate feeder monitoring and transmission of data to the central control room allow AUB to determine the section of a feeder on which load growth is occurring. The monitoring system can show startup currents and the trend (increase or decrease) in base current. AUB has determined that remotely controlling in-line and intertie switches that do not have fault sensors is unnecessary. Outages are detected by the automation system, but some cannot be corrected from the control room. AUB uses a data base to correlate customer phone calls with switch locations and compares trouble calls from customers to determine the location and type of fault.

Voltage monitoring has been important during reduced loading conditions, especially when capacitors are switched in. Before automating the system, only a few fixed-capacitor banks were available. The new monitoring system has identified new locations for capacitor banks, a particularly important accomplishment because TVA has imposed a cost penalty if power factor on the AUB system is not held within close tolerances.

Since the start of the experiment, AUB has more than doubled the number of capacitor banks. Before the system was automated, 12 banks were controlled by time clocks with a mechanical timer and by voltage control with high and low set limits. Eleven new capacitor banks have been installed for var control.

A change in reactive power injection when a capacitor bank is closed or opened is easily detected by the substation monitoring system. Substation monitoring confirms that the capacitors at a remote site have been switched. Single-phase monitoring on feeders has little value other than to provide voltage measurement at the end of the feeders; as a result, AUB has removed all phone lines to the single-phase monitoring points.

The load relief achieved by turning off appliances cannot be accurately monitored using the slow-speed monitoring equipment on the feeders. The number of appliances dropped at one time may be small, and the natural variation in demand on a feeder between readings may mask the true amount of relief. Therefore, accurate determination of the magnitude of load change due to switching out loads is difficult with standard monitoring equipment. High-speed monitoring equipment allows accurate determination of the amount of load dropped and restored. Figures 6-42, 6-43, and 6-45 illustrate how the response of the system to a load control action can be tracked with high-speed monitoring. Monitoring equipment with a sampling rate of five samples/second is fast enough to track load control events.

Automated system reconfiguration operations normally performed on the AUB involve only load transfers from a faulted feeder to a supporting feeder to isolate a fault or from an overloaded circuit to relieve the overload condition. If the overload condition occurs on a frequent basis, a permanent reconfiguration of the circuit is performed. Automated system reconfiguration is not used by AUB to reduce peak feeder loads or to reduce feeder losses for the reasons described in Chapter 4, even though the monitoring and control functions do exist. Analysis (see Chapter 4) indicates that the automation system at AUB will not decrease losses and peak loading because (1) AUB is a relatively small system and the diurnal cycles of the loads on the 12 feeders are similar, (2) the AUB feeders are "telescoped"* so that any deviation from the nominal feeder configuration will increase the impedance between source and load, and (3) automated switches installed at AUB are only sufficient to sectionalize feeders into three or four zones involving 25% to 33% of the feeder load per zone. Frequent automated system reconfiguration operations will require an on-line assessment of the automated operation prior to its implementation and an assessment of how long the feeders can be reconfigured. The substation monitoring of the voltage and power flow injections of the AUB feeders and the monitoring of automated in-line and intertie switches on the AUB system along with the SYSRAP Program are capable of this decision making.[3] Determining the length of time the feeders can be reconfigured requires the incorporation of a load forecasting model into the SYSRAP program. However, because analysis indicates that frequent reconfigurations will not decrease losses or peak loading on the AUB system, the operators do not need to use the program on a regular basis.

MONITORING VERSUS MODELING

Simulation programs that model the performance of the system under proposed control actions can be used to reduce the number of monitoring stations required for an automated system. A simulation program, SYSRAP (see Chapter 8), was developed to predict the effects of a proposed control action.[3] This program includes a voltage-sensitive load model that uses data gathered at the substation and a knowledge of the distribution of load. The model assumes that all loads on the feeder are voltage sensitive and that there is no diversity between feeder loads. The program was validated by actual data taken during the control actions. Analysis of the data can show which monitoring points should be eliminated.

The substation data containing (real and reactive) power and voltage are necessary to determine the effects of control actions on the system. This information combined with aggregate information of the customer's loads is normally enough to determine the effects of control actions; however,

*Large conductor sizes are installed close to the substations with wire sizes decreasing toward the end of the feeder.

monitoring at intertie switch locations can give more detailed information about feeder behavior.

There are two basic approaches to modeling load control actions. The first is to build a table based on previously monitored control actions that estimates the impact of a control action. For space-conditioning appliances, the table might include outdoor temperature, intensity of control, and the estimated load relief per unit controlled. Because water heating demand is seasonal and more behaviorally driven, a water-heating table might include season, length of control action, time of day, and estimated relief per unit controlled.

A more sophisticated approach is to develop computer-based models that use monitoring information either on or off line to update the models. These models use the same data as the tabular approach, in addition to other information. Sophisticated models for estimating the impacts of space-conditioning control are based on duty cycle and/or thermal time constants.

Both methods of modeling the impacts of control share some common problems. The most fundamental of these is that the phenomenon being modeled is constantly changing. In Athens, the use of space-cooling appliances is increasing, the efficiency of replacement installations is increasing, and the demographics of the population and the associated usage patterns are changing. This means that the accuracy of any model will decline through time. Some utilities have reported large fluctuations in load relief from year to year in response to system changes made over time and to changes in the reliability of the control equipment.

The system operator needs to know the available controllable load. However, the current state of the art does not lend itself to real-time monitoring, prediction, and control. Thus, whole-household and end-use monitoring are used to evaluate the impact of control after the fact and to construct and update models to predict the impacts of control. The use of high-speed monitoring holds promise for implementing real-time control in the future.

SUMMARY

Automation of electric distribution systems necessitates a higher resolution of monitoring of power flow, voltage, and equipment status than is normally used on distribution systems. When a system is operated near its capacity, load transfers in particular may need to be assessed before implementation to avoid overloading of conductors and loss of critical loads. A system can be designed to monitor every remotely and manually controlled capacitor, regulator, in-line and tie switch, and circuit breaker to give a real-time power flow to the electric system every 20 seconds; however, a simulation program that models the performance of the system for automated control functions can eliminate the necessity for many feeder monitoring points. In addition, a load prediction model can be designed for a distribution system that can be used to determine the impacts of volt/var control, load control, and system reconfiguration control actions before they are implemented.

The original instrumentation installed when the Athens system was automated is sufficient for the day-to-day operation of the electric system. The data resolution of the equipment provides the ability to monitor power and voltage changes due to capacitor switching, voltage changes due to voltage control, and voltage and power flow changes due to load transfers. However, the data resolution is insufficient for determining load changes due to load control and real power changes due to capacitor switching. Further, the resolution is insufficient for measuring switching transients due to load transfers that can momentarily overload conductors. Application of a high-speed data acquisition system was necessary to measure switching transients associated with load transfers and to determine the load sensitivity to voltage for model development.

REFERENCES

1. D. T. Rizy, J. S. Lawler, J. B. Patton, and W. R. Nelson, "Measuring and Analyzing the Impact of Voltage and Capacitor Control with High Speed Data Acquisition," IEEE Paper No. 88 WM 098-6, presented at the IEEE PES Winter Meeting, New York, February 1988; published in *IEEE Trans. Power Delivery,* 4(1), 704–14 (January 1989).
2. J. H. Reed, W. R. Nelson, G. R. Wetherington, and E. R. Broadaway, "Monitoring Load Control at the Feeder Level Using High-Speed Monitoring Equipment," IEEE Paper No. 88 WM 095-2, presented at the IEEE PES Winter Meeting, New York, February 1988; published in *IEEE Trans. Power Delivery,* 4(1), 694–703 (January 1989).
3. J. B. Patton, D. T. Rizy, and J. S. Lawler, "Applications Software for Modeling Distribution Automation operations on the Athens Utilities Board," IEEE Paper No. 89 TD 424-3 PWRD, presented at IEEE Transmission and Distribution Exposition, New Orleans, April 1989.

4

SYSTEM RECONFIGURATION EXPERIMENT*

J. S. Lawler, D. T. Rizy, J. P. Stovall, J. B. Patton, L. D. Monteen, and J. S. Lai

This chapter discusses the results of the system reconfiguration experiments. Automatic switching experiments were performed and analyses were conducted to determine the increase in reliability that could be attributed to the automated system. Also, switching experiments were conducted to determine whether automatic switching could enhance utilization of existing system capacity. Other benefits of automating the AUB Athens Utilities Board (AUB) system are also discussed.

Analytical studies show the improvement in conventional distribution system reliability indices that was achieved at AUB as a result of automation. Operating experience shows that significant intangible benefits and tangible cost benefits associated with automation are outside the scope of conventional reliability indices. Case studies of AUB operations that resulted in significant cost savings and increased reliability are presented. While these specific benefits may not be applicable to other utilities, similar benefits specific to individual utilities should be realized. These benefits, which may be difficult to quantify, add to the value of and the justification for distribution automation.

---

*This chapter is based on material in IEEE Paper No. 88 WM 087-9, "Impact of Automation on the Reliability of the Athens Utilities Board's Distribution System," by J. S. Lawler, J. S. Lai, L. D. Monteen, J. B. Patton, and D. T. Rizy, which was first presented at the IEEE Power Engineering Society Winter Meeting, February 1988, New York (copyright 1988 by the IEEE).

The impact of automation on capacity utilization for AUB was studied. The potential improvements in capacity utilization effected by automation are system loss reduction and peak load reduction. The benefits to Athens in these areas were less than anticipated because of the AUB system characteristics. These characteristics, which precluded an enhancement of capacity utilization or a reduction of system losses, are discussed to help other utilities evaluate the potential benefits of automation to their systems.

INCREASE IN RELIABILITY ON THE AUB SYSTEM

SCADA and telephone communications provide substation monitoring and control at the 3 AUB substations, while remote terminal units, power line carriers, and telephone communication provide feeder monitoring and equipment control on the 12 feeders. Automation equipment that is particularly relevant to enhancing system reliability includes substation and feeder monitoring, 12 feeder circuit breakers, 12 power reclosers, 35 load break switches, and 21 fault detectors.

Automated fault detectors combined with remote control of distribution circuit breakers, power reclosers, and load break switches can (1) significantly reduce the time required to detect and locate faults, (2) increase the speed of isolating faulted equipment, and (3) provide faster load restoration above and below a faulted feeder zone. These benefits of automation can be quantified using historical records and conventional reliability assessment tools such as the Predictive Reliability Assessment Model (PRAM) computer code developed by EPRI.[1] This chapter discusses the use of PRAM to study the improvement in reliability at AUB as a function of the number of automated switches installed on a feeder. The value of automation is heavily dependent on the historical outage data used to establish component failure rates and on the value of economic worth assigned to reliability.

AUB has documented many instances in which automation has increased system reliability and provided substantial cost savings that seem to fall outside of the standard indices that normally reflect system reliability. AUB has prevented outages or greatly reduced the outage area and number of customers affected, provided cost savings through automation system use during daily and routine events (that were previously performed manually), improved system safety, and detected failing equipment before catastrophic equipment failure and subsequent outage. These improvements have provided substantial economic benefits. While each case study reflects a unique set of circumstances and is perhaps peculiar to AUB, it is highly likely that AUB and other utilities will receive similar benefits on a continuing basis from automated operations.

Based on the experience with AUB's automated system, we conclude that the value of automation in improving system reliability is understated if the value is determined solely from conventional distribution reliability assessment indices. Many engineers and department supervisors have supported distribution automation concepts but have been unable to provide sufficient data to convince their managers to invest in an automated system. The added benefits attained at AUB may help to convince utility management of the advantages of distribution automation.

Analytical Reliability Studies

To quantify the effect of automated switching capability on reliability on the AUB distribution system, the PRAM computer program was used to calculate three industry-recognized reliability indices. Because automation costs were well known on the Athens system,[2] the cost of incremental improved reliability associated with various automation equipment was of interest.

Using the explicit perfect protection feature in PRAM (where the protection system always functions properly), it was possible to quantify the effects of feeder protection coordination and alternative remotely controlled feeder supplies (interties) on feeder reliability. Three feeders on AUB's South Athens Substation were analyzed: circuit 7 (SA-7), circuit 8 (SA-8) and circuit 9 (SA-9). One-line diagrams of these feeders and some of the other circuit information needed as input to PRAM are given in Figures 4-1 through 4-3. SA-7 serves a mixture of residential, commercial, and industrial users; SA-8 is composed primarily of residential loads and has the longest lines, the most individual customers, and the least load; and SA-9 serves mostly industrial and commercial customers and has the fewest number of customers and the highest load.

Reliability indices. PRAM calculated the load-point reliability at each load on the Athens feeders by combining a structural description of the AUB distribution feeders with remotely controlled and manual switch-operating times, line-related failure frequency data, and customer interruption duration data. The calculated load point results are combined by PRAM to determine three reliability indices for each feeder:

- System Average Interruption Frequency Index

$$\text{SAIFI} = \frac{\text{total number of customer interruptions}}{\text{total number of customers served}},$$

- System Average Interruption Duration Index

$$\text{SAIDI} = \frac{\text{sum of customer interruption durations}}{\text{total number of customers}}, \text{ and}$$

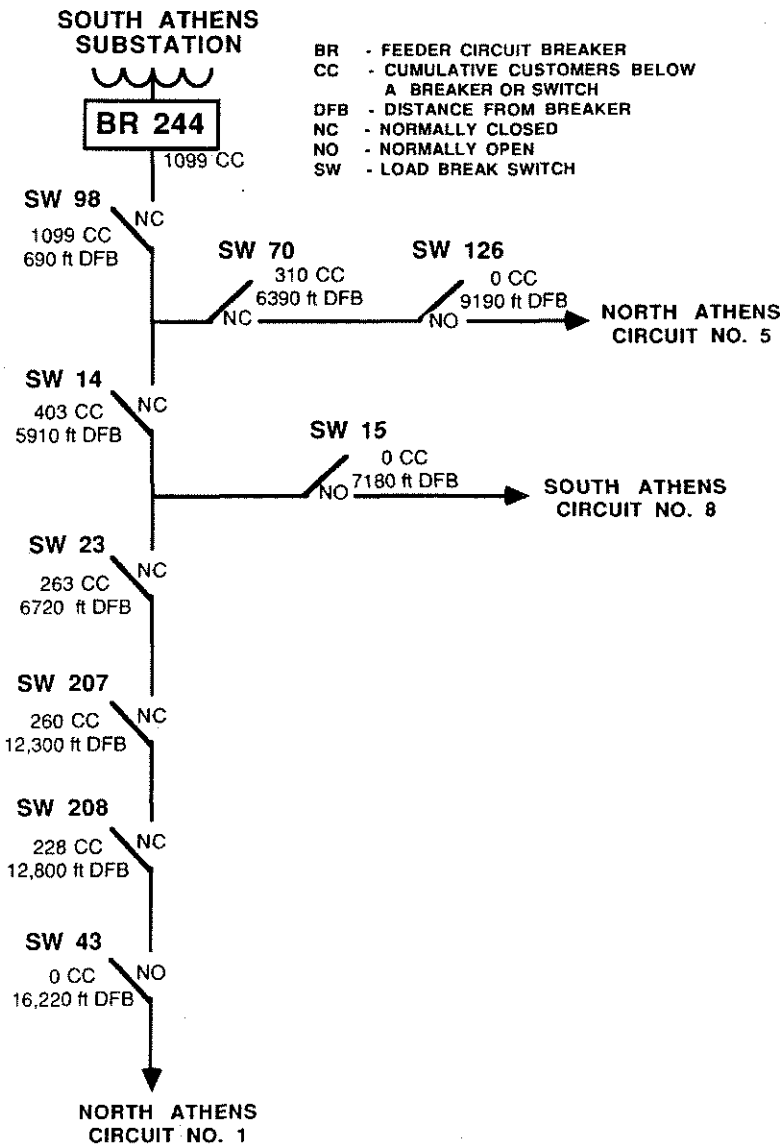

Figure 4-1 One-line diagram of SA-7 (copyright 1988 by the IEEE).

- Customer Average Interruption Duration Index

$$\text{CAIDI} = \frac{\text{sum of customer interruption durations}}{\text{total number of customer interruptions}}.$$

SAIDI and CAIDI are highly sensitive to the switching time required to sectionalize a feeder and restore service after a fault; and implementing remotely controlled switches instead of manual switches results in an improvement in reliability measures. SAIFI is a measure of the number of outages and is not affected by the amount of automation equipment.

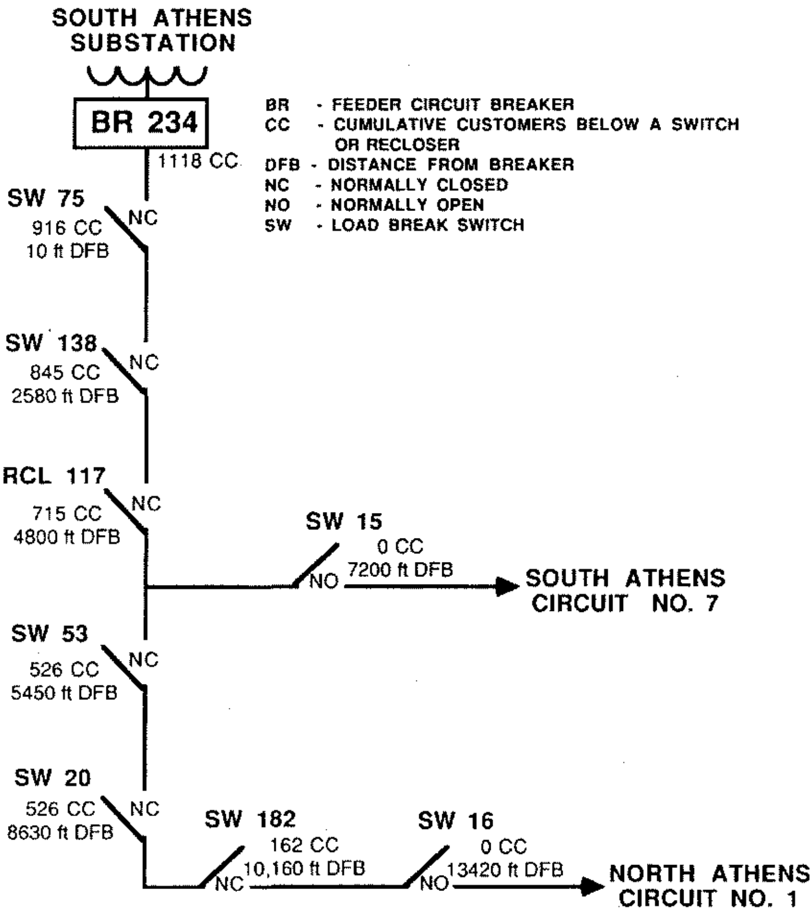

Figure 4-2 One-line diagram of SA-8 (copyright 1988 by the IEEE).

Input data description. Trouble service summaries for 1 year were examined to analyze the three South Athens feeders. The total number of primary circuit outages on all AUB feeders was determined, and the number was averaged over the total circuit miles to obtain a primary circuit failure frequency. This frequency was calculated to be 1.53 failures/(year·mile). This failure rate was assumed to be uniform on the three feeders used for the study. No attempt was made to account for weather, and minor outages caused by transformer fuse openings or secondary faults were not counted. Only the effects of automation on primary line reliability were of interest.

During the course of the Athens experiments, it was observed that restoring service using the automation equipment took an average of 3 minutes, while manual switching requires approximately 20 minutes. Line repair takes approximately 45 minutes for all but the most severe failures.

Study scenarios and PRAM results. Four to five automation scenarios were studied for each feeder. In general, the base case (scenario 1) uses all

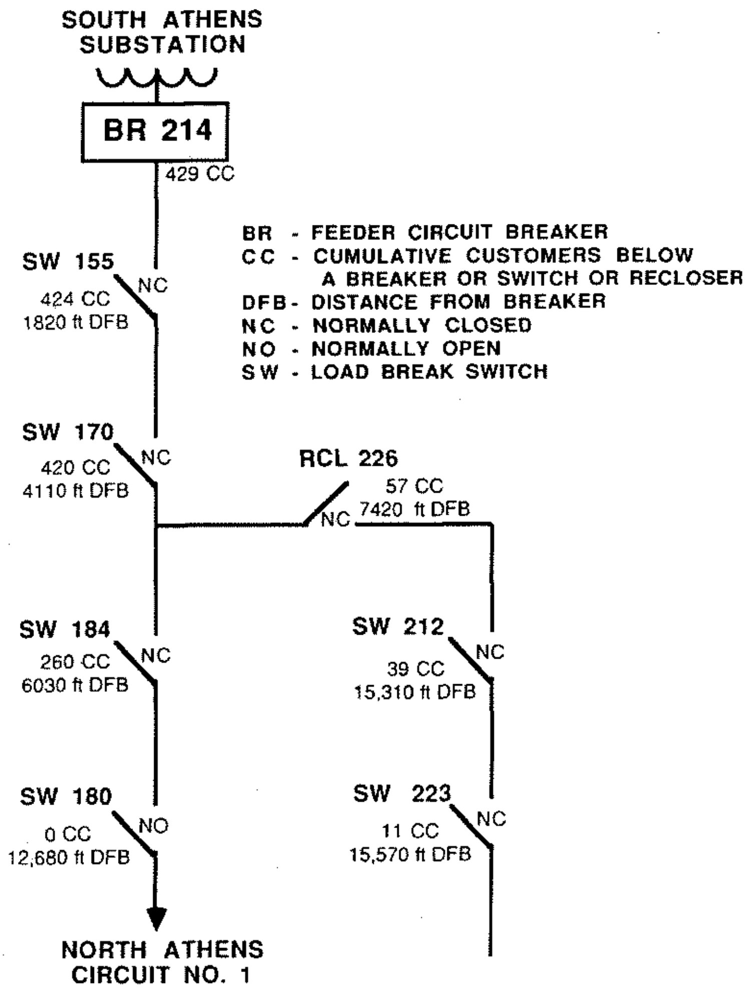

Figure 4-3 One-line diagram of SA-9 (copyright 1988 by the IEEE).

the protection equipment and switches shown on the feeder one-line diagrams. They were operated in a purely manual mode, and all switching times are set to 20 minutes. The second scenario is to automate the feeder breaker such that it can be remotely reclosed after line repair. This is accomplished in PRAM by setting the breaker switching time to 3 minutes. Subsequent scenarios involve automating a switch pair consisting of one in-line switch and one tie switch. Such a switch pair will allow the feeder to be sectionalized (by opening the in-line switch), and a portion of the feeder can be transferred to another feeder to restore load by closing the tie. PRAM assumes that any tie switch can support the load that might be connected to it. As with the feeder breaker, the automation of the switch pair is simulated in PRAM by changing the operating time from 20 minutes to 3 minutes. Additional switch pairs are automated until the design configuration of the feeder is reached. Typically, each feeder can be remotely sectionalized into 3 or 4 zones.

The specific automation penetration scenarios for feeder SA-7 are as follows:

1. base case, no automation;
2. automate the feeder breaker BR244;
3. automate BR244 and switch pair SW14 and SW43 (two zones);
4. automate BR244, SW14, SW43, SW70, and SW126 (three zones);
5. automate BR244, SW14, SW43, SW70, SW126, SW207, and SW15 (four zones).

Four automation cases are defined for feeder SA-8:

1. no automation;
2. automate BR234;
3. automate BR234, recloser RCL117, and SW16 (two zones);
4. automate BR234, RCL117, SW16, SW20, and SW15 (three zones).

Finally, the cases studied for feeder SA-9 are as follows:

1. no automation;
2. automate BR214;
3. automate BR214, SW170, and SW180 (two zones);
4. automate BR214, SW170, SW180, and RCL226 (three zones).

For each feeder and automation case, four combinations of manual switching time and line failure rate were investigated with PRAM. These combinations are as follows:

A. 20 minutes, 1.53 failures/(year·mile) (the nominal values);
B. 40 minutes, 1.53 failures/(year·mile) (high switching time);
C. 20 minutes, 0.765 failure/(year·mile) (low failure rate);
D. 20 minutes, 3.06 failures/(year·mile) (high failure rate).

The reliability calculations are contained in Figures 4-4 through 4-6 for feeders SA-7, SA-8, and SA-9, respectively. The figures confirm the expected improvement in system reliability resulting from automation. All of the indices monotonically improve as additional automation equipment is added and tend to remain constant when one automated in-line switch and one automated tie switch on each major branch of the feeder are added. The flattening of the curves in Figures 4-1 through 4-6 suggests that a point of diminishing returns is reached when the addition of another automated switch provides little benefit.

Three factors are required to conduct a cost/benefit analysis of the impact of automation on distribution system reliability: the cost of automation equipment, the quantified improvement in reliability through

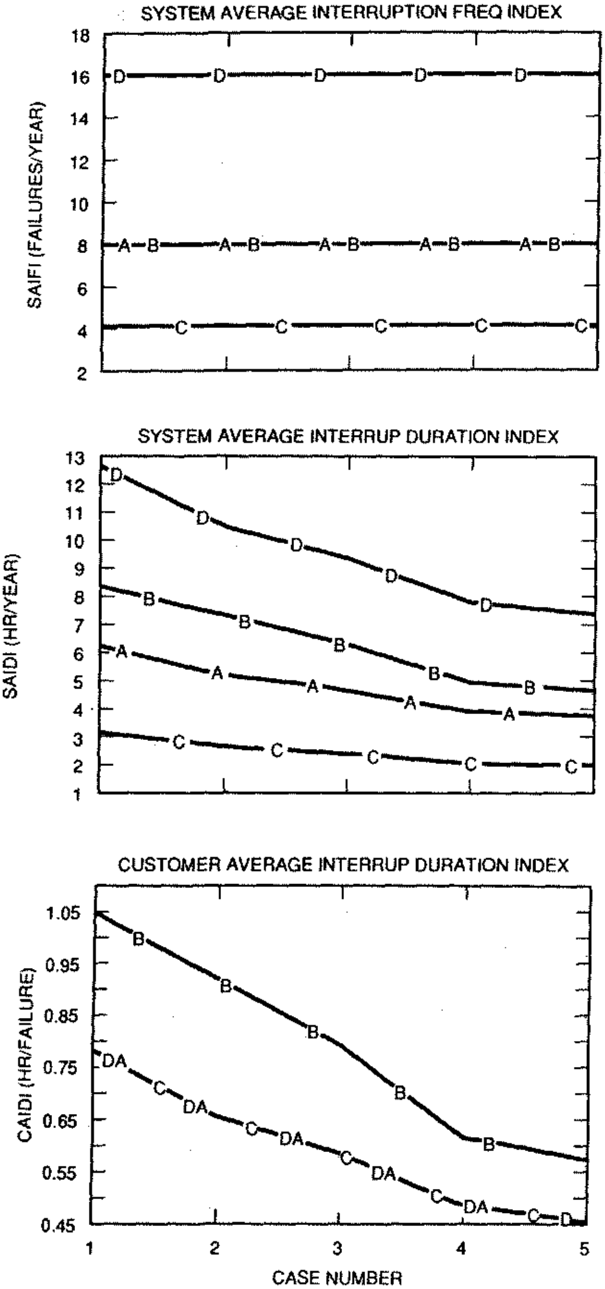

Figure 4-4 Reliability assessment of SA-7 for increasing levels of automation (copyright 1988 by the IEEE).

Case A. 20 minutes, 1.53 failures/(year·mile) (the nominal values);
Case B. 40 minutes, 1.53 failures/(year·mile) (high switching time);
Case C. 20 minutes, 0.765 failure/(year·mile) (low failure rate);
Case D. 20 minutes, 3.06 failures/(year·mile) (high failure rate).

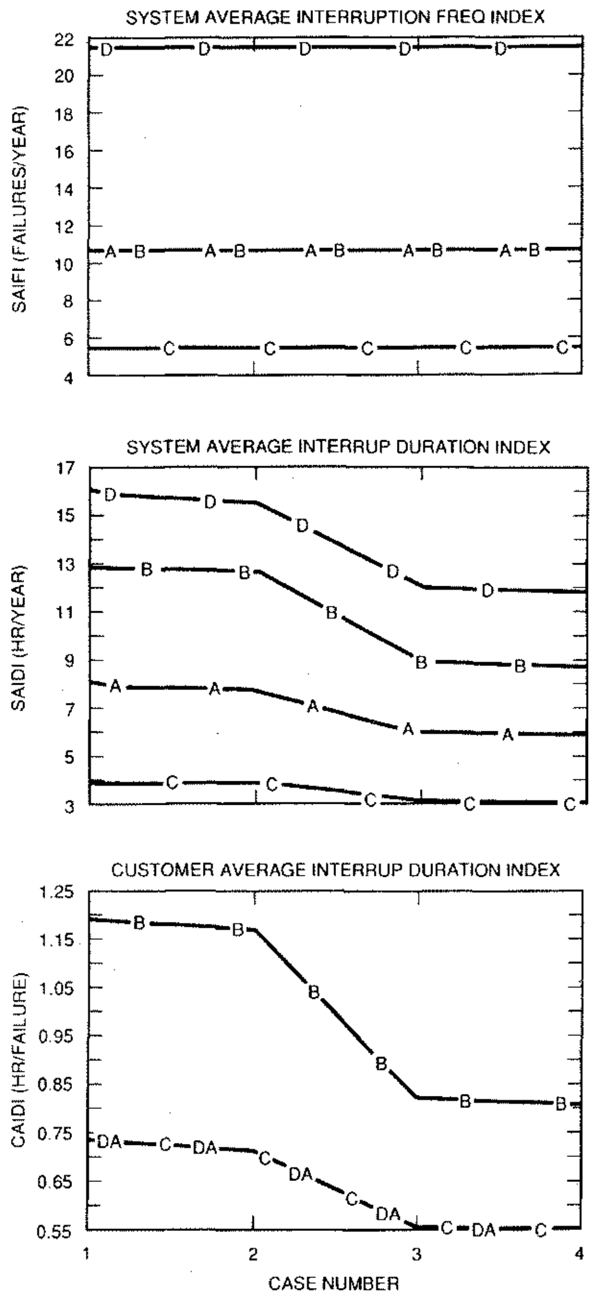

Figure 4-5 Reliability assessment of SA-8 for increasing levels of automation (copyright 1988 by the IEEE).

Case A. 20 minutes, 1.53 failures/(year·mile) (the nominal values);
Case B. 40 minutes, 1.53 failures/(year·mile) (high switching time);
Case C. 20 minutes, 0.765 failure/(year·mile) (low failure rate);
Case D. 20 minutes, 3.06 failures/(year·mile) (high failure rate).

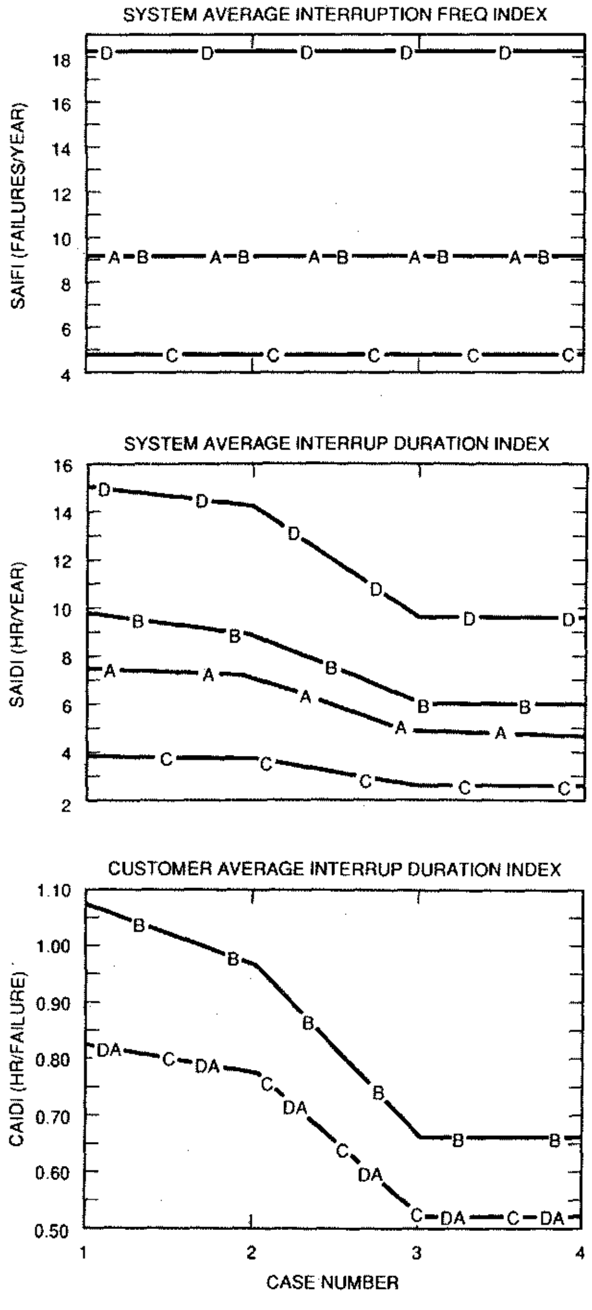

Figure 4-6 Reliability assessment of SA-9 for increasing levels of automation (copyright 1988 by the IEEE).

Case A. 20 minutes, 1.53 failures/(year·mile) (the nominal values);
Case B. 40 minutes, 1.53 failures/(year·mile) (high switching time);
Case C. 20 minutes, 0.765 failure/(year·mile) (low failure rate);
Case D. 20 minutes, 3.06 failures/(year·mile) (high failure rate).

automation, and the worth of reliability. While the cost of automation is well documented for the AACE[2] and the impact of automation on reliability indices is easily assessed using the analytical tool PRAM, the worth of reliability is highly controversial. Several studies have been conducted, but assessments of the worth of reliability vary greatly. A summary of outage cost studies can be found in reference 3.

Table 4-1 shows the incremental cost (1986 dollars) of the automation equipment installed on feeder SA-9. Using the table, the equipment cost for scenario 2 (automate BR214) is $10,232; for scenario 3 (automate BR214, SW170, and SW180), the cost is $34,972; and for scenario 4 (automate BR214, SW170, SW180, and RCL226), the equipment cost is $41,592.

Attempts to accurately determine the cost of outages for customers at AUB were not made. Such costs would likely be as controversial as other published data and at best applicable only to AUB. The costs of outages are highest in the industrial sector, although cost estimates still vary widely.

To demonstrate cost/benefit analysis, we have used the short-duration (1-hour) outage cost data for the industrial sector given by SRI.[3] These data were used to analyze feeder SA-9. According to reference 3, the average outage cost for an industrial customer in the United States is $6.56/kWh, with extremes of $3.21/kWh and $14.46/kWh (1977 dollars). Using the consumer price indexes[4] for 1986 (3.284) and 1977 (1.815) to adjust these costs to 1986 dollars, and assuming an average load of 6,000 kW on feeder

TABLE 4-1 Remote switch and recloser cost (copyright 1988 by the IEEE)

Material	Cost/h ($)	Labor ($35/h)	Total cost (1986 dollars)
BR214 (feeder circuit breaker) – automated switching with status indication and three-phase monitoring	3,337	197	10,232
SW180 (tie switch) – automated load/break switch with status indication	6,500	51	8,285
SW170 (in-line switch) – automated load/break switch with status indication and three-phase monitoring	11,100	153	16,455
RCL226 – automated switching and status indication (without recloser cost)	3,750	82	6,620

SA-9, low, average, and high estimates of the yearly outage cost to customers on feeder SA-9 are given by 5.81 × SAIDI × 6,000, 11.87 × SAIDI × 6,000, and 26.16 × SAIDI × 6,000, respectively. Note that the customer outage costs are linear in SAIDI, which is heavily dependent on the historical outage frequency.

Using these expressions and the cost data from Table 4-1 yields the cost/benefit analysis shown in Table 4-2 for 1.53 failures/(year·mile), a manual switching time of 20 minutes, and an automated switching time of 3 minutes. The table shows that even when we assume the lowest outage cost ($5.81/kWh), the automated cases appear to be fully justified on the feeder. However, the equipment costs represent only the incremental cost of added switching capability; they do not account for the basic system cost, which includes SCADA and communications systems.

Table 4-3 gives the cost/benefit for feeder SA-9 and shows that the benefits of reliability of automating a system decrease with outage frequency. This result stresses the importance of using accurate historical outage data in making cost/benefit studies.

Because outage costs for residential and commercial circuits are lower than for industrial circuits, a similar cost/benefit analysis for feeders SA-7 and SA-8 will show lower benefits of automation than for feeder SA-9. However, the community hospital in Athens is connected to feeder SA-7 and the outage cost could be assigned a higher value to justify extensive automation to improve the reliability of the circuit. AUB has realized public

TABLE 4-2 Cost/Benefit for SA-9 assuming 1.53 failures/(year·mile), 20 minutes for manual switching time, 3 minutes for automated switching time, and 6,000 kW average average load for 1 year (copyright 1988 by the IEEE)

	Study case	Outage cost (1986 dollars)			Reliability benefits (1986 dollars)		
		low	average	high	low	average	high
1	Base case – no automation – SAIDI = 7.58	264,239	539,848	1,189,757			
2	Automate BR214 – cost = $10,232 – SAIDI = 7.11	247,855	506,374	1,115,986	16,384	33,474	73,771
3	Automate BR214 – SW170 and SW180 – cost = $34,972 – SAIDI = 4.77	166,282	339,719	748,699	97,957	200,129	441,058
4	Automate BR214, SW170, – SW180, and RCL226 – cost = $41,592 – SAIDI = 4.74	165,236	337,583	743,990	99,003	202,265	445,767

TABLE 4-3 Cost/Benefit for SA-9 assuming 0.765 failure/(year·mile), 20 minutes for manual switching time, 3 minutes for automated switching time, and 6,000 kW average load for 1 year (copyright 1988 by the IEEE)

	Study case	Outage cost (1986 dollars)			Reliability benefits (1986 dollars)		
		low	average	high	low	average	high
1	Base case – no automation – SAIDI = 3.93	137,000	279,895	616,853			
2	Automate BR214 – cost = $10,232 – SAIDI = 3.68	128,285	262,090	577,613	8,715	17,805	39,240
3	Automate BR214 – SW 170 and SW180 – cost = $34,972 – SAIDI = 2.47	86,104	175,913	387,691	50,896	103,982	229,162
4	Automate BR214, SW170, – SW180, and RCL226 – cost = $41,592 – SAIDI = 2.46	85,756	175,201	386,122	51,244	104,694	230,731

relations benefits from improved service to the hospital as a result of the AACE.

Cost/benefit assessments to evaluate reliability gained from automation require accurate historical outage frequency data and an appropriate value for the worth of reliability.

After operating the automation system for 30 months, AUB has encountered many instances in which the automation system has provided intangible reliability benefits (benefits that are not evident from standard reliability indices) and significant cost savings to AUB.

Reliability Improvement

AUB's automation system was installed and tested over a 30-month period from January 1985 to June 1987. During this period, AUB personnel gained confidence in the system and began to realize its value to system operations, especially in diagnosing and resolving system problems before they escalate into serious outages. Eight specific cases are described below, along with estimated cost savings to AUB.

Case 1: prevention of a load-tap-changing transformer failure. Most utilities make and record periodic readings of breaker, switch, and tap changer counters. These readings are taken weekly (time permitting) at AUB and are used for general maintenance information and to check trouble reports. Typically, detecting a trend toward increased operations of a piece of equipment takes several weeks. However, AUB's control room operators were able to observe a substantial increase in the frequency of operations on both of the load-tap-changing (LTC) transformers at AUB's South Athens Substation. They reported that the transformers were changing as much as four steps at a time and then back again. On several occasions, two or three raise or lower commands were required to produce a one-step change in tap position. The maintenance crews' observations at the substation verified the operators' findings. Further investigation revealed an extraordinary increase in counter readings between the last reading and the current reading. Historically, these tap changers averaged 20 operations per day, but for the 6 days between readings, the operation count averaged over 200 per day. As a result, a decision was made to lock out the tap changers and to check the unit completely.

The results of subsequent overhaul showed that one of the LTC sensing units was out of calibration, resulting in the frequent tap changes. Because the two transformers are connected in parallel, the other LTC followed the malfunctioning LTC to stay within two steps of it. Both seal-in relays which ensure that the tap changers advance a full step were faulty; as a result, all contacts on the tap changers were damaged to the point of failure.

The cost of repairs to the transformers was $24,000, compared with $250,000 for the replacement of major LTC components, lost revenue, and labor costs. This represents a potential avoided cost of $226,000.

Case 2: complex maintenance operation. The repair of the transformer tap changers required AUB to transfer, on three successive nights; all of the load on the South Athens Substation to the North Athens Substation. This presented a unique opportunity to quantify the benefits of the automation system. To transfer the South Athens load to North Athens, one set of line regulators was set to the nominal tap position and nine distribution switches were operated on the first night; this transfer was done without the use of the automation system. Twelve linemen, two supervisors, and one dispatcher were involved in the operation. Nine linemen were used to manually transfer the load, and five of them returned to the substation to assist in repairs. On the first night, 27 minutes were required to disconnect the first transformer and 2 hours and 13 minutes were needed to manually execute all necessary switching. After completion of work in the substation, the five men who originally transferred the load returned to the field to retransfer the load to the South Athens substation. The total duration of the transfer was 2 hours and 40 minutes, requiring 15 men (40 man-hours).

On the following two nights, the load transfer was accomplished with the use of the automated system. Table 4-4 shows the reduction in manpower required as confidence was gained in the automated system. Manpower was reduced from 15 on the first night to 10 and then to 8 on the last night.

TABLE 4-4 AUB load transfer times (copyright 1988 by the IEEE)

	Night 1 manual	Night 2 automated	Night 3 automated
Total duration (h)	2:40	1:48	1:16
Switching time (h)	2:13	1:20	0:44
Man-hours required	40	18	10:13
Workers dispatched	15	10	8

Man-hours were reduced from 40 to 18 to 10.13 on consecutive nights. The reduction in manpower resulted in a labor savings of 51.9 man-hours ($1,945, assuming $37.5 per man-hour for overtime work).

AUB has made this same load transfer on two subsequent occasions to repair bus current transformers damaged by lightning. Fully automated switching times have been further reduced to 18 minutes and 12 minutes. Assuming that manual switching requires 2 hours and 13 minutes and 7 additional people, the labor savings on these two operations was 27.5 man-hours ($1,033).

Case 3: detection of a capacitor bank failure. In October 1986, the Tennessee Valley Authority (TVA) increased its power factor billing requirement from 0.85 lagging on-peak to 0.93 and added an off-peak power factor requirement of 0.97 leading. As a result, many TVA distributors have installed var-controlled capacitor banks to regulate power factor and avoid these penalties. By measuring real and reactive power flow, the automated feeder monitoring system at AUB has helped to determine where banks should be placed. Some distributors have had problems in determining proper locations for the banks and in detecting defective capacitors and controllers.

The monitoring system has prevented two outages on the North Athens Substation by alarming neutral currents that were 95% of the trip value at the substation. In response to each of these alarms, operators surveyed power flow data and were able to locate two capacitor banks that appeared to have one open phase. By remotely operating these banks and observing var flows, this suspicion was confirmed. The early detection of these two malfunctions resulted in a cost savings to AUB of $3,500 ($1,800 labor and $1,700 lost revenue).

Case 4: detection of a tap changer failure in a line regulator. The early detection of a malfunctioning tap changer motor in a line regulator prevented an outage and possibly the destruction of the regulator. Cost savings to AUB are estimated to be $6,100 ($5,000 cost of regulator, $800 lost revenue, and $300 labor costs).

Case 5: industrial accident. An industrial customer called AUB to report that during roof repairs, a strip of metal had fallen off the roof into the power transformers and had damaged the secondary leads such that the conductors were burning. Primary conductors were damaged and getting hot. AUB was able to remotely transfer half of the circuit to another feeder, open the reclosing relay cutout switch to the feeder breaker, and open a sectionalizing switch near the plant to de-energize the transformers. AUB removed the jumpers to the transformers, and the sectionalizing switch was closed 10 minutes after it was opened.

AUB was able to prevent an outage to 90% of the customers on the feeder, and the remaining 10% were out of service for only 10 minutes. The cost savings to AUB is estimated at $4,200 ($4,000 cost of transformer and $200 lost revenue).

Case 6: automated blocking of circuit breaker reclosure. The reclosing relay in a feeder breaker or distribution power recloser serves to automatically reclose the breaker or recloser a specific number of times before locking out the interrupter due to a fault. The reclosing relay cutout switch is opened to prevent the breaker from reclosing when switching is performed to transfer load, when linemen are working, or for various other reasons. Over the past two and a half years, AUB has averaged one operation per day of a reclosing relay cutout switch by remote operation. The ability to remotely operate reclosing relay cutout switches has enabled AUB to reduce outage times, increase productivity, reduce labor costs, and increase system and personnel safety. Each manual operation of a reclosing relay cutout switch requires about 0.5 man-hour. Assuming one such operation per day, at $25 per man-hour, the labor costs savings to AUB over the last 30 months are estimated at $11,406 (January 1985 through June 1987).

Case 7: detection of an abnormal load condition. In June 1987, just after 1 p.m. on weekdays, high-current alarms on one of AUB's feeders were reported by the automation system. The high-current readings lasted only a few minutes and then dropped below alarm limits. Because the duration was short, ammeters in the breakers could not verify this behavior. Calibration of the watt/var and voltage transducers in the breaker was checked and found to be within tolerance. As a result, AUB studied all monitored data and determined that two industrial customers, who had recently expanded operations, were creating a short demand peak for about 5 minutes during their afternoon startup operations. Current levels at the breaker were a value of 98% of relay pickup during this short time. This type of short-term peak could not have been detected so quickly without the automated system. Several circuit breaker operations, and at least one outage, likely would have occurred before the operators determined the exact nature of the problem. As a result, AUB designed a more optimum feeder configuration and remotely reconfigured the system. Cost avoidance to AUB is estimated at $1,800 ($1,000 lost revenue, $800 labor cost).

Case 8: insulator failure. Early in the morning on two consecutive days, the automation system recorded a protective device operation on one of AUB's circuits. Of particular concern was a hospital located on the feeder. AUB decided to switch the hospital to another feeder and transfer two other feeder sections to other feeders in hopes of determining the area that was causing the breaker to operate. Three days later, another operation was detected on the same circuit. AUB was able to isolate the search area to a half-mile section of line. A failing insulator found in this section was replaced before prolonged outage occurred. AUB was then able to transfer the hospital, a large shopping center, and a commercial sector back to a more stable and reliable circuit. The cost avoidance to AUB was estimated at $400 ($300 lost revenue, $100 labor costs).

These eight case studies are representative of the intangible reliability benefits and cost savings that have been achieved at AUB through automation. Because the AUB distribution system is typical of many distribution systems across the country, the same types of benefits should be applicable to these systems.

The Athens experiments have shown that system reliability can be increased when a distribution system is automated. The analyses also have shown that events not accounted for by standard reliability indices can produce substantial cost savings to the utility. The case studies presented show a direct benefit to AUB of $256,384 over a period of 30 months. These savings could not have been predicted by analytical studies.

Many of the major benefits of an automation system result from the diagnostic ability to prevent small problems and outages from escalating into large outages. Using analytical techniques to justify automation from an improved reliability standpoint clearly requires accurate historical outage data and careful use of advanced reliability evaluation models. At best, the cost/benefit conclusions resulting from such a study are tenuous in the absence of good "worth of reliability" data.

One other case study deserves mention even though costs savings cannot be assigned. On July 29, 1987, at 3:28 p.m., the automation system reported two operations of the feeder circuit breaker on North Athens circuit 2. A supervisor at the console at the time received a call from a customer at 3:30 p.m. reporting that a truck had hit a power pole in her front yard. Lines were down across the truck, and the driver was trapped inside. The breaker had reclosed on the high resistance fault. At 3:30:56, the supervisor remotely opened the breaker, and de-energized the circuit. The driver left the vehicle safely.

IMPACT OF AUTOMATED FEEDER RECONFIGURATION ON CAPACITY UTILIZATION AT THE ATHENS UTILITIES BOARD

Substation and remote feeder monitoring combined with remote control of distribution switches can significantly improve the capacity utilization of distribution system equipment. Enhanced capacity utilization can defer capacity expansion and can also allow the operation of existing facilities at higher load factors than are possible with a conventional (nonautomated) system. The addition of feeder monitoring to substation SCADA provides an opportunity to follow system operating conditions and detect evolving problems. Remote control of switches corrects problems such as an imminent overload of a component before they become major. Remote load transfers between feeders allow surplus capacity of equipment at one location to be made available to other locations quickly and easily. Such transfer capability reduces the need for redundant capacity, thereby reducing capital cost. The ability to reconfigure distribution circuits by remote commands may reduce system losses, conserve additional equipment capacity, and reduce operating costs.

Experience at Athens shows that the expected potential of distribution automation to improve capacity utilization was not fully realized. On the AUB system, a load transfer to reduce peak load on one feeder increases the peak load on the supporting feeder. A more advantageous situation may exist on other utility systems where there is sufficient difference in the times of peak loads on individual feeders to allow a sequence of load transfers to reduce the noncoincident peaks on all the feeders.

The AUB feeders are "telescoped" with conductor diameters that decrease in discrete steps with distance from the substation. Almost any deviation in system configuration from the nominal condition at Athens will increase the impedance between source and load (thereby increasing the losses, reducing the voltage, and decreasing customer load). Distribution systems that do not telescope feeders have a greater potential for loss reduction through feeder reconfiguration than is possible at AUB.

The number of automated switches installed at AUB will sectionalize each feeder into three or four zones so that even the smallest possible transfer of load from a feeder will transfer a significant portion of the load on that feeder (25–33%). Capability to transfer smaller loads would require additional remotely controlled switches and would increase the cost of the automation. It should be noted, however, that the reliability improvement at AUB resulting from automated fault isolation and service restoration tends to be maximized at three to four zones per feeder.[5]

Reducing Peak Feeder Loads

A potential benefit of automated feeder load transfers is to reduce the noncoincident peak loads on two or more adjacent feeders. When two feeders peak at different times, load may be transferred from one feeder before its peak and restored after its natural peak; then, the process can be reversed for the second feeder as the peak period approaches. This type of daily "multishift" operation can delay the need for increasing conductor size on both feeders. The avoided capital cost of reconductoring may easily justify the cost of the automated switches. Unfortunately, this type of benefit was not demonstrated at AUB because AUB feeder loads peak at about the same time.

In October 1985, two load transfer experiments were conducted between AUB's circuit 1 on the North Athens Substation (NA-1) and circuit 7 on feeder SA-7. One-line diagrams of these feeders are shown in Figure 4-7. Switch 43 (SW43) is a normally open tie switch between the two feeders, and SW14 and SW207 are normally closed sectionalizing switches on feeder SA-7. Under fairly typical autumn peak load conditions, a load of about 800 kW exists between SW207 and SW43 and a load of about 1800 kW exists between SW14 and SW43. Closing tie switch SW43 and opening one of the in-line sectionalizing switches (either SW207 or SW14) will transfer load from feeder SA-7 to feeder NA-1. Because these two feeders do not have significant load diversity, reducing the peak on feeder SA-7 will result in an increase in the peak on feeder NA-1. At 11 a.m. on Tuesday, October 8, SW43 was closed and SW207 was opened and about 800 kW was transferred from feeder SA-7 to feeder NA-1. The transfer was made for a 24-hour period to ensure that the peak load reduction on feeder SA-7 and the peak load increase on feeder NA-1 could be observed. Figure 4-8 is a plot of the

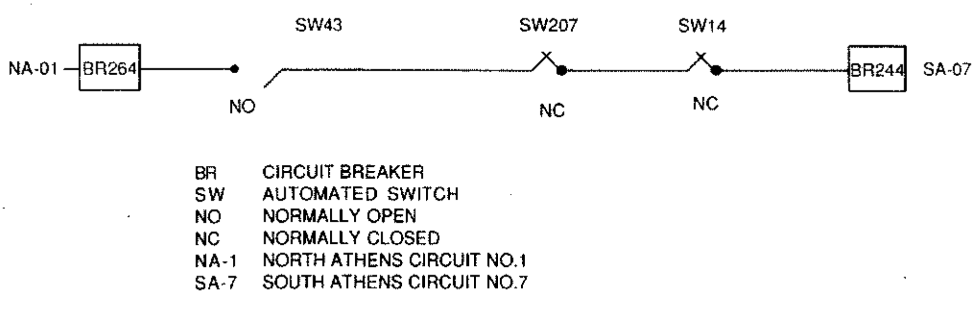

Figure 4-7 Simplified one-line diagram of NA-1 and SA-7.

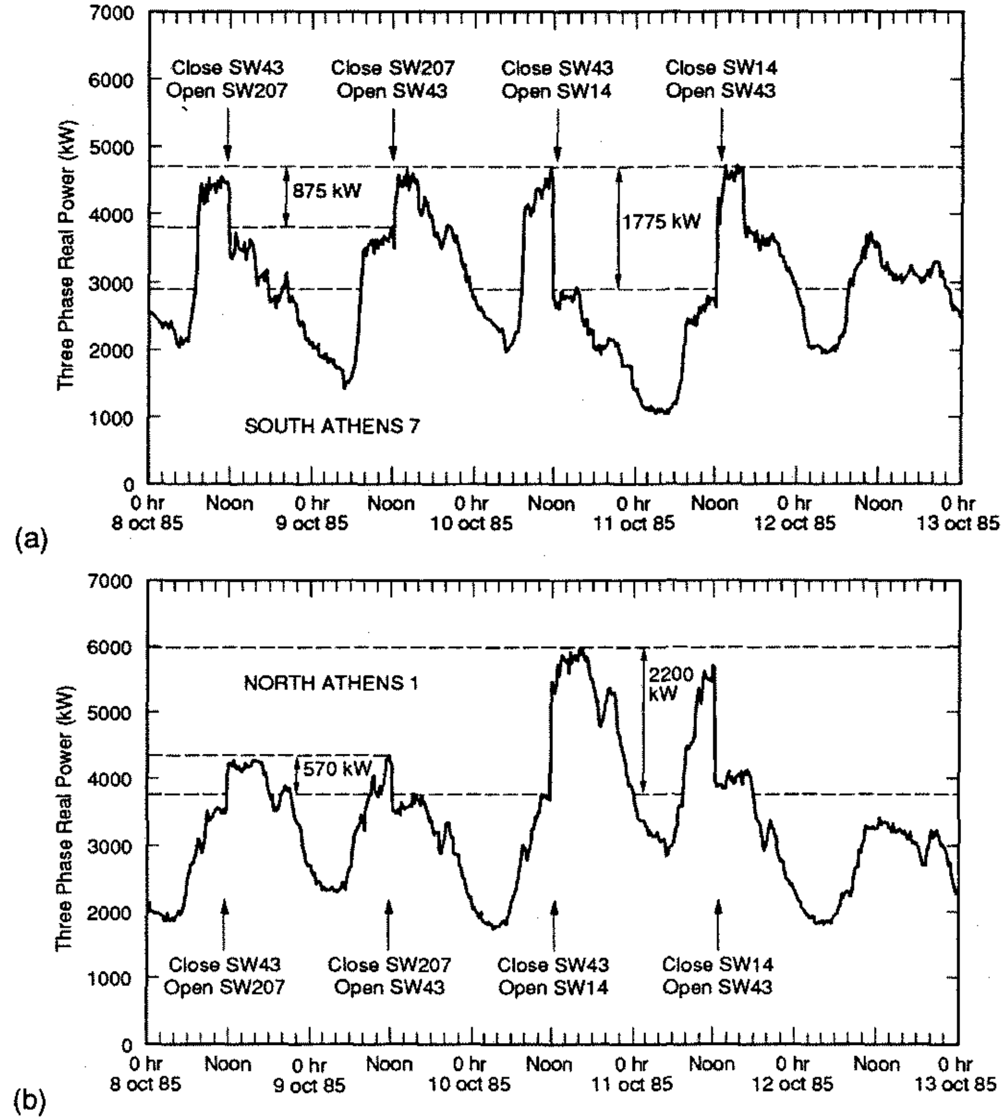

Figure 4-8 Power transfer between feeders SA-7 and NA-1.

three-phase real power observed at the circuit breaker on feeders SA-7 and NA-1. The data show that the peak on feeder SA-7 was reduced by 875 kW and the peak on feeder NA-1 was increased by 570 kW. Between 11 a.m. on October 9 and 11 a.m. October 10, the two feeders were maintained in their normal configuration (SW43 open, SW207 closed). At 11 a.m., Thursday, October 10, a large load transfer was initiated by closing SW43 and opening SW14, transferring approximately 1800 kW from feeder SA-7 to feeder NA-1. This transfer was left in place for 24 hours. Figure 4-8 shows that the peak on feeder SA-7 decreased by 1775 kW and the peak on NA-1 increased by 2200 kW. These tests reveal that unless peak loads on two feeders occur at different times, load transfers merely reduce the peak on one feeder while increasing the peak on a supporting feeder.

Switching Transients

Load transfer between two feeders involves two switch operations. A tie switch between the feeders is closed and, subsequently, an in-line sectionalizing switch is opened on one of the feeders to complete the load transfer. This switching sequence ensures that the customers in the zone where load is transferred do not experience a temporary outage. The initial closing of the tie switch results in a tying together of the two feeders. The feeders are likely to be tied together long enough for the system operator to verify that the tie switch is closed before opening the sectionalizing switch.

The protection system is designed and coordinated to protect radial feeders in their normal configuration. The performance of the protection system may be difficult to predict should a fault occur when the feeders are tied together; however, this problem may be lessened by minimizing the time the feeders are tied together. Reconfiguration of the feeder may require a change in short-circuit duty and protective relay setting.

Another concern during reconfiguration operations is the magnitude of the switching transient when closing the tie switch. The transient is dictated by the magnitude and phase of the voltage across the tie switch in the pretransfer state. Ideally, the location of normally open tie switches between two feeders would avoid a transient following the closing of the switch. A transient implies that moving the normal tie-switch location toward the circuit breaker of the new feeder reduces losses. The optimal location for the tie switch may vary through the diurnal load cycles, and physical constraints (such as the availability of a suitable utility pole) may preclude locating the tie switch to minimize the transient. Because the AUB system is supplied from the TVA system at a single point, these concerns were not serious and measurements of the differential voltage across tie switches were not provided. An experiment was performed to investigate the switching transients using a high-speed data acquisition system[6] (see Chapter 3). The experimental plan was to close the tie switch (SW43) and then open the in-line switch (SW14) to transfer approximately 1800 kW from feeder SA-7 to feeder NA-1 (see Figure 4-8a). To observe the transient associated with the load transfer and to monitor the behavior of the two feeders when they are tied together, the high-speed monitoring system was used to measure system parameters at the NA-1 feeder breaker. The high-speed monitoring system recorded real and reactive power flow and voltage on all three phases at a rate of 1000 samples per second. Another permanently installed monitoring system was used to record real and reactive power and voltage every 7 seconds on the NA-1 and SA-7 feeders. The load transfer was executed manually when SW14 was opened approximately 10 seconds after SW43 was closed.

Both the real and reactive power observed on phase b of the two circuits are shown in Figures 4-9 and 4-10. Figure 4-9 shows the high-speed data for real and reactive power for the North Athens circuit. Figure 4-10 is the slower-speed data for NA-1 and SA-7 for the same time interval. The switching transient was shown by the high-speed monitoring system and the closing of SW43 and the opening of SW14 are easily discerned in Figure 4-9.

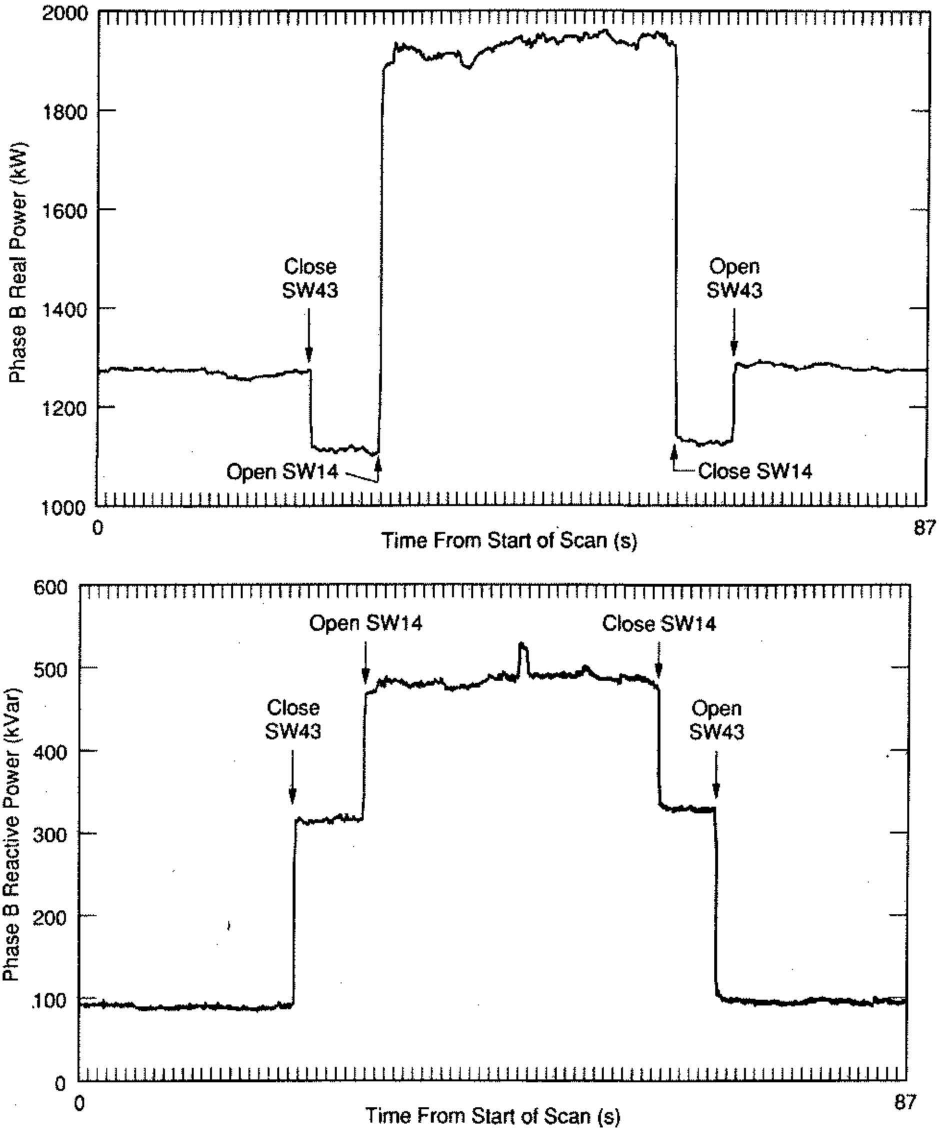

Figure 4-9 Real and reactive power taken by high-speed monitoring system on NA-1.

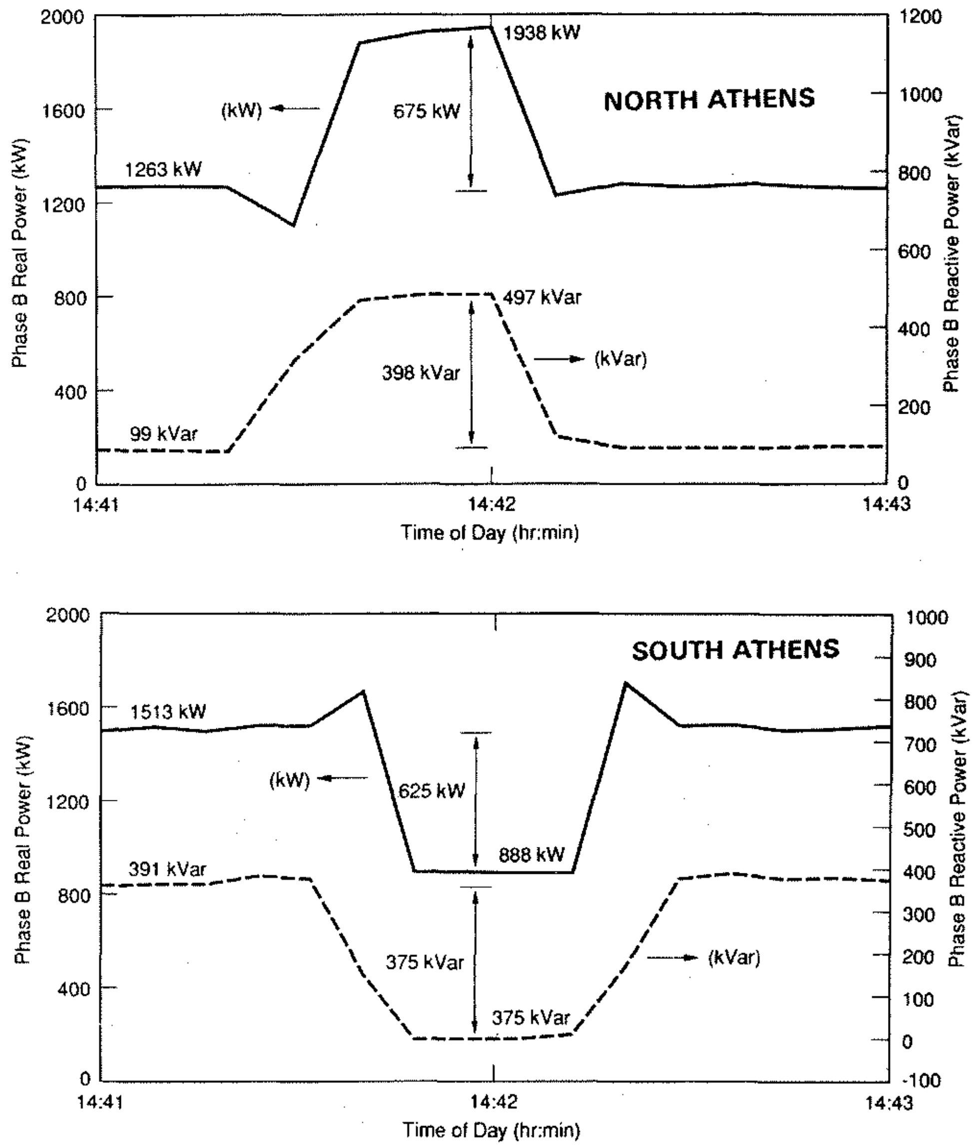

Figure 4-10 Real and reactive power on the South Athens and North Athens feeders taken at 7-second intervals during a switching transient.

The switching transients are not so noticeable in the data taken on the feeders with the slower data acquisition system (see Figure 4-10). Note (Figure 4-9) that when SW43 closed, the real power injection on feeder NA-1 decreased and the real power on feeder SA-7 increased (which is counter to the objective in transferring load from feeder SA-7 to feeder NA-1). The behavior of the reactive power with the feeders tied together is the opposite. This experiment demonstrates that switching transients can be significant and that operators need guidance in predicting the magnitude of such transients.

Load Sensitivity to Voltage

AUB feeders are "telescoped" (i.e., conductor diameters decrease in discrete steps with distance from the substation). In general, when a block of load is transferred from one feeder to another, there is an effective increase in the total impedance between the transferred section and the substation breaker feeding that section. This increase in impedance results from the fact that the conductor size at the sectionalizing switch (which is the supply point to the section of interest before transfer) is generally larger than the conductor size at the tie switch (which is the supply point to the zone after the transfer). Consequently, the losses in the transferred area would be expected to increase following the transfer.

If loads respond as constant power usage, then the total power injected on the two feeders should be larger in the posttransfer state than in the pretransfer condition because of the increase in losses. The load transfer experiments at AUB resulted in a reverse behavior. The net power injected at the substation on the two feeders is smaller in the posttransfer condition than in the pretransfer state. Because it was suspected that the difference resulted from changes in feeder voltage profile and the sensitivity of feeder loads to voltage, an investigation was conducted using SYSRAP[7] (see Chapter 8).

Figure 4-11 is a simplified one-line diagram of circuit 9 on the South Athens Substation (SA-9) and circuit 5 on the North Athens Substation (NA-5). Switch 170 (SW170) is a normally closed sectionalizing switch on SA-9, and SW180 is a normally open tie switch between the two feeders. The total load connected to SW170 and SW180 is about 4 MW during weekday afternoons. Closing SW180 and opening SW170 transfers the 4 MW from feeder SA-9 to feeder NA-5. This transfer was performed on the actual system, and the measured data were compared with results obtained with the simulator (SYSRAP).

Simulation results were obtained with three different load models: constant power, constant current, and constant impedance. In each modeling case, the pretransfer feeder voltage profiles were identical and total substation power injection agreed with the pretransfer experimental data.

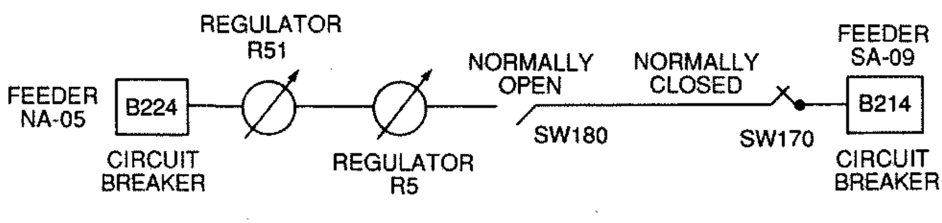

Figure 4-11 Simplified one-line diagram of SA-9 and NA-5.

Figure 4-12 shows a comparison of the pre- and posttransfer values for real power injection obtained experimentally and the SYSRAP predictions for each of the load models. Note that in the measured data (Figure 4-12a), the total power decreased by 273 kW following the load transfer (11,992 kW to 11,719 kW). In the three simulation cases, only the constant power model predicts an increase in the total power. The predictions from the constant current model are closer to the actual data (i.e., predicting a net decrease of 230 kW compared with the actual value of 273 kW). The constant impedance model predicts a decrease of 621 kW. Note that the largest difference (964 kW) in the net posttransfer real power is between the constant power model (with no voltage dependence) and the constant impedance load model (quadratic dependence on voltage). Figure 4-12b shows the total pretransfer and posttransfer power predictions for feeders SA-9 and NA-5 for the different load models. Figure 4-12c shows a 126-kW spread in calculated line losses between the SYSRAP constant power and constant impedance models. This value is a difference of 82% from the pretransfer line losses. This study shows that commonly used constant power load models are inadequate to predict the effect of load transfers.

Minimizing Losses by Reconfiguration

The objective of this analysis was to determine whether diversity of feeder peaking can produce switching opportunities to reduce losses. The approach for the analyses was to (1) identify feeders having the diversity to accomplish load transfers; (2) determine the potential switch operations based on installed automated or manual switches (and the loads in each switchable zone); (3) use the SYSRAP program to generate loss profiles (for the base configuration and switched configuration); and (4) calculate the total energy losses and compare them for the normal and switched configurations.

The analysis indicates that intertie switches on the AUB system were installed to increase reliability rather than to optimize feeder loading and shows that a design configuration that increases system reliability may not produce an ideal system for reducing feeder losses.

An initial goal of the experiments was to study the diversity on the system for one month to determine the length of time that a switching scheme is effective. Data from four Thursdays in August 1987 were chosen for the experiments. Thursdays were selected to avoid holidays and nontypical weekend activities. August was selected as a peak load month when losses were expected to be maximum. The analysis was later repeated with data from four Thursdays in March 1988.

Power data for these days were taken every 15 minutes by the MODSCAN SCADA system. Figures 4-13 and 4-14 show the load profiles on feeders SA-7 and SA-8. The load profiles were considered to be consistent over the four experimental days and, thus, typical for the proposed load

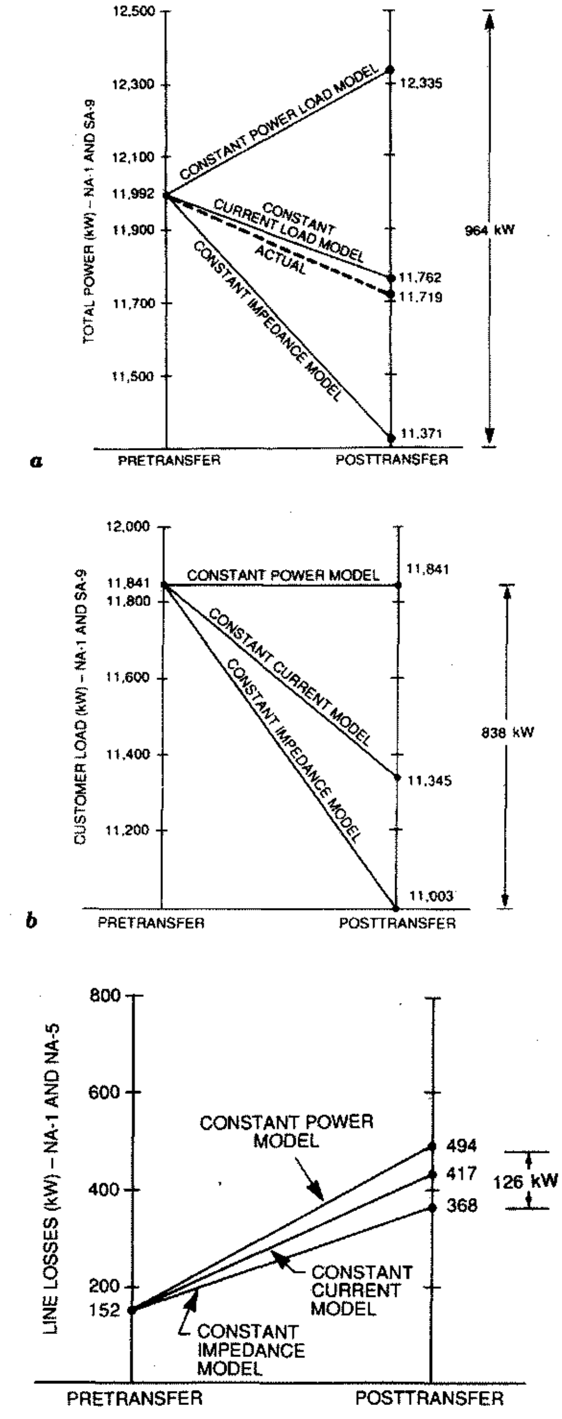

Figure 4-12 SYSRAP predictions of (a) total real power for transfer of load from SA-9 to NA-5, (b) customer load for transfer of load from SA-9 to NA-5, and (c) line losses for transfer of load from SA-9 to NA-5.

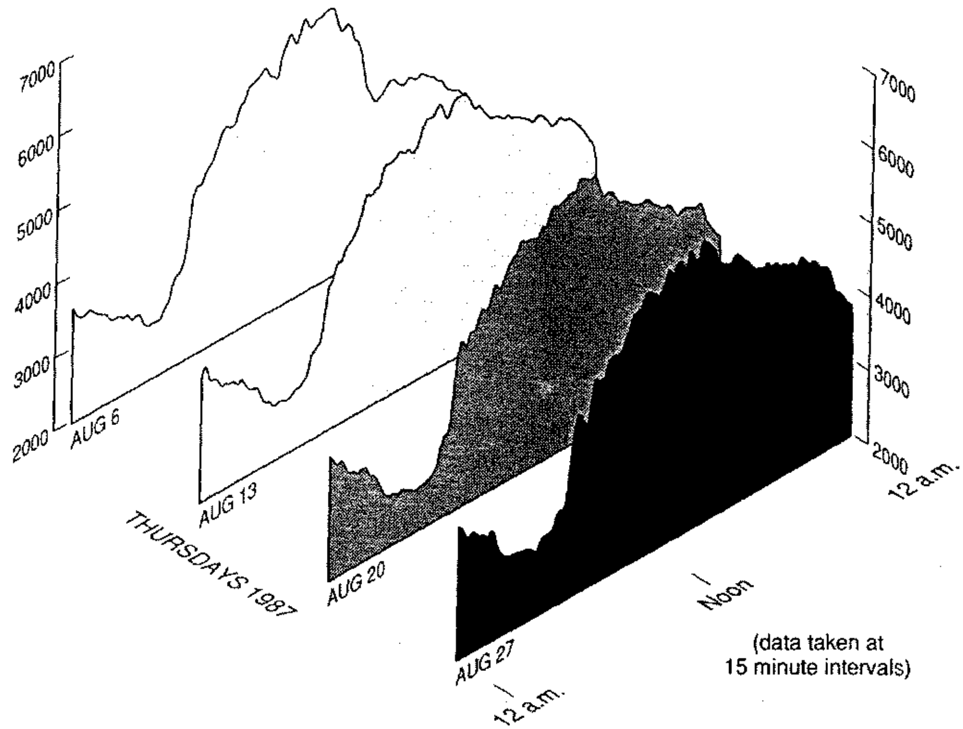

Figure 4-13 August daily load profiles for SA-7.

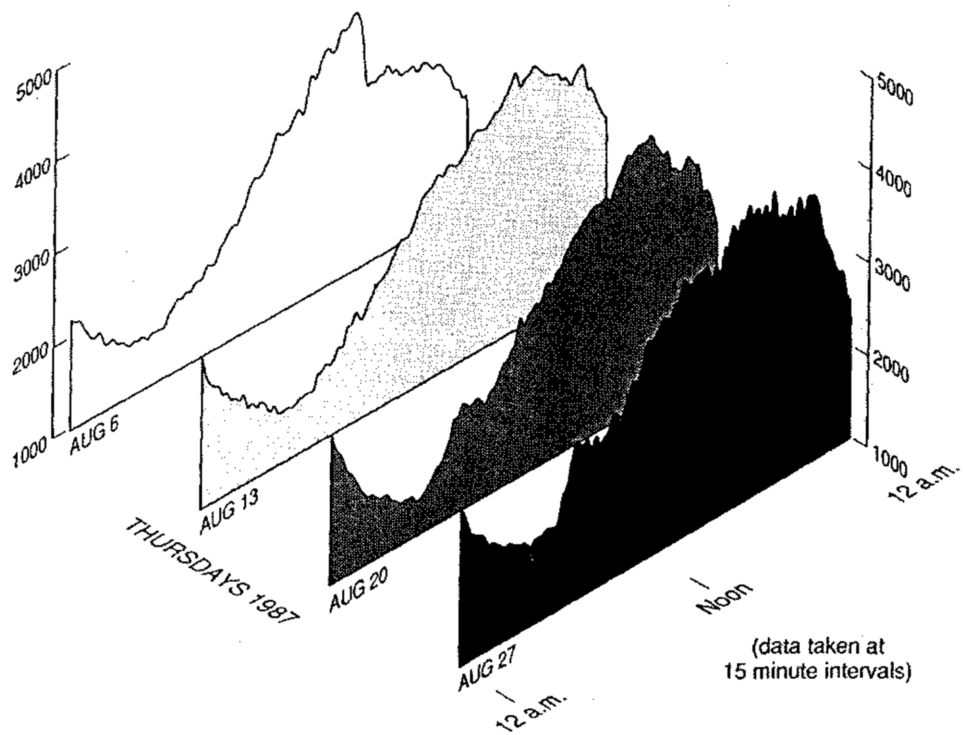

Figure 4-14 August daily load profiles for SA-8.

transfer schedules. (Examination of the load profiles and consideration of th anticipated load transfer time led to the conclusion that data taken hourl were sufficient for studying feeder load transfers.)

Figure 4-15 shows differences between loads on feeders SA-7 and SA-8 Insufficient diversity exists in the other interconnected feeders to allow a loa transfer without increasing the peak on the supporting feeder. Typical Augus load profiles of the Englewood, South Athens, and North Athens substation are shown in Figures 4-16, 4-17, and 4-18.

Assuming consistent diversity on Thursdays, the data in Figure 4-15 fo feeders SA-7 and SA-8 suggested that loads of 600 to 1000 kW could b transferred from feeder SA-7 to feeder SA-8 at 10 a.m. and restored t feeder SA-7 at 5 p.m. This transfer could achieve load leveling between feeders. Note that both the width of the feeder load peaks and their time displacement contribute to the magnitude and duration of load transfers.

The load transfer opportunities for these feeders are limited by the number of switches installed. Figure 4-19 is a one-line diagram of the two feeders and shows the amount of load in each section that can be switched. One remotely controlled intertie switch is installed between feeders SA-7 and SA-8 (intertie switch 15). Figure 4-19 shows there are no switching opportunities on feeder SA-7 to transfer a load less than 1000 kW to feeder SA-8. The closest in-line switch on feeder SA-7 that can be opened is SW14, and it will transfer 2241 kW to feeder SA-8.

A fictional switch A on feeder SA-7 was assumed. If such a switch existed, 1164 peak kW could be transferred to feeder SA-8 (see Figure 4-20). The load profiles before and after transferring the load with this switch are

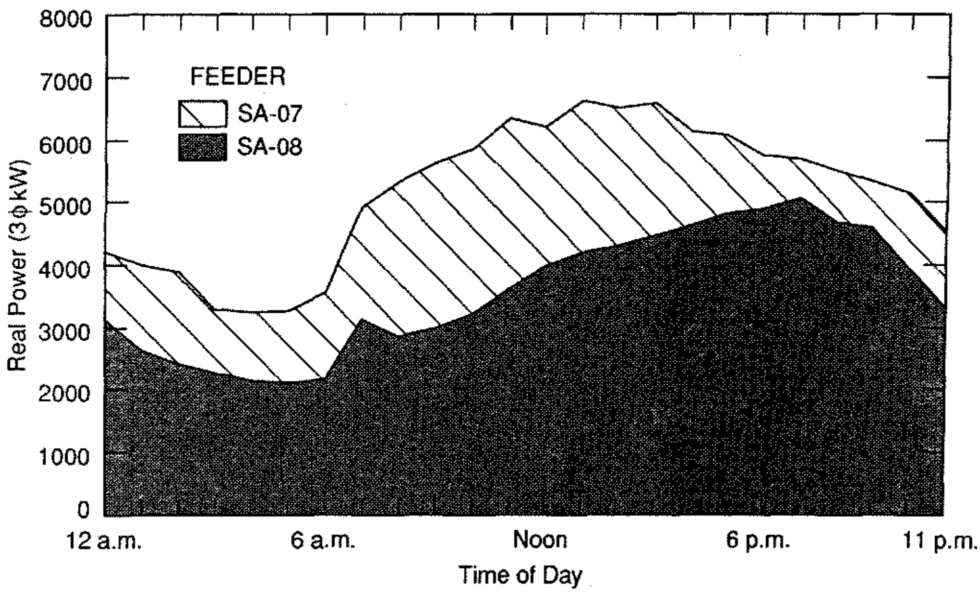

Figure 4-15 Load diversity between SA-7 and SA-8.

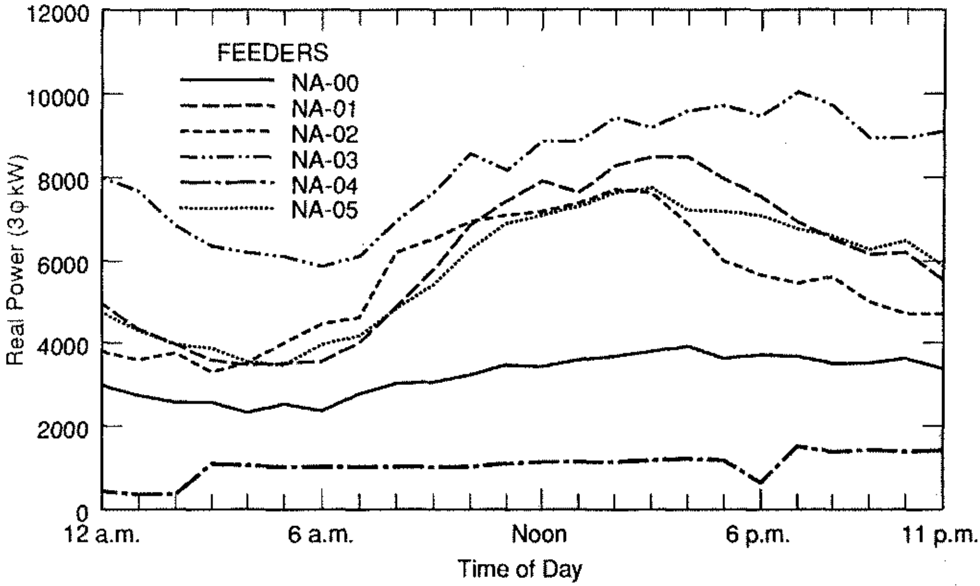

Figure 4-16 Load profile of North Athens substation.

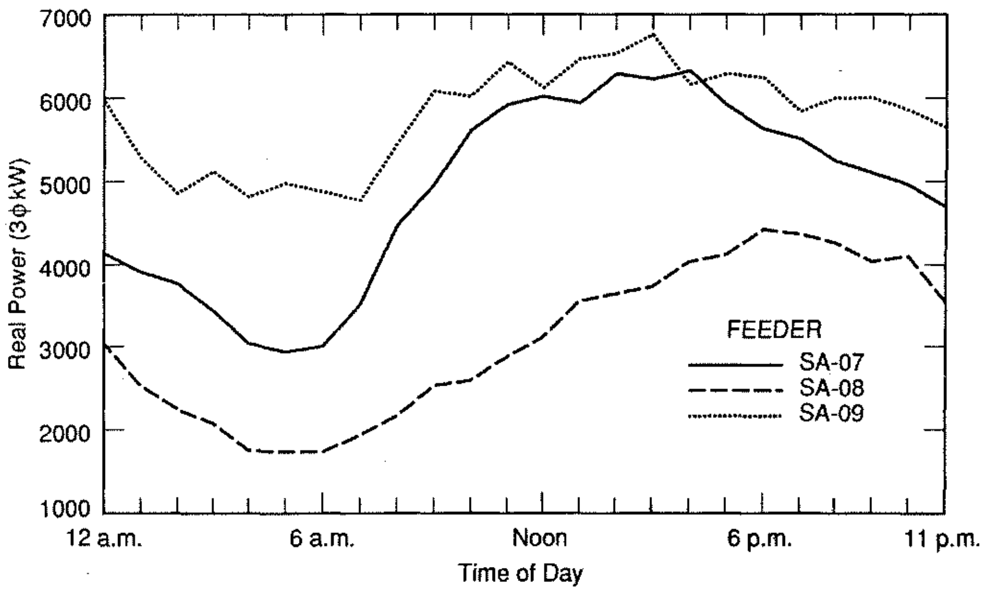

Figure 4-17 Load profile of South Athens substation.

shown in Figure 4-20. The following assumptions were made for the load transfer analysis using the SYSRAP computer program:

1. All load on feeders SA-7 and SA-8 was coincident. Uniform diversity between loads on the feeders implies that the transferred load peaks at the same time as the load on the original feeder.

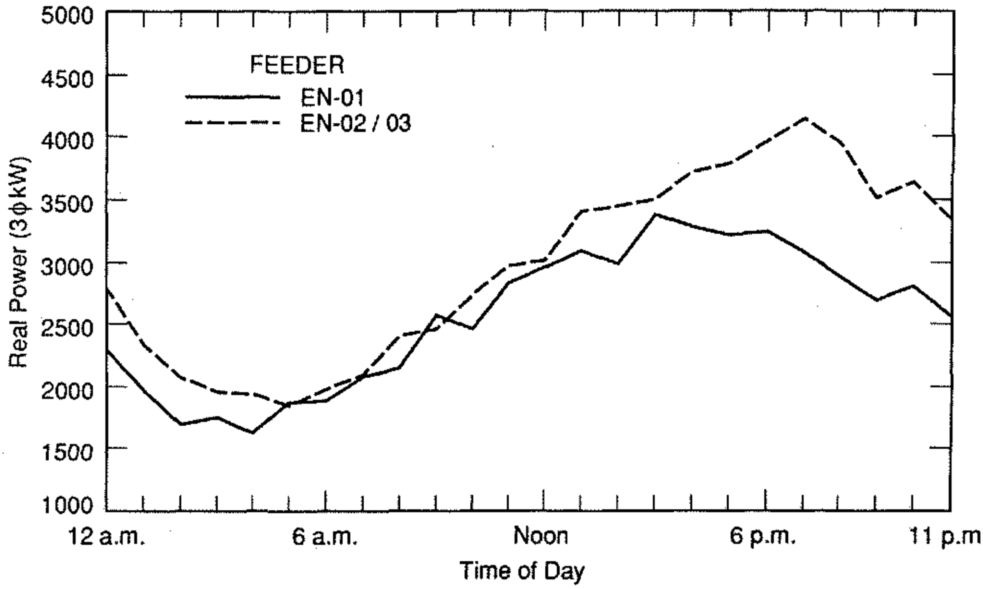

Figure 4-18 Load profile of Englewood substation.

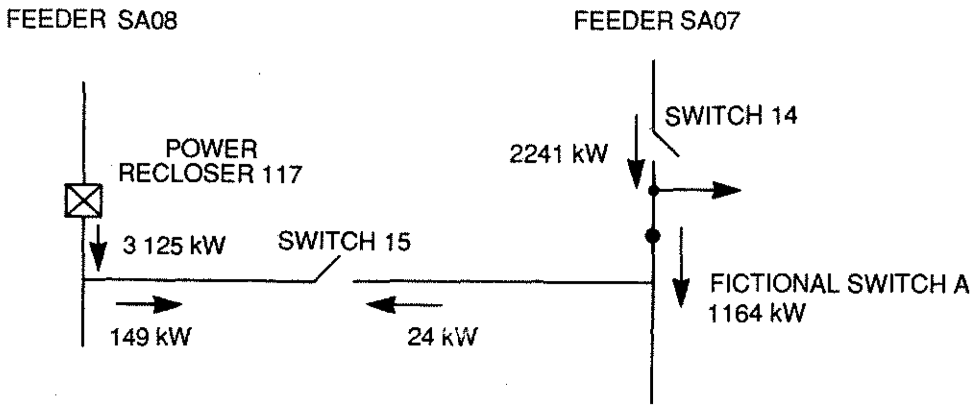

Figure 4-19 Simplified one-line diagram of SA-7 and SA-8 showing load transfer capabilities.

2. Constant impedance and constant power models were used.
3. Capacitor configuration was not changed during the runs. The capacitor bank on feeder SA-8 was connected, and the bank on SA-7 was not.
4. Voltage was assumed constant at 7.6 kV for the analysis.

The results of the computer analysis shown in Table 4-5 are for the August 1987 data and in Table 4-6 for the March 1987 data.

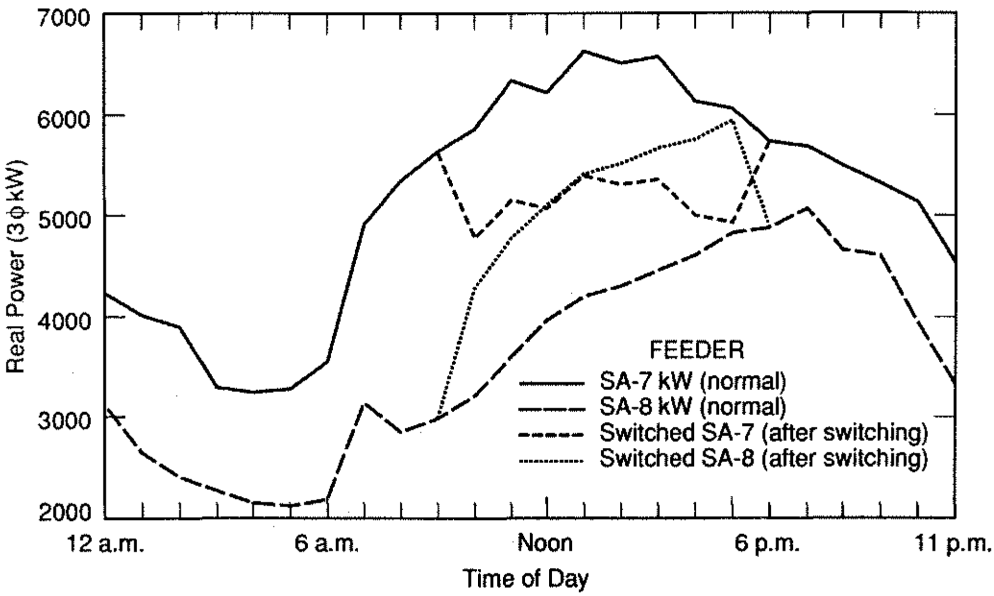

Figure 4-20 Simulation of transfer of 1164 kW from feeder SA-7 to feeder SA-8.

TABLE 4-5 SYSRAP results for August 1987 SA-7 and SA-8 data

	Energy use			Line loss		
	7 (MWh)	8 (MWh)	7+8 (MWh)	7 (MWh)	8 (MWh)	7+8 (MWh)
	Constant Impedance Load Model					
Normal configuration	123619.3	85565.09	209184.4	828.21	632.48	1460.69
Switched configuration	114325.0	95274.85	209599.8	687.23	801.53	1488.76
	Constant Power Load Model					
Normal configuration	123619.3	85565.09	209184.4	828.21	632.48	1460.69
Switched configuration	114358.8	94856.55	209215.3	676.11	791.65	1467.76

The assumptions used for analyzing the March data are as follows:

1. All capacitor banks were energized for both base and switched configurations.
2. Constant impedance and constant power calculations were made for the base loss profiles and the switching period profiles.
3. SCADA voltage values were input along with the kW and kVARs values.
4. No diversity of load existed on feeders SA-7 or SA-8.

Analysis of the August data shows that the losses increased by 2% when the system was reconfigured using the constant impedance load model. The increase was less than 0.5% when a constant power load model was used.

TABLE 4-8 SYSRAP results for March 1987 SA-7 and SA-8 data

	Energy use			Line loss		
	7 (MWh)	8 (MWh)	7+8 (MWh)	7 (MWh)	8 (MWh)	7+8 (MWh)
Constant impedance load model						
Normal configuration	100691.0	70310.83	171001.8	525.79	427.54	953.33
Switched configuration	93857.9	77170.12	171028.0	453.03	511.41	964.44
Constant power load model						
Normal configuration	100687.3	70313.99	171001.3	526.47	428.09	954.56
Switched configuration	94596.25	76412.9	171009.1	460	502.3	962.3

The March data agree reasonably well with the August data. An increase of 1.2% in energy use was observed using the constant impedance load model, and an increase of 0.8% was seen using the constant power load model.

It should be noted that the AUB system has a great deal of spare capacity. As a result of this spare capacity, the losses are so small that I^2R losses resulting from feeder peaking were not readily noticeable. The analyses show that reconfiguration did not have an appreciable effect on loss reduction. Potential opportunities for loss reduction were difficult to identify and even the most obvious load transfer did not produce conclusive results.

Because of the homogeneous nature of the diurnal load cycle on the 12 AUB feeders, it was not possible to reduce the daily peak load on two adjacent feeders by load transfer. The peak on one feeder could be reduced while the peak on the supporting feeder was increased. Such transfers will not be needed daily and can be made by manual switching.

Load sensitivity to voltage was found to be an important factor in predicting conditions after load transfer when the power flow program was used. Constant power load models show inaccurate results while a constant current model agreed reasonably well with experimental data. Accurate models will be required for operators to make switching decisions in highly automated systems where reconfiguration is a daily operation and load factors are high.

SUMMARY

ORNL and AUB have been able to show that system reliability has been increased due to automation, based on standard reliability measurement indices. They have also shown that events take place, outside the realm of these standard indices, that produce substantial cost savings to the utility. The case studies presented show a direct benefit to AUB of $256,384 (1986 dollars) over a period of 30 months. These savings could not have been predicted by analytical studies, and, as the time goes on, other cost savings will add to the total. Many of the major benefits of an automation system result from the diagnostic ability to prevent small problems and outages from escalating into large outages. Using analytical techniques to justify automation from an improved reliability standpoint clearly requires accurate historical outage data and careful use of advanced reliability evaluation models.

The capacity utilization enhancement benefits of automated feeder reconfiguration are disappointing at AUB. However, the AUB system is relatively small, and lacks sufficient load diversity to realize the full potential of automated feeder reconfiguration in reducing feeder and substation peak loads. Due to the homogeneous nature of the diurnal load cycle on the 12 AUB feeders, it was not possible to reduce the daily peak on two adjacent feeders by load transfer. It was possible to reduce the peak on one feeder while increasing it on the supporting feeder. Such transfers are not likely to be needed on a daily basis and can be handled by infrequent manual switching. Any departure from the normal system configuration resulted in an increase in losses. The primary reason is that the Athens feeders are telescoped and a reconfiguration generally results in the power routed to the transferred zone passing through a larger impedance than in the normal system configuration.

It was experimentally observed that load transfers at AUB are not conservative. That is, the relieved feeder sheds more or less load than is picked up by the supporting feeder. The decrease in load is due to the voltage sag on the transferred zone that results in a decrease in customer load that exceeds the increase in losses. Thus, load transfers between telescoped feeders can have a double drawback in that the losses go up and customer load (sales) goes down. Aggravating this phenomenon is the fact that relatively few automated switches are available on any given feeder and, consequently, the smallest load transfers that can be initiated by remote control involve 25 to 33% of the feeder load. Less voltage sag and less increase in losses might be achievable if smaller portions of feeder load could be transferred. This would require more automated switches which may not be economically justified.

Load sensitivity to voltage was found to be an important factor in being able to accurately predict post load transfer conditions using a power flow program. Constant power load models were shown to yield inaccurate results, while a constant current model agreed reasonably well with experimental data. Accurate models will be required to support operators in making switching decisions in highly automated systems where reconfiguration is a routine daily operation and load factors are high.

Feeder tie switches are seldom in their optimal location and significant transients can be observed once a tie switch is closed looping two radial feeders (as the first step in a load transfer). To avoid closing tie switches that would result in objectionable transients the differential voltage magnitude and phase angle across the tie can be measured (increasing the cost of automation) or an on line power flow calculation can be used to predict the acceptability of the system state in the loop condition. This problem was not critical at AUB which is fed from a single supply point from the TVA system.

The automation system has significantly improved system reliability, ease of maintenance and operation, improved the quality of service to customers, and reduced system costs. Additional study is needed to determine if systems without telescoped feeders and/or systems with more load diversity can gain greater capacity utilization benefits through automated switching than those observed at AUB.

REFERENCES

1. *Development of Distribution System Reliability and Risk Analysis Models*, EL-2018, Research Project 1356-1, Electric Power Research Institute (August 1981).
2. S. L. Purucker et al., *Athens Automation and Control Experiment: Substation and Distribution System Automation Designs and Costs*, ORNL/TM-9596, Oak Ridge National Laboratory (June 1986).
3. *The National Electric Reliability Study: Technical Study Reports*, DOE1EP-0005, Appendix B, p. 525 (April 1981).
4. *Suvey of Current Business*, Bureau of Economic Analysis, U.S. Department of Commerce, Washington, D.C.
5. J. S. Lawler, J. S. Lai, L. D. Monteen, J. B. Pattton, and D. T. Rizy, "Impact of Automation on the Reliability of the Athens Utilities Board's Distribution System," IEEE Paper No. 88 WM 087-9, presented at the IEEE PES Winter Meeting, New York, February 1988; published in *IEEE Trans. Power Delivery*, 4(1), 770–80 (January 1989).
6. D. T. Rizy, J. S. Lawler, J. B. Patton, and W. R. Nelson, "Measuring and Analyzing the Impact of Voltage and Capacitor Control with High-Speed Data Acquisition," IEEE Paper No. 88 WM 098-6, presented at the IEEE PES Winter Meeting, New York, February 1988; published in *IEEE Trans. Power Delivery*, 4(1), 704–14 (January 1989).
7. D. T. Rizy, J. S. Lawler, J. B. Patton, and N. H. Fortson, "Distribution Automation Applications Software for the Athens Utilities Board," IEEE Paper No. 88 WM 097-8, presented at the IEEE PES Winter Meeting, New York, February 1988; published in *IEEE Trans. Power Deliver*, 4(1), 715–24 (January 1989).

5

VOLT/VAR EXPERIMENT*

D. T. Rizy, J. S. Lawler, J. B. Patton, and W. R. Nelson

The effectiveness of real-time control of regulators and capacitors on the distribution system was evaluated as part of the Athens Experiment. The evaluation included testing real-time, computer-activated capacitor and regulator control along with load control and system reconfiguration over a 2-year period (1986–1987).[1,2] The capacitor and regulator experiments involved controlling load-tap-changing (LTC) transformers at the substation and voltage regulators and shunt capacitors on the distribution feeders.

The objectives of the capacitor and regulator control experiments were to

1. determine the line loss reduction of computer-automated capacitor and regulator control;
2. determine the effectiveness of computer-automated regulator control in leveling voltage profiles, reducing voltage drop, and reducing energy use;
3. develop software that can be used for capacitor and regulator control;
4. identify hardware and software requirements for implementing capacitor and regulator control on a future distribution automation system; and
5. transfer experimental results to the electric utility industry.

*This chapter is based on material in IEEE Paper No. 88 WM 098-6, "Measuring and Analyzing the Impact of Voltage and Capacitor Control with High Speed Data Acquisition," by D. T. Rizy, J. S. Lawler, J. P. Patton, and W. R. Nelson, which was first presented at the IEEE Power Engineering Society Winter Meeting, February 1988, New York (copyright 1988 by the IEEE).

Objective 1 was accomplished by determining the response of the feeder to capacitor switching and regulator control. A distribution system analysis tool that combines a power-flow analysis, a short-circuit analysis, and a data base manager was developed to analyze experimental data and to meet project objectives 1 and 2.[3] The computer tool allows the feeder loads to be represented as voltage-sensitive or -insensitive load models (any load composition of constant power, constant current, and constant impedance). In addition, the real-power load composition can be specified differently from the reactive power composition. For objective 3, a control procedure that minimizes var flow on each of the 12 AUB feeders was implemented on the central control computer. The computer control procedure maintains a slightly lagging power factor because TVA has a cost penalty for a leading power factor and for a power factor <0.95 lagging. For objective 4, one-way communication via power line carrier has been shown to be adequate for conducting capacitor control on the system. When a capacitor is switched either in or out, the reactive-power changes can be observed by the substation remote terminal unit, which updates the analog data at the screens of the distribution dispatch control center every 20 seconds.

Capacitor and regulator control experiments were conducted in the fall of 1985 and in January, April, and July 1986. Real-time data were collected at three different sampling rates (a sample every 20 seconds but recorded only every 15 minutes, a sample every 7 seconds, and 1000 samples every second) in an attempt to determine the changes in system parameters due to capacitor switching. The results of capacitor-switching experiments with data collected at the sampling rate of 1000 samples per second are presented and discussed.

THE DISTRIBUTION SYSTEM

The 12 distribution circuits on the AUB system are "telescoped circuits," with the three-phase primary consisting of 556 aluminum cable steel-reinforced (ACSR) conductors and 336 ACSR conductors with smaller three-, two-, and one-phase laterals and sublaterals consisting of 4/0, 3/0, 1/0, 2, and 4 ACSR and copper conductors. The power-flow analysis models of the 12 radial circuits used in the analyses ranged in size from 11 buses to 97 buses per phase. In some cases, entire subdivisions and multiple loads have been lumped together into one bus. The number of buses on a feeder correspond to electronic data points (EDPs) for which AUB maintains records of the total number of customers connected, connected transformer kilovolt-amperes, and appropriate kilowatt-hours billing data. The average number of buses per phase per feeder is 50.

The automated system uses a two-way communications system and remote terminal units (RTUs) to monitor the status of capacitors, single-phase bus voltages, real-power flows, and reactive-power flows on each feeder and near the capacitors. Three substations, 12 feeders, 2 substation LTC transformers, 4 line regulators, and 29 feeder capacitors are controlled with telephone and power line carrier communications. The substations and an average of four locations per feeder are monitored to collect analog data (i.e., real- and reactive-power flows and bus voltages) and equipment status data (i.e., tap positions of the LTC transformers and on/off status of capacitor banks). The data are sent to the AUB distribution control center.

The three-phase capacitor banks under control on the North Athens, South Athens, and Englewood substations are shown in Table 5-1. The capacitors are controlled to maintain the total feeder reactive power between zero and the rated size of the smallest capacitor installed on the feeder [0 to +200 kvar per phase (a 600-kvar, three-phase bank) for the North Athens and South Athens circuits and Englewood circuit No. 1; and 0 to +100 kvar per phase (a 300-kvar, three-phase bank) for Englewood circuit No. 2]. Normally, the utility controls the capacitors to maintain a slightly lagging power factor.

Voltage regulation on the North Athens feeders is achieved by three-phase line regulators (Table 5-2). The South Athens and Englewood feeders

TABLE 5-1 Shunt capacitors on the North Athens, South Athens, and Englewood distribution circuits (copyright 1988 by the IEEE)

Substation	Circuit	Number and size of capacitors (kvar)
North Athens	0	1 (600)
North Athens	1	2 (600), 2 (1200)
North Athens	2	3 (600),[a] 2 (1200)
North Athens	3	1 (900), 3 (1200)
North Athens	4	No capacitors
North Athens	5	2 (600), 2 (1200)
South Athens	7	1 (600), 1 (900), 1 (1200)
South Athens	8	2 (600)
South Athens	9	3 (600),[a] 2 (1200)
Englewood	1	1 (600)
Englewood	2	1 (150),[a] 1 (300)
Englewood	3	No capacitors

[a]One capacitor is fixed (there are 28 switchable capacitors and 3 fixed capacitors).

TABLE 5-2 Voltage regulation on the North Athens, South Athens, and Englewood distribution circuits (copyright 1988 by the IEEE)

Substation	Circuit	Voltage regulation
North Athens	0–5	No substation regulation
North Athens	0	2 line regulators
North Athens	3	1 line regulator
North Athens	5	2 line regulators
South Athens	7–9	LTC[a] transformer
Englewood	1–3	Substation regulator
Englewood	1	1 line regulator

[a]LTC = Load-tap-changing.

have substation-level voltage regulation. Englewood circuit No. 1 is the only feeder with both substation-level regulation and a line regulator. The LTC transformers at the South Athens substation, the substation regulator at the Englewood substation, and the line regulators on the North Athens feeders and Englewood circuit No. 1 control voltage in the range ±10% over 32 tap settings.

There are three types of capacitor control installations. Eleven installations are of the first type and have two-way RTUs that both monitor and control a capacitor. The RTU sends analog and equipment status data to the distribution control center by telephone. An open or close control signal that switches the capacitor bank in or out is transmitted from the distribution control center to the substation by dedicated telephone and from the substation to the RTU by power line carrier. The two control modes for this type of installation are (1) remote control, which allows the RTU to read data and control the capacitor; and (2) local control, which allows the RTU to read data but has no control over the capacitor (the local var controller is enabled if installed at this installation). One of these installations has a var controller.

A second type of installation has a capacitor controlled by a one-way communication RTU device. In the 17 installations of this type, the control signal is transmitted in the same manner as in the first type, but no monitored analog or status data are collected. Data are collected by the nearest upstream two-way RTU. Ten of these capacitor installations have var controllers.

The third type of installation has a capacitor bank that is not automatically controlled. The capacitors are switched manually at the three fixed-capacitor-bank installations.

The LTC transformers at the South Athens substation are controlled by a two-way RTU that uses a dedicated telephone between the control center and the substation. The RTU is used to raise or lower the transformer taps sequentially, and a resistive bridge on the transformer tap controller monitors the tap position of the transformer.

The line regulators on the North Athens and Englewood circuits are controlled also by a two-way RTU with a dedicated telephone line for communications. Supply-side and load-side voltages of each line regulator are used to determine the tap position of the regulator.

CAPACITOR SWITCHING TEST RESULTS

The results of real-time capacitor switching tests conducted on South Athens circuit No. 9 and North Athens circuit No. 5 in 1986 are presented in this chapter. During the tests, real-time data (bus voltages, real-power flows, and reactive-power flows on phases a, b, and c at the feeder breaker) were collected at a sample rate of 1000 samples every second. Analysis was conducted before the experiment to determine what to expect from capacitor switching on all the AUB circuits. A distribution system analysis tool developed by the project team[3] was used for analyzing the experimental results.

Expected Results

Before the experiments were conducted in 1986, the 12 AUB feeders were analyzed with a Newton-Raphson power flow computer program.[4] The 1983 winter peak load data were used as input to determine what could be expected from capacitor switching. The objective of the 1983 data analysis was to determine the effect of capacitor control on line losses and the subsequent change in real-power flow on the feeders due to the switching in of capacitors. The North Athens and South Athens circuits were later reanalyzed from the 1986 winter peak load data; Table 5-3 summarizes the peak load data collected for this period.

Most utilities switch capacitor banks to improve the power factor on distribution feeders and to reduce the reactive-power (var) transport along the feeder. When feeder loads are modeled as constant power, a capacitor-switching operation that moves the power factor of a feeder closer to unity from a lagging power factor condition should be accompanied by a reduction in reactive-power injection, an increase in line-to-neutral voltages, and a reduction in real-power injection. The switching operation should result in reduced feeder losses.

To determine the real- and reactive-line losses without compensation, the power flow analyses were first conducted with all the capacitors on the circuits switched out. The analyses were rerun with capacitors switched in to quantify the line losses with compensation. The LTC transformers and

TABLE 5-3 1986 Winter peak load data for North Athens and South Athens distribution circuits (copyright 1988 by the IEEE)

Circuit	Real power (kW)				Reactive power (kvar)				Bus voltage (kV)		
	a-phase	b-phase	c-phase	3-phase sum	a-phase	b-phase	c-phase	3-phase sum	a-phase	b-phase	c-phase
North Athens											
No. 0	1,249	1,116	1,125	3,490	605	573	641	1,819	7.44	7.39	7.47
No. 1	2,197	2,210	2,354	6,761	1,515	1,404	1,576	4,495	7.44	7.39	7.47
No. 2	2,376	2,454	2,363	7,193	1,857	1,872	1,976	5,705	7.44	7.39	7.47
No. 3	4,104	3,884	4,127	12,115	2,086	2,085	2,217	6,388	7.44	7.39	7.47
No. 4	326	475	394	1,195	92	109	134	335	7.44	7.39	7.47
No. 5	2,611	2,614	2,680	7,905	1,793	1,786	1,982	5,561	7.44	7.39	7.47
Total	12,863	12,753	13,043	38,659	7,948	7,829	8,526	24,303			
South Athens											
No. 7	2,530	2,693	2,594	7,817	866	792	896	2,554	7.52	7.54	7.60
No. 8	2,470	2,440	1,979	6,889	908	948	870	2,726	7.52	7.54	7.60
No. 9	4,372	4,366	4,217	12,955	1,882	1,924	2,062	5,868	7.52	7.54	7.60
Total	9,372	9,499	8,790	27,661	2,790	2,872	2,932	8,594			

regulators at the substation and the line regulators were set at the nominal tap position (zero: no voltage increase or decrease) for both computer runs. The difference in the line loss results (all capacitors switched out vs all capacitors switched in) gave the maximum reduction in line losses on all 12 circuits. These results are shown in Table 5-4. North Athens circuits Nos. 0–3 and 5 have the highest ratio of line loss to loading because they are the longest circuits and have more small conductors than any of the other AUB circuits.

The results of the power flow analyses indicate that the line losses with all the capacitors switched out are expected to be ~0.9% (South Athens circuit No. 7) to ~3.8% (North Athens circuit No. 5) of the power flow. The switching in of all the capacitors is expected to reduce the line losses on the circuits by ~3.3% to ~30%. A line loss reduction was not indicated for North Athens circuit No. 4 because there are no capacitors on that feeder.

The common assumption in power flow analyses is that the customer loads respond as constant power loads, which presumes that the customer loads are not a function of voltage. Thus, the capacitor-switching experiments were expected to yield an observable decrease in real-power flow at the feeder breaker on each phase about equal to the loss reduction achieved by switching in the capacitors.

Actual Results

The experiments to determine feeder response for capacitor switching were conducted in 1985. During these experiments, data were sampled every 15 minutes (actually sampled every 20 seconds but recorded on history files every 15 minutes), every 20 seconds (obtained by recording operator screen data), and every 7 seconds. The reactive power and voltage data from sampling at these rates verified the expected effects of capacitor switching on reactive power and on phase voltage. The data taken at these sample rates showed that the reactive power decreased by approximately the capacitor kvar rating per phase and that phase voltage increased with the switching in of a capacitor bank. The data showed also that the reactive-power reduction varied with voltage levels, as would be expected (because a capacitor is a constant-impedance rather than a constant-power device), and was different on the three phases because of the unbalanced loading and the differences in impedance of the phases and in the voltage profile of the three phases. However, the real-power data collected at these low sample rates did not show a discernible change (either increase or decrease) as a result of the switching in or switching out of the capacitors.

In 1986, the capacitor switching experiments were repeated and new experiments were conducted with a high-speed data acquisition system (see Chapter 3) collecting data at 1000 samples per second at the feeder breaker. The high-speed data acquisition system was employed to eliminate concerns

TABLE 5-4 Line loss calculations for the North Athens and South Athens circuits from the 1986 winter peak load data (copyright 1988 by the IEEE)

Circuit	Load		Line losses with capacitors switched out				Total installed capacitor kvars on feeder (kvar)	Line losses with capacitors switched in		Line loss reduction due to capacitor compensation			
	Real power (kW)	Reactive power (kvar)	Real power		Reactive power			Real power (kW)	Reactive power (kvar)	Real power		Reactive power	
			(kW)	%[a]	(kvar)	%[b]				(kW)	%[c]	(kvar)	%[d]
North Athens													
No. 0	3,490	1,819	93	2.65	113	6.21	600	90	103	3	3.3	10	8.8
No. 1	6,761	4,495	170	2.52	397	8.84	3,600	121	278	49	29.0	120	30.1
No. 2	7,193	5,705	121	1.68	262	4.59	4,200	88	187	32	26.7	75	28.8
No. 3	12,115	6,387	394	3.25	681	10.66	4,500	352	583	42	10.7	97	14.3
No. 4	1,195	335	15	1.26	15	4.37	0	15	15	0	0.0	0	0.0
No. 5	7,906	5,561	302	3.82	734	13.19	3,600	221	521	81	26.9	212	29.0
South Athens													
No. 7	7,817	2,554	71	0.91	224	8.78	2,700	65	204	6	8.4	20	6.7
No. 8	6,890	2,726	102	1.48	170	6.23	1,200	96	157	6	6.2	13	8.8
No. 9	12,955	5,868	189	1.46	626	10.67	4,200	164	536	25	13.4	90	2.4

[a][The real line loss (column 3) divided by the total real power of the feeder (column 1)] multiplied by 100%.

[b][The reactive line loss (column 5) divided by the total reactive power of the feeder (column 2)] multiplied by 100%.

[c][The real line loss reduction (column 10) divided by the real line loss for the feeder with capacitors switched out (column 3)] multiplied by 100%.

[d]The reactive line loss reduction (column 12) divided by the reactive line loss for the feeder with capacitors switched out (column 5)] multiplied by 100%.

that the slower sampling rates might be introducing too much time skew between the voltage and power data. The high-speed data acquisition system was used because it was anticipated that the real-power data were fluctuating so fast that the 7-second sampling rate was too slow to measure the changes resulting from capacitor switching.

The results presented below are from the capacitor-switching experiments that were conducted on South Athens circuit No. 9 and North Athens circuit No. 5. On circuit 5, the line-loss reduction for capacitor compensation was expected to reduce the real-power flow by $\leq$1.02% (100 $\times$ 81/7906). On circuit 9, the line-loss reduction for capacitor compensation was expected to reduce the real-power flow by $\leq$0.19% (100 $\times$ 25/12955). Table 5-5 summarizes the capacitor-switching experiments and their results. Experiments 1 through 3 were conducted on North Athens circuit No. 5 in April 1986. Experiments 1 and 2 were repeated several times to ensure repeatability of results. Experiments 4 through 8 were conducted on South Athens circuit No. 9 in July 1986. Figures 5-1 and 5-2 show the capacitor control points and the controllable switches on circuits 5 and 9. There are 4 three-phase switchable capacitor banks on circuit 5: 102 (200 kvar/phase), 119 (400 kvar/phase), 121 (400 kvar/phase), and 123 (200 kvar/phase). Circuit 9, primarily an industrial circuit, has four switchable capacitor banks: 101 (200 kvar/phase), 109 (400 kvar/phase), 110 (400 kvar/phase), and 122 (200 kvar/phase). Capacitor 111 is fixed bank, 200 kvar/phase.

The experiments were to switch capacitors in and out on circuit 9 while the substation LTC transformers were maintained at a fixed-tap position and to switch capacitors on circuit 5 while the line regulators were maintained at nominal tap positions. Initially, on circuit 5, capacitors 121 and 123 were out of service and capacitors 102 and 119 were in service. In Experiment 1, capacitor 102 was remotely switched out. Table 5-5 shows the condition of the feeder immediately before (preswitched state) and after (postswitched state) the switching out of the capacitor. Figure 5-3 shows the real and reactive power and the bus voltage on the a-phase, taken at a rate of 1000 samples per second. The data indicate an increase in the reactive-power flow of the circuit approximately equal to the kilovolt-ampere reactive per-phase rating of the switched three-phase capacitor bank and a decrease in the voltage with the switching out of the capacitor. The real-power flow on the feeder follows the bus voltage and decreases as the capacitor is switched out. The real power decreases from 1441 to 1421 kW [a decrease of 20 kW (1.4%)] in a little more than 0.25 second. The b- and c-phase real power decreased by 1.5% after the capacitor was switched out.

In Experiment 5, capacitor 109 on circuit 9 was switched in. At the start of this experiment, capacitors 101, 110, 111, and 122 were in service. Figure 5-4 shows the a-phase data during this switching operation. As in Experiment 1, the feeder reactive power decrease is about the same as the capacitor rating. However, the real power and bus voltage increased when the capacitor

TABLE 5-5 Capacitor switching experiments conducted on North Athens circuit No. 5 and South Athens circuit No. 9 (copyright 1988 by the IEEE)

Experiment	Capacitor switching	Phase	Preswitched state: Real power (kW)	Preswitched state: Reactive power (kvar)	Preswitched state: Bus voltage (kV)	Postswitched state: Real power (kW)	Postswitched state: Reactive power (kvar)	Postswitched state: Bus voltage (kV)	Change: Real power (kW)	Change: Real power (%)	Change: Reactive power (kvar)	Change: Bus voltage (kV)	Change: Bus voltage (%)
1[a]	102	a	1441.0	630.0	7.678	1421.0	805.0	7.650	−20.0	−1.4	175	−0.028	−0.4
	Switched	b	1527.5	692.5	7.596	1505.0	867.5	7.569	−22.5	−1.5	175	−0.027	−0.4
	out	c	1511.0	840.0	*c*	1488.0	1015.0	*c*	−23.0	−1.5	175		
2[a]	102	a	1344.0	860.0	7.681	1350.0	680.0	7.694	6.0	0.4	−180	0.013	0.2
	Switched	b	1429.0	925.0	7.598	1439.0	735.0	7.608	10.0	0.7	−190	0.010	0.1
	in	c	1424.0	1053.0	*c*	1439.0	865.0	*c*	15.0	1.1	−188		
3[a]	121	a	1385.0	665.0	7.706	1392.0	305.0	7.722	7.0	0.5	−360	0.016	0.2
	Switched	b	1533.0	735.0	7.621	1536.0	355.0	7.632	3.0	0.2	−380	0.011	0.1
	in	c	1483.0	905.0	*c*	1490.0	505.0	*c*	7.0	0.5	−400		
4[b]	109	a	3267.0	1185.0	7.499	3233.0	1575.0	7.450	−34.0	−1.0	390	−0.049	−0.7
	Switched	b	3330.0	1250.0	7.541	3295.0	1635.0	7.497	−35.0	−1.1	385	−0.044	−0.6
	out	c	3157.0	1340.0	7.595	3122.0	1680.0	7.554	−35.0	−1.1	340	−0.041	−0.5
5[b]	109	a	3270.0	1490.0	7.489	3298.0	1095.0	7.521	28.0	0.9	−395	0.032	0.4
	Switched	b	3384.0	1585.0	7.544	3404.0	1195.0	7.578	20.0	0.6	−390	0.034	0.5
	in	c	3131.0	1635.0	7.596	3152.0	1280.0	7.626	21.0	0.7	−355	0.030	0.4
6[b]	101	a	3319.0	1305.0	7.488	3335.0	1130.0	7.504	16.0	0.5	−175	0.016	0.2
	Switched	b	*d*	1365.0	7.527	*d*	1190.0	7.543			−175	0.016	0.2
	in	c	3200.0	1460.0	7.595	3219.0	1275.0	7.610	19.0	0.6	−185	0.015	0.2
7[b]	101	a	3409.0	1165.0	7.532	3379.0	1335.0	7.521	−30.0	−0.9	170	−0.011	−0.1
	Switched	b	*d*	1230.0	7.583	*d*	1400.0	7.572			170	−0.011	−0.1
	out	c	3269.0	1310.0	7.634	3237.0	1485.0	7.623	−32.0	−1.0	175	−0.011	−0.1
8[b]	122	a	3489.0	1595.0	7.506	3515.0	1435.0	7.519	26.0	0.7	−160	0.013	0.2
	Switched	b	*d*	1675.0	7.560	*d*	1505.0	7.571			−170	0.011	0.1
	in	c	3286.0	1745.0	7.615	3323.0	1580.0	7.627	37.0	1.1	−165	0.012	0.2

[a]Experiments 1–3 conducted on North Athens circuit No. 5 in April 1986.

[b]Experiments 4–8 conducted on South Athens circuit No. 9 in July 1986.

[c]Data not collected.

[d]Bad data.

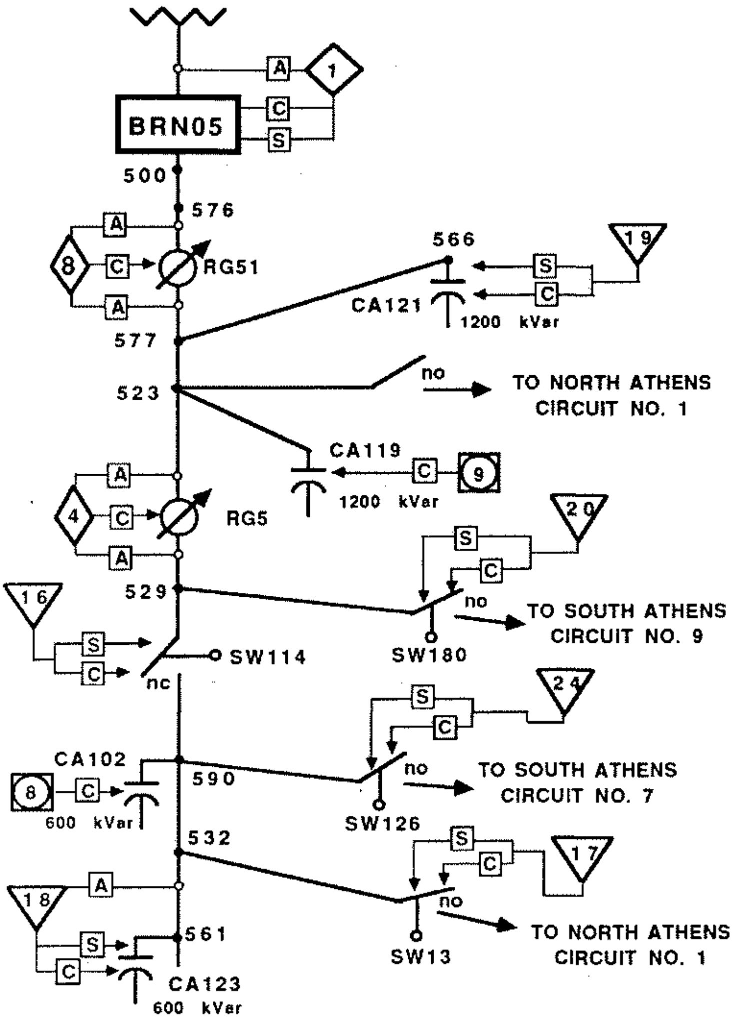

◇ = substation remote terminal unit (RTU) with two-way telephone communication
◇ = two-way feeder RTU with telephone communication
▣ = one-way feeder RTU with powerline communication
▽ = two-way feeder RTU with powerline and telephone communication
[A] = monitors analog power system values: power flows and voltage
[C] = control capacitor oil switch or load break switch
[S] = monitors status of capacitor oil switch or load break switch
BR = feeder circuit breaker
CA = three-phase capacitor bank
SW = motor-operated load break switch

Figure 5-1 Simplified one-line diagram of North Athens circuit No. 5 (copyright 1988 by the IEEE).

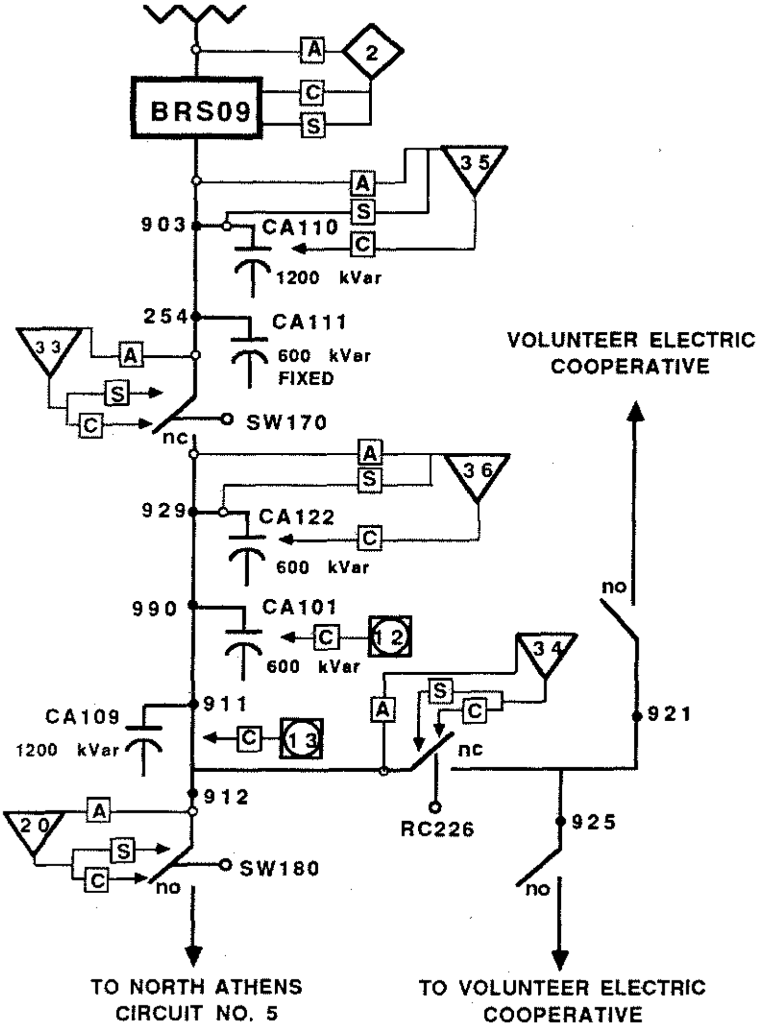

◇ = substation remote terminal unit (RTU) with telephone communication

□ = one-way RTU with powerline communication

▽ = two-way feeder RTU with powerline and telephone communication

[A] = monitors analog power system values: power flows and voltage.

[C] = controls capacitor oil switch or load break switch

[S] = monitors status of capacitor oil switch or load break switch

BR = feeder circuit breaker

CA = three-phase capacitor bank

SW = motor-operated load break switch

Figure 5-2 Simplified one-line diagram of South Athens circuit No. 9 (copyright 1988 by the IEEE).

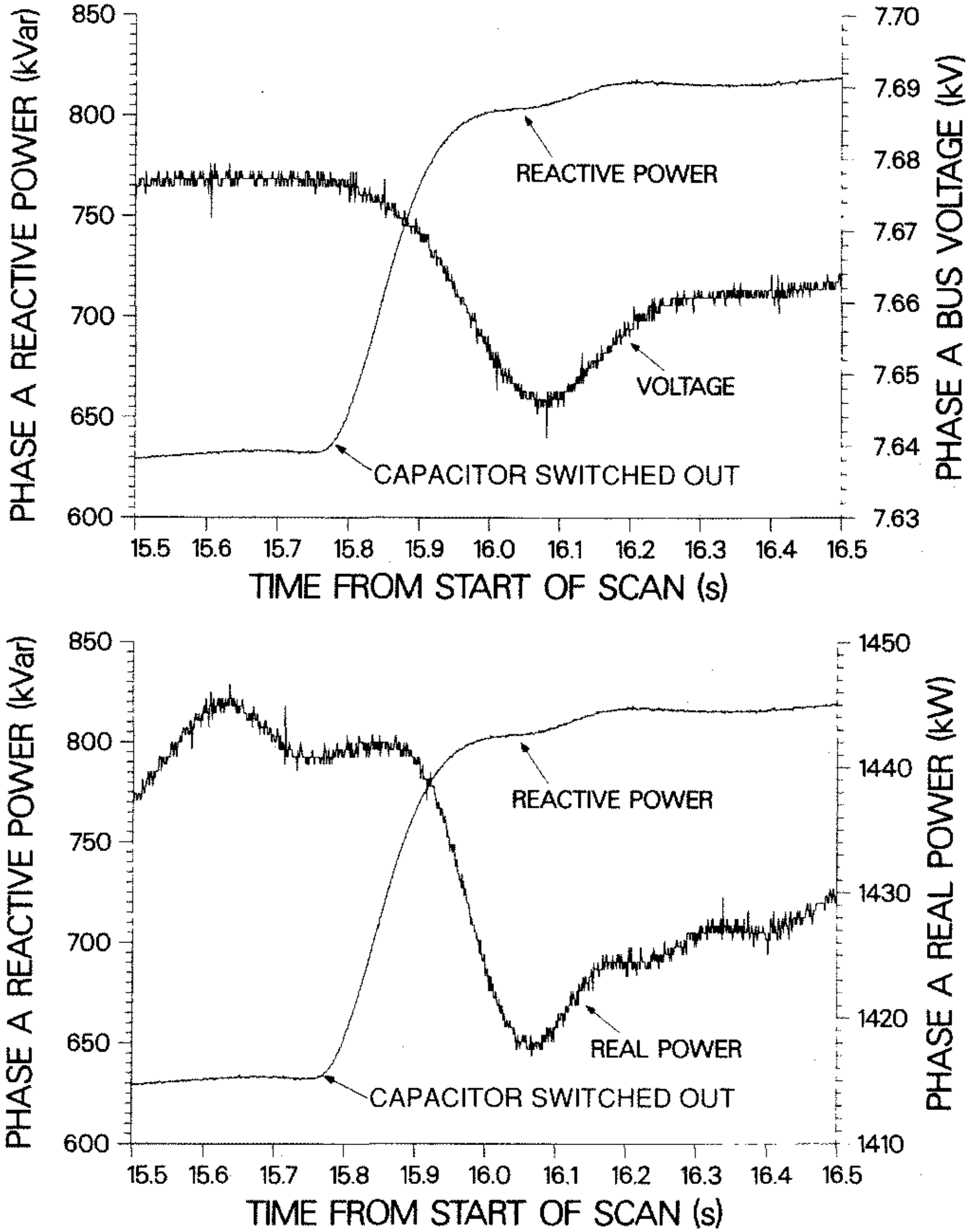

Figure 5-3 Measured bus voltage, real power, and reactive power for the switching out of a capacitor (copyright 1988 by the IEEE).

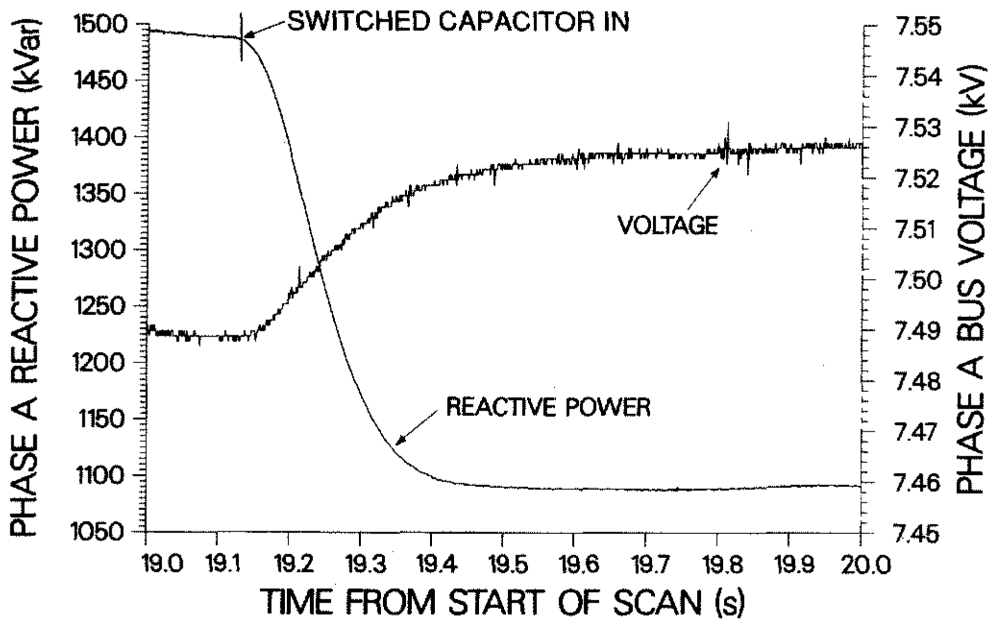

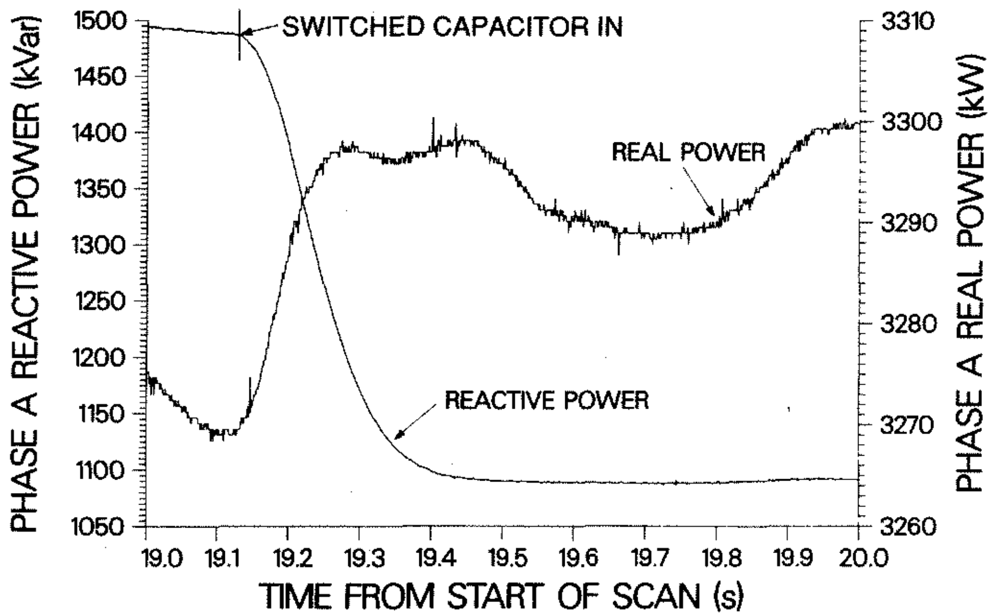

Figure 5-4 Measured bus voltage, real power, and reactive power for the switching in of a capacitor (copyright 1988 by the IEEE).

was switched in. The real power increased 0.9% on phase a, 0.6% on phase b, and 0.7% on phase c.

A postexperiment analysis was conducted to explain why the real power on circuit 5 decreased when capacitor 102 was switched out and why the real power on circuit 9 increased when capacitor 109 was switched in. These effects are contrary to those shown by simulation models that are not sensitive to voltage, which are common models in some traditional computer programs.

Postexperiment Analysis

A computer program[3] was developed to assess feeder load transfers with respect to the pre- and posttransfer voltage profile, losses, conductor thermal loading, and protection coordination. This program is described in Chapter 8. The program combines a three-phase power-flow analysis (three decoupled single phases per feeder that need not be balanced), short-circuit analysis (three-phase balanced fault), and data base manager. Subsequently, the program was modified to assess volt/var control functions such as capacitor switching and voltage regulator tap setting and to include voltage-sensitive load models. The program is designed to scale (1) the real component of the total power injection to the feeder at each bus or node on the basis of the actual kilowatt-hour billing data compiled by AUB and (2) the reactive-power injection of the total power on the basis of the capacity kilovolt-ampere rating of each distribution transformer on the AUB system. The three load models considered are constant power (power does not change as a function of voltage), constant current (sensitive to voltage), and constant impedance (sensitive to voltage squared). As shown in Table 5-5 and the data plots of Figures 5-3 and 5-4, the real power increased or decreased as the voltage increased or decreased when the capacitor was switched in or out, indicating that the loads are sensitive to voltage.

The analysis of the switching out of the capacitors illustrates how different load models affect the simulation results (feeder real-power flow and line losses) differently. The preswitched and postswitched conditions of circuit 5 for experiment 1 are given in Table 5-6 along with the calculated line losses for the actual postswitched state. The sum of the a-, b-, and c-phase real-power flows decreased by 65.5 kW, while the total calculated real-line loss increased by 7.2 kW.

In the four simulation cases of experiment No 1 (Table 5-7), the line losses increased when the capacitor bank was switched out, as would be expected; however, the greatest increase occurs for the loads modeled as constant power. There is <4% difference between case 1 (constant-power load model) and case 4 (the best voltage-sensitive representation). The error between the actual postswitched data and simulation data is the smallest for case 4, when the real load is modeled as constant impedance and the reactive load is modeled as constant current. This case results in a lower line-loss increase than when the loads are modeled as constant power. However, the feeder real-power flows differ as follows: (1) for the constant-power load representation, real power increases by 0.2 to 0.3%; (2) for the constant-current load representation, real power decreases by 0.6 to 0.7%; (3) for the

TABLE 5-6 Preswitched and postswitched data for experiment 1 (switching out of capacitor) (copyright 1988 by the IEEE)

Capacitor state	Bus voltage at breaker (kV) phase			Total feeder real power (kW) phase			Total feeder reactive power (kvar) phase			Total feeder real losses[a] (kW) phase			Total feeder reactive losses[a] (kvar) phase		
	a	b	c	a	b	c	a	b	c	a	b	c	a	b	c
Preswitched state (in)	7.678	7.596		1441	1527.5	1511.0	630.0	692.5	840.0	23.8	25.8	29.6	55.5	58.9	70.6
Postswitched state (out)	7.650	7.569		1421	1505	1488	805.0	867.5	1015.0	25.9	27.9	32.6	61.1	64.7	78.5
Change	−0.4%	−0.4%		−1.4%	−1.5%	−1.5%	27.8%	25.3%	20.8%	8.8%	8.1%	10.1%	10.1%	9.8%	11.2%

[a]Calculated with a decoupled radial power-flow program.

[b][(Postswitched value minus preswitched value) divided by preswitched value] multiplied by 100%.

TABLE 5-7 Simulated postswitching states for experiment 1 (switching out of capacitor) (copyright 1988 by the IEEE)

Postswitching simulation cases[b]	Bus voltage at breaker (kV) phase			Total feeder real power[a] (kW) phase			Total feeder reactive power[a] (kvar) phase			Total feeder real losses[a] (kW) phase			Total feeder reactive losses[a] (kvar) phase		
	a	b	c	a	b	c	a	b	c	a	b	c	a	b	c[c]
Case 1: CP	7.650	7.569		1444.0	1530.6	1514.8	819.4	881.8	1028.2	26.7	28.9	33.4	63.2	67.0	80.6
Error[d]				1.6%	1.7%	1.8%	1.8%	1.6%	1.3%	3.1%	3.6%	2.5%	3.4%	3.6%	2.6%
Change[e]				0.2%	0.2%	0.3%	30.1%	27.3%	22.4%	12.2%	12.0%	12.8%	13.9%	13.8%	14.2%
Case 2: CI	7.650	7.569		1431.3	1517.5	1501.4	808.1	870.3	1018.5	26.2	28.3	33.1	61.9	65.6	79.7
Error[d]				0.7%	0.8%	0.9%	0.4%	0.3%	0.3%	1.2%	1.4%	1.5%	1.3%	1.4%	1.5%
Change[e]				−0.7%	−0.7%	−0.6%	28.3%	25.7%	21.3%	10.1%	9.7%	11.8%	11.5%	11.4%	12.9%
Case 3: CZ	7.650	7.569		1419.3	1505.2	1488.6	797.5	859.4	1005.8	25.7	28.8	32.4	60.7	64.4	78.1
Error[d]				0.1%	0.0%	0.0%	0.9%	0.9%	0.9%	0.8%	0.4%	0.6%	0.7%	0.4%	0.5%
Change[e]				−1.5%	−1.5%	−1.5%	26.6%	24.1%	19.7%	8.0%	7.8%	9.5%	9.4%	9.3%	10.6%
Case 4	7.650	7.569		1419.1	1505	1488.3	807.3	869.5	1017.5	26.0	28.1	32.8	61.4	65.0	79.0
Error[d]				0.1%	0.0%	0.0%	0.3%	0.2%	0.2%	0.4%	0.7%	0.6%	0.4%	0.5%	0.6%
Change[e]				−1.5%	−1.5%	−1.5%	28.1%	25.6%	21.1%	9.2%	8.9%	10.8%	10.6%	10.4%	11.9%

[a]Calculated by a decoupled radial power flow program.

[b]Case 1: real and reactive loads modeled as constant power (CP); Case 2: real and reactive loads modeled as constant current (CI); Case 3: real and reactive loads modeled as constant impedance (CZ); and Case 4: real load component modeled as constant current and reactive load component modeled as 50% constant current and 50% constant impedance.

[c]Calculated assuming that the phase c voltage was the same as the phase b voltage.

[d]Error = {absolute value of [(calculated postswitched value minus experimental postswitched data) divided by experimental postswitched data]} multiplied by 100%.

[e]Change = [(calculated postswitched value minus experimental preswitched data) divided by experimental preswitched data] multiplied by 100%.

constant-impedance load representation, real power decreases by 1.5%. The experimental data showed that the real power decreased by 1.4 to 1.5%. The reactive power was not as sensitive to voltage in this experiment as was the real power, so simulation case 4 was performed. Case 4 resulted in the smallest error between the measured and calculated real- and reactive-power flows.

The preswitched and postswitched conditions of circuit 9 for experiment 5 are given in Table 5-8 along with the calculated line losses for the actual postswitched state. The sum of the a-, b-, and c-phase real-power flows increased by 69 kW, while the calculated total real-line loss decreased by 9 kW. In the four simulation cases of this experiment, given in Table 5-9, the line losses decreased when the capacitor bank was switched in, as would be expected; however, the greatest decrease occurred for the loads modeled as constant power. There is <2% difference between case 1 (constant-power load model) and case 4 (the best voltage-sensitive representation). The error between the actual postswitched data and the simulation data is the least for case 4, when the real load is modeled as constant current and the reactive load is modeled as a combination of constant current and constant impedance. This case results in a smaller decrease in line loss than when the loads are modeled as constant power. However, the feeder real-power flows differ as follows: (1) for the constant-power load representation, the real power decreases by 0.1%; (2) for the constant-current load representation, real power increases by 0.7 to 0.8%; (3) for the constant-impedance load representation, real power increases by 1.4 to 1.6%. The experimental data showed that the real power increased by 0.6 to 0.9%. For this experiment, the reactive power was more sensitive to voltage than was the real power, so simulation case 4 was performed. As in the simulation cases for experiment 1, case 4 resulted in the least error between the measured and calculated real- and reactive-power flows.

LOAD-TAP-CHANGING TRANSFORMER TEST RESULTS

In June 1986, the two 20-MVA load-tap-changing (LTC) transformers at the South Athens Substation were controlled for 40 seconds to observe the response of real power and reactive power with changes in bus voltage. A high-speed data acquisition system (see Chapter 3) was used to collect the real and reactive power and bus voltage for South Athens circuit No. 9 at the circuit breaker. The LTC transformer tap changers were initially set at tap position −3 (3 positions below the nominal setting) when the experiment began. During the experiment, the tap settings of the LTC transformers were raised from position −3 to position 7 in a sequential fashion within 15 seconds, kept at position 7 for ~15 seconds, and then lowered from position 7 to position 3 in 10 seconds.

TABLE 5-8 Preswitched and postswitched data for experiment 5 (switching in of capacitor) (copyright 1988 by the IEEE)

Capacitor state	Bus voltage at breaker (kV) phase			Total feeder real power (kW) phase			Total feeder reactive power (kvar) phase			Total feeder real losses[a] (kW) phase			Total feeder reactive losses[a] (kvar) phase		
	a	b	c	a	b	c	a	b	c	a	b	c	a	b	c
Preswitched state (out)	7.489	7.544	7.596	3270	3384	3131	1490	1585	1635	39.8	42.3	36.4	129.5	136.8	118.5
Postswitched state (in)	7.521	7.578	7.626	3298	3404	3152	1095	1195	1280	36.9	39.1	33.5	119.0	125.1	107.9
Change[b]	0.4%	0.5%	0.4%	0.9%	0.6%	0.7%	−26.5%	−24.6%	−21.7%	−7.3%	−7.6%	−8.0%	−8.1%	−8.6%	−8.9%

[a]Calculated by a decoupled radial power flow program.

[b]Change = [(postswitched value minus preswitched value) divided by preswitched value] multiplied by 100%.

TABLE 5-9 Simulated postswitching states for experiment 5 (switching in of capacitor) (copyright 1988 by the IEEE)

Postswitching simulation cases[b]	Bus voltage at breaker (kV) phase			Total feeder real power[a] (kW) phase			Total feeder reactive power[a] (kvar) phase			Total feeder real losses[a] (kW) phase			Total feeder reactive losses[a] (kvar) phase		
	a	b	c	a	b	c	a	b	c	a	b	c	a	b	c
Case 1: CP	7.521	7.578	7.626	3266.3	3380	3127	1058.7	1157.2	1246.8	36.1	38.4	32.8	116.2	122.7	105.7
Error[c]				1.0%	0.7%	0.8%	3.3%	3.2%	2.6%	2.2%	1.8%	2.1%	2.4%	1.9%	2.0%
Change[d]				−0.1%	−0.1%	−0.1%	−28.9%	−27.0%	−23.7%	−9.3%	−9.2%	−9.9%	−10.3%	−10.3%	−10.8%
Case 2: CI	7.521	7.578	7.626	3295.1	3410	3152	1081.3	1181.2	1268.3	36.8	39.2	33.4	118.6	125.3	107.7
Error[c]				0.1%	0.2%	0.0%	1.3%	1.2%	0.9%	0.3%	0.3%	0.3%	0.3%	0.2%	0.2%
Change[d]				0.8%	0.8%	0.7%	−27.4%	−25.5%	−22.4%	−7.5%	−7.3%	−8.2%	−8.4%	−8.4%	−9.1%
Case 3: CZ	7.521	7.578	7.626	3323.2	3439	3176	1103.3	1204.6	1289.2	37.5	40.0	34.0	120.9	127.8	109.7
Error[c]				0.8%	1.1%	0.8%	0.8%	0.8%	0.7%	1.6%	2.3%	1.5%	1.6%	2.2%	1.7%
Change[d]				1.6%	1.6%	1.4%	−26.0%	−24.0%	−21.1%	−5.8%	−5.4%	−6.6%	−6.6%	−6.6%	−7.4%
Case 4	7.521	7.578	7.626	3295	3410	3152	1091.4	1192	1278.1	36.9	39.2	33.5	118.8	125.5	108
Error[c]				0.1%	0.2%	0.0%	0.3%	0.3%	0.1%	0.0%	0.3%	0.0%	0.2%	0.3%	0.1%
Change[d]				0.8%	0.8%	0.7%	−26.8%	−24.8%	−21.8%	−7.3%	−7.3%	−8.0%	−8.3%	−8.3%	−8.9%

[a]Calculated by a decoupled radial power flow program.

[b]Case 1: real and reactive loads modeled as constant power (CP); Case 2: real and reactive loads modeled as constant current (CI); Case 3: real and reactive loads modeled as constant impedance (CZ); and Case 4: real load component modeled as constant current and reactive load component modeled as 50% constant current and 50% constant impedance.

[c]Error = {absolute value of [(calculated postswitched value minus experimental postswitched data) divided by experimental postswitched data]} multiplied by 100%.

[d]Change = [(calculated postswitched value minus experimental preswitched data) divided by experimental preswitched data] multiplied by 100%.

As the LTC tap settings were raised from position −3 to position 7, the voltage on circuit 9 increased from 7.24 to 7.61 kV; and as the LTC tap settings were lowered from position 7 to position 3, the voltage decreased from 7.61 to 7.46 kV. Figure 5-5 shows the real and reactive power and the bus voltage data collected at the circuit breaker of circuit 9 for each LTC transformer tap setting. The experiment resulted in a less than ±5% change in circuit voltage and real power and a less than ±20% change in reactive power. From the raw data, the real and reactive power injected into the circuit was observed to increase with increasing substation bus voltage and to decrease with decreasing bus voltage.

In the previous section, a polynominal in voltage was used to analyze the real and reactive power change due to capacitor switching. In this section, a

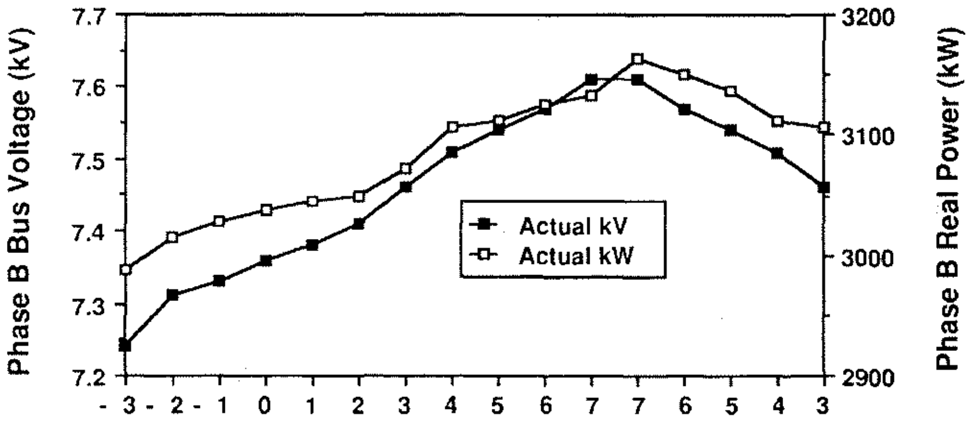

a

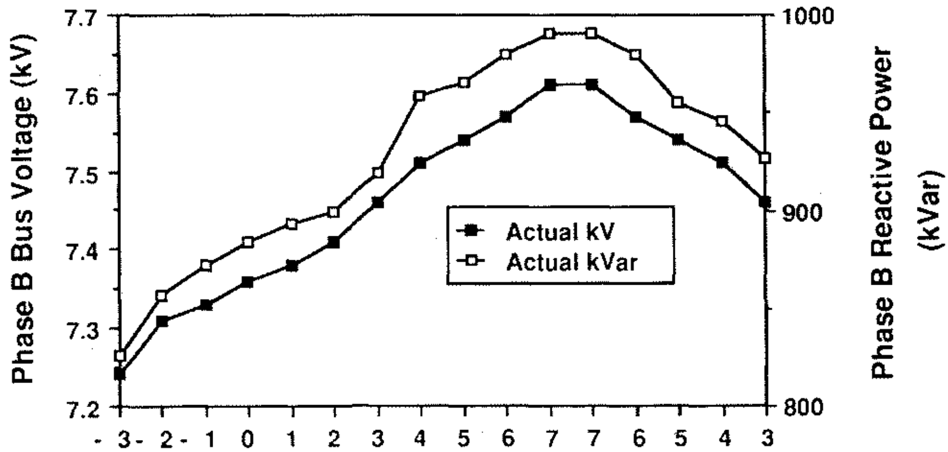

b

Figure 5-5 Actual real and reactive power and bus voltage for load-tap-chaning (LTC) transformer tests.

much simplier approach is applied to assess the voltage sensitivity of real and reactive power changes due to LTC control actions. In Chapter 8, the approach of using a polynominal in voltage is also applied to the LTC test results. Both approaches are consistent as they show that load is sensitive to voltage change.

The changes in real power from the initial value for tap position −3 were computed for real power; it was assumed that (1) the changes are due only to losses (known as a constant-power model), (2) real power is a function of voltage to the first power (the entire feeder represented as a constant-current model), and (3) real power is a function of voltage squared (the entire feeder represented as a constant-impedance model). The changes in reactive power from the initial value for tap position −3 were computed for the same three models and an additional model that considered reactive-power changes as a function of voltage to the fourth power. A power-flow program was used to calculate the values for the constant-power model, and the following equation was used to calculate the real and reactive power for the constant current, constant impedance, and fourth-order voltage models.

$$P_{t+1} = \left\{\frac{V_{t+1}}{V_t}\right\}^n P_t \quad ,$$

where

P_{t+1} = the calculated real-power value for the next tap setting;
P_t = the calculated real-power value for the previous tap setting;
V_{t+1} = the actual voltage for the next tap setting;
V_t = the actual voltage for the previous tap setting;
n = power value (1 for constant current, 2 for constant impedance, 4 for fourth-order model);
t = 1 to 15, where 1 represents the starting tap setting of −3 and 15 represents the next to the last tap setting of 3.

To start the calculations, the real-power value for tap position −2 was computed from the above equation, and the actual real power and bus voltage for tap setting −3 and the bus voltage for tap setting −2 were used. Only the values of 1 and 2 for n were used for calculating real power. This procedure was repeated to obtain the fifteen calculated values for the constant-current and constant-impedance models. An identical equation was used to calculate reactive-power data for n equal to 1, 2, and 4.

A comparison of calculated and actual real and reactive power is shown in Figure 5-6. The decreasing trend of the real and reactive power with increasing voltage and the increasing trend with decreasing voltage for the constant-power models (constant P and constant Q) are quite contrary to the trend observed for the actual real- and reactive-power data. The voltage-

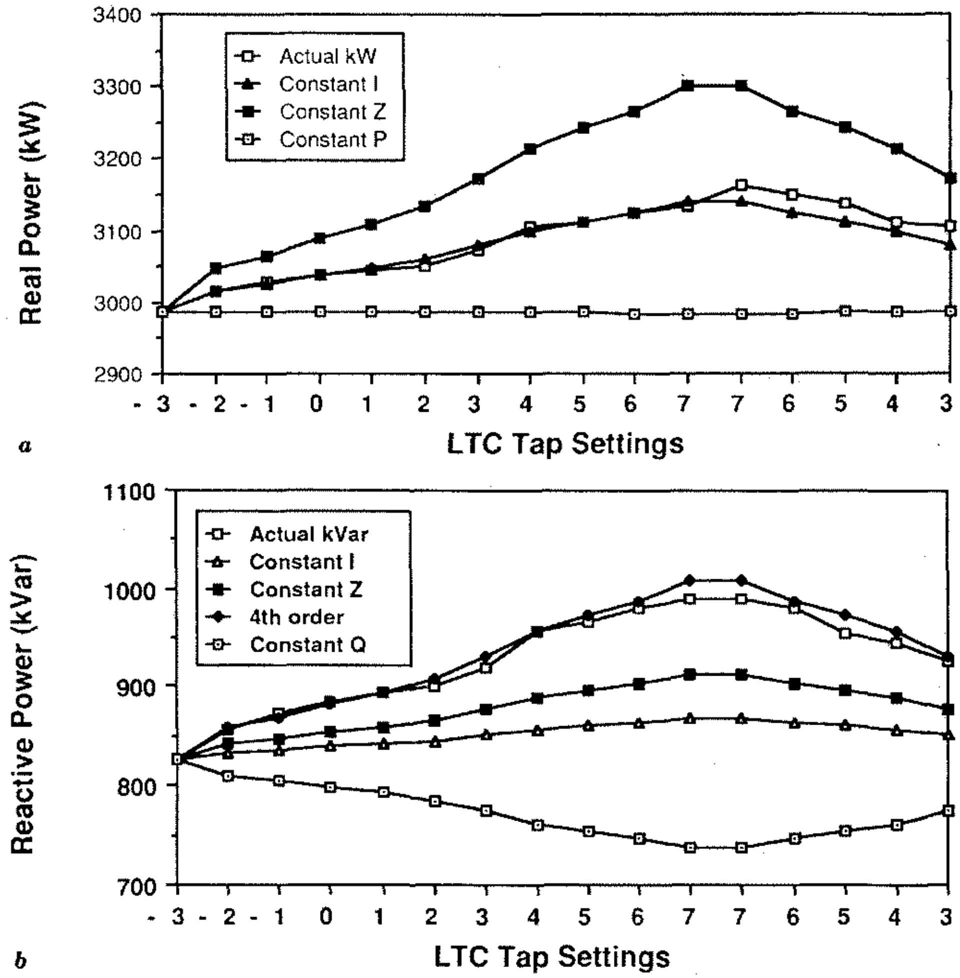

Figure 5-6 Comparison of actual and calculated real, and reactive power data.

sensitive models more correctly simulated the trend. Further, the calculated data seem to indicate that the reactive power is more sensitive to voltage changes than is the real power. A pure constant-current feeder model closely replicates the actual real-power data of the LTC transformer test. A pure fourth-order feeder model closely replicates the reactive-power data of the LTC transformer test. Figure 5-7 plots the error percentage in each of the simplified model calculations and shows that the constant current model is within a 1% error of the actual real-power data and the fourth-order voltage model is within a 2% error of the actual reactive-power data. The above LTC transformer test data are again considered in Chapter 8, in which the actual data are more correctly modeled by using a Taylor series expansion of the real and reactive power consumed by the circuit loads.

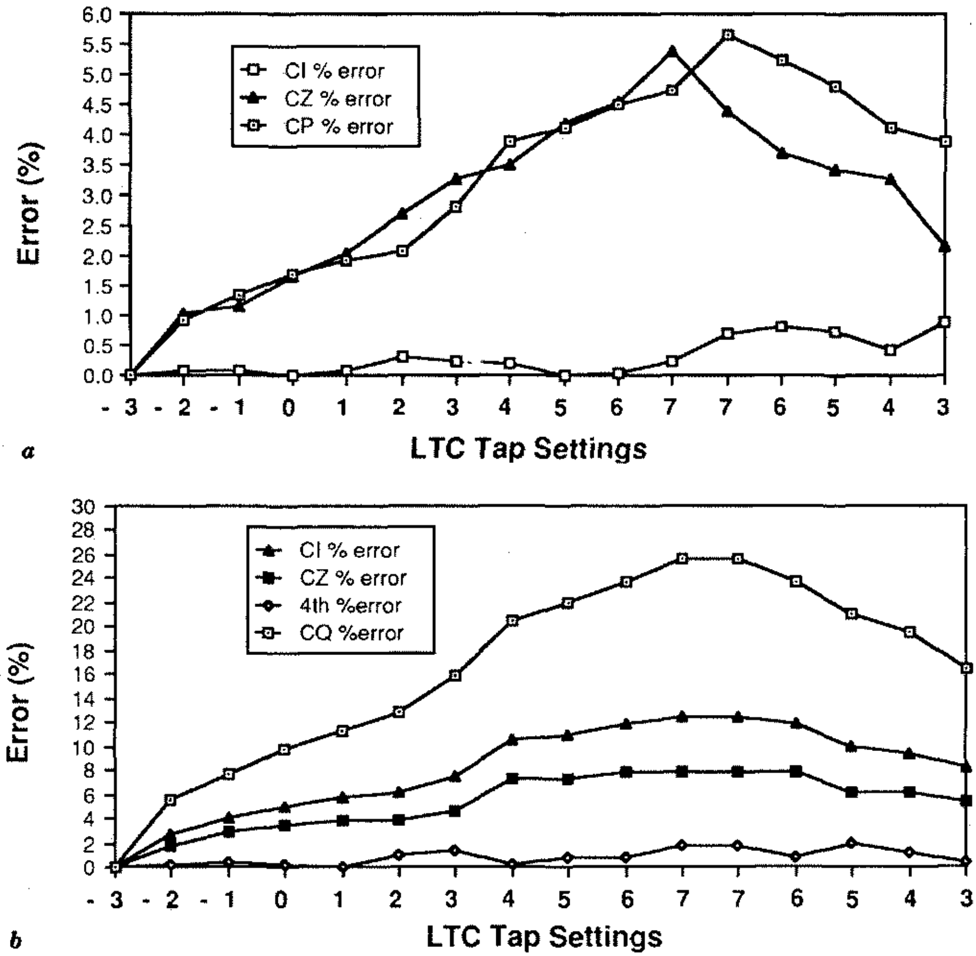

Figure 5-7 Relative error between computed and actual real, and reactive power.

SUMMARY

Field experiments were conducted to determine the effects of capacitor switching and voltage control on feeder operating variables as measured at the feeder breaker by three types of data acquisition systems. The slower data acquisition rate of the distribution automation system (one sample every 20 seconds) and the data acquisition rate of a commercial high-speed data acquisition system (one sample every 7 seconds) were adequate to measure the effect of capacitor switching and voltage control on the reactive-power injection and phase voltage but were not adequate to measure the effect on real-power injection. A high-speed data acquisition system (1000 samples/second for each channel) with filtering was necessary to measure the effect of capacitor switching and voltage control on the real-power injection.

A sampling rate of 1000 samples per second per channel is much faster than necessary to separate changes in real power due to the capacitor switching from noise, but this sampling rate is what was available at the time the tests were performed. Sampling rates of 50 samples were made available later and found to be adequate to separate load noise from changes due to load control experiments (see Chapter 6).

Consistent with expectations, the switching in of a capacitor bank to improve the power factor results in decreased reactive-power (var) injection and increased phase voltages. However, contrary to some simulation models and pre-experiment analysis that assumed constant-power load representations, a reduction in real-power injection, reflecting reduced line losses, is not observable at the substation. In fact, the measured real-power injection increases. Similarly, the switching out of the capacitor bank results in increased var injection, decreased phase voltages, and decreased real-power injection. The experiments were repeated several times to confirm the repeatability of the results.

Analysis of the capacitor switching experimental results with voltage-sensitive load models shows that, while feeder losses are reduced following feeder power factor correction, the attendant improvement in voltage profile results in an increase in load that exceeds the amount of loss reduction. Further, the postexperiment analysis shows that the line loss reduction is slightly less for a voltage-sensitive load model than for a voltage-insensitive load model (constant power). Consequently, distribution system operators employing supervisory control and data acquisition systems will not be able to observe the loss reduction associated with capacitor switching to improve the power factor. System planners will need to know the exact nature of load sensitivity to voltage to precisely quantify the economic benefits of installing and operating capacitor banks. Fortunately, high-speed data acquisition provides a convenient means of obtaining the data necessary to determine the load sensitivity to voltage.

Analyses of the LTC transformer tests confirm the conclusions of the capacitor switching test results. Real and reactive power are sensitive to voltage changes, and reactive power can be more sensitive than real power. In the above analysis, simplified voltage-sensitive models of the entire feeder were needed to simulate the effects of voltage control on real and reactive power for circuit 9. In Chapter 8, a Taylor series expansion of real and reactive power is used to more correctly model the load sensitivity to voltage.

REFERENCES

1. S. L. Purucker et al., "Automation and Control of a Distribution Power System," *1984 Control of Power Systems Conference*, IEEE Conference Record 84-CH-2027-1 (March 1984).

2. S. L. Purucker, R. J. Thomas, and L. D. Monteen, "Feeder Automation Designs for Installing an Integrated Distribution Control System," *IEEE Trans. Power Appar. Syst.* **PAS-104**(4), 2929–34 (October 1985).
3. D. T. Rizy et al., "Distribution Automation Applications Software for the Athens Utilities Board," IEEE Paper No. 88 WM 097-8, presented at the IEEE PES Winter Meeting, New York, February 1988; published in *IEEE Trans. Power Delivery,* **4**(1), 715–24 (January 1989).
4. W. F. Tinney and C. E. Hart, "Power Flow Solution by Newton's Method," *IEEE Trans. Power Appar. Syst.* **PAS-86,** 1449–60 (November 1967).

6

LOAD CONTROL EXPERIMENTS*

J. H. Reed, R. P. Broadwater,
A. Chandrasekaran, and W. R. Nelson

This chapter describes the structure and the results of the load control experiments that were conducted as part of the AACE. Customers' water heaters, air conditioners, and heat pumps were systematically controlled to evaluate the effectiveness and impacts of load control.

The findings show that water heater control is an effective way of shifting load without causing notable impact to customers. Air conditioner cycling is also an effective way to shift load, although customers are more aware of the impacts. Under certain circumstances, heat pump control may lead to larger peaks and increased energy use by customers. To be effective, heat pump control must be done at temperatures below 20°F or with specific (new) types of control circuits.

The chapter includes the objectives of the load control experiment, the experiment design, the placement of equipment, customer recruiting, the results of the experiments, and recommendations for load control design. The

*This chapter is based on material in IEEE Paper No. 88 WM 095-2, "Monitoring Load Control at the Feeder Level Using High-Speed Monitoring Equipment," by J. H. Reed, W. R. Nelson, G. R. Wetherington, E. R. Broadaway; and material in IEEE Paper No. 88 WM 095-5, "Load Control Experiments with Heat Pumps During the Winter," by J. H. Reed, R. P. Broadwater, and A. Chandrasekaran, which were first presented at the IEEE Power Engineering Society Winter Meeting, February 1988, New York. The chapter also contains material in IEEE Paper No. 88 SM 596-9, "Analysis of Water Heater Data from Athens Load Control Experiment," by J. H. Reed, J. C. Thompson, R. P. Broadwater, and A. Chandrasekaran, which was first presented at IEEE Summer Meeting, July 1988, Portland, Oregon (copyright 1988 by the IEEE).

chapter also describes experiments in which high-speed monitoring equipment was used to take measurements during the experiments. The results from these experiments suggest new methods of analyzing and recording customer loads.

Utilities have conducted over 200 load control studies in recent years.[1] While these studies give some indication of the promise and problems of load control, they raise as many questions as they answer. Many of the studies were either poorly designed or deficient in monitoring. Often, results have not been available to other utilities or are not transferable. Only one study of heat pump control is cited in the Institute of Electrical and Electronics Engineers (IEEE) Bibliography.[2] Almost all of these experiments assume that customers' electric power usage is uniform, and the strategies that have been used have controlled the customers uniformly.

The objectives of the Athens experiments were to

- evaluate the ability to shift electric power demand on the system by controlling water heaters, central air conditioners, and space heaters;
- evaluate whether the utility or customers gained or lost energy when load was shifted;
- evaluate the impact of direct load control on customers;
- segment customers into classes and differentially control customers to distribute the impacts of load control;
- use the data collected to develop generalized models that could be used by other utilities to evaluate the load control option; and,
- evaluate the reliability of the equipment.

Delays in equipment installation and problems with the equipment made it impossible to successfully meet all of these ambitious objectives. However, accomplishments related to these objectives significantly advanced the understanding of customer loads and load control.

CONTROLLING THE LOAD

The objective of a load control program is to reduce system peaks by transferring demand from the peak period to a time of day when the demand is lower. To effectively accomplish this objective, information is needed to determine when to control the load, how much load is to be controlled, and how this will be accomplished

For the AACE, the basic load control objective was to reduce the system peak. During the winter, this was done by controlling the morning peak and deferring that load until mid- to late morning. Similarly, energy from the winter evening peak can be deferred until later in the evening. Control periods were selected to maximize the coincidence between the peak system load and peak appliance load. During the summer, the objective was to defer load from midday until late evening. Controlling loads in the morning would shift load to midday and add to the midday peak.

Deciding when to control loads was determined by comparing diversified demand curves for individual appliances with the system load shape. The diversified demand of an appliance is the average load for all units of a specific type of appliance at a specific time. If 25 of 100 air conditioners on a feeder are each using 4 kW at 4 p.m., the diversified demand is 1 kW [(25 × 4)/100]. Figure 6-1 illustrates how the control period was selected using winter load curves. The x-axis represents the hour of the day, and the y-axis represents the percentage of the daily peak. This percentage is calculated by dividing the hourly value by the value for the peak and multiplying by 100. The solid curve represents the system load, and the curve illustrated by the broken line is the water heating curve. The latter curve was derived from data supplied by TVA. A comparison of the two curves shows that the greatest load relief will occur if water heaters are controlled in the morning and in the evening, when appliance demands coincide with system peaks.

The concept of duty cycle* provides a useful tool for evaluating load control. The duty cycle of an appliance is determined by the demand for

Duty cycle is the proportion of a specified time interval, usually an hour, that an appliance is operating. An air conditioner duty cycle of 0.33 means that the air conditioner is running 10 minutes during a half hour. Normally, the duty cycle of an appliance is not constant but changes throughout the day in response to human behavior, environmental conditions, etc. Sometimes the term "natural duty cycle" is used to describe the duty cycle of an uncontrolled appliance.

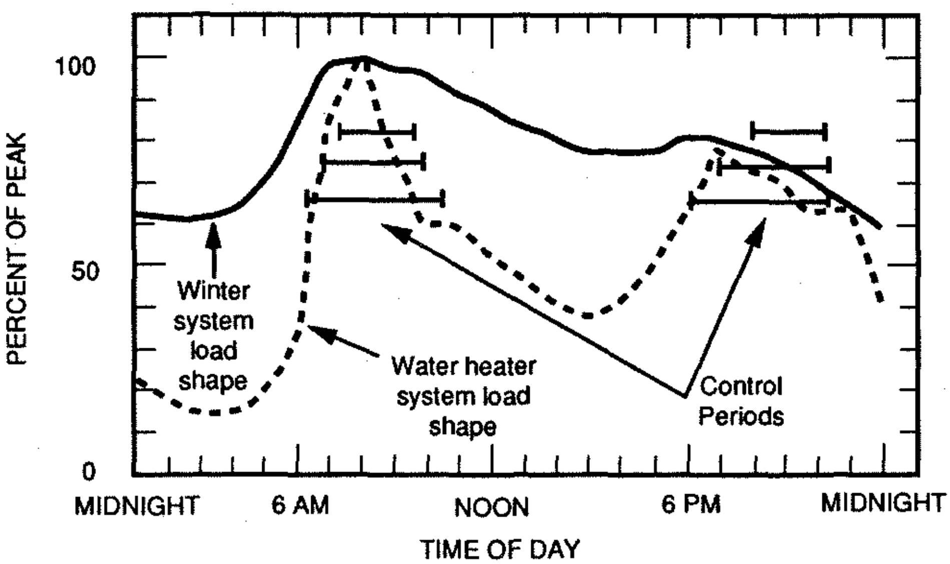

Figure 6-1 System load and water heater load shapes with control period overlays.

service and the capacity of the appliance to meet the demand. The demand for service is conditioned by the desired level of service (e.g., thermostat setting, environmental conditions, and occupant behavioral patterns).

Figure 6-2 shows typical summer and winter load shapes for the AUB system. The winter load shape is bimodal, with a morning peak and a secondary peak in the evening. The summer system curve shows a midday peak that is sustained until evening, when the load decreases.

An important objective of load control is that the demand for service can be deferred without seriously affecting a customer's comfort. The amount of demand that can be deferred and the length of time it can be deferred depend on the service. Thus, if an air conditioner has a duty cycle of exactly 0.5 (15 minutes out of 30), control must be exercised for more than 15 minutes during the half hour for the utility to experience any relief. The utility will benefit from load control only when the intensity of control is greater than one minus the duty cycle.

The duty cycle of an appliance normally varies throughout the day as conditions influencing demand change and from user to user (because the conditions influencing demand are not identical). Figure 6-3 shows the distribution of the duty cycles for air conditioners being monitored at Athens on a 94°F day for half-hour periods beginning at 10 a.m., 2 p.m., and 10 p.m. No control actions were implemented on this day. The *x*-axis represents the six categories of duty cycle, or the percentage of the half hour into which air conditioners were placed. The *y*-axis is the percentage of machines in the duty cycle classification. At 10 a.m., 90% of the air conditioners are running less than 60% of the time. As the afternoon progresses, the duty cycles

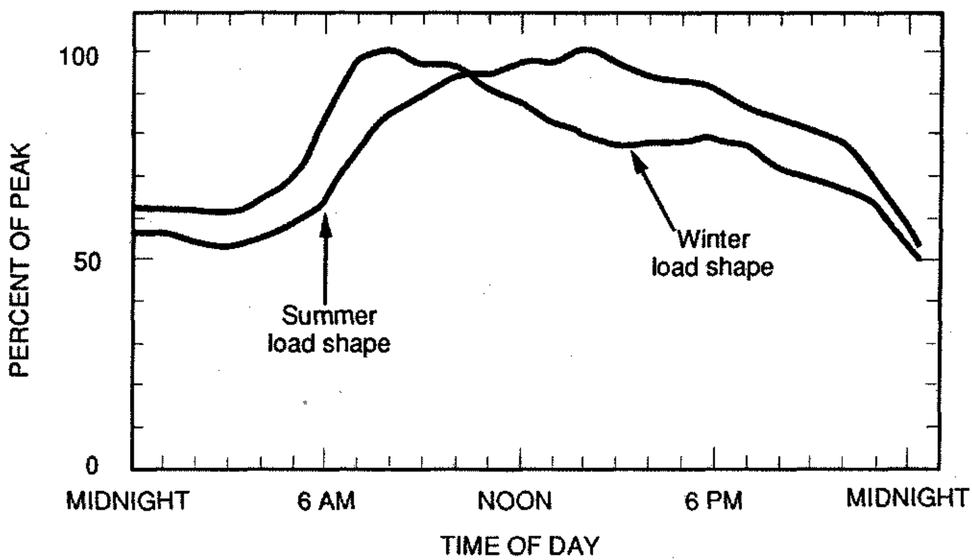

Figure 6-2 Summer and winter load shapes at Athens, Tennessee.

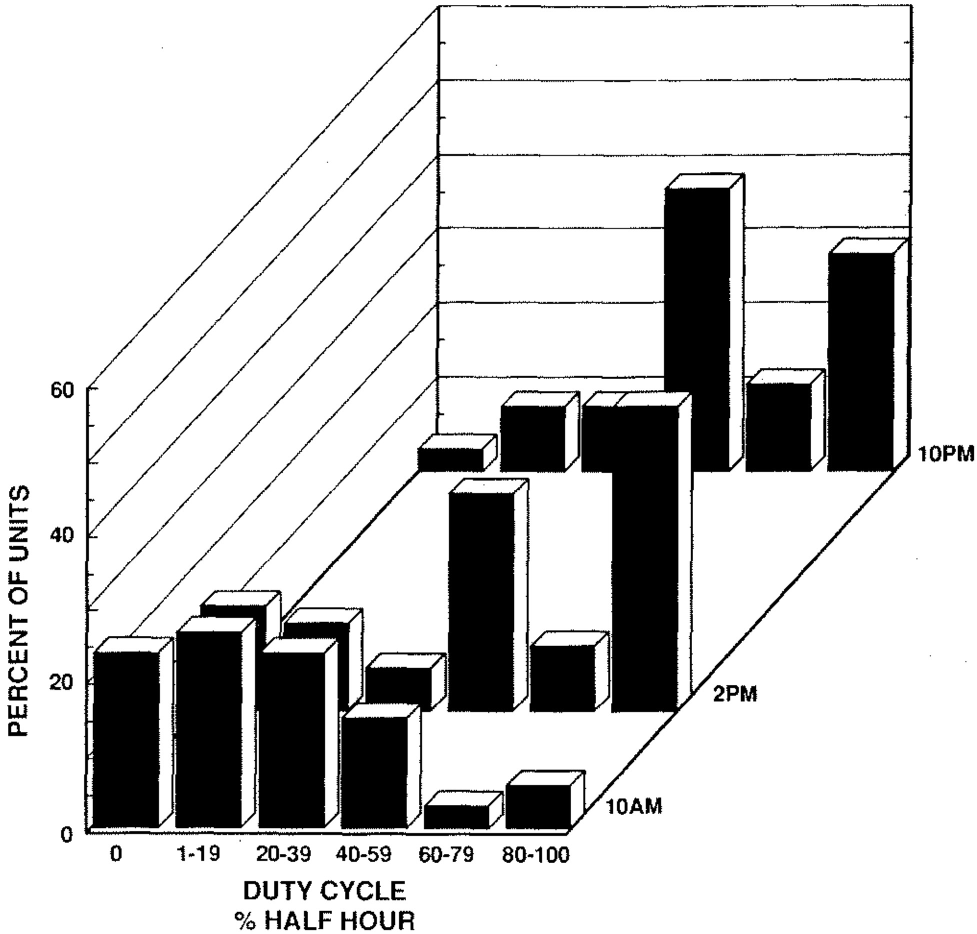

Figure 6-3 Distribution of air conditioner duty cycles in Athens, Tennessee—July 20, 1986.

become longer. By 2 p.m., more than half the air conditioners are running more than 60% of the time. At 10 p.m., after the sun has set and the outdoor temperature cools, almost half the air conditioners are running 40–60% of the time.

As Figure 6-3 illustrates, customers do not have the same duty cycles. At 10 a.m., customer duty cycles are spread across the entire spectrum. If the utility controlled air conditioners at an intensity of 0.33 (10 minutes out of 30) at 10 o'clock, about 10% of the customers (those with duty cycles greater than 0.66) would actually experience a reduction in the amount of time their air conditioner was running. Actually, the latter statement is true only in a theoretical sense. A customer whose appliance has a duty cycle less than 0.66 may experience some effect if the appliance is in use when the control action occurs. The effect may continue until the quiescent period of the appliance and the off portion of the control cycle* coincide.

The duty cycles of water heaters are driven by behavior rather than temperature. Unlike buildings, water heaters have sufficient storage so that they may be controlled for several hours.

LOAD CONTROL GROUPS

The preceding discussion shows that exercising the same intensity of control† over every customer causes some customers to notice greater effects of control because of the normal (natural) variations in duty cycle between households.

To equalize the impacts of control, we grouped households with similar duty cycles and varied the intensity of control for each group so that the impacts would be about equal. For example, if the goal is to reduce the duty cycle of all households by 0.1 or 0.2, the households should be grouped and then the intensity of control set at 1 minus the duty cycle plus 0.1 or 0.2. This is a crude but effective way of accomplishing the goal.

In attempting to equalize the impact, a concept of "sizing ratio" was developed. Sizing ratio is the number of Btu's required for heating or cooling a thermal envelope to a desired level (at a specified outdoor temperature) divided by the rating of the heating or cooling appliance. Households with large-capacity units relative to the space-conditioning loads have a sizing ratio greater than 1. Households with small-capacity units relative to space-conditioning loads have a sizing ratio less than 1 and would not meet the cooling load under extreme conditions.

The AUB load control equipment installers calculated the heating and/or cooling load for each home. Then, a ratio of the heating/cooling load to the capacity of the heating/cooling unit was formed. Units with a sizing ratio of 1.1 or less were assigned to the undersized category, and units with a ratio greater than 1.1 were assigned to the oversized category.

A slightly different approach was used for classifying water heater customers. TVA guidelines for establishing water heater tank sizes take into account the number of persons in the household, the number of bathrooms, and the presence or absence of a clothes washer and/or dishwasher. Using census data as a guide, customers were assigned to a small, medium, or large expected usage category (see Figure 6-4). This categorization was independent of the actual tank size.

**Control cycle* refers to the length of time between control actions. The control cycle includes the period during which energy to the appliance is interrupted and the period following the interruption before the next control action. If an appliance is cycled for 10 minutes on the half hour, there are two control cycles in an hour.

†*Intensity of control* is the proportion of a specified time interval that the utility has an appliance under control. An intensity of control of 0.33 is equivalent to interrupting the flow of energy to an appliance 10 minutes in a half hour.

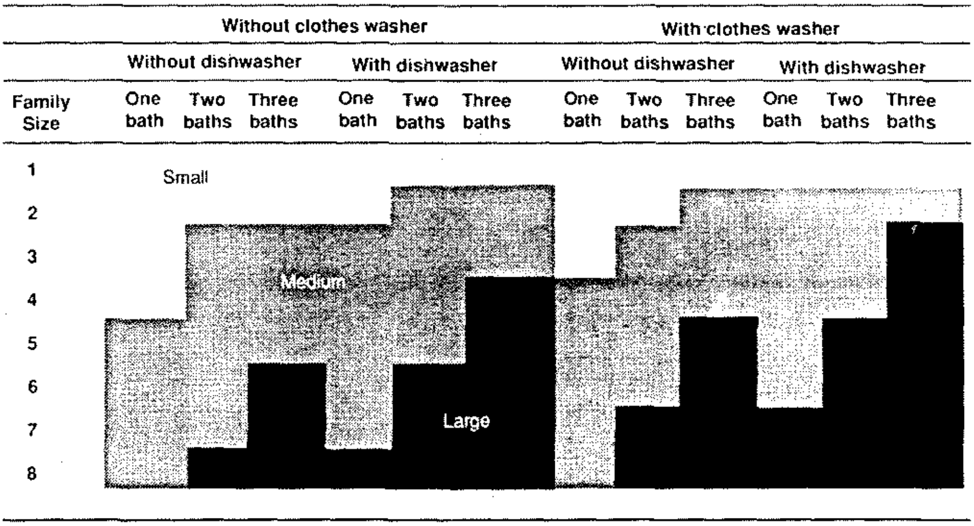

Figure 6-4 Classification criteria for water heater customers.

Typically, load control customers are assigned randomly to groups so that the impact of starting numerous appliances simultaneously will be distributed over the system. Because the impacts at the feeder level were of interest to us, customers were assigned to a group based on their feeder location.

CUSTOMER RECRUITING

Customer marketing is one of the most important aspects of a direct-load-control program, although it often receives less attention and fewer resources than other aspects of the program. Marketing includes identifying the customers to be targeted, designing methods for informing customers of the program, establishing contact with customers, minimizing obstacles to participation, recruiting customers, and retaining customers throughout the life of the program.

At Athens we used recruiting methods to target customers in a way that will improve the efficiency of the load control system and eliminate costs associated with installing equipment at households that provide no load relief. These methods differed from the traditional methods used by utilities, which generally ignore customer differences. This section describes the method used at Athens. It proved effective in achieving high customer acceptance of a direct-load-control program through careful customer selection and recruitment—and without the use of incentives.

Many utilities practicing residential load control do not select customers but simply accept customers who respond to the advertisement if the customers have appropriate appliances. This reduces the recruiting cost per household. However, the number of households recruited by this method is often very low (less than 10%), and the method often results in the placement of equipment in locations that result in no net load relief.[3] The lack of load relief occurs because the correlation between appliance installations and appliance usage is far from perfect. Load relief is achieved only when appliances are switched off. Customers who do not use their appliances but who are controlled do not contribute to load relief. Such "free riders" reduce the effectiveness of a program because of the costs of recruiting, equipment, equipment installation, and any incentives that may be offered.

A major objective of the Athens experiment was to place load control switches at effective locations. This required a method of selecting or targeting households which provided the most load relief when it was desirable to exercise control. Marketing experts refer to this as market segmentation. Cluster analysis was the method used at Athens. Observations of customers' monthly consumption over a period of months were compared, and customers with similar patterns were placed into the same category. An advantage of cluster analysis is that neither the number nor the nature of the patterns has to be specified before the analysis. (Left completely unconstrained, cluster analysis will identify every household as a separate cluster.) There are no accepted procedures for determining the number of clusters. An arbitrarily finite number of clusters is normally specified, and the number of clusters is then varied until a set of clusters to which meaning can be assigned is reached.

Other literature has suggested that cluster analysis may not be sufficiently robust for adequately grouping customers.[4] Given the variety of factors influencing daily load patterns, the conclusion appears reasonable. However, the lack of robustness probably is not a problem when considering monthly data because the interaction of seasonal weather patterns with usage is likely to overwhelm other considerations such as daily changes in behavioral patterns. This does not mean that errors will not be made in assigning customers to groups. However, the object of this exercise is to provide a working categorization of customer usage.

The FASTCLUS algorithm from the Statistical Analyses System (SAS) package was used to reduce the Athens billing data for the period from March 1982 to May 1983.[5] The problem was initially constrained to ten clusters. After inspection, the number of clusters was reduced to six and then to five.

Cluster analysis provided some valuable insights into the customer base. Figure 6-5 shows the average monthly consumption for each of the five groups that emerged from the cluster analysis. The basic user group is composed of households with low and fairly stable consumption (less than 500 kWh per month) throughout the year. This group probably contains many of the 5–10% of Athens households that, according to the Census

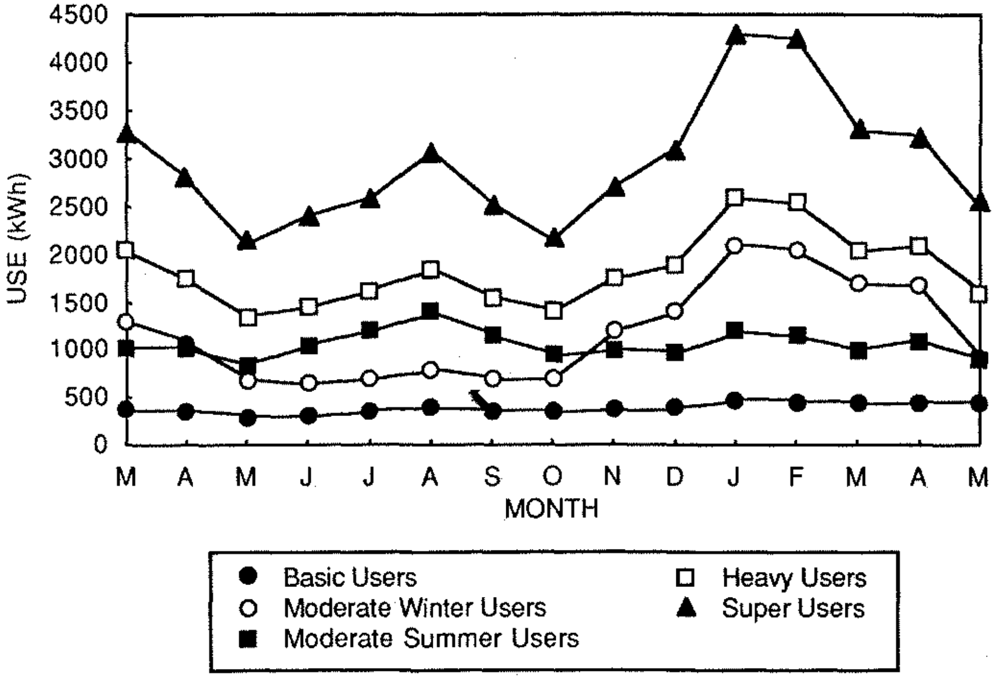

Figure 6-5 Patterns of monthly electricity usage at AUB.

Bureau, do not heat water with electricity. The clustering algorithm distinguished two groups of customers, subsequently named "heavy users" and "super users," who use substantial amounts of electricity in the summer and winter seasons. These households are likely to have electric central space conditioners and are likely to contribute substantial load relief during periods of control. Heavy users and super users have similar patterns of consumption from month to month, but the differences in the magnitude of their monthly consumption make it worthwhile to treat them separately for analytical purposes.

The two remaining groups, moderately high summer users and moderately high winter users, are also of interest because they should include the households that have either electric air conditioning or space heating. It is probable, however, that many of these households have decentralized space-conditioning appliances (window air conditioners or baseboard heat) that could not be effectively controlled with the hardware available at Athens.

Figure 6-6 shows the distribution of the percentage of customers in each group. Athens has about 7800 potentially controllable customers. Of these, about 29% are basic-user households that were not primary targets for the initial recruiting efforts because they probably have either no controllable appliances or only one, an electric water heater. About 24% of the Athens customers fall into the heavy-user and super-user groups. The remaining 47% of the customer base may have two controllable appliances—one space-

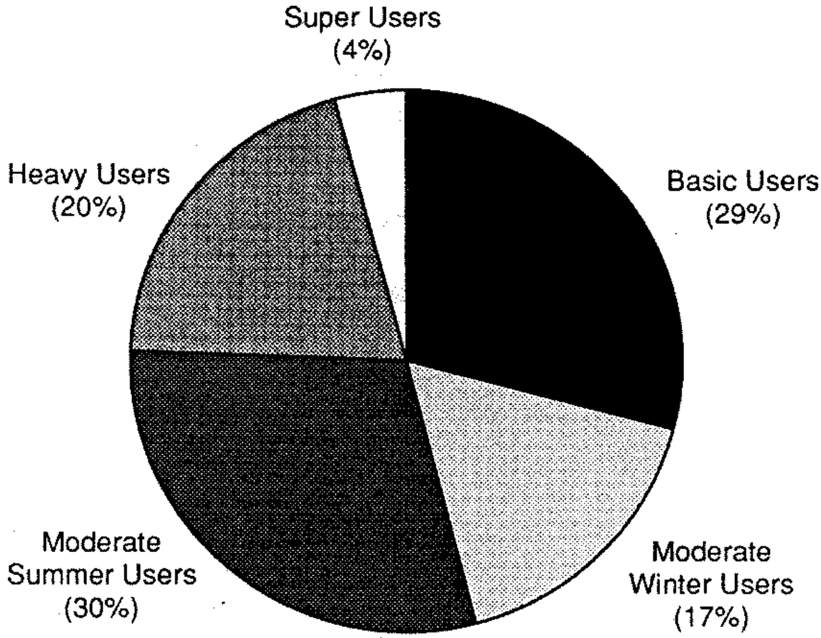

Figure 6-6 Percentage of electricity customers of each type at AUB.

conditioning appliance and a water heater. The households in the moderately high summer and moderately high winter groups are likely to have decentralized systems with appliances not available for control. Thus, to make the most efficient use of the 1000 load control receivers in the experiment, a very high penetration rate was needed in the heavy-user and super-user groups, and a high penetration rate was needed among those in the moderately high summer and winter user groups (when those households have central space-conditioning appliances).

Some knowledge of the social and demographic characteristics of the target audience is crucial to the recruiting process. Figures 6-7 through 6-10 show the distribution of selected social and demographic characteristics by the usage groups identified in the previous section. The data for these distributions were obtained from a 1981 survey of Athens customers conducted by Van Liere and Ploch.[6] Figure 6-7 shows the percentage of households within income categories by user type. For example, the percentages of households with incomes less than $14,000 summed across user type is equal to 100% of those with that income. Likewise, the sums of the percentages of households within each of the other categories across user groups also total 100% of those within the categories. If the height of the bars within a usage group is relatively the same, no relationship exists between the characteristic and the usage group.

Figure 6-7 shows that among basic users, the relative proportion of households decreases as income increases. Just the opposite is true among

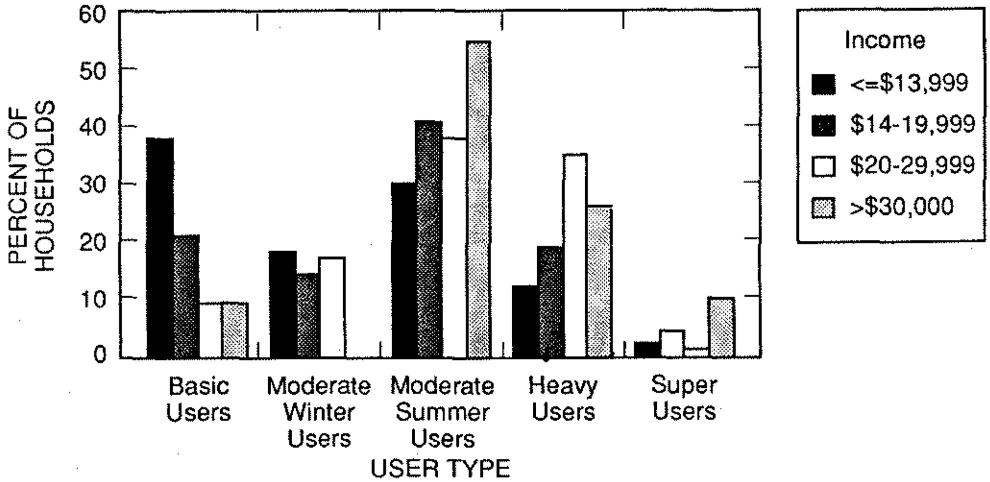

Figure 6-7 Percentage of households in income category by user type.

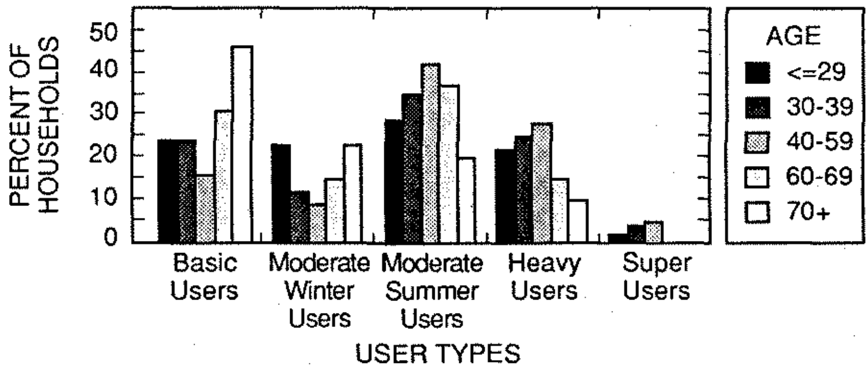

Figure 6-8 Percent of households in age group by user type.

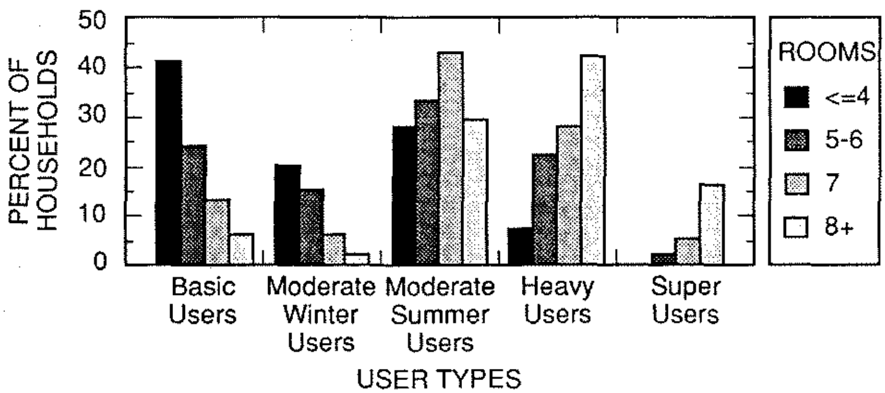

Figure 6-9 Percentage of households with number of rooms by user type.

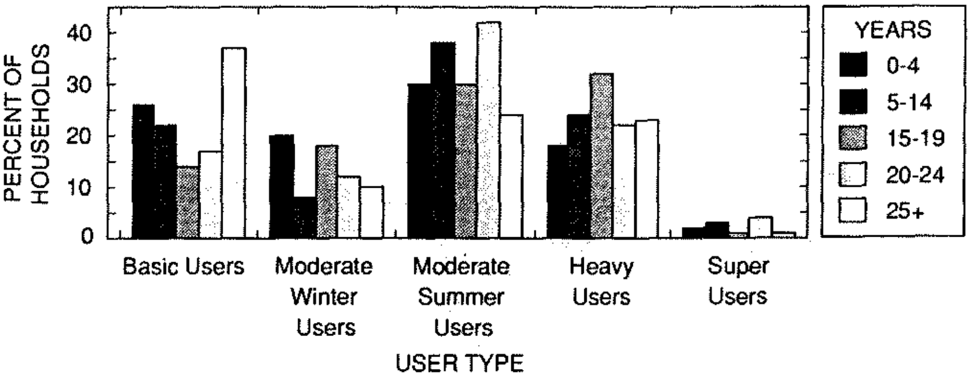

Figure 6-10 Percentage of households in length of residence category by user type.

super users. Those with lower incomes tend to be basic users while those with higher incomes tend to be super users. This is not surprising because energy use is probably a reasonable proxy for household economic status.

The primary targets for load control were heavy users and super users, and the secondary targets were the moderate summer user and (perhaps) moderate winter users. We were able to identify the characteristics of the target households. The target households tend to have higher incomes, have adults in the 40–59 age range, and have seven or more rooms in the house. Figures 6-8, 6-9, and 6-10 show the percentage of households in user groups relative to age, number of rooms, and length of residence, respectively.

Once the target audience was identified and characterized, the next step was to recruit customers. Recent papers on the subject of load control have concluded that the key to recruiting is to conduct a broad range of marketing activities.[7,8] These activities include the market segmentation procedures described previously. Additional activities include creating public awareness, making personal contact, providing customers with information, and minimizing the obstacles to customer participation. Recruiting is best described as being divided into a preparation phase and an implementation phase.

At Athens, the preparation phase involved organizing the marketing activities into an overall strategy and defining the activities in detail. Once this was accomplished, the procedures were reviewed by management and staff at AUB. A focus group was then formed to evaluate the procedures. The focus group was composed of 24 AUB customers, mostly couples. The couples were chosen to reflect the diversity of the AUB customer base. However, no attempt was made to make the group representative of the composition of the AUB customer base. The individuals were selected because of their ability to articulate how various segments of the community would respond to load control.

Those chosen to participate in the focus group received a personal letter from the AUB manager asking them to attend a two-hour meeting. They were told that they would be asked for advice about a new program to be launched by the utility. This letter was followed by a call from the utility manager's office answering any questions that may have arisen and asking for a commitment to attend the meeting.

The focus group meeting had three objectives. The first was to explain the program. The second was to explain the strategy that had been devised to recruit customers. The third objective was to determine how best to describe the program to customers and what concepts and vocabulary might be used effectively. The meeting was conducted by the utility manager. Formal presentations were followed by opportunities to ask questions and to get reactions. The overall strategy was then adjusted to reflect the opinions of the group.

After the strategy was devised, the implementation phase began. The first step was to create public awareness because initial perceptions are very important in determining whether a customer will respond positively or negatively to load control and recruiting activities. Public awareness activities were not used directly for recruiting, although people who volunteered as a result of such activities were not turned away.

In Athens, the public awareness function was handled in several ways. The utility manager spoke with community groups about the project. This was effective because members of the community organizations to which he speaks are likely to be members of target households. Members of the community were used as advisers to the project. AUB employees were carefully briefed about the project and were encouraged to discuss the project with other residents in the community. Articles describing the project appeared in the local newspaper.

Figure 6-11 shows the AUB customer recruitment procedure. Customers were sent a personal letter stating that an AUB employee would contact them by phone about participating in an important project. This was done to differentiate the phone call from telephone marketing and survey calls from other groups. Citizens responded positively to the AUB letterhead and the personal nature of the letter.

A telephone call to the customer was then made. The purpose of the phone contact was to provide additional information to the customer and to make an appointment for an interview in the customer's home. Some screening was done to ascertain that the customer had a controllable appliance. Experience indicates that few people refuse an appointment or indicate that they do not wish to participate at this stage. Indeed, several people indicated at the time of the call that they wanted to participate and would like to have the equipment installed without further explanation. This

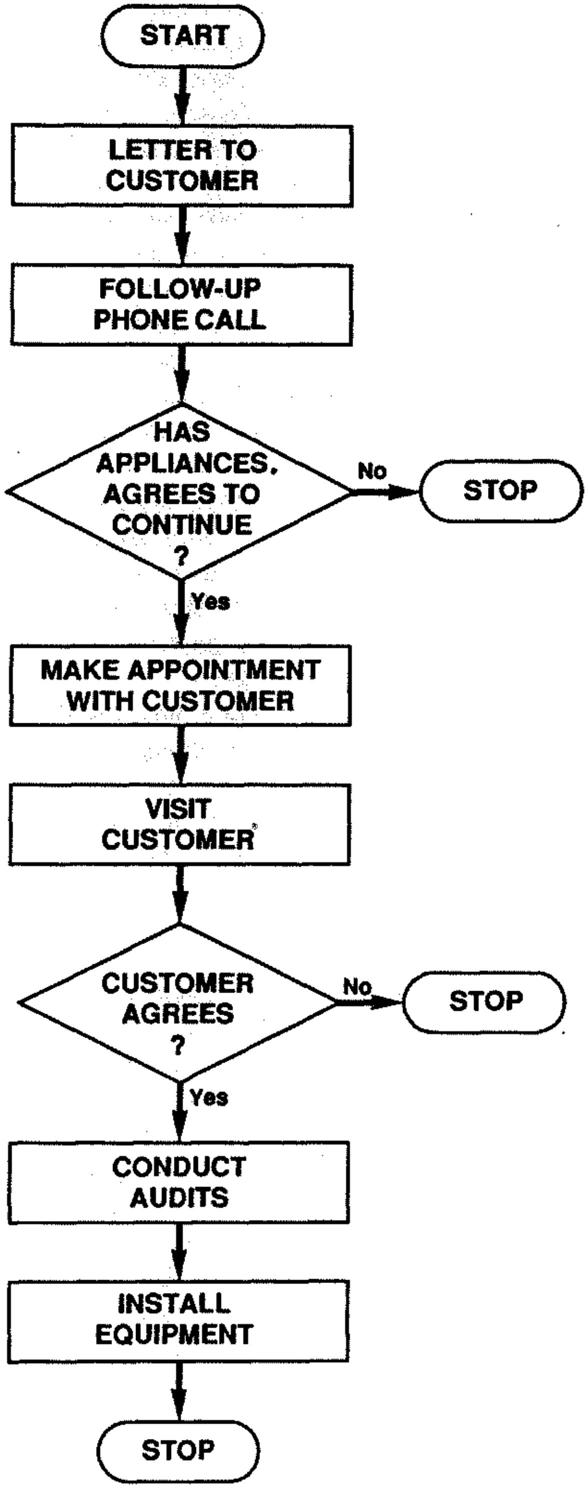

Figure 6-11 Customer recruitment procedure.

indicates the effectiveness of public awareness activities and confidence in the utility.

The site visit and interview were then made to provide information to the customer and to gain the customer's consent to participate. The visit was made by an AUB employee who used posters to explain the operation of the load control receiver and monitoring equipment. Customers were told that the program was voluntary and that it would help to limit electric rates in the long term. They were also told that if they agreed to participate, their appliances would be checked for proper operation before installation of the new control equipment. In addition, the customers were told that they might become aware of control actions, although one of the goals of the project was to minimize effects on customers' comfort.

Once the customer agreed to participate, the final step was installation. The installer made an energy audit of the house and appliances, and the customer completed a lifestyle audit. The installer completed some site engineering to determine the best way to install the equipment and either completed the installation on the initial visit or made an installation appointment.

An important key to success is minimizing obstacles to customer participation. This was done in several ways. Customer contact was limited to that essential to recruiting and getting the equipment installed. An attempt was made to complete all installation requirements in one visit. If additional trips were required, these visits were confined to an outside location and did not require the presence of the customer. Once the equipment was functional, only essential return trips were made. Studies show that repeated visits to customer locations are the primary reason for dropouts from programs.[3] Customers were not asked to sign a contract because studies[7] reveal that signing a contract is an obstacle to participation.

Athens customers are not receiving direct monetary incentives. The decision not to use incentives was based on several studies. One of these[3] shows little support for the notion of a robust relationship between financial incentives and attitudes toward participation in load control programs. Behavioral studies support the data from attitudinal studies. Based on a telephone survey of utilities that conducted load management programs, Burby et al. published two tables that show either no relationship between incentives and participation or that the higher the incentive, the lower the rate of participation.[7] At Athens, recruiting relied on an effective marketing and customer relations program.

Figure 6-12 shows the success of the AUB recruiting plan. Thirty-eight percent of those contacted had appropriate appliances and agreed to participate in the program. Another 37% agreed to participate but did not meet the pre-established characteristics. Many of these people can be included in the program at a later time. Thus, the potential participation rate was about 75%.

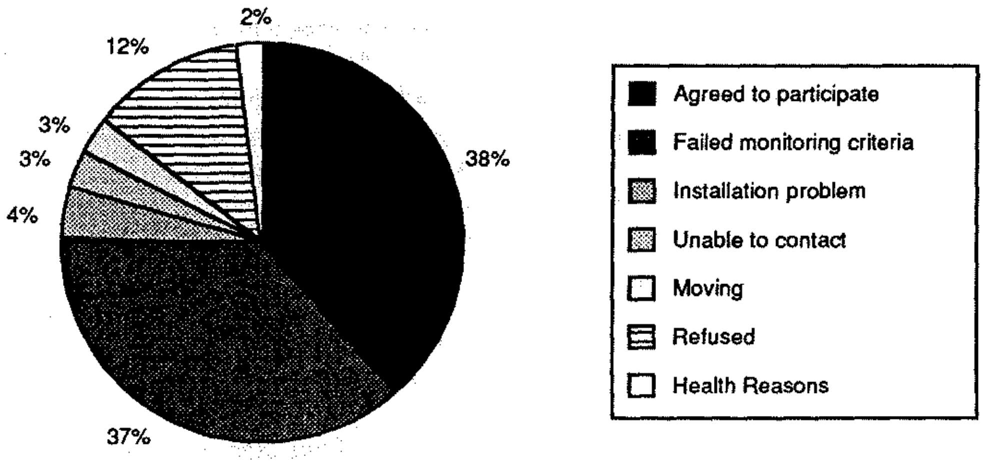

Figure 6-12 Patterns of success in recruitment.

The remaining 25% could not be recruited for a variety of reasons. Only 12% of those contacted refused to participate.

THE EQUIPMENT

A detailed description of the control and monitoring equipment can be found in Chapter 2. However, some details essential to understanding the experimental results are included here. The control equipment on the feeder includes a Brown Boveri Corporation (BBC) signal injection unit at the substation and BBC load control receivers installed at customer locations. A signal injection unit receives an encoded command from a central control computer and finds the message corresponding to that command in its "read only" memory. The message is injected at 340 Hz on the power line.

Residential load control receivers are preset so that their relays open or close if the 340-Hz signal is present during a particular interval. Messages can be coded to deactivate appliances by feeder, feeder section, and appliance group. The relays in the load control receiver are closed either by a timer or by a message received over the power line. Figure 6-13 shows the turnoff and restore messages for air conditioners.

Two basic types of monitoring equipment were used to gather the data used for the load control experiments. The first type were Appliance Research Meters (ARMs); each ARM can gather four channels of data from a combination of appliances, an interior household temperature sensor, and/or a household watt-hour meter. These units were furnished by the Electric Power Research Institute (EPRI) for use at Athens. A data sample consisting of one to four measurements is stored once every 5 minutes, or 288 times per day. The devices use the customer's phone lines to call a central

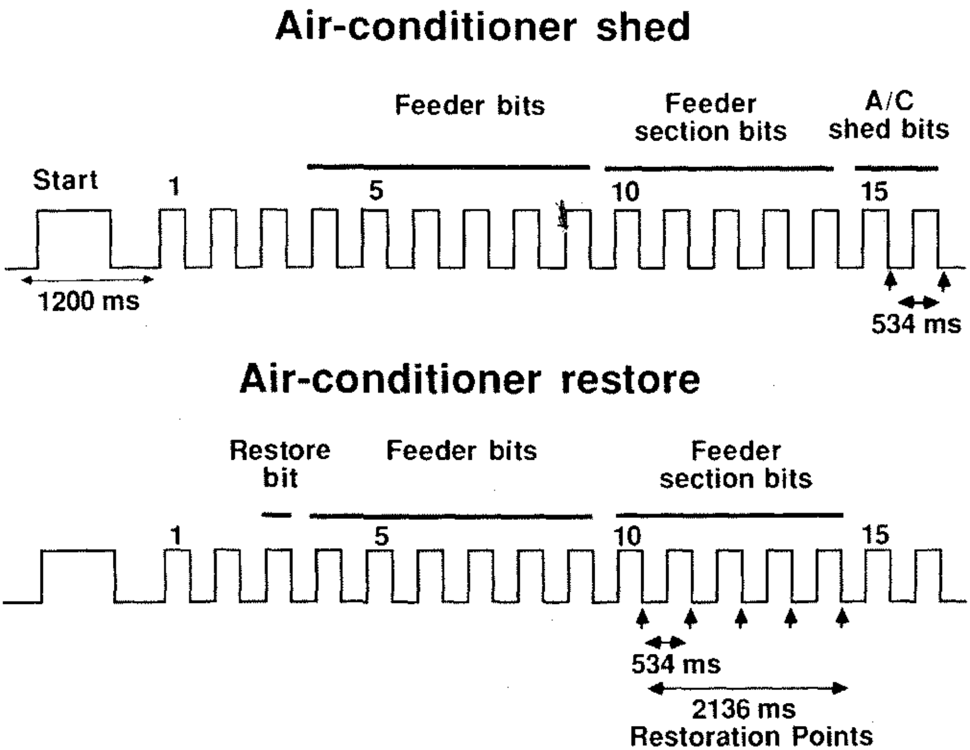

Figure 6-13 Messages sent to shed and restore air conditioners (copyright 1988 by the IEEE).

computer between midnight and 6 a.m. about every two days and transmit data for each channel to the computer. Because of the way the ARMs and the central computer interact, the data for different households may include a time skew of a few minutes.

The second type of monitoring equipment was the high-speed data acquisition system, which is described in detail in Chapter 3. This equipment consists of a Digital Equipment Corporation PDP 11/23 minicomputer and peripheral equipment; a 10-channel, 14-bit analog-to-digital converter; a bank of instrumentation filters; an oscilloscope; an external trigger; a voltage reference; a portable personal computer; and specialized cabling. The cabling connects the system to watt, var, and voltage transducers mounted in the distribution substation. For the air-conditioning experiment, the equipment was adjusted to scan each channel at a rate of 50 samples per second.

DATA

It was necessary to deal with large quantities of data. For example, the winter data from the ARMS units included a maximum of four observations every 5 minutes from 74 households. This is approximately half a megabyte of data per day. Approximately 286.7 million heat pump power measurements and 62 million interior house temperature measurements were recorded over the 3-month period. Each data set includes the load control receiver address, a date/time stamp, an appliance code, a channel number, and the channel measurement for the previous 5 minutes.

Weather variables were measured at the substation every 15 minutes. The weather measurements included air temperature, barometric pressure, humidity, solar radiation, wind direction, and wind speed.

All load control actions initiated at the control center are logged in a data file, which includes a date/time stamp and a description of the control action.

The basic data management tasks were to organize the data for efficient analysis and to perform data validation checks. SAS was used to analyze the data.[5]

WATER HEATING CONTROL

This section describes the analysis of the water heater data. The analysis compares winter control days with no–control days. The analysis focuses on the impacts of control on the utility and the customer. Water heaters were controlled for 2, 3, and 4 hours in the morning and evening. These winter control strategies are illustrated in Figure 6-2.

Figure 6-14 shows the distribution of water heater tank sizes for the experimental group. The smallest water heater was a 40-gal tank, and the largest was a 66-gal tank. The predominant size was 40 gal.

Figure 6-15 shows the average demand for all water heater customers for noncontrol days. The diversified demand for water heating for the Athens sample peaks at about 1060 W at 7 a.m. on winter mornings. However, this is not the only peak. Usage decreased but peaks again at 980 W at about 9 a.m. Water heater power demand then decreases until late afternoon, when the load begins to increase to a secondary evening peak of 700 W, which lasts from about 7 to 11 p.m.

Figure 6-16 shows for noncontrol days the percentage of water heaters operating any time during the monitoring interval, the percentage that activate during the interval, and the percentage that operate throughout the entire 5-minute monitoring interval.

The percentage of units operating is greatest (35%) around 7 a.m., with a secondary peak at 9 a.m. (when about 30% of the units are operating). The number of operating units then declines until about 5 p.m., when the percentage begins to increase to a peak of 25%. The percentage of units operating declines to about 7% in the early morning hours. This is a consistent pattern of daily behavior.

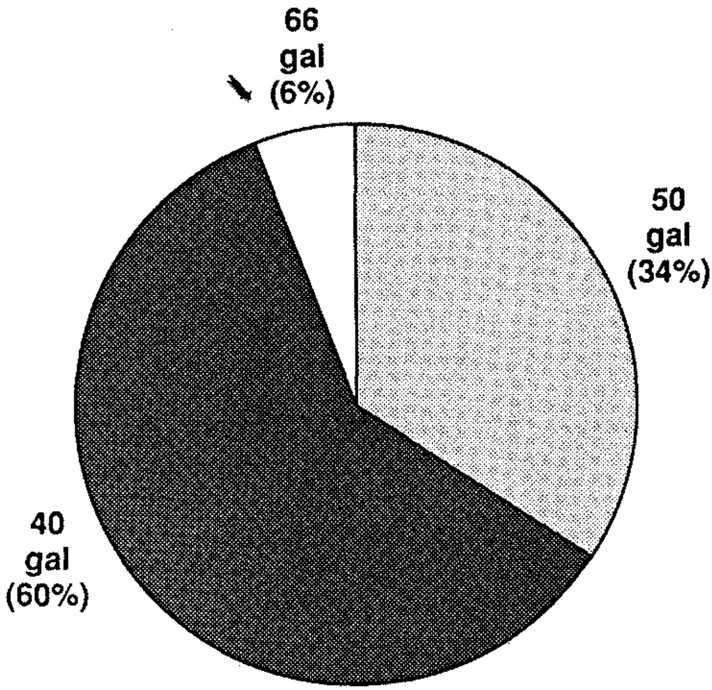

Figure 6-14 Distribution of water heater tank sizes among monitored customers at Athens, Tennessee.

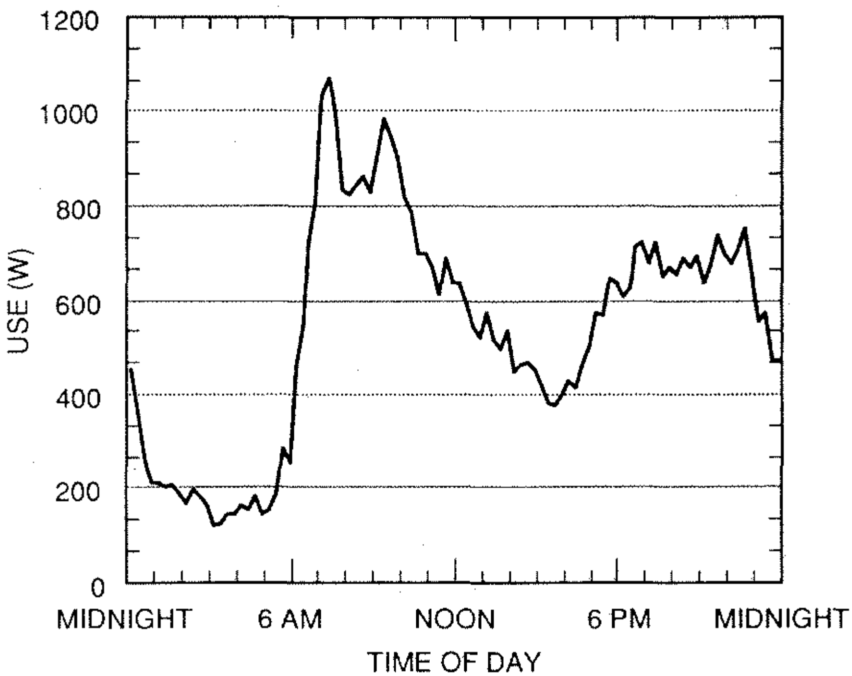

Figure 6-15 Diversified water heater load for noncontrol days.

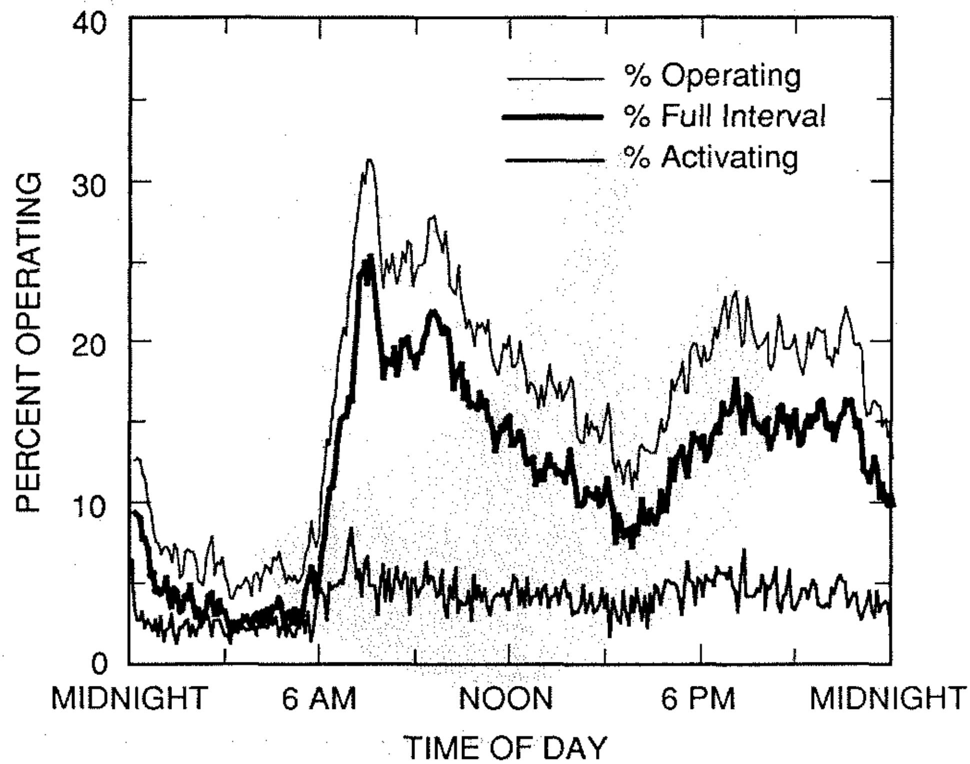

Figure 6-16 Percentages of units starting, running for a 5-minute monitoring interval, and running less than monitoring interval.

The percentage of units operating for each full 5-minute monitoring interval tracks very closely the percentage of units operating at any time during the interval. The percentage of units activating within a 5-minute interval shows a somewhat surprising characteristic. During the early morning hours, the percentage of units activating is fairly stable at about 3%. After the early morning increase, the number of units activating is about 6% and remains fairly constant throughout the day. Thus, consumption does not seem to be directly proportional to the number of units activating within an interval.

As previously noted, customers were categorized by expected usage on the assumption that there would be differences in behavior patterns. Also, the morning peak is actually two peaks separated by about 2 hours. Figure 6-17 shows water heater usage by expected-usage groupings and also differences in the patterns. The medium-expected-usage group peaks at 7 a.m., the small-expected-usage group peaks at around 7:40 a.m., and the large-expected-usage group peaks at about 8:45 a.m. The different peak times for the different groups explain the bimodal morning peak.

Load control strategies could use these patterns to more effectively shift loads. Households in which energy usage peaks early could be controlled in

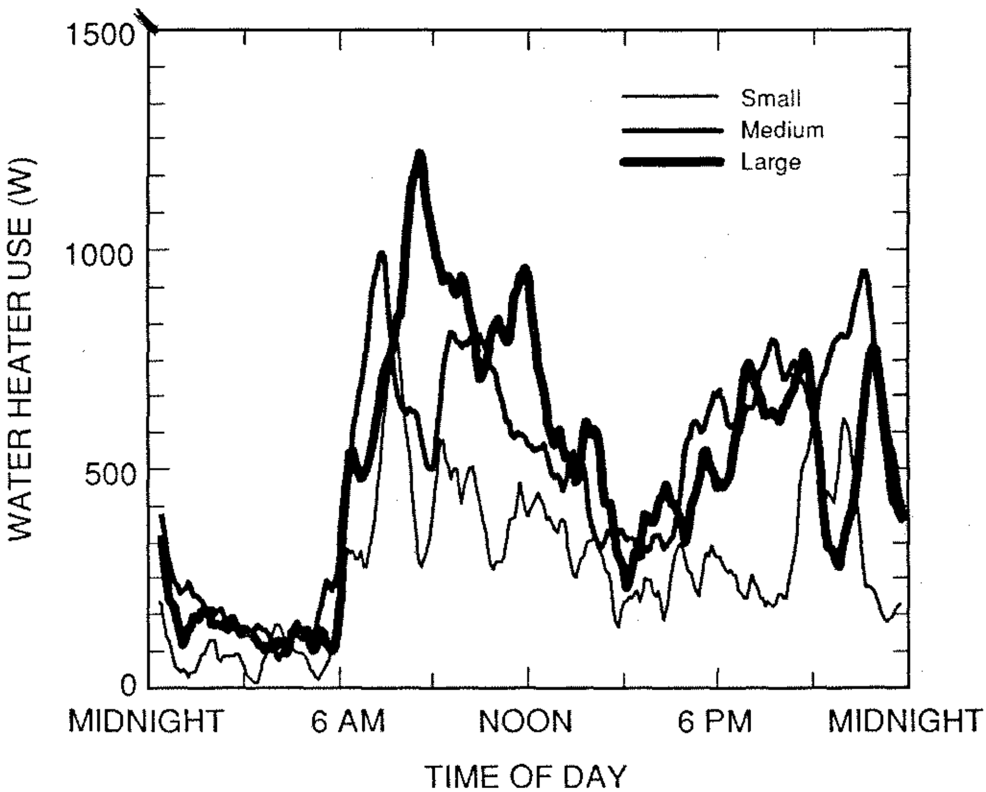

Figure 6-17 Diversified water heater demand for customers classified as having small, medium, and large expected usage.

the early morning hours, and load could be released at about mid-morning. Households in which usage peaks late could be controlled from just before mid-morning until about noon to permit the shifting of significant amounts of load from early morning to noon.

There is strong evidence that these variations in the patterns of water heater use are linked to social characteristics. The medium-expected-usage group is made up of blue collar and white collar workers. The large-use households appear to be headed by professionals, while the small-use households appear to be those with older members. The linkage of these different patterns to social characteristics is being investigated with the help of survey data.

Figure 6-18 is a plot of the diversified water heater load with and without control. The control action shown here is the 4-hour morning control action from 6:30 a.m. to 10:30 a.m. The diversified load during control was expected to go to zero but did not. The low level of demand shown in the figure is attributed to load control receivers that did not function reliably. The graph also shows the payback peak when control was released after 4 hours. In this case, the diversified load reached almost 2 kW per unit.

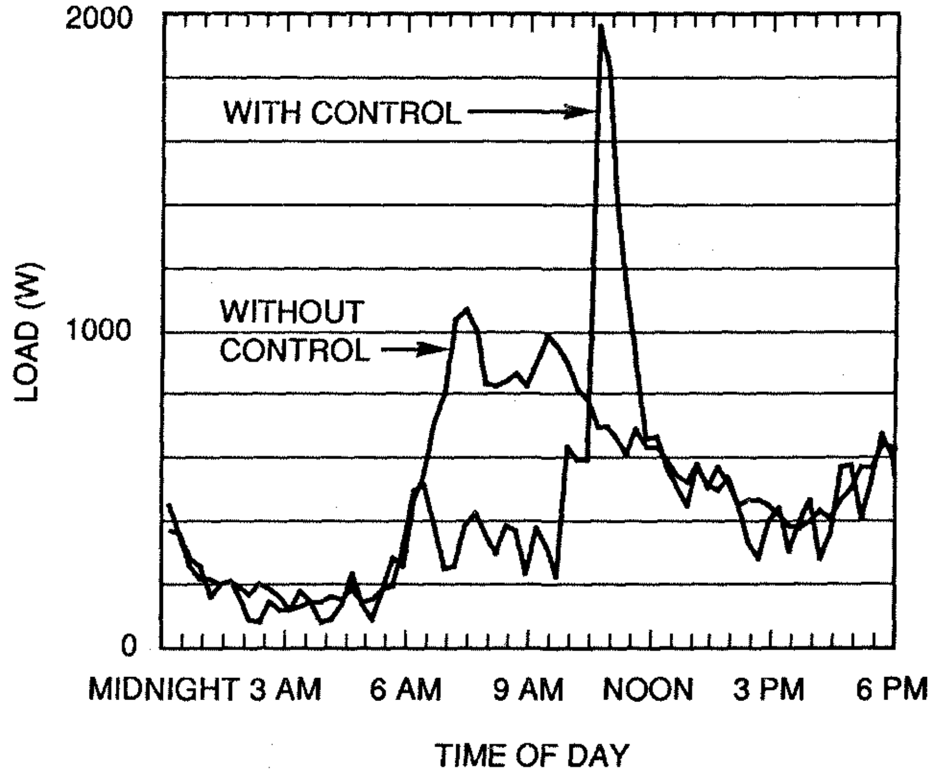

Figure 6-18 Diversified water heater load with and without control.

Figure 6-19 is a graph comparing the expected water heater demand for noncontrol days with that for control days. Each column represents one of six control periods. Column height represents the average demand per water heater for that control period* on a noncontrol day. Depending on the control period, the expected demand reduction is between 700 and 920 W per unit. This is the load that may be potentially deferred, assuming that the load control units operate with 100% reliability.

The segment at the bottom of the column represents the average deferred demand during the control period. This actual deferred demand ranged from about 375 to 500 W per unit depending on the control period. The average deferred demand was obtained by subtracting the average demand for a control day from the average for a noncontrol day. The shaded segment at the top represents average demand that went undeferred on control days. Because the load control receivers frequently failed to operate, reduction in demand in each control period is about 50% less than was expected.

**Duration of control* or the *control period* refers to the time of day during which control actions are occurring, for example, between noon and 10 p.m.

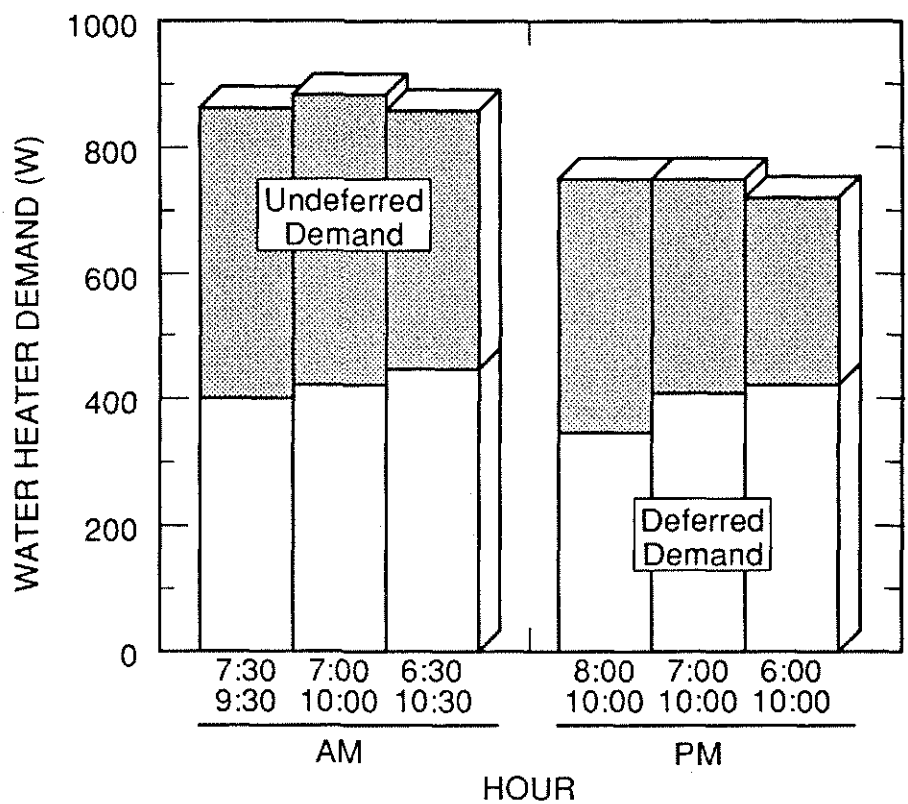

Figure 6-19 Average deferred water heater demand per water heater compared with demand on a no-control day.

Load control may result in a coincidence of load. This coincidence of load may result in a new system peak, thereby defeating the purpose of load control. Thus, the magnitude of the peak after the load is controlled and the length of time the effects of control remain in the system are of interest. To investigate the length of time the effects of coincidence remain in the system, the difference in average energy use for control and noncontrol days was calculated. Figure 6-20 is a graph of these differences plotted from the end of a 4-hour control period. The effects of control are largely dissipated when the difference in diversified demand reaches zero and begins to oscillate about zero. The difference between the average diversified load without control and the diversified load just after control is released is about 1550 W. The graph shows that the effects of coincidence for a 4-hour load control action are largely dissipated in about 1 hour 15 minutes. For a 3-hour control action, the diversity is reestablished in about the same amount of time. For a 2-hour action, the diversity is reestablished in slightly less time.

One of the rationales for load control of water heaters is that demand can be deferred without a substantial reduction in energy sales. For each of

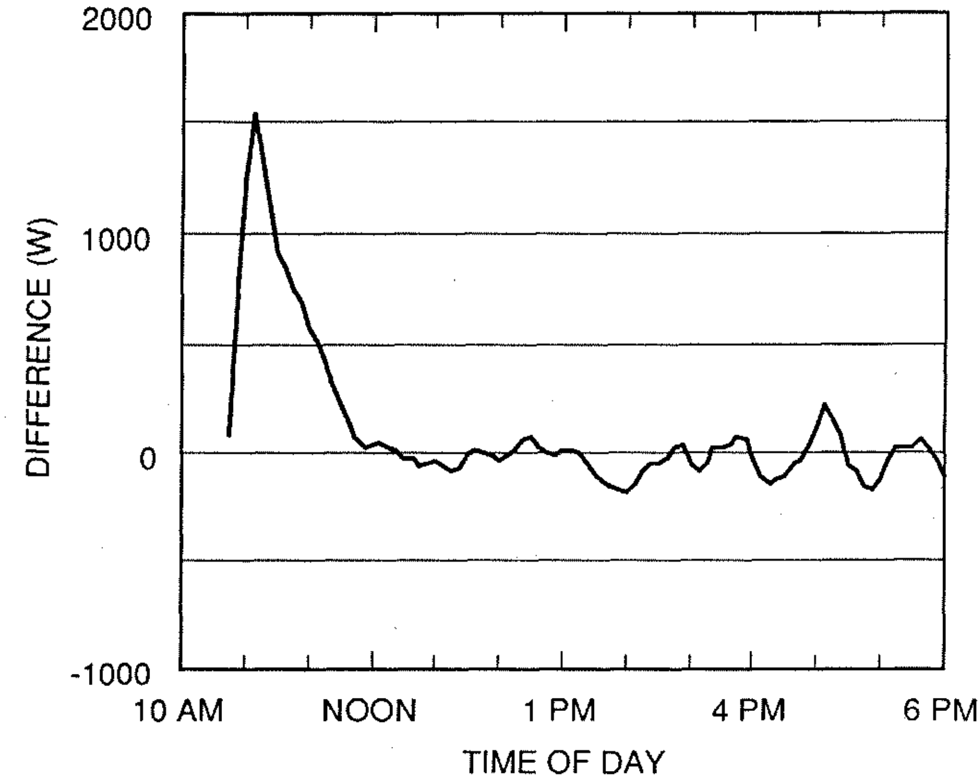

Figure 6-20 A plot of the difference in diversified load on a control and noncontrol day after a 4-hour control action.

the morning control actions, the average total energy used was calculated from the beginning of the control action to 7½ hours after control was released. Table 6-1 shows the results of these calculations as well as the analogous calculation for the no-control days and the differences. These data show that total energy supplied by the utility was reduced by about 1 kWh for each of the three control actions.

TABLE 6-1 A comparison of energy consumption during and after control actions on control and no-control days

Control action	Energy consumption on control day (Wh)	Energy consumption on no-control day (Wh)	Difference (Wh)
7:30–9:30 a.m.	5120	6040	920
7:00–10:00 a.m.	5618	6852	1234
6:30–10:30 a.m.	6630	7554	1194

An important issue in direct load control is whether a customer identifies a reduction in service, for instance, a lack of hot water. Most studies have determined the effects of direct control by waiting for customer complaints. AUB did receive complaints from customers. However, we have no way of knowing if those represent all those experiencing problems. A more direct method of ascertaining the impact of load control on customers is to examine the amount of hot water used by the customers and then compare this with the amount available. This can be estimated by calculating the amount of water heated based on the amount of electricity used and comparing that with the effective size of the tank. The calculation of the amount of hot water is:

$$m = \frac{E}{Cp\,\Delta T}$$

where

m = mass pounds of water;
ΔT = the temperature difference between the inlet temperature and the temperature after heating in °F;
Cp = the specific heat of water $= \frac{(1\ \text{Btu/lb})}{°\text{F}}$;
E = the energy used to heat the water (a watt hour = 3.415 Btu and a gallon of water is 8.3 lb).

This calculation requires both the inlet temperature and the actual temperature of the tank. Neither of these values is known directly. However, for the period of interest, the water temperature at the AUB supply tank was about 50°F. The movement of the water through underground pipes and the location of water heaters in heated and unheated spaces make it unlikely that water at the inlet is the AUB water temperature. The amount of variation is unclear. Nonetheless, the system temperature provides a useful guide. In lieu of a measurement of the temperature in the tank, we assumed that the water would be heated to 140°F. This is consistent with the set points recorded by the installers. Thus, the estimates are based on the assumptions of a 90°F temperature rise. Thermal losses also have been ignored.

Figure 6-21 shows the cumulative percentage of households by gallons of water consumed on a noncontrol day. The x-axis represents gallons of water per day, and the y-axis shows the cumulative percentage of households. The household with the largest consumption used about 146 gallons of water. Half the households use less than 45 gallons of hot water per day; 90% use less than 100 gallons of hot water per day.

Figure 6-22 is a series of plots displaying the percentage of water in a tank used during a control period and the cumulative percentage of households at that percentage level. The columns in the plots differentiate the morning and evening control periods, and the rows of plots differentiate the

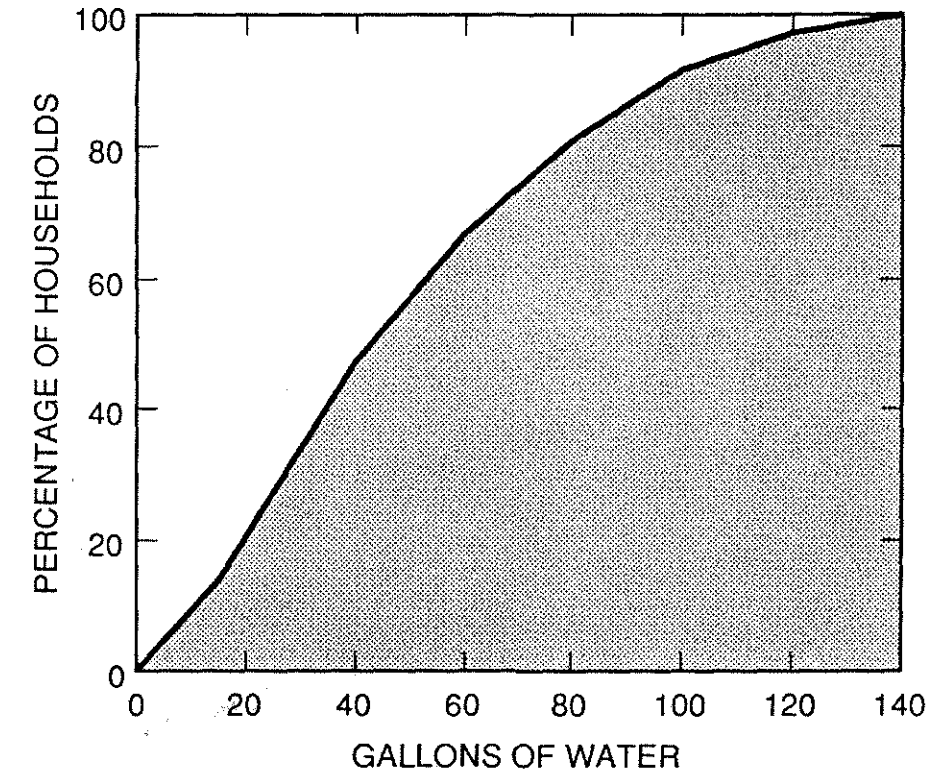

Figure 6-21 Cumulative percentage of households by total gallons of water used per day.

control actions. The percentage of water in a tank can exceed 100% if the tank size is smaller than the amount of "hot" water used.

According to water heater manufacturers, the hot water user will begin to experience a decrease in water temperature when 60% of the water in a tank has been used. The effective sizes of our 40-, 50-, and 60-gallon tanks are 28, 35, and 42 gallons, respectively. The hatched rectangular area in Figure 6-22 shows where consumption exceeds 60% of the tank size and represents the area of insufficient service. The intersection of the cumulative use curve with the area of insufficient service gives the percentage of customers experiencing a shortage of hot water. This percentage of customers is represented by the solid dark area in each graph.

Several observations are evident from these plots. Consumption is greater during the morning control periods than during the evening control periods. A maximum of 13% of the customers experienced a shortage of hot water (solid dark area) during the 4-hour morning control period, and less than 7% experienced a shortage in either of the other two morning control periods. No customers experienced a shortage of hot water during the 2- and 3-hour control periods in the evening, and less than 5% experienced a shortage

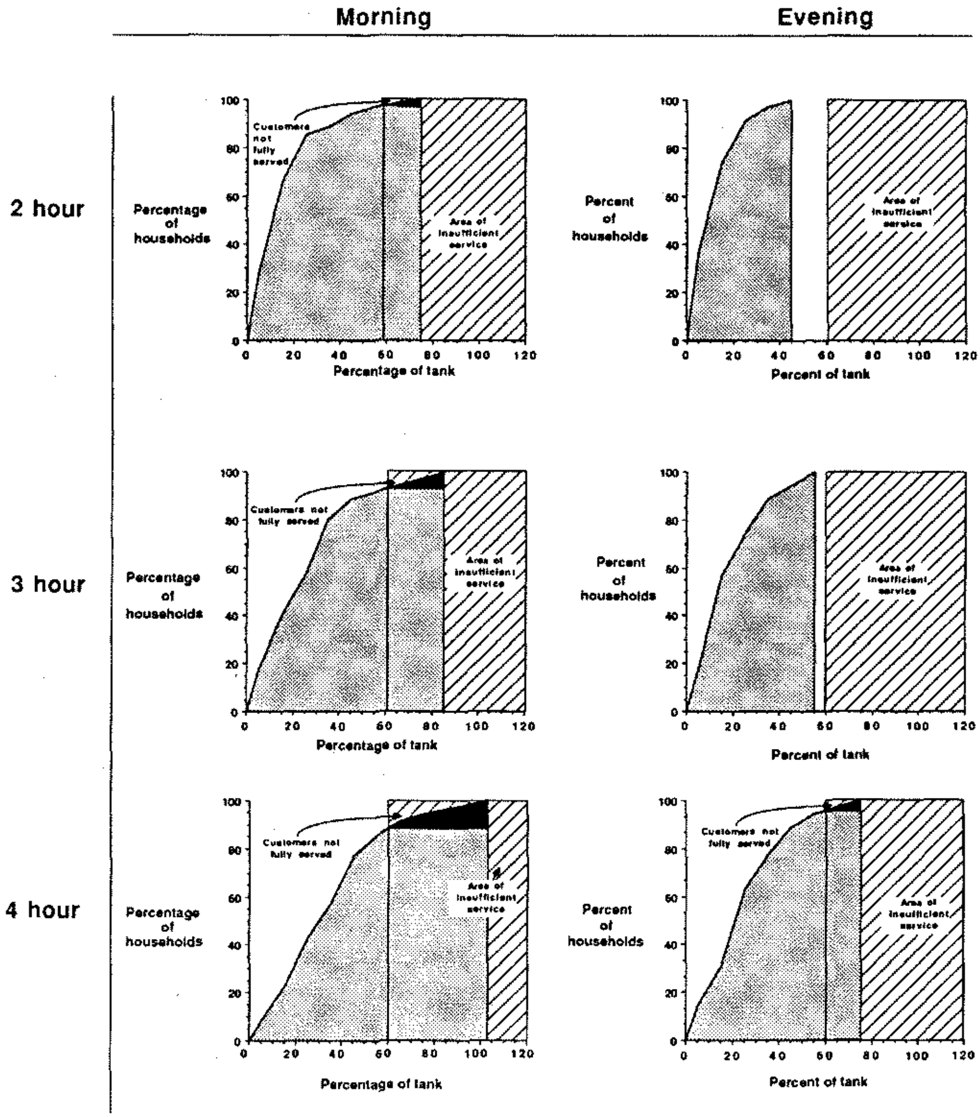

Figure 6-22 Customers experiencing deficient service as a result of water heater load control actions.

during the 4-hour evening control period. Some users experienced a shortage during the 4-hour evening control period. AUB reported that fewer than 5% of its customers complained of shortages during water heater control.

Summer hot-water-use patterns have not been examined. However, electricity use for hot-water heating in summer is somewhat less than in winter. This probably reflects differences in inlet water temperatures and usage between seasons and has not been investigated at this time.

Summary of Water Heater Effects

The effects of six different water heater load control strategies were extensively investigated. The expected demand reduction ranged between 700 and 920 W per unit depending on the control strategy and the time of day. Because the load control receivers did not function reliably, the actual reduction range was between 375 and 500 W per unit. The highest diversified payback demand at restoration was approximately 2 kW, which was about four times the expected load at that hour. The main effect of synchronization of appliances as a result of control was largely dissipated within 1 hour 15 minutes after control was concluded.

If it is assumed that (1) a load control receiver costs about $80 per unit, (2) customer recruiting takes 2 person-hours, (3) installation requires 3 hours inclusive of paper work, and (4) personnel costs average $30 per hour, then the cost per kilowatt of load control installed can be estimated by dividing the installation cost by the amount of actual relief obtained per unit. Based on the expected relief, the cost per kilowatt is about $270. Based on the actual relief, which is lower than the expected relief because of the reliability problems with the load control receivers, the cost per kilowatt of relief is $575. It should be kept in mind that control results in an average 1-kWh loss of energy sales for a control action lasting 2 or more hours. This must be included in the cost-benefit estimates for load control.

An alternative method of water heater control would be to replace the standard 4-kW heating elements in the tank with smaller elements (e.g., 2.5 kW). Recent reports (informal) suggest that this might significantly reduce peak water heating load. The rationale for using the large elements was that they were needed for rapid recovery so that electric water heaters can be competitive with gas heaters. The Athens data suggest that with a sufficiently large tank, downsizing the element will not lead to a shortage of hot water. Some preliminary investigation suggests that downsizing is effective if there are sharp peaks but much less effective if the peak is fairly broad. Thus, downsizing of the heating elements might have different effects on the morning and evening peak for utilities like Athens.

Another control method would be to use larger water heaters or two tanks in series. The consumption data presented here clearly imply that larger tanks are a viable alternative. Approximately 80% of AUB's customers would manage nicely with a 120-gallon tank. Such usage reduces daytime load and can be used to build nighttime load, which may be particularly attractive to utilities with low load factors at night. To be successful with larger water storage, new control circuit designs are needed.

SPACE HEATING CONTROL

This section discusses the load control experiments performed using heat pumps during the winter. The experiments are of interest because few utilities have performed load control experiments on heat pumps.[9,10] The data indicate that control of heat pumps can result in a higher energy use because of the design of the auxiliary heater circuits. Current heat pump technology is designed so that a small deviation of household temperature from set point, generally in the neighborhood of 2–3°F, will cause the auxiliary heat to operate. This feature ensures that when compressors lose their efficiency at extremely low temperatures, the temperature in the building will be maintained at the desired value. Load control causes the interior household temperature to deviate from the small deadband range, thereby causing the auxiliary heat to operate. The power rating of the auxiliary heat is generally 2 to 4 times that of the compressor, thereby increasing energy usage.

Heat pumps were controlled at Athens from 6 to 9 a.m. on weekday mornings when the forecast temperatures fell into the desired range. The determination of whether a day was to be a control or a no-control day was based on a simple algorithm[11] designed in advance to ensure that the choice of days was not biased. Control was done in 30-minute cycles. For each control strategy, the heat pump was turned off for a certain fraction of the 30-minute cycle. The control strategies were 0, 7.5, 10, 12, and 15 minutes per half hour. The more intense strategies were omitted for severe temperature days.

Two strategies consisting of intensities of 0.25 and 0.33 and referred to as SH1 and SH2, respectively, are discussed here. For SH1, the heat pumps were turned off 7.5 minutes of every 30 minutes between 6 and 9 a.m. For SH2, the heat pumps were turned off 10 minutes of every 30 minutes. Table 6-2 displays the two control strategies and intensities and the corresponding times.

TABLE 6-2 Control strategies

Control type	Control intensity	Control period	Control cycle (minutes)	Time off during control (minutes)
SH1	0.25	6–9 a.m.	30	7.5
SH2	0.33	6–9 a.m.	30	10.0

Because we wanted to ensure that no household was left without space heating, the relay that interrupts the power to the heat pump compressor, fan, and auxiliary heat was installed with a 15-minute timer. Thus, if the relay received no further signals, it automatically closed in 15 minutes, thereby restoring space heating. To implement control intensities of less than 0.5, a message had to be sent to cause the relay to close. Thus, the SH1 and SH2 control strategies, required that a load turnoff signal and a load restore signal be sent at the proper time.

The data were recorded by the ARMs between December 1, 1986, and February 28, 1987. Total heat pump energy usage was monitored in 29 houses. Of these, there were eight in which both the auxiliary heating unit and the compressor for the heat pump were monitored separately. The interior temperature also was monitored in eight of the houses.

Seven days of SH1 control and 4 days of SH2 control were selected for analysis. The set of no-control days was then analyzed to determine a subset of days whose temperature variations closely matched those of the control days. Seven no-control days of similar temperature variations were found. All days included in the analysis are weekdays.

Figure 6-23 shows the mean temperature variations for each grouping of days. Table 6-3 shows the average temperatures over the 24-hour period and

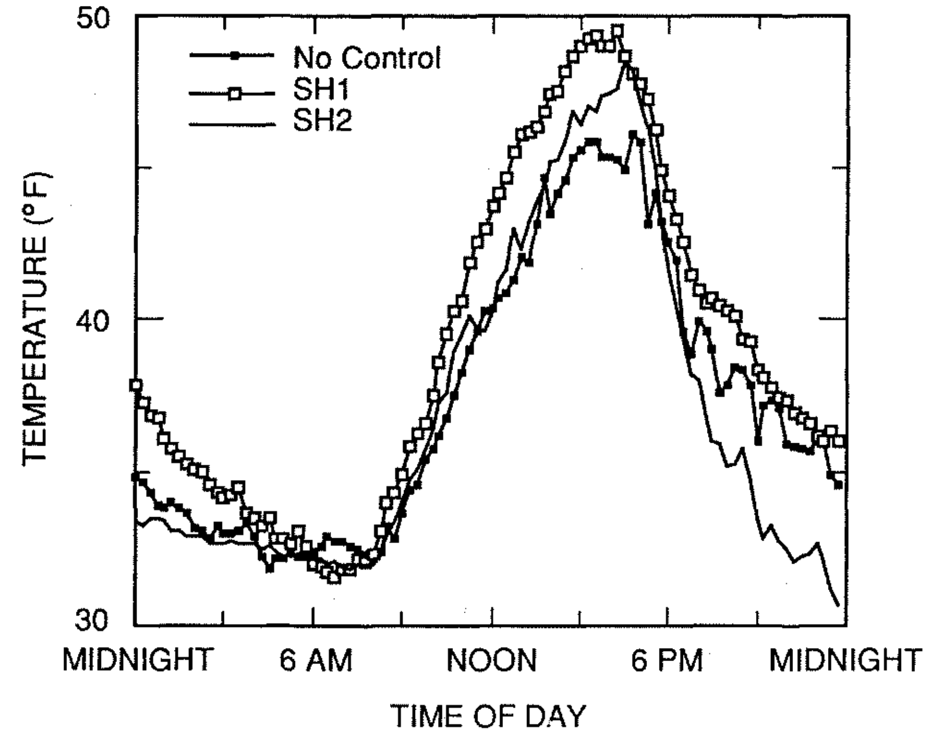

Figure 6-23 Mean temperature variations for similar days of noncontrol, SH1 control, and SH2 control (copyright 1988 by the IEEE).

TABLE 6-3 Average temperatures for three groupings of similar days (copyright 1988 by the IEEE)

Type of day	Temperature for control period (6 to 9 a.m.) (°F)	Temperature over 24-hour period (°F)
7 days of no control	32.7	37.3
7 days of SH1 control	32.6	39.1
4 days of SH2 control	32.4	36.9

the average over the 3-hour control period from 6 to 9 a.m. for each grouping of days. Figure 6-23 and Table 6-3 reveal that the temperature variation is small among the three groups of days. This is especially true between the hours of 6 and 9 a.m. Assuming the thermal mass effects are not great, differences in the energy usage of the heat pumps due to outside temperature on noncontrol days and control days should be small.

Diversified Load Analysis

For each of the groupings, a diversified energy demand was calculated for the heat pumps by time of day. Hence, for the no-control days or the control days of SH1, the diversified energy demand at a given time of day included 7 days of measurements for 29 heat pumps, and each mean was calculated from 203 measurements.

Figure 6-24 shows the diversified load of the heat pump averaged over 7 noncontrol days that correspond to the average temperature day plotted in Figure 6-23. Figure 6-24 has several interesting features. The spikes at noon and 1 p.m. represent cases where thermostat settings were increased during the lunch hour after having been set back earlier in the day. There is also a substantial increase shortly after 4 p.m. that can be attributed to people increasing their thermostat set points at that hour. A similar increase in the morning as people awakened was anticipated; however, the data did not reflect an increase, possibly because of the small sample size.

Figures 6-25 and 6-26 show the diversified loads of the heat pumps corresponding to the average temperatures plotted in Figure 6-23 for SH1 and SH2 control, respectively. Because only 4 days of data were used for SH2 control, each mean for SH2 was calculated from 116 measurements.

Figures 6-25 and 6-26 show that during the control period, the heat pump diversified-energy-usage peaks are much higher than on the noncontrol

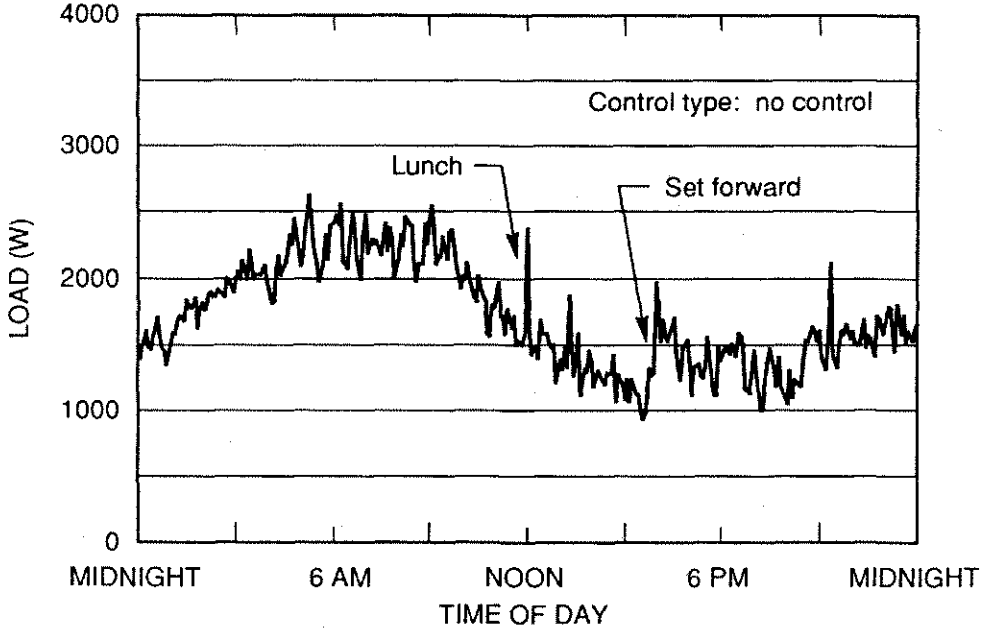

Figure 6-24 Diversified demand for heat pumps averaged over seven noncontrol days (29 heat pumps included in the sample) (copyright 1988 by the IEEE)

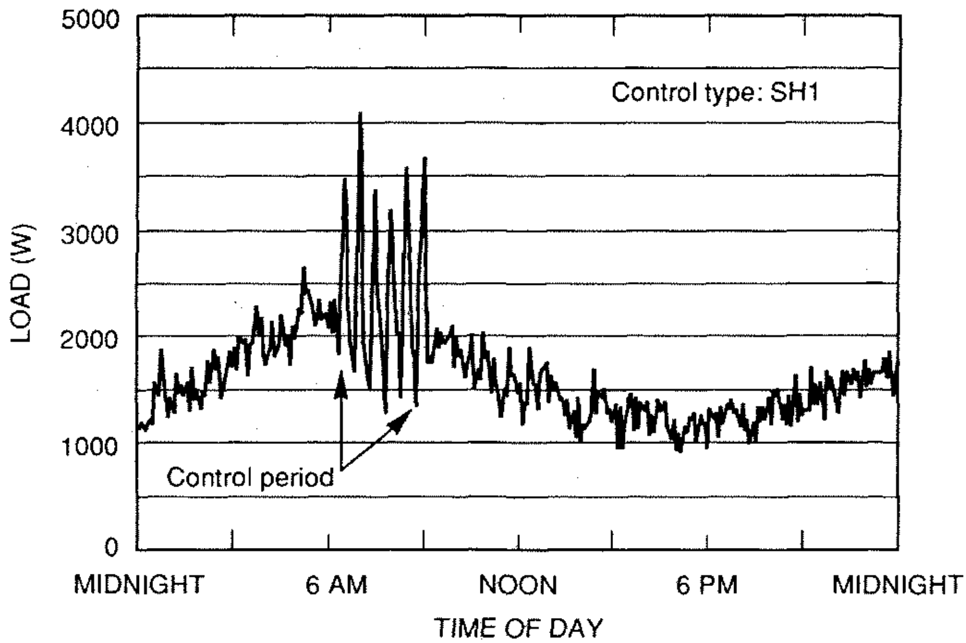

Figure 6-25 Diversified demand for heat pumps averaged over seven SH1 control days (29 heat pumps included in the sample) (copyright 1988 by the IEEE).

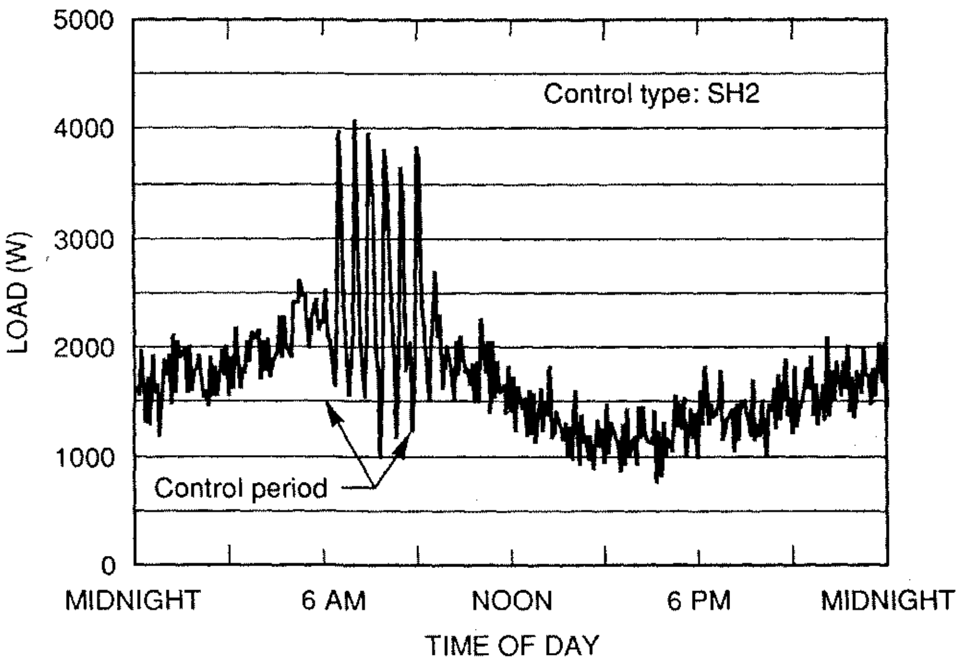

Figure 6-26 Diversified demand for heat pumps averaged over four SH2 control days (29 heat pumps included in the sample) (copyright 1988 by the IEEE).

days. The diversified energy usage never goes to zero because of the time skew associated with the ARMs' measurements and the reliability problems with the load control receivers.

Diversified Energy Analysis

Table 6-4 gives the total energy use between 6 and 9 a.m. for the average heat pump. The table shows that energy use increases with the intensity of control. This is contrary to what is desired because for load control to be effective the energy use should decrease or remain constant during the control period. The increase is attributed to the operation of the auxiliary heat.

During normal operations, heat pump customers would be controlled in groups to level the system load; the Athens experiments controlled customers as a single block. Figure 6-27 is a simulation of what might have happened if heat pumps had been controlled as three groups. The effect of using auxiliary heat during the control period is obvious.

At eight homes, both the energy use of the heat pump compressor and the auxiliary heat were monitored. The diversified energy use for both the compressor and the auxiliary heat was calculated over the groupings of similar days for each control type. Figures 6-28–6-33 illustrate the results of

TABLE 6-4 Total energy use for average heat pump during control period (copyright 1988 by the IEEE)

Day type	Energy use (Wh)
No-control day	7027
SH1 control day	7398
SH2 control day	7573

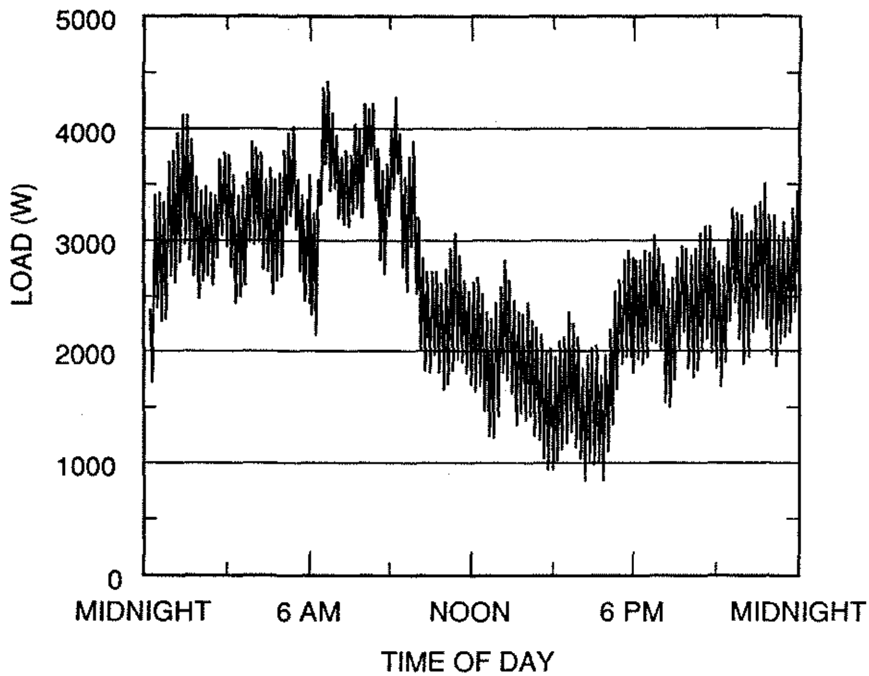

Figure 6-27 Simulation of the operational control of heat pumps on a winter day.

these calculations. For the noncontrol day, Figure 6-28 shows the diversified auxiliary heat energy use vs time of day, and Figure 6-29 shows the diversified compressor energy use vs time of day. Figures 6-30 and 6-31 show diversified auxiliary heat energy use and the diversified compressor energy usage, respectively, for SH1 control. During the 6 to 9 a.m. control period, the auxiliary heat uses significantly more energy than on the no-control days. A similar observation may be made for SH2 control (see Figures 6-32 and 6-33).

Table 6-5 presents the total energy use between the hours of 6 and 9 a.m. for the average auxiliary heat, compressor, and total heat pump loads

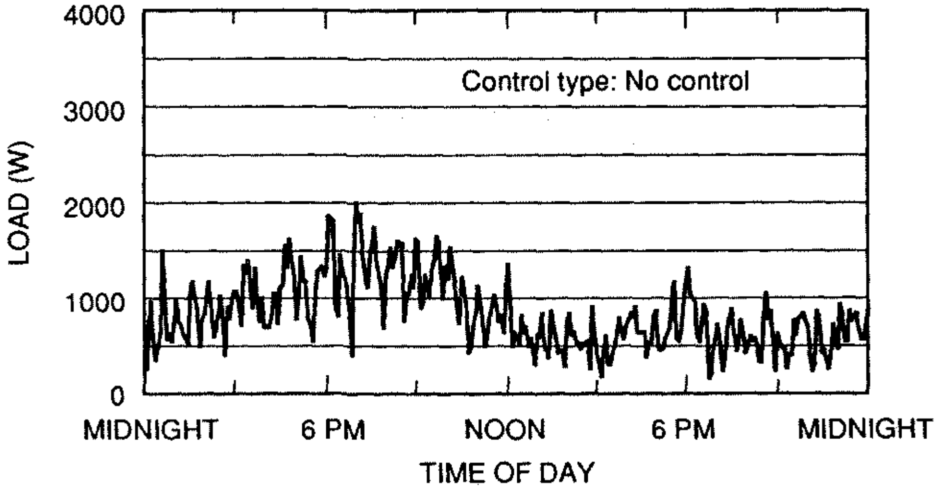

Figure 6-28 Diversified demand of the auxiliary heaters averaged over seven noncontrol days (copyright 1988 by the IEEE).

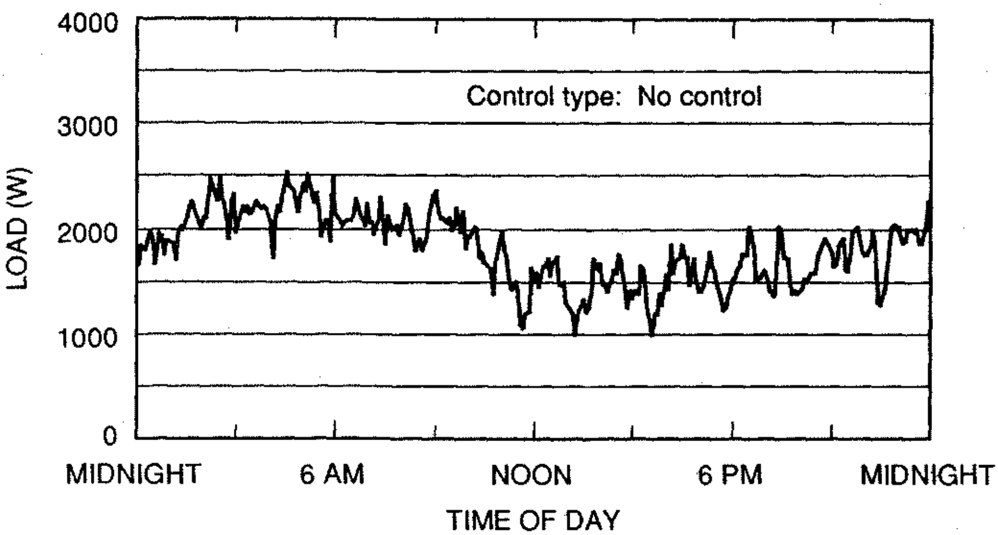

Figure 6-29 Diversified demand of the compressors averaged over seven noncontrol days (copyright 1988 by the IEEE).

during the time of control. The heat pump uses more energy during control periods primarily because of the increased use of the auxiliary heat during the control period. The average size of the heat pumps in Table 6-5 is larger than that for the overall sample of 29 heat pumps.

Interior House Temperature

Figure 6-34 shows a scatter plot of the interior house temperature measurements for the noncontrol days. Figure 6-35 shows a similar plot for

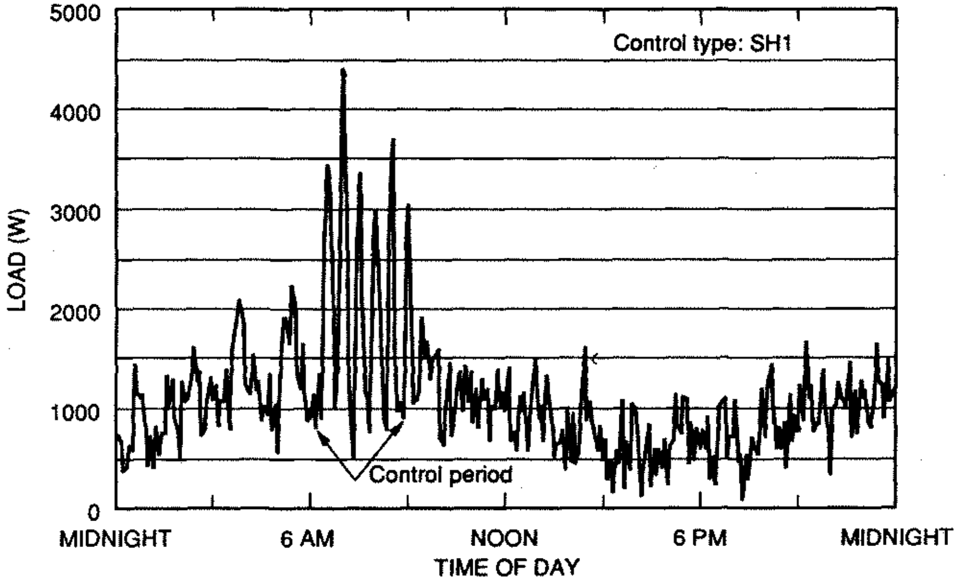

Figure 6-30 Diversified demand of auxiliary heat averaged over seven SH1 control days (copyright 1988 by the IEEE).

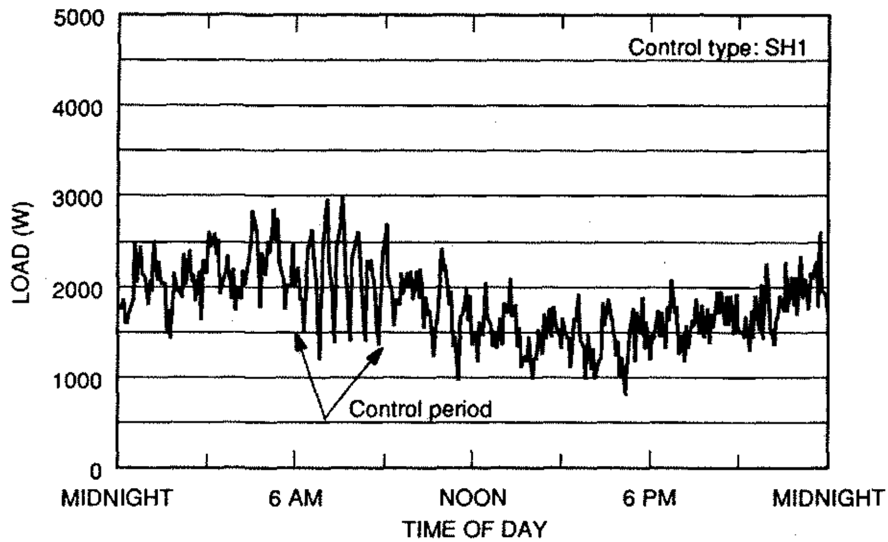

Figure 6-31 Diversified demand for compressors averaged over seven SH1 control days (copyright 1988 by the IEEE).

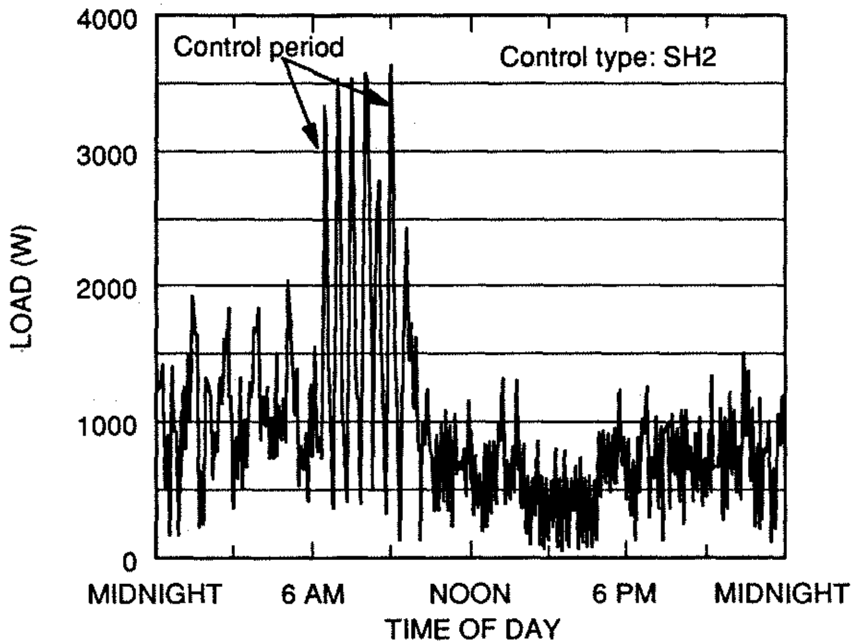

Figure 6-32 Diversified demand for compressors averaged over four SH2 control days (copyright 1988 by the IEEE).

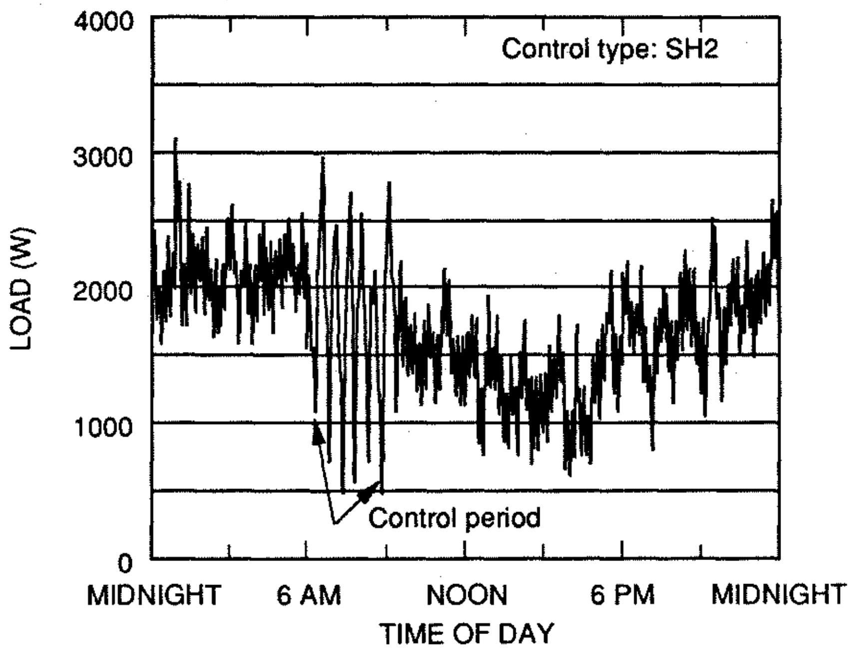

Figure 6-33 Diversified demand for compressors averaged over seven SH2 control days (copyright 1988 by the IEEE).

TABLE 6-5 Total energy use for diversified auxiliary heat, compressor, and total heat pump loads between 6 and 9 a.m. (copyright 1988 by the IEEE)

	Auxiliary heat (Wh)	Compressor pump (Wh)	Total heat (Wh)
No-control day	4,100	6,362	10,462
SH1 control day	5,961	6,669	12,630
SH2 control day	5,776	5,451	11,227

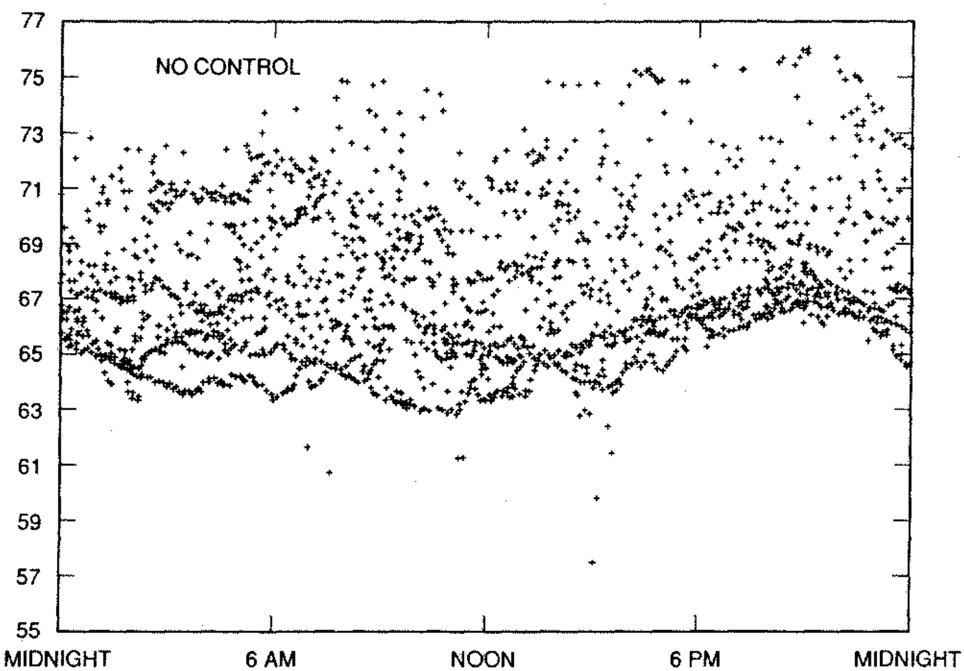

Figure 6-34 Scatter plot of interior house temperatures over noncontrol days (copyright 1988 by the IEEE).

the control days. The interior temperatures for the no-control days are slightly higher than the temperatures for the control days.

AIR-CONDITIONING CONTROL

The air-conditioning experiment reported here was performed under different conditions than the previous load control experiments. High-speed monitoring equipment was used in place of end-use monitoring equipment.

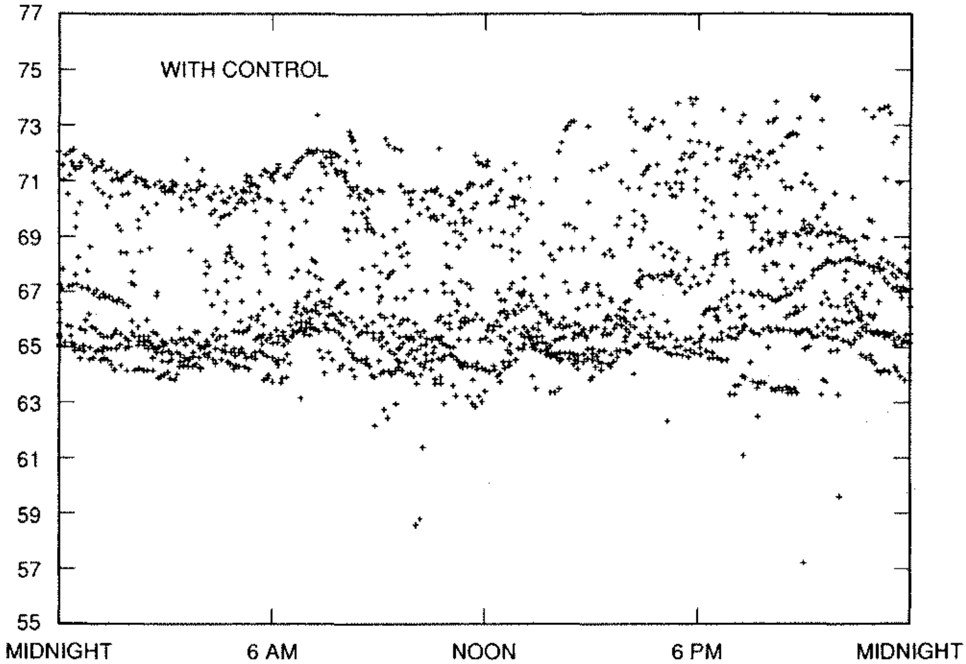

Figure 6-35 Scatter plot of interior house temperatures over control days (copyright 1988 by the IEEE).

The high-speed monitoring equipment is described in Chapter 3. The initial experiment was conducted on August 1, 1986. The circuit used for testing was a residential feeder with approximately 1000 customers, although some small commercial enterprises and a school are also on the feeder.

When the experiment was conducted, there were 152 customers on the feeder with controllable air-conditioning loads. The control strategy was to turn off all controlled air conditioner loads for 12 minutes during each half hour. Control was initiated on the hour and the half hour and was deactivated at 12 minutes and 42 minutes after the hour. The control period was from noon to 10 p.m., although high-speed monitoring was done only during the 2½-hour interval from 12:27 to 2:57 p.m. This limitation was a function of the data storage capacity of the high-speed monitoring equipment.

Measurements were taken for the total real and reactive power injection and bus voltage on each phase of the feeder—a total of nine parameters. In addition, a constant-source parameter was recorded on a tenth channel for purposes of calibration. Each parameter was sampled every 20 ms.

The experiment was conducted on a typical summer day in east Tennessee. The temperature ranged from a low of about 68°F at 7 a.m. to a high of 94°F at 4 p.m. Figure 6-36 shows the temperature and solar insolation data for August 1. The right axis gives the temperatures, and the left axis gives the solar radiation in langleys per minute. Langleys are a unit

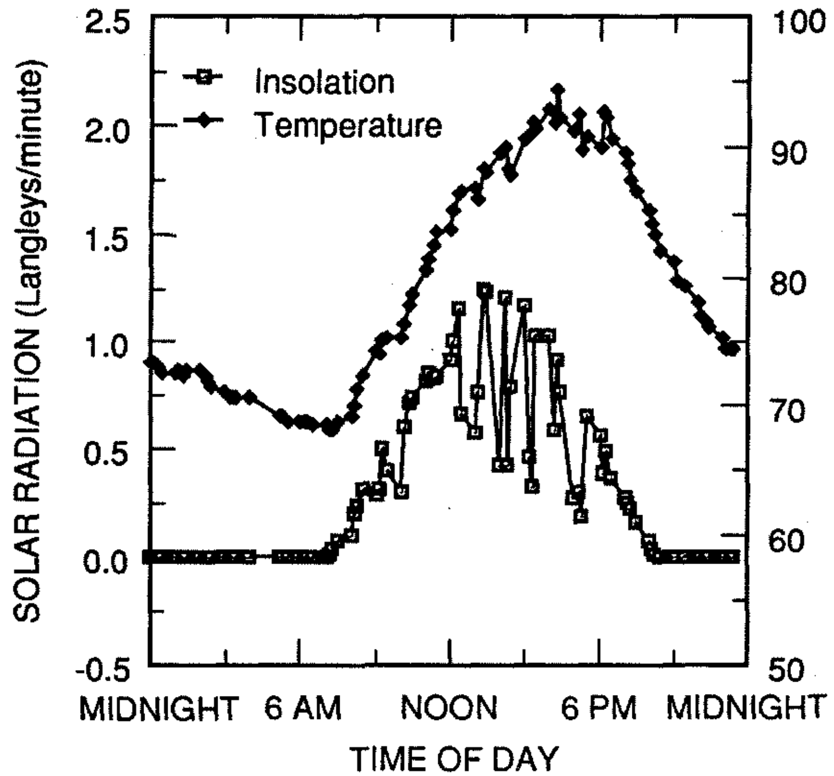

Figure 6-36 Temperature and solar insolation on August 1, 1986 (copyright 1988 by the IEEE).

of intensity of solar radiation equivalent to 1 gram-calorie per square centimeter. Of course, the solar radiation at night is 0 unless there is strong moonlight.

During the monitoring period, the temperature increased from 85 to about 90°F, although a slight dip in temperature occurred shortly after 2 p.m. The solar insolation data show that clouds passed through the area at that time.

Figure 6-37 shows the real power for the B-phase of the test circuit from shortly before the 1 p.m. load drop until shortly after load restoration at 1:12 p.m. The load drop is quite noticeable, as is restoration.

Figure 6-38 shows the amount of load dropped and restored by phase for the five load control actions during the monitoring period. The first bar in each pair is the amount of load that was dropped on the half hour, and the second bar is the amount of load that was restored when the control action was terminated 12 minutes later. The segments within the bars are the values for each of the monitored phases.

The values for the load dropped were calculated by subtracting the average of the ten measurements taken in the 200 ms after the load drop

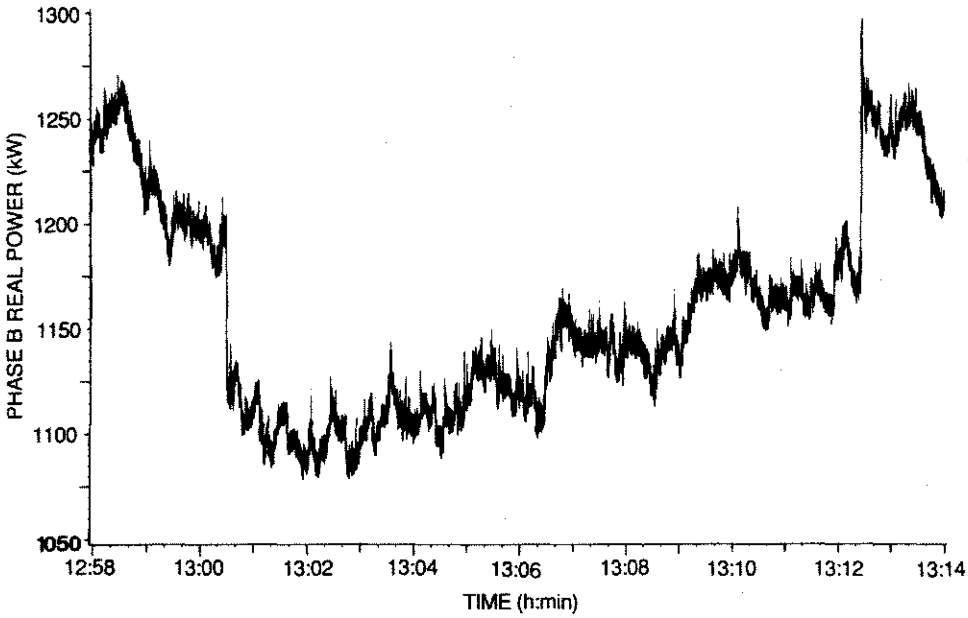

Figure 6-37 Load shed and load restore actions on B-phase of the test circuit on August 1, 1986 (copyright 1988 by the IEEE).

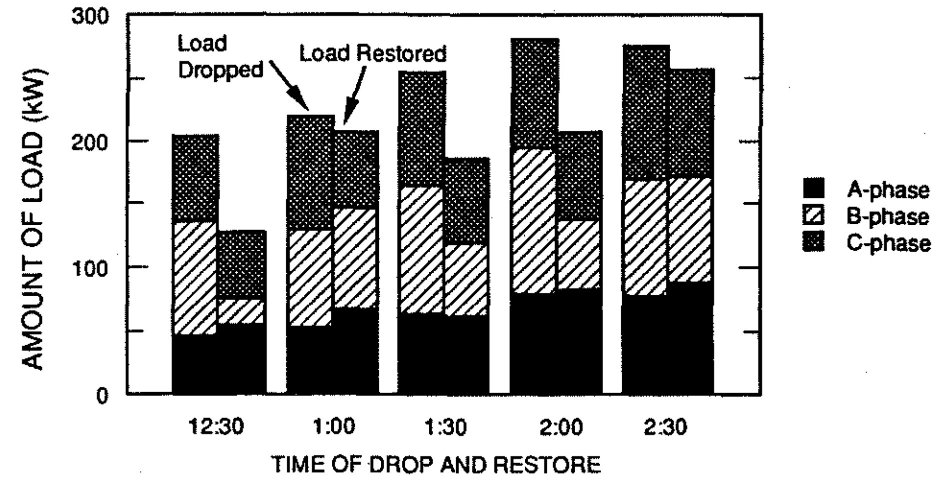

Figure 6-38 Load dropped and restored by phase for five load control actions on August 1, 1986 (copyright 1988 by the IEEE).

from the average of the ten measurements taken in the 200 ms preceding the drop. The average was used to eliminate the effects of low-level noise in the data. The values for restored load were calculated by subtracting the average of the ten measurements taken just before restoration from the average of ten measurements taken after restoration.

Each load drop caused a total load reduction of greater than 200 kW. The 2 p.m. drop is the largest, although the one at 2:30 was expected to be larger because the temperature should have been higher than before. Cloud cover during the latter portion of the experimental period reduced the amount of load dropped. It has been assumed that the internal temperatures of buildings change fairly slowly in response to changes in external environmental conditions. However, these data suggest that change occurs within a matter of minutes.

Based on monitoring data from 49 homes, the average air conditioner size in Athens is 4.5 kW. The distribution of air conditioner sizes based on the end-use monitoring data is shown in Figure 6-39.

Table 6-6 shows the estimated number of air conditioners dropped during each of the five control periods. The estimate was calculated by dividing the total load dropped by the average air conditioner size. The second value in the table is the estimated percentage of air-conditioning units running at the time of the load control action. This percentage is the estimated number of units divided by the number of installed load control receivers.

The estimate of the percentage of the units controlled appears to be slightly lower than the expected values based on end-use monitoring data. Figure 6-40 shows, by time of day (for 3 days with similar weather), the average percentage of units operating. These data were obtained from the end-use monitoring system. It appears that the average from the end-use monitoring data is about 10 to 15% higher in each of the relevant time periods. We attribute this difference to the smaller sample size for the end-use monitoring units and to the possibility that the units in the end-use monitoring sample may tend to be relatively undersized compared with the community as a whole or operated more frequently.

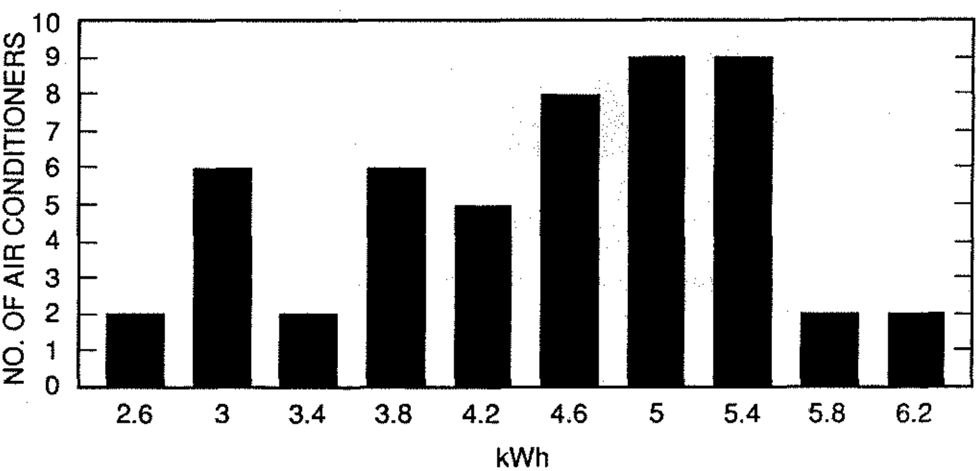

Figure 6-39 Distribution of air conditioner sizes in Athens, Tennessee, based on a sample of 49 units (copyright 1988 by the IEEE).

TABLE 6-6 Estimate of the number of air conditioner loads shed and the diversified demand at the time of the shed (copyright 1988 by the IEEE)

Time of shed	Estimated number of units shed	Estimated percent of units controlled
12:30 p.m.	45	30
1 p.m.	49	32
1:30 p.m.	57	38
2 p.m.	62	41
2:30 p.m.	61	40

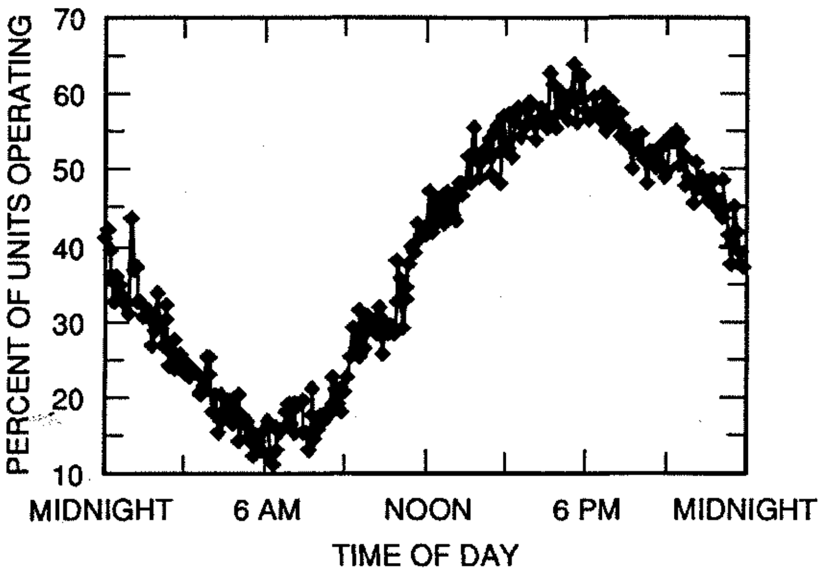

Figure 6-40 Average percentage of air conditioners operating on three summer days (copyright 1988 by the IEEE).

For each of the five load drops and restores (Figure 6-37), the total restored load was less than the total load dropped. The restored load was expected to be larger than the dropped load because units that were turned off would be restored and additional households with demand requirements deferred during the control period would also be restored.

The individual phases exhibit slightly different patterns with respect to dropped and restored load. For four of the five actions, the restored load on the A-phase is larger than the load dropped. For the other phases, the load dropped is always larger than the restored load.

One possible explanation is that air conditioners were not turned off long enough for the head pressure to equalize. Most air conditioners have circuit protection that prevents restart until head pressure is equalized. However, this usually takes 5 minutes or less, so this is not a likely explanation. A more likely explanation is that many air-conditioning units have almost satisfied the building's demand for cooling before the control action. When the air conditioner is turned off during the control period, the air stratifies and the thermostat setting is satisfied. Thus, sufficient cooling is stored in the building before the control action to satisfy the cooling requirement until after the control has been completed. The installers report an analagous phenomena that if a unit is operating when they shut it off to install load control receivers, the thermostat must sometimes be lowered to test the installation once work is complete.

Figure 6-38 implies that in a number of homes, the length of time that a unit normally would be off in a half-hour period is less than the length of the control action. For those homes, load control does not reduce operating time but, instead, changes the air conditioner cycling pattern. In these cases, the utility is receiving little or no load relief for its efforts, particularly when many units being controlled are oversized.

Figure 6-41 is similar to Figure 6-38 except that it displays the measurements for reactive power. For the five load drops, the change in reactive power ranged between 90 and 140 kvar. The restoration actions resulted in the return of a slightly smaller reactive load than was dropped.

Heat pumps and air conditioners are reactive rather than resistive devices. Thus, little fluctuation in voltage is expected when air conditioners are switched. The largest change in voltage on any of the three feeders was

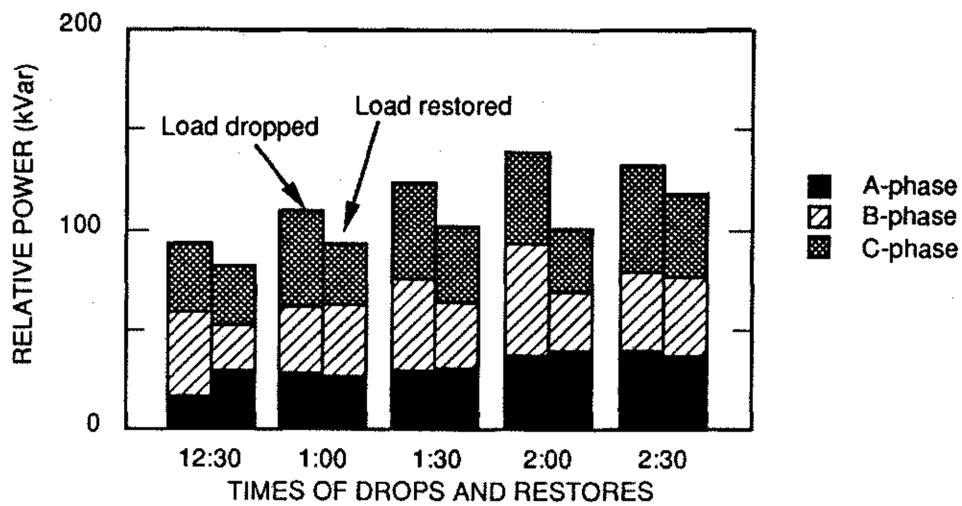

Figure 6-41 Change in kvars by phase for five sheds and restoration on August 1, 1986 (copyright 1988 by the IEEE).

about 9 V. At 7.6 kV, this is a change of slightly more than one-tenth of a percent, and most of the changes were less than half this amount. Furthermore, the changes had no consistent pattern. Such small changes approach the accuracy limits of the measurement equipment.

Feeder Level Management

The data gathered in these experiments demonstrate that effects of load control can be calculated from measurements taken at the feeder level. While this provides "after the fact" confirmation that load control is effective, system operators need to predict in advance the amount of load that can be dropped.

Many of the early load control experiments relied on monitoring at the feeder level to determine the impact of load control actions. While it is possible to evaluate load control using these methods, the methods proved unsatisfactory for the Athens data for a variety of reasons. For example, the feeder monitoring was designed for distribution system management and sampling rates were slow. Distinguishing the normal changes in feeder load from changes resulting from load control actions was difficult. Feeder level monitoring, because it often produced conflicting results, did not answer many of the questions about load control.

As a result of the difficulties with feeder level monitoring, experimenters turned to end-use appliance monitoring to provide direct feedback about the effects of load control actions. However, end-use monitoring also has limitations. For example, magnetic tape recorders originally proved to be ineffective because of the logistics of using the devices. End-use monitoring technology has been improved. However, data collection, data filtering, data reduction, and the assembling of reliable and usable results are still time consuming and costly. More importantly, end-use monitoring does not effectively address the system operator's need for real-time information about the available controllable load.

The Athens experiment indicates that the idea of returning to feeder level monitoring has merit. The experiments show that high-speed monitoring (i.e., sampling feeder parameters at the rate of 25 or 50 times a second) can be used to accurately show load changes due to load control actions. High-speed monitoring may make it feasible to detect at the feeder level the natural cycling of large individual appliances such as central air conditioners. If so, relatively inexpensive devices can be designed that will reduce the amount of data at the point of collection and pass small amounts of higher-level information to system operators. An example of the type of data that an operator might use is the average duty cycle of air conditioners on the system. Combining these new monitoring systems with load control receivers that have programmable addressing capability may be an alternative to costly end-use monitoring systems.

If the system operator could identify controllable load from real-time system data, the use of load control techniques would be enhanced. If loads, such as air conditioners, could be identified at the feeder level, the operator could determine the maximum effective level of load reduction. The Athens data indicate that such a technique may be feasible if duty cycle of electrical equipment can be identified.

To construct an index of a parameter such as duty cycle, it is necessary to identify when air conditioners are running. This requires that the unique characteristics of air conditioners be identified.

Central air-conditioning loads have distinctive startup patterns. Real and reactive power increase dramatically at unit startup. After the initial surge, real and reactive power decline to steady state operation. These changes occur within a definable time period. If these changes can be observed at the feeder level, then an air conditioner startup can be detected.

Some characteristics of air conditioner operation have been identified (see Figure 6-37). Figure 6-42 is the rescaled version of the data used to plot Figure 6-37. This graph has two significant features. As discussed earlier, the restore action takes place in five steps since air conditioners are restored by

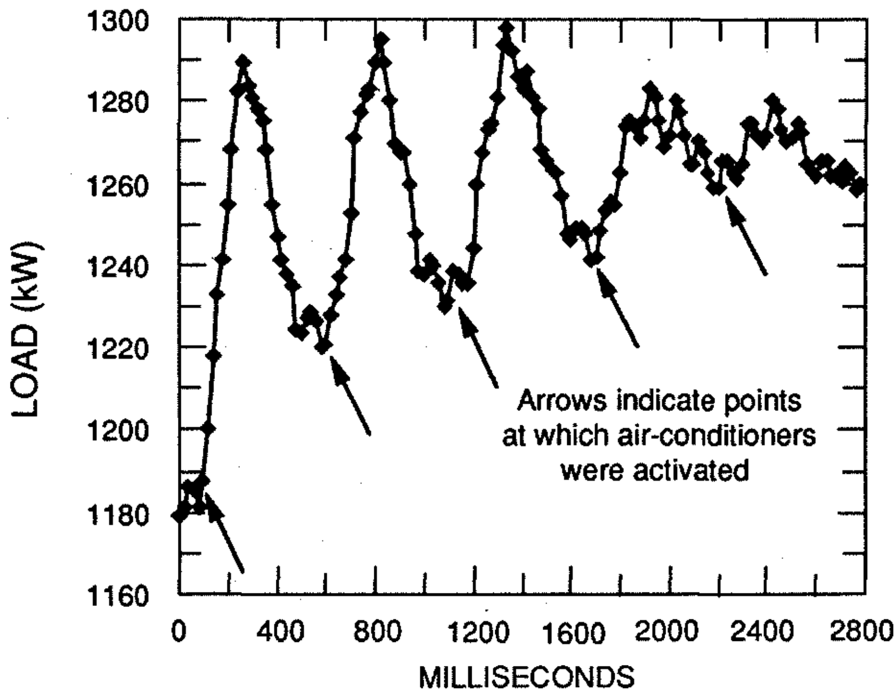

Figure 6-42 Air conditioners being activated by feeder section during a load control restore action (copyright 1988 by the IEEE)

feeder sections. The timing shown is very close to that of the design specification shown in Figure 6-13. With respect to this, the load appears to reach a new steady state level several measurements before the next control action takes effect.

Figure 6-42 also shows the effect of the air conditioner compressor motor startup. The rapid inrush power peaks and is followed by a decrease to steady state values, followed by the rapid increase as the next group of air conditioners is restored.

Figure 6-43 is a rescaled version of a single restore action and shows the power increase during inrush and the power decrease to a steady state value.

Twenty-five load restorations and ten load turnoffs were analyzed. These numbers were selected because five feeder sections were restored for each load control action and two groups were turned off for each action. Several parameters were calculated for each load turnoff and load restoration.

The average of the values before the restore action, the peak value at inrush, and the subsequent steady state value were calculated for both real and reactive power for load-restoring actions. The average value before turnoff and the average value after turnoff were calculated. In addition, each action was inspected to determine the time between initiation and peak value at inrush and the time between initiation and return to steady state values.

The inrush time for air conditioner compressor startup is about 200 ms. The postpeak values decrease to steady state in about 220 ms. The entire startup event lasts about 420 ms as shown in Figure 6-43.

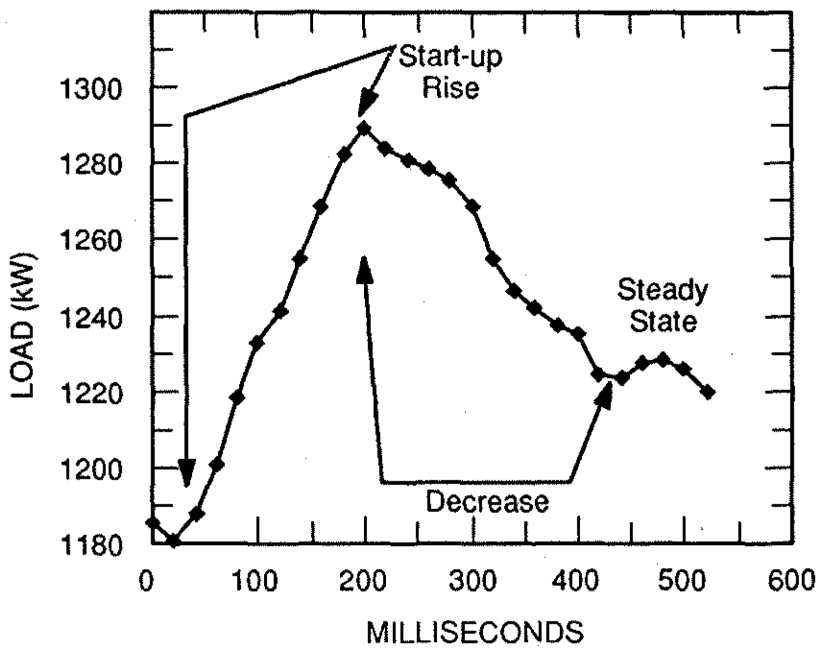

Figure 6-43 Rescaled version of a single load control action (copyright 1988 by the IEEE).

Based on data from the end-use monitoring equipment, air conditioner steady state operating values are determined to be in the range of 2.5 to 6.0 kW. The calculated difference between the prestart load consumption and the inrush peak consumption is 3 to 4 times greater than the steady state value, with some values ranging higher. Changes in the values of reactive power range between 34% and 57% of the changes in real power (see Figure 6-44).

The air conditioners were dropped in two groups. Figure 6-45 is a rescaled version of the 1 p.m. load drop. This graph shows that the load drop takes place in two steps separated by a short interval. The first load drop lasts 260 ms and is followed by a 340-ms interval and then a second load

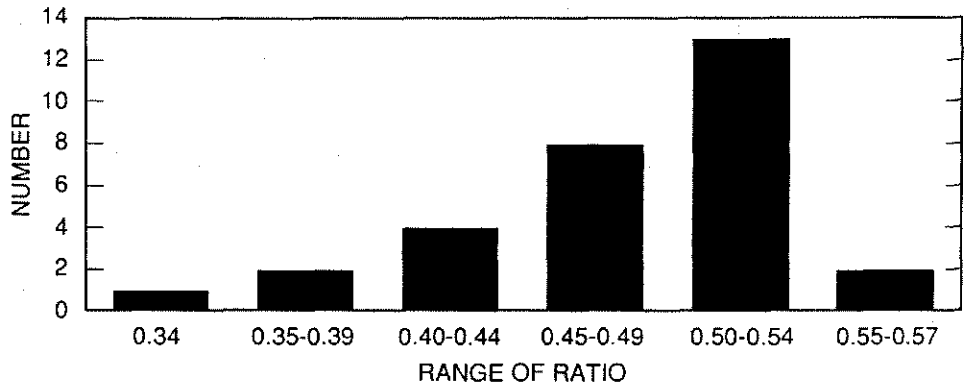

Figure 6-44 The ratio of changes in reactive power to changes in real power (copyright 1988 by the IEEE).

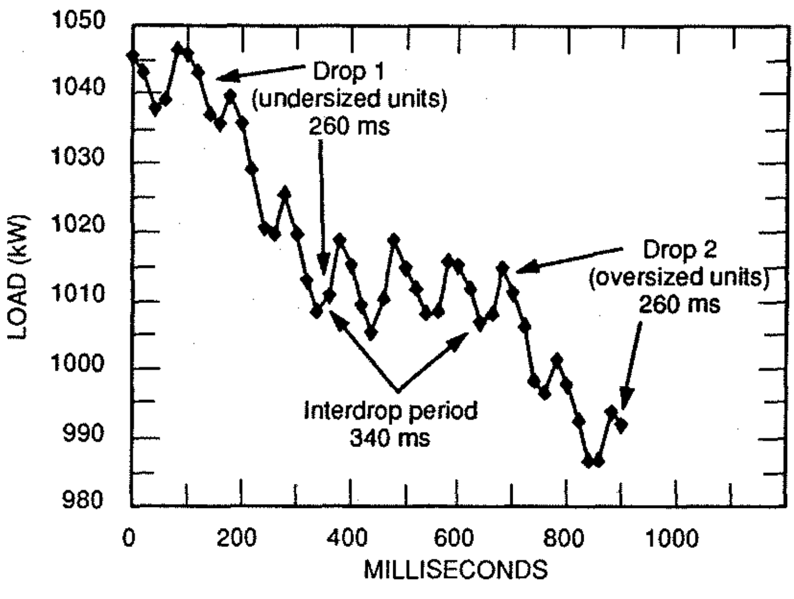

Figure 6-45 Air conditioners being deactivated by group during a load control shed action (copyright 1988 by the IEEE).

drop. The first decrease in real power corresponds to the time the drop message is received for the "undersized" air-conditioning group, while the second decrease corresponds to the time the load drop message is received for the oversized group. The interval is the remainder (100) of the 267 ms of silence between bits after the decrease has been measured plus the 267 ms required to send the next bit. This is consistent with the design specifications (see Figure 6-13).

Use of expert systems for load control. Based on observations of the air-conditioning experimental data, a set of rules was constructed for detecting air conditioner starts and stops in the high-speed data. These rules are applied to data in a window that contains all readings occurring within a 440-ms period. As an example, if data are taken every 20 ms, then the first window contains the first through the twenty-first measurements, the second window contains the second through the twenty-second measurements, etc. The rules are as follows:

- *Rule 1.* If the difference between the first (T1) and either of the last two readings [400 or 420 ms (T_{400}, T_{420})] in a window is between 2.0 to 6.6 kW, then the data in the window meet the criterion for an air conditioner having started and reached steady state operation.
- *Rule 2.* If the difference between the first reading in the window and either of the readings at 200 or 240 ms (T_{200}, T_{240}) in the window is between 5.0 and 30 kW, then the data in the window meet the criterion for the change in kilowatts for the inrush portion of an air conditioner start.
- *Rule 3.* If the difference between the first reading in the window and either of the readings at 200 or 240 ms (T_{200}, T_{240}) in the window is between 1.7 kvar and 18 kvar, then the data in the window meet the criterion for reactive power consumption for an air conditioner start.
- *Rule 4.* An air conditioner startup is detected only if rules 1, 2, and 3 are met.
- *Rule 5.* If the difference between the first kilowatt reading in the window and the reading at 260 ms (T_{260}) is in the range of -2.0 to -6.6 kW, then the data in the window meet the criterion for a change in kilowatts for an air conditioner from on to off.
- *Rule 6.* If the difference between the first kvar reading in the window and the reading at 260 ms (T_{260}) in the window is in the range of -0.65 kvar and -4.0 kvar, then the air conditioner meets the criterion for a change in kvar from on to off.
- *Rule 7.* An air conditioner stop is detected only if rules 5 and 6 are met.

Table 6-7 shows the number of air conditioner startups detected in each 30-minute interval of the time period examined.

It is interesting that the number of air conditioner startups decreases during the afternoon. To gain additional perspective on this phenomenon, a calculation was made to determine the number of air conditioner startups for the three comparison days in the summer of 1986. Figure 6-46 shows the frequency of the number of air conditioner startups each half hour and reveals a declining pattern of startups throughout the afternoon. We attribute this declining pattern of starts to the longer run times needed to meet the

TABLE 6-7 Number of air conditioner starts detected by high-speed monitoring on August 12, 1987

Time	Number
1:30–2:00 p.m.	191
2:00–2:30 p.m.	143
2:30–3:00 p.m.	115

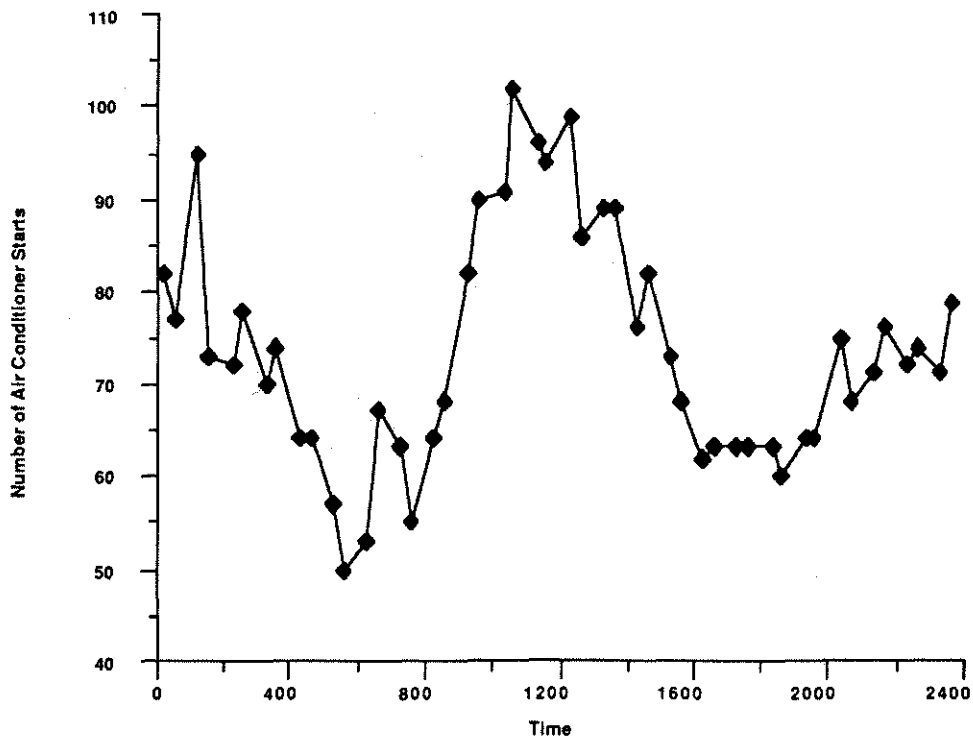

Figure 6-46 Number of air conditioner starts per half hour for three summer days in 1986.

increased cooling load as the day progresses. The number of startups is minimal at 4 p.m., when many air-conditioning units are operating for a substantial portion of the time.

The decline in the number of startups appears to be related to changes in the weather. A weather front moved through the Athens area as data acquisition began, causing the temperature to decrease 4°F just after 1 p.m. At 2:30 p.m., the solar radiation declined from 1.0 to about 0.5 langley/minute. This type of change could have reduced the run times of the air-conditioning loads.

Figure 6-47 plots the three values used to detect an air conditioner startup. The z-axis is the change in real power corresponding to inrush. The y-axis is the change in real power from prestart to steady state. The x-axis is the change in kvars associated with inrush.

The points in the graph are not randomly placed in the cubic space defined by the start rules. As expected, the points run from what would be the smaller-sized motors in the lower right corner to the larger sizes at the left rear.

It is not clear whether we can identify air conditioner startups from the high-speed data. However, the data give indications that the theory is correct and that further work is justified.

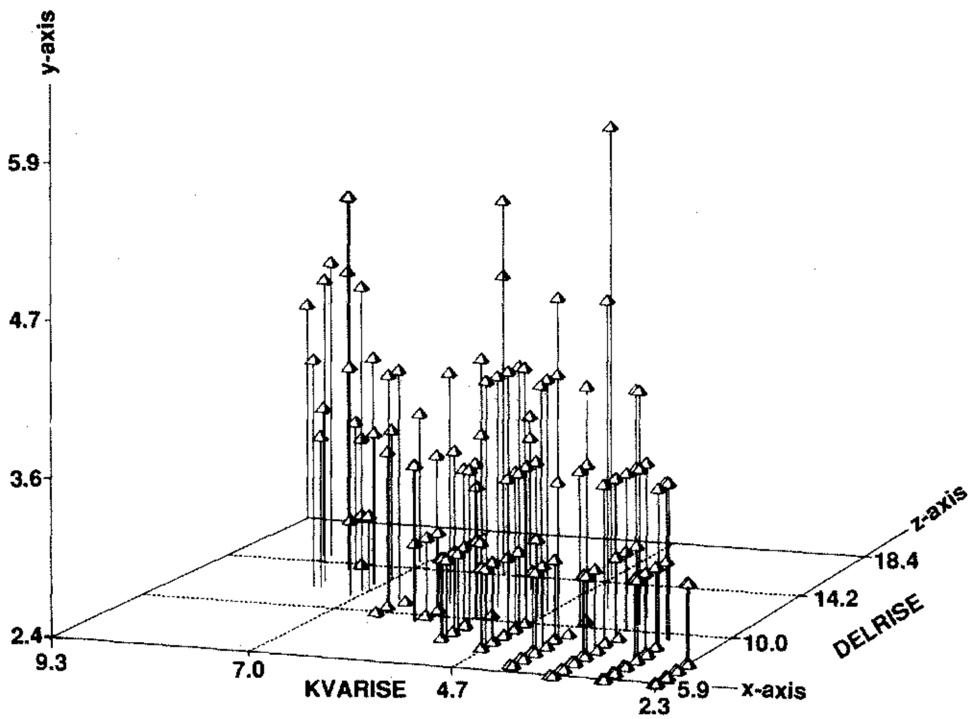

Figure 6-47 A plot of the sets of three values used to detect an air conditioner start.

These rules were applied to data for a 90-minute period when there was no control. Air conditioner startups appear to have been successfully identified. The rules for air conditioner shutdowns were so general that excessive numbers of air conditioner shutdowns were detected. We conclude that rules 5, 6, and 7 are not adequate to define when an air conditioner stops operating.

SUMMARY

Direct control of water heating is an effective method of shifting load. Installation of larger storage tanks and smaller heating units can be an effective way of reducing water heating load during peak loads.

With current technology, the control of heat pumps for space heating is difficult and not very practical. Existing control circuitry in heat pumps is designed to ensure, by turning on supplementary resistance heating, that buildings do not get cool when the compressor loses efficiency at lower temperatures. This usually means that customers who set back their thermostats will use the more costly resistance heating when they set them forward. Because this same problem may occur with direct control, controlling heat pumps is effective only on days when the temperature is low, the compressor has lost its efficiency, and heating is essentially resistive.

Control of resistive heating is effective if it is central heating and can be centrally controlled. The control of decentralized electric resistance heating requires circuit breakers equipped with relays that can be operated by 24-V supplies. The cost of the additional equipment required to provide the control voltage and installation may make them impractical.

Direct space heating and cooling control can benefit greatly from advanced-design solid state thermostatic controls. Thermostats are now available that allow customers to set back thermostats connected to heat pumps. Such thermostats do not call for resistance heating unless the compressor is unable to raise the temperature at an acceptable rate.

Between 200 and 250 kW was dropped on the test circuit each time air-conditioning load was controlled. In every case, the total amount of load that was restored was less than the amount dropped. This indicates that in some households, the heat gains due to load control did not exceed the cool-storage capacity of the building envelope. The results from high-speed data also correspond with the changes in solar radiation. Changes in solar radiation result in almost immediate changes in demand patterns.

If all customers are controlled with equal intensity, those whose cooling demands are larger relative to the capacity of their air conditioners will experience greater effects of control than those whose air conditions tend to be oversized.

Customer recruiting was done through personal contact and included a letter from the utility, a follow-up phone call, and on-site interviews. The customer acceptance rate was high, and the approach was very successful.

Many of the original concerns of dealing with customers were perceived rather than real. Far more effort was expended in dealing with predictions of how customers would respond to load control concepts than was expended responding to customer complaints. Although the various scenarios constructed were useful, many were simply wrong. The experiments showed that customers are much more tolerant than originally anticipated and more willing to participate than predicted.

A cluster analysis of monthly billing data was used to identify and recruit customers who have and use central electric space-conditioning appliances and/or electric water heaters.

Many customers are not appropriate targets for direct load control. Utilities should screen for customers who either do not have the proper appliances or do not use the appliances. Such screening can be done by the creative use of billing data and by the use of marketing segmentation studies.

Use of incentives is not necessary to the success of a load control program. Incentives are costly, encourage "free riding," and are difficult to administer. The Athens experiments and other studies show that an effective multifacted marketing program can achieve the objectives without the use of incentives. Direct-control programs can have a positive impact on customer relations.

Some equipment problems were encountered during the experiments. Utilities who are serious about load control should

- Check to see if the equipment has been used previously in the exact application.
- Be prepared for extended periods of debugging if the equipment has not been used previously in the exact application.
- Carefully evaluate the equipment that they are going to use. The experiences of other utilities with similar equipment should be examined. Equipment should also be checked for adequate lightning protection. Electronic components often do not function well in the extreme environments into which they are placed. The temperatures under a glass meter cover can range as high as 150°F. Electronic equipment does not function well in environments with high voltages, high currents, and electrical noise.
- Institute a comprehensive quality control program. The program should include observation of quality control procedures at the factory, predelivery testing at the factory, a thorough testing of each piece of equipment after delivery, and a postinstallation test before operation.

- Hire qualified instrument technicians to perform the checks and to maintain the equipment once it is installed.

Successful monitoring requires significant design effort. The following rules provide general guidelines for early planning, but they should be refined for individual applications.

- End-use monitoring, preferably with a sampling rate of 15 or 30 minutes, will provide useful data; however, 5-minute data are more useful.
- Whole-house usage data require a sampling rate of 1 minute or faster to be effective.
- Sample sizes can be less than 200 points; however, the observation of more events is required to produce statistically significant results.
- A plan for handling and maintaining data is essential because of the large amount of data that will be gathered. A full-time employee is needed to handle data maintenance problems. Data maintenance and screening tasks should be automated.
- New types of monitoring equipment that reduce data at the point of collection are needed.

REFERENCES

1. *1983 Survey of Utility End-Use Projects,* EM-3529, Electric Power Research Institute, May 1984.
2. A. B. Calsetta, M. A. Sager, and B. Edwards, *Bibliography on Load Management,* IEEE 85JH 7337-9-PWR, 1985.
3. T. A Heberlein et al., *Customer Acceptance of Direct Load Controls: Residential Water Heating and Air Conditioning,* EA-2152, Electric Power Research Institute, 1981.
4. D. R. Limaye and C. Whitmore, *Selected Statistical Methods for Analysis of Load Research Data,* EA-3467, Electric Power Research Institute, Palo Alto, Calif., 1984.
5. *SAS User's Guide: Basics,* Version 5, SAS Institute Inc., Cary, N.C., 1985.
6. K. D. Van Liere et al., *Public Reactions to Load Management: A Summary of Baseline Community Data for the Athens Automation and Control Experiment,* ORNL/TM-7961, Oak Ridge National Laboratory, 1982.
7. R. Burby et al., *Electric Utility Load Management: Marketing Strategies and Tactics,* Rowman and Allanheld, Totowa, N.J., 1983.
8. A. G. Lawrence, T. A. Heberlein, and R. M. Baumgartner, *Customer Attitudes and Response to Load Control,* RDS95, Electric Power Research Institute, 1984.
9. W. Meyer, C. Harbourt, N. Pazokki, and R. Jobe, "Impact of Heat Pumps on Load Shape and Load Control," *Proc. Am. Power Conf.* **44,** 159–60 (1978).

10. W. J. Smolinski, "Determination of Potential Demand Reduction on Residential Electric Heating Systems with Load Management," presented at the IEEE Power Engineering Society Winter Meeting, February 1988, New York; published in *IEEE Trans. Power Appar. Syst.* **PAS-97**(4), 1012 (August 1978).
11. J. H. Reed, *Test Plan for the Load Control Experiments: Athens Automation and Control Experiment,* ORNL/TM-9796, Oak Ridge National Laboratory.

7

MODEL FOR DIRECT LOAD CONTROL*

J. D. Birdwell and D. Bargiotas

Accurate single-customer models are vital to the development of aggregate dynamic load models that can predict response to direct-load-control actions. Without such aggregate models, optimal scheduling of direct-load-control actions in a manner that accounts for constraints upon customer comfort is not possible. In this chapter, a dynamic model of the response of a single residential air conditioner load to weather conditions is developed. The model's performance is evaluated from data obtained from the Athens Automation and Control Experiment (AACE), and some novel approaches to the determination of the parameters of a customer's thermal envelope model are discussed. The model is used to make a preliminary assessment of the effect of the level of detail upon model accuracy. For the limited number of customers with suitable data and survey information who were available in the experiment, the variability of parameters and responses is assessed.

The use of sophisticated and more accurate power system load models has the potential to significantly improve the operation and planning of utility distribution systems. Recently, utilities have shown great interest in load models that can be used in direct load management. Such load models generally represent space conditioning and water heater loads aggregated over a group of customers. For direct load management applications, load models

*This chapter is based on material in IEEE Paper No. 88 WM 066-3, "Residential Air Conditioner Dynamic Model for Direct Load Control," by D. Bargiotas and J. D. Birdwell, which was first presented at the IEEE Power Engineering Society Winter Meeting, February 1988, New York (copyright 1988 by the IEEE).

based only on the statistical analysis of historical data are not sufficient—they cannot predict the effects of direct load control. For this purpose, either historical data that include the response to extensive direct-load-control experiments or physically based models that are capable of accurately predicting the response are required.

This discussion concentrates on residential load models for space conditioning. The methodology suggested can be expanded to develop models for other types of loads. To construct an accurate, physically based load model of a space conditioner, the thermal characteristics of the house are required. The thermal characteristics can be calculated from survey data or by estimation techniques. Survey data are more accurate but may be economically less suitable. Combining estimation techniques with a limited amount of survey data and historical consumption data would yield less costly results; however, these techniques have yet to be developed and tested.

An accurate space-conditioning load model should incorporate, in addition to the house thermal characteristics, the effects of weather (temperature, humidity, solar radiation, and wind speed); the effects of lifestyle; and possibly the effects of voltage and frequency fluctuations. It is clear that load management and direct-load-control strategies cannot be based upon a collection of load models for each house. Rather, aggregate load models, each representing customers having "similar" characteristics and, therefore, belonging to the same classification group, are desirable. The classification of the groups can be based on historical load data and/or survey data (size of house, type and size of space conditioning unit, and insulation level of the house). For each group, a model of the aggregate load of the group members is desired. The model should be based upon either general characteristics of the group or specific characteristics of the members of the group. The latter method appears more complicated but promises better results.

Given accurate, physically based models of a collection of customers, it appears possible to produce a model that can predict with reasonable accuracy the aggregate response to direct-load-control actions.[1,2] These results, however, have been based upon (1) customer models that use unverified assumptions, such as uniform customer characteristics or the uniform or Gaussian distribution of customer parameters; and (2) the independence of model behavior on exogenous variables, such as indoor and outdoor humidity or solar insolation.

This research addresses five issues: (1) development of a detailed model of air-conditioning load for a single customer; (2) information required to evaluate the parameters of this model; (3) model accuracy using collected data, and possible unmodeled effects that contribute to errors; (4) variability of customer parameters and responses; and (5) effect of model detail upon accuracy. The long-term goal of the research project is the development of a dynamic, physically based, single-customer load model. The model must be easily and inexpensively customized to individual customers and sufficiently accurate for the subsequent development of an aggregate model based upon individual models of a sample population of the controlled customers.

SUGGESTED METHODOLOGY

An accurate space-conditioning load model for use in direct-load-control strategies should incorporate a mathematical description of the nature of the load and the weather conditions that affect the load shape, based upon the theory of the underlying physical processes. Because a theoretical load model can easily incorporate house parameters, air-conditioning parameters, and weather conditions, it is very promising for use in determining direct-load-control strategies. Furthermore, such models can be recalibrated periodically or adjusted for use in different locations, possibly using on-line parameter identification. The development of a residential load model should include the following steps:

- classification of the population into groups,
- development of an aggregate load model for each group, and
- validation of the aggregate load model from high-frequency real data.

The classification of the population could be based on historical consumption data, parameters of the house, parameters of the space-conditioning unit, and lifestyle pattern.

The development of the aggregate model for each classification group can be based on fairly detailed dynamical load models of a representative sample of houses belonging to the same group. Each single-house load model includes the effects on load shape of the house thermal characteristics, performance of the space-conditioning unit, indoor temperature and humidity, weather conditions (temperature, humidity, solar radiation, and wind speed), and lifestyle (thermostat setting). The house thermal characteristics are determined by the size and shape of the house, the insulation levels, and other measurable parameters.[3]

Knowledge of the performance of the space-conditioning unit is considered necessary in developing an accurate load model because the power consumption and the thermal power output change drastically with weather fluctuations, especially with temperature and humidity.

The dependence of the residential load space-conditioning model on the weather conditions is fairly obvious. Although temperature is the main factor affecting the demand, the addition of humidity, wind speed, and solar radiation could increase the accuracy of the load model without increasing significantly the computational requirements. Prior to this research, the relative contribution of these factors was unknown. Humidity has been included in the model reported here; wind speed and solar insolation have not. As will be demonstrated, humidity effects may be neglected for cooling loads; this may not generalize to heating loads.

Because of the sensitivity of the space-conditioning load shape to lifestyle, the dependence of the load model on lifestyle should not be ignored. Unfortunately, lifestyle effects are poorly understood and tend to be erratic. We suspect that a substantial portion of the errors in predictions using the model results from (unmodeled) lifestyle dynamics. Lifestyle is represented as only an unmeasurable indoor thermostat set point in the model; for some customers, the assumption that the set point is constant is clearly violated. A possible avenue of future research would be set point identification and tracking.

THE MODEL

The model is based upon equations for energy balance and mass balance for the air inside a customer's residence. Because a significant portion of an air conditioner's thermal power is committed to the extraction of water vapor from the house, equations relating both indoor temperature and humidity to outdoor temperature and humidity were developed.

This model depends upon several parameters that are unique to each customer: insulation characteristics, air conditioner efficiency curves as a function of outdoor temperature and outdoor humidity, indoor temperature and humidity, and thermostat set point. Insulation characteristics for the customers included in this study were estimated from a site survey. This survey also collected data on customers' answers to questions about thermostat set point and how the set point might be changed on a regular basis. Unit efficiency curves were obtained from manufacturers' data sheets, with nameplate data recorded as part of the survey. Unfortunately, for most units it proved necessary to use efficiency curves for a similar unit, because the older the unit, the less likely the chance of finding a matching data sheet.

For a large customer base, a sufficient set of statistics cannot be gathered on all units. Our goal is to provide some validation for a dynamic model and assess in the process the relative effects of model parameter errors and excursions in outdoor temperature and humidity. Second, we wish to assess the likelihood of using this model as a basis for estimating model parameters from time series data. Third, we expect to use this model as a way to predict the effect of load control strategies on the customers. Specifically, we seek to evaluate the variations in indoor temperature and humidity caused by cycling load control strategies used within the Athens system.

The authors have developed a single-house air conditioner load model for use in the evaluation of direct-load-control strategies, which can easily be modified to represent other types of space conditioners. The model is described by two coupled differential equations.[4] The first equation of the model, which tracks the temperature inside the house (T_{in}) as a function of constants and either measurable or estimated variables, is given by

$$\dot{T}_{in} = [k_1(T_{out} - T_{in}) + e_1 V S_{vap}(T_{out} H_{out} W_{sat-out} - T_{in} H_{in} W_{sat-in}) \tag{1}$$

$$- sw\, E_{sen}]/[V(D_{air} S_{air} + H_{in} W_{sat-in} S_{vap})] \ ,$$

where

k_1 = the house thermal coefficient, including only dry air effects (Btu/°F·hour);
T_{out} = the outdoor temperature (°F);
T_{in} = the indoor temperature (°F);
V = the total volume of the house (ft^3);
S_{vap} = the specific heat of water vapor (Btu/lb·°F);
H_{out} = the outdoor relative humidity;
H_{in} = the indoor relative humidity;
$W_{sat-out}$ = the density of saturated water vapor as a function of T_{out} (lb/ft^3);
W_{sat-in} = the density of saturated water vapor as a function of T_{in} (lb/ft^3);
e_1 = the percent of the total indoor air that is exchanged every hour with the environment (or the percent of the total energy leaving the house if the energy lost due to the condensation in the unit is not included), in the range [0,1];
sw = the switch process of the air-conditioning unit ($sw = 1 \Rightarrow$ unit = 'ON'; $sw = 0 \Rightarrow$ unit = 'OFF');
E_{sen} = the rate of energy transfer from indoors to outdoors caused by the air-conditioning unit (Btu/hour) (= sensible capacity of the unit);
D_{air} = the density of the dry air at a given temperature (lb/ft^3); and
S_{air} = the specific heat of the dry air (Btu/lb)c.°F).

The second equation, which tracks the humidity inside the house (H_{in}) as a function of constants and either measurable or estimated variables, is given by

$$\dot{H}_{in} = \frac{e_1(H_{out} W_{sat-out} - H_{in} W_{sat-in})}{W_{sat-in}} - \frac{sw\, E_{unit}}{E_{cond} W_{sat-in} V} \ , \tag{2}$$

where

E_{unit} = the rate of transfer of energy from indoors to outdoors due to the moisture condensation caused by the air-conditioning unit (Btu/hour) (= total capacity − sensible capacity) and

E_{cond} = the heat of condensation (or vaporization) of the water (= 970 Btu/lb).

VALIDATION OF THE MODEL

The model was tested with data from ten customers participating in the AACE. For each of the houses, air-conditioning consumption data, recorded in a 5-minute cycle using Robinton Electric Appliance Research Meters (ARMs), and weather data are available for the summer of 1986. We used data from the month of August 1986. The combined file of ARMs and weather data contains information on the outdoor temperature, outdoor humidity, status of the air-conditioning unit (whether the unit is on or off), and the power consumption of the unit.

For each of the houses, using real data, we estimate the duty cycle of the air-conditioning unit (T_{dc}), the cycle time of the unit (T_{cyc}), the time the unit is on (T_{on}), the average power (P_{avg}), and the maximum power consumption (P_{max}) per cycle with respect to outdoor temperature (T_{out}) and humidity (H_{out}). The same quantities are also calculated from data taken from a simulation of the model under a variety of values of outdoor temperature, humidity, and thermostat set point (T_{sp}). Specifically, the temperature ranged from 70 to 100°F, the relative outdoor humidity ranged from 50 to 100%, and the thermostat set point ranged from 65 to 75°F. The data used to calculate these quantities represent steady state values.

For each possible combination of the outdoor temperature, outdoor humidity, and thermostat set point, the model was simulated until approximately steady state was reached, and then data were recorded over a 3-hour period with a time interval of 0.01 hour. The data recorded from the simulation were time, indoor temperature, indoor humidity, average power demand, and status of the air-conditioning unit (*sw*). Sample values for the parameters and constants for one of the tested houses (corresponding to house 9 in Table 7-1) used for the validation of the single-house model are listed in Table 7-2.

The output of the model (with the exception of the indoor humidity) appears to be affected little by the outdoor humidity. The dependence of the duty cycle, the maximum power demand, and the average power demand on the outdoor humidity is summarized in Table 7-1. The table gives the maximum percent deviation in these three variables for the ten customers

TABLE 7-1 Dependence of results upon outdoor humidity (copyright 1988 by the IEEE)

Customer	Percent change (Δ / mean value)		
	Duty cycle	Maximum power	Average power
1	8.99	1.17	9.81
2	9.58	0.84	10.25
3	11.65	1.80	13.17
4	11.85	1.27	12.72
5	8.50	1.95	9.40
6	9.25	1.94	10.09
7	12.66	2.25	14.46
8	9.49	1.50	10.63
9	12.22	2.76	11.30
10	7.51	2.36	9.76

TABLE 7-2 Parameters of the model (copyright 1988 by the IEEE)

Volume, ft^3	15872
Thermal house coefficient, Btu/°F·hour	1366
Unit brand	General Electric BWC030B
Total capacity, Btu/hour	27,200
Air exchange rate, %/hour	10

studied. As a consequence, the remaining results assume a constant outdoor humidity of 100%, which is a good approximation for Athens in August.

A family of curves, one for each value of the thermostat set point (T_{sp}), was derived from the simulation for each customer. The curves represent the behavior of T_{dc} (Figure 7-1), P_{max} (Figure 7-2), and P_{avg} (Figure 7-3), as a function of the outdoor temperature, for customer 9. Curves extracted from ARMs data for the same customer are presented in Figure 7-4 (T_{dc}), Figure 7-5 (P_{max}), and Figure 7-6 (P_{avg}). The theoretical and actual (estimated from collected data) slopes of the average power demand are similar, indicating that the model should be useful in predicting average power and duty cycle, as a function of outdoor temperature. From a comparison of the zero intercepts of the curves, we hypothesize that the thermostat set point of the house is approximately 65°F. Theoretical and actual slopes of average power demand and estimated thermostat set point for each of the ten houses studied are summarized in Table 7-3. For the simulation data, slopes are averaged over the linear portion of the curves; for the collected data, slopes use the maximum values along the curves.

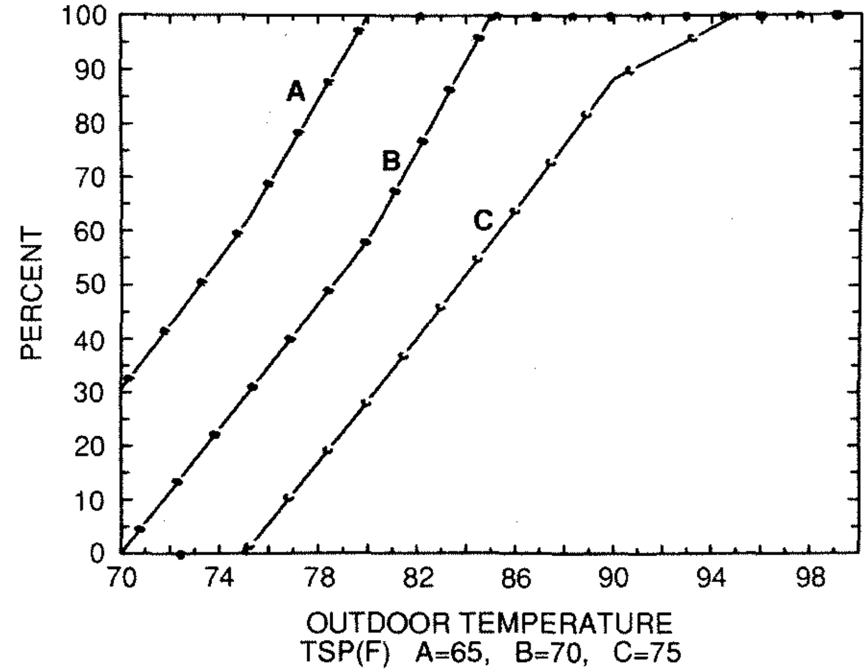

Figure 7-1 Steady state simulated duty cycle as a function of outdoor temperature for various values of thermostat set point (T_{sp}) (copyright 1988 by the IEEE).

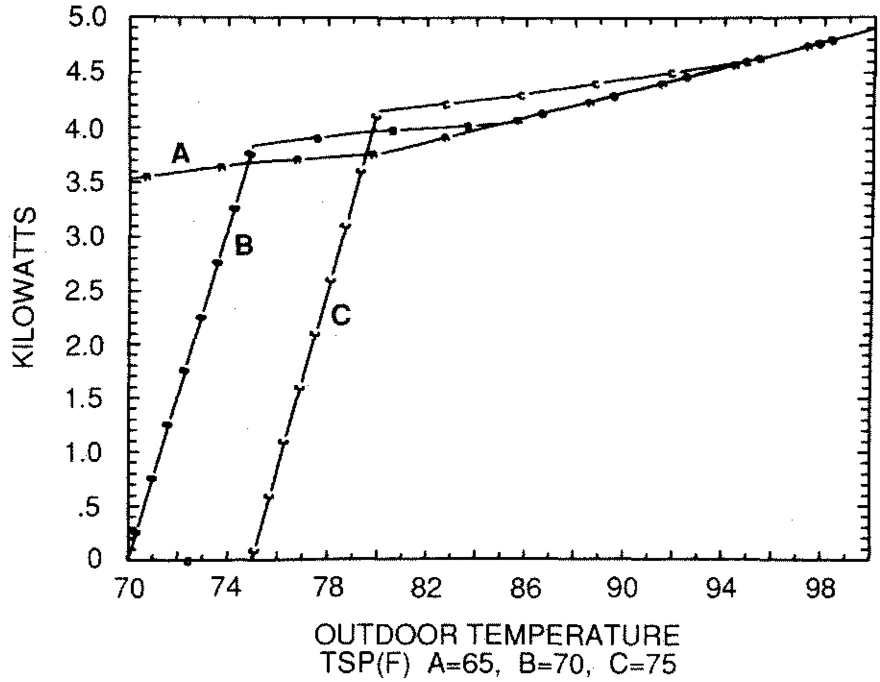

Figure 7-2 Steady state simulated peak power demand as a function of outdoor temperature for various values of thermostat set point (T_{sp}) (copyright 1988 by the IEEE).

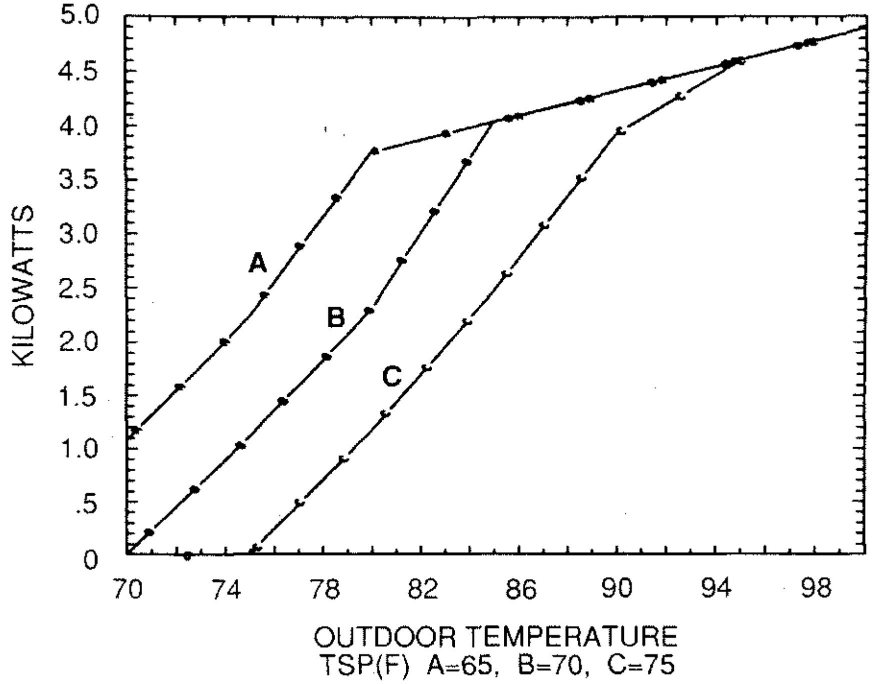

Figure 7-3 Steady state simulated average power demand as a function of outdoor temperature for various values of thermostat set point (T_{sp}) (copyright 1988 by the IEEE).

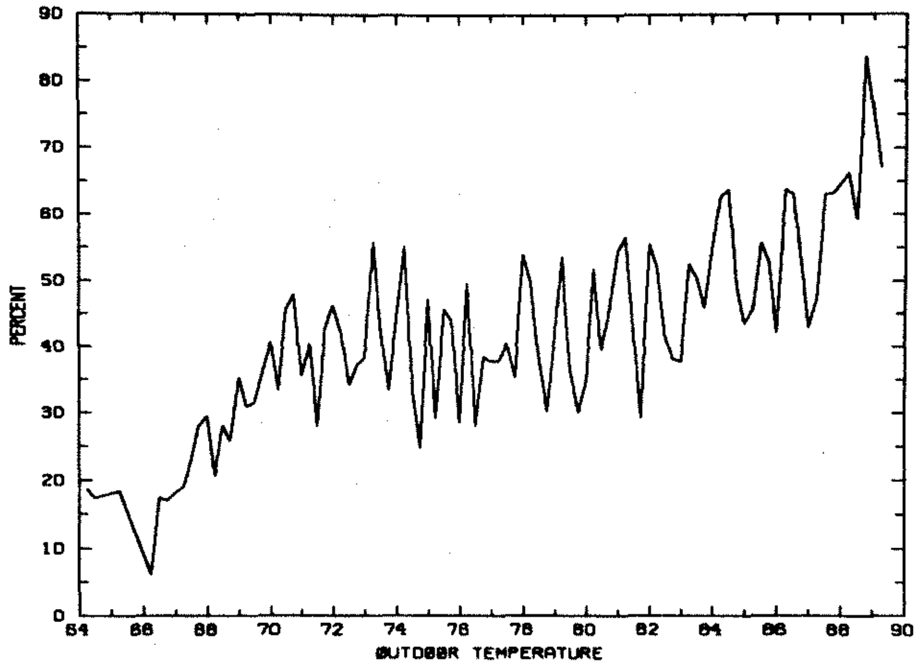

Figure 7-4 Actual air conditioning duty cycle (copyright 1988 by the IEEE).

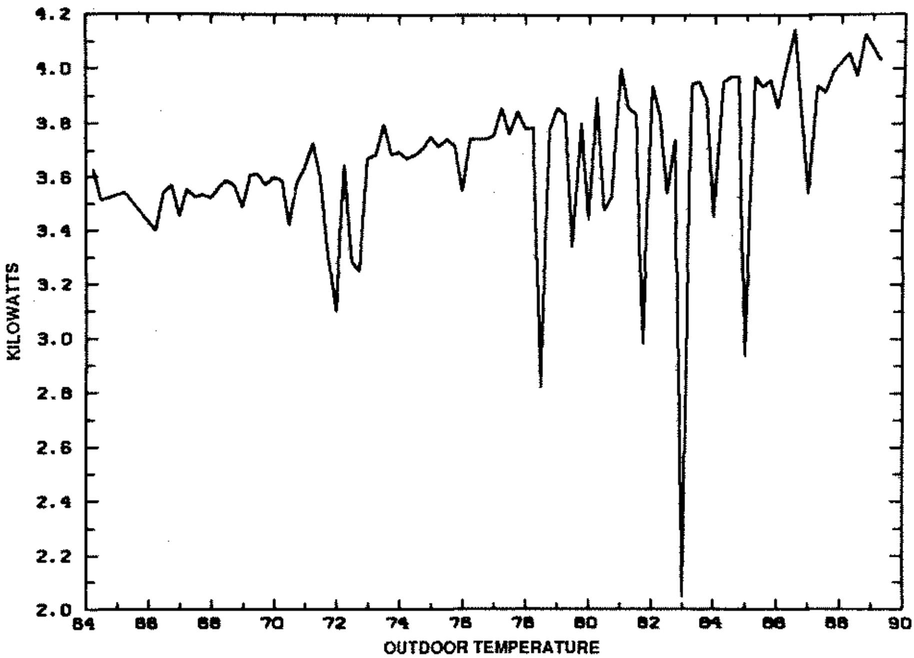

Figure 7-5 Actual peak air conditioning power demand (copyright 1988 by the IEEE).

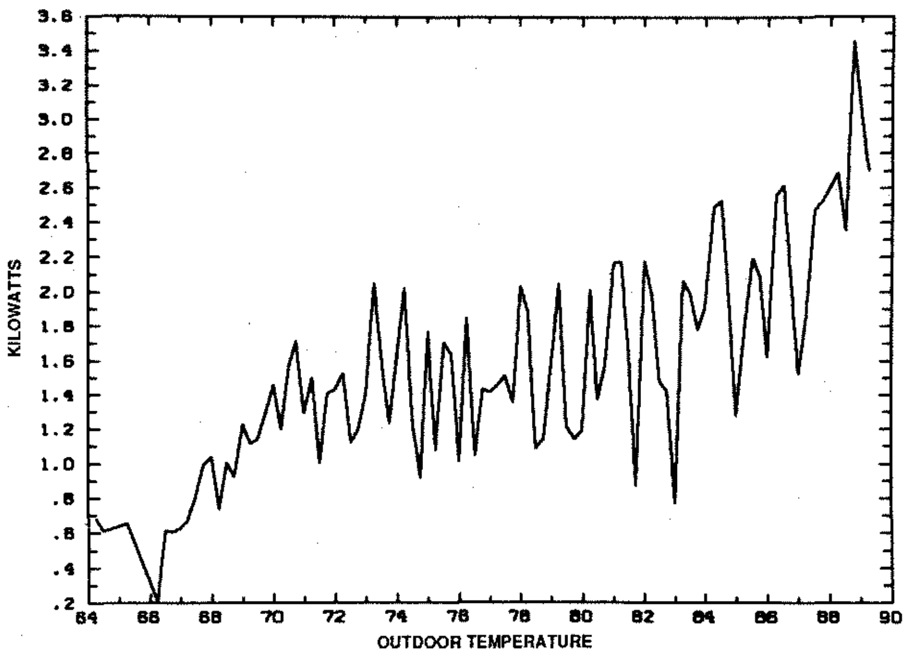

Figure 7-6 Actual average air conditioning power demand (copyright 1988 by the IEEE).

TABLE 7-3 Comparison of slopes for average power demand vs temperature and the estimated thermostat set point (copyright 1988 by the IEEE)

Customer	Theoretical slope (P_{avg})	Actual (estimated) slope (P_{avg})	Estimated T_{sp}
1	0.97	1.07	66
2	1.28	1.07	72
3	0.87	1.04	65
4	0.78	0.90	64
5	0.81	0.78	63
6	0.87	0.97	61
7	1.28	0.90	61
8	1.00	1.04	59
9	0.97	1.00	65
10	1.48	0.97	63

PREDICTION OF DIRECT-LOAD-CONTROL EFFECTS

The single-house model has been used to predict the effects of direct load control on the customer. Figure 7-7 gives an example of such an action. After the system reaches its steady state (3 hours), a control action is introduced into the system. The control action forces the air-conditioning unit to turn off for 10 minutes at the beginning of each 30-minute cycle. The figures overlay all the cycles on one 30-minute period. Successive cycles are indicated by the letters A, B, C . . . . This simulation demonstrates two effects of direct load control:

1. The peak indoor temperature is increased.
2. The control action causes the unit cycles to synchronize with the direct-load-control system cycles.

This result predicts that the direct load control will cause a loss of diversity among the load control customers. Consequently, direct load control, as described above, may negatively affect the peak power demand.

More information on the effects of load control actions are shown in Figure 7-8. The control action forces the unit to turn off for 0, 7.5, 10, 12, 15, and 18 minutes at the beginning of each 30-minute load control cycle. The temperature excursions within the houses depend on the parameters of the customer (insulation, volume, etc.); these parameters are costly to measure; however, some estimate of those parameters is necessary for accurate grouping of customers with similar responses.

We suspect that a control action that has little effect on one customer could severly affect another customer. For the test house, control actions of

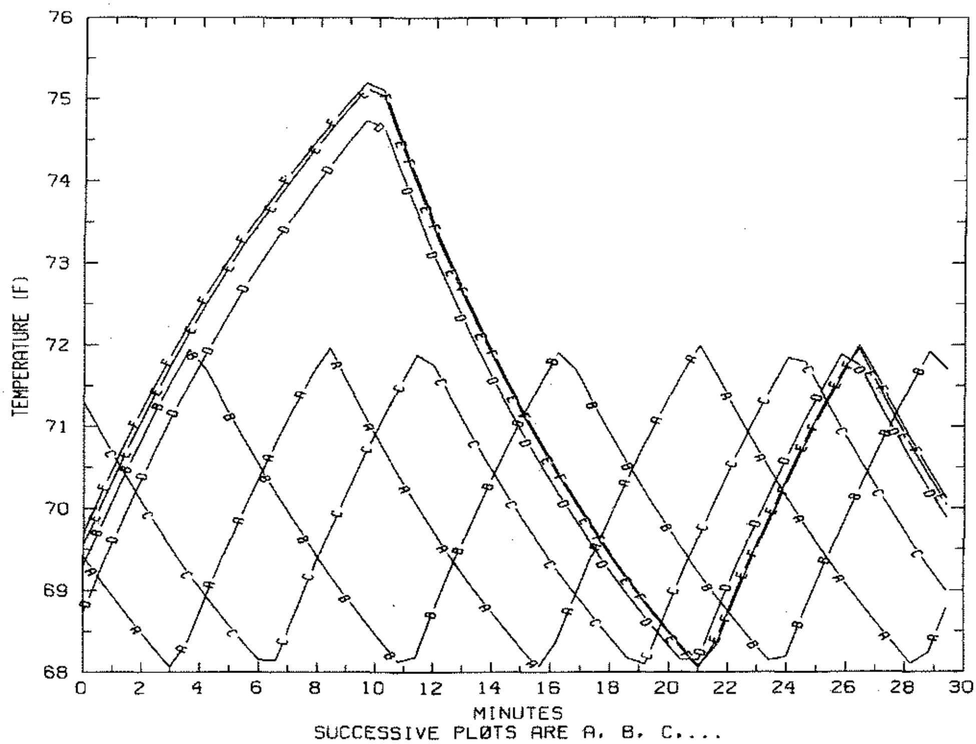

Figure 7-7 Synchronization effect (simulated) of direct load control on the indoor temperature cycle (copyright 1988 by the IEEE).

12 minutes or less may not be of concern to the utility's customers. Control actions lasting more than 15 minutes result in indoor temperature changes severe enough to be noticeable and may not be acceptable by the customer. Table 7-4 summarizes the temperature excursion vs load control action in each of the ten customer houses under study. All illustrated data assume a thermostat set point of 70°F, an outdoor temperature of 80°F, and an outdoor humidity of 100%. Although there are as yet no data on the dropout rate of customers participating in the AACE, it will be interesting to correlate the dropout rate with the predicted temperature excursions.

In a load management program of Pacific Gas and Electric (PG&E) Company,[5] the observations agree with our predictions. It is worth noting that about 70,000 customers are participating in the PG&E load control program. Initially, the program cycling strategies were 9 and 12 minutes for every 30-minute cycle, without any significant controversies. The later-introduced 15- and 18-minute cycling strategies for every 30-minute cycle, were too severe for many customers. As a consequence, PG&E had to eliminate the 18-minute strategy.

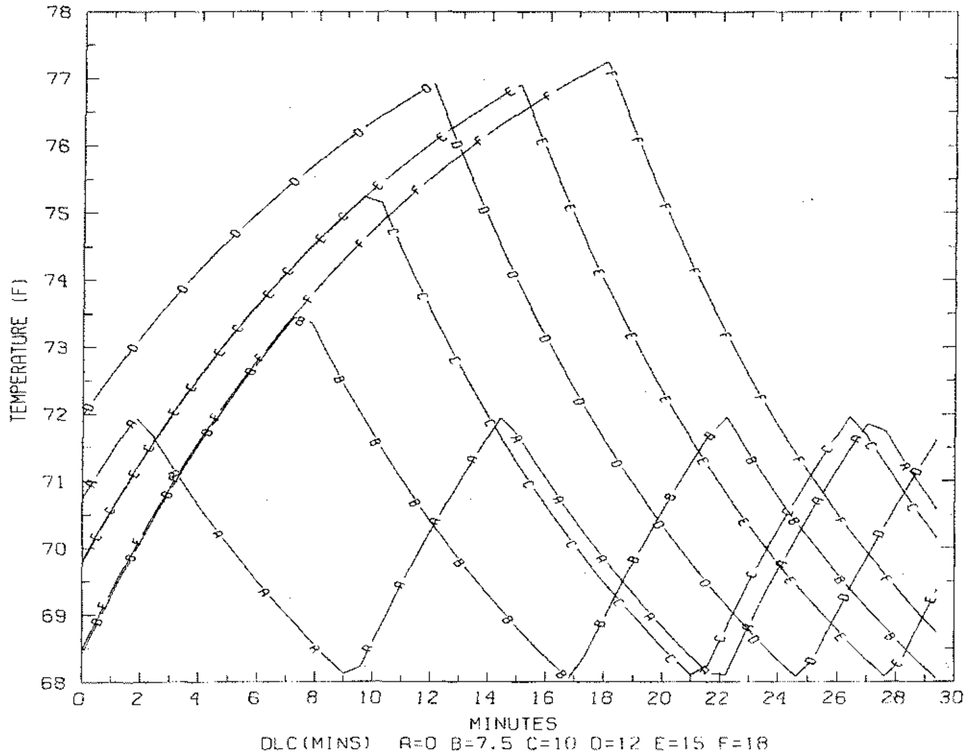

Figure 7-8 Effect of direct load control on the indoor temperature (copyright 1988 by the IEEE).

TABLE 7-4 Indoor temperature excursions as a function of load control strategy (copyright 1988 by the IEEE)

Customer	Temperature excursion for strategy (°F)					
	A (0%)	B (25%)	C (33%)	D (40%)	E (50%)	F (60%)
1	3.8	8.3	8.2	9.2	10.6	10.6
2	3.9	7.2	9.0	9.7	9.8	10.7
3	3.9	7.3	7.3	7.3	9.4	9.7
4	3.8	6.7	7.7	7.9	9.2	9.8
5	4.0	5.4	8.1	8.3	8.7	10.1
6	3.8	7.7	8.8	9.2	10.5	10.7
7	3.7	7.7	8.2	8.3	9.3	10.2
8	4.0	5.2	8.0	8.5	8.6	10.1
9	4.0	5.4	7.2	8.9	8.9	9.2
10	3.9	7.3	8.6	9.4	10.3	10.9

SUMMARY

An accurate single–customer load model is required for development and testing of aggregate load models useful for direct load control. This model is used to portray a sample population of customers within the controlled customer group, and it should be easy and inexpensive to define, or customize, for individual customers. Our immediate goal is to determine in such a model the correct level of detail consistent with accuracy and economy. We experienced considerable difficulty in obtaining a sufficiently uniform quality in survey data taken to establish model parameters and in procuring manufacturers' efficiency specifications on installed units. These two items represent a significant portion of the project cost, and their necessity should be avoided if possible. A procedure for economically estimating the required parameters for a single-customer load model using readily available data would be quite valuable.

We believe that the agreement between the slopes of the average power–outdoor temperature curves and the ability to estimate the thermostat set point from actual data lend credence to our model; however, the model is probably overly complex. Given the small variation in average power demand vs humidity, the dependence upon both indoor and outdoor humidity can probably be removed. We stress, however, that prior to this study, this probability was an unverified assumption in other works. Noting the rough order-of-magnitude difference between the variation due to humidity in average and peak power demand, we hypothesize that the characteristics of the thermostat, which is essentially a closed-loop control around the unit, allow the reduction in model complexity.

Finally, we believe that the loss of diversity due to direct-load-control cycling strategies is a significant effect and that it should receive more attention. This effect may be limiting the possible energy recovery due to load control, and if so, other control strategies should be investigated.

REFERENCES

1. H. T. T. Nguyen and J. D. Birdwell, "A Physically-Based Low-Order Model for Aggregate Air Conditioner Loads," *Proc. 1982 American Control Conference*, Arlington, Virginia, June 1982.
2. R. E. Mortensen and K. P. Haggerty, "A Stochastic Computer Model for Heating and Cooling Loads," *IEEE Power Engineering Society Summer Power Meeting*, July 1987.
3. J. Reed et al., *Test Plan for the Load Control Experiments Athens Automation and Control Experiment*, ORNL/TM-9796, Oak Ridge National Laboratory, September 1985.

4. D. Bargiotas and J. D. Birdwell, "Residential Air Conditioner Dynamic Model for Direct Load Control," *IEEE Trans. Power Delivery,* 3, 2119–26 (October 1988).
5. D. L. Becker, "Load Management Direct Control: Fact or Simulation," IEEE Publications 85 SM 477-5, presented at the 1985 IEEE PES Summer Meeting.

8

AUTOMATION SOFTWARE

**E. R. Broadaway, J. B. Patton, J. S. Lawler,
D. T. Rizy, and G. R. Wetherington**

While the principles of distribution system analysis and operation are well known, no applications software packages are suitable for supporting the operators of automated distribution systems. The packages that are available were generally developed for planners rather than operators, run on mainframe computers, have long execution times, and are cumbersome to use.[1] The development of a distribution automation applications software package for assessing system reconfiguration opportunities and volt/var control on radial distribution feeders is discussed in this chapter.

Several computer programs were written for the AACE. The System Reconfiguration and Analysis Program (SYSRAP), an off-line personal-computer-based feeder analysis program used primarily to support the research experiments, is discussed in this chapter. The development of SYSRAP was motivated by the needs of automation system designers and researchers to determine the optimum location, number, and characteristics of automation equipment and the need of system operators to predict the effect of automation system control actions. The Athens Automation and Control Experiment Test System (AACETS), also discussed in this chapter, is a scaled-down laboratory prototype of the full Supervisory Control and Data Acquisition (SCADA) system in Athens. SCADA was used to develop real-time control programs and test the custom real-time software necessary to support the Brown Boveri Control Systems, Inc., SCADA software. Some of the special SCADA software tools developed on AACETS are described.

SYSRAP combines power-flow and short-circuit analyses with data base management. Many unique features of the code have evolved from experience with the AUB automation system and operator concerns. The program is especially well suited for answering "what if" questions posed by the operator with respect to switch orders, capacitor bank dispatch, and regulator tap adjustments. The program runs on a personal computer, interfaces with the mainframe computer that controls the real-time data acquisition and control system at AUB, and executes power-flow and short-circuit analyses for detailed feeder models in tens of seconds. Reorganizing the data base to reflect switching operations and changes in the status of volt/var control equipment is easily accomplished.

One important observation of the AACE is that feeder load sensitivity to voltage is a significant effect that cannot be neglected in simulating system response to control actions that alter feeder voltage profile.[2] An operator support tool that accurately predicts the impact of reconfigurations, capacitor switching, and regulator tap adjustments must include load sensitivity to voltage as part of the feeder model. Feeder load distribution, the voltage-sensitive load model used by SYSRAP, the power-flow analysis procedure, and two applications of SYSRAP on the AUB system are presented. Finally, some observations on the software development and directions for future development of operations support software for automated distribution systems are given.

Functional Capability

SYSRAP is a menu-driven computer program developed for analyzing electric distribution systems and supporting the operator of an extensively automated system. The program is written in PASCAL and runs on an IBM-compatible personal computer. SYSRAP was developed by ORNL over a 3-year period for simulating and analyzing distribution automation functions such as feeder load transfers and volt/var control. A user's manual for this program has been prepared and published by ORNL (report number ORNL-6575) and can be obtained from the Department of Energy, Technical Information Center, P.O. Box 62, Oak Ridge, TN 37831. The program combines three-phase power flow analysis (three decoupled, single phases per feeder that need not be balanced), short-circuit analysis (three-phase balanced fault), and data base manager.

SYSRAP is capable of three major functions: conducting distribution system studies, interrogation of the feeder data base, and data base editing. The data base organization exploits the feeder's radial structure and allows accumulation of data related to load, losses, number of customers, voltage drop, and impedance. Twelve feeders of the Athens Utilities Board have been modeled and are being analyzed by SYSRAP as part of the AACE.

Distribution system studies. The program can perform six different distribution system studies: load transfer alternatives study, load transfer simulation study, voltage study, short-circuit study, postfault load transfer study, and capacitor dispatch study. SYSRAP maintains a static data base of line parameters and a dynamic data base of load and status parameters that allow the operator to perform these various studies interactively without extensive additional calculations (except when a reconfiguration or capacitor dispatch is performed). The dynamic data base is periodically updated from the SCADA real-time data base, while static data parameters are changed when physical changes are made to the distribution system.

Load transfer alternatives study. A simple feeder-to-feeder load transfer involves two switch operations: a tie switch (normally open) between the two feeders must be closed, and an in-line sectionalizing switch (normally closed) on the feeder to be relieved of load is opened to complete the load transfer to the supporting feeder. An operator has four primary concerns in developing a switch order for such transfers: what are the switching alternatives?; is the conductor capacity adequate?; will the voltage/loss profile be acceptable on both feeders?; and will there be drastic changes in short-circuit duty that may disrupt protection? The load transfer alternatives study was developed to identify candidate switch orders and provide the operator with answers to the capacity issues.

For each line section of each feeder, the data base includes (1) the temperature-dependent ampere capacity as calculated by the Schurig and Frick equations[3] and (2) the through load (in amperes) on the basis of the existing load condition. The difference, capacity minus load, is the "margin" that is the increment in through load that can be added to the section without overload.

Because the conductor capacity is temperature dependent, the user specifies an ambient temperature and the feeder from which the load is to be transferred. The data base is then searched to identify all candidate in-line switches and the total ampere load below each such switch. The user selects one sectionalizing switch to be opened, and a search is initiated to find all possible tie switches to be closed to an alternate feeder.

For each tie switch, the "minimum margin" is located on the supporting feeder and the minimum capacity is located on the area to be transferred. The minimum margin is the smallest margin on any line section in the direct path between the tie switch and the feeder breaker on the supporting feeder. The location of the minimum margin is the potential bottleneck on the supporting feeder. The minimum margin must be greater than the total load to be transferred. The minimum capacity on the section to be transferred is also important because it also represents a potential bottleneck. After the transfer is completed, the section that is transferred will be fed from the tie switch rather than from the in-line sectionalizing switch. Consequently, the capacity of the conductor in the vicinity of the tie switch must exceed the total ampere load in the area to be transferred. This is an important consideration in systems that are telescoped, that is, where conductor size decreases with distance from the substation.

When multiple tie switch options exist, they are displayed in the order of largest to smallest minimum margin on the supporting feeder. If the minimum margin and minimum capacity values exceed the load to be transferred by a substantial amount (≥100 A), an operator may be sufficiently comfortable to execute the transfer without additional study. Other than the adjustment of capacity for temperature, the procedure involves only data base searching rather than calculations, and the total time required is a few seconds.

Load transfer simulation study. This study simulates an actual load transfer from one feeder to a neighboring feeder by changing the normal feeder configuration and feeder data base. The load is transferred to the neighboring feeder by rewriting the connectivity pointers for the affected feeders, and a power-flow analysis is performed for each feeder to determine new voltages, power flows, and line losses. Pre- and posttransfer summaries are displayed to show the change in line power flows, losses, and minimum/maximum feeder voltages resulting from the transfer. After the load-flow calculations are completed, a new set of margins is computed for the line sections on the feeders involved. For two feeders involving 300 nodes (50 nodes per phase on each feeder), the entire process requires 45 seconds on an IBM/AT compatible with math coprocessor.

Voltage study. The voltage study was developed to provide fast, approximate answers on the changes in the voltage/loss profile that result from volt/var control actions or feeder reconfigurations. The existing voltage/loss profile from the substation to any desired point can be graphically displayed for any phase of any feeder. A control action is then specified, such as a capacitor switching or regulator tap adjustment, and the resulting voltage/loss profile is overlayed on the original. In this study, the data base is not actually reorganized to simulate the specified control action. Rather, the affected feeder is represented by about five line sections, and loads are represented as pure constant-current sinks. These simplifications allow the necessary load-flow calculations to be executed in a matter of seconds. Actually implementing the control action and generating a detailed power flow are accomplished through the data base editing feature described under "Software Development Procedure."

Several unique features support rapid assessment of voltage/loss profiles associated with load transfers. An in-line switch on any feeder can be opened to simulate a load transfer to another feeder. The voltage/loss profile above the opened switch is then graphically displayed back to the feeder breaker. This feature is important because capacitor banks above the opened in-line switch may have to be switched out to avoid objectionable voltage increases following the load transfer. It is also possible to display the voltage/loss profile from an in-line switch on one feeder through a specified intertie to the substation breaker on a supporting feeder. This feature allows quick assessment of how much voltage sag will occur on the supporting feeder and the transferred section following reconfiguration.

Short-circuit study. The short-circuit study was designed to allow quick assessment of the effect of feeder reconfiguration on the settings and ratings of protection equipment. For each interrupting device on the feeder backbone, it is important to determine how the normal load and short-circuit duty will differ between the normal and the reconfigured state. The user can specify any location on a feeder and display the normal load (in amperes) and the short-circuit duty for that point when supplied in the normal feeder configuration and when supplied through an intertie from a neighboring feeder. From this information, it can be determined whether recloser relay settings need to be adjusted, the rating of the interrupting device needs to be upgraded, the feeders need to be restored to their original configuration, or the feeders can be permanently left in the reconfigured state without compromising the feeder protection. This study mode executes quickly because loads are neglected in computing short-circuit duties and because accumulated load data are stored in the data base.

Postfault load transfer study. The postfault load transfer study was designed to assist operators in developing switch orders to restore service above and below a faulted line section. The user specifies a fault location, and the program searches the data base for a set of automated in-line switches to be opened to isolate the faulted zone. Once the faulted zone is isolated, the fault-clearing element above the faulted zone can be reclosed (if possible) and tie switches can be closed to restore service below the fault. All transfers are checked with regard to acceptable feeder margin on the neighboring feeders and capacity on the line sections to be transferred. A tabulation of total unserviced customers and load is maintained, and alternative switching actions above and below the fault are identified.

Capacitor dispatch study. SYSRAP can be used to determine how to dispatch capacitors to move the power factor of a feeder closer to unity from a lagging or leading power factor condition. The package has been designed to display the low/high voltages, total line losses, total real- and reactive-power injection for a feeder, and the status of all the capacitor banks on the feeder. When a change in capacitor status is indicated, the study procedure performs a power-flow analysis to calculate the new low/high voltages, total line losses, and total real- and reactive-power injections. The pre- and postcapacitor switching values are displayed together for comparison to allow an operator or planner to determine if a capacitor switching is necessary to readjust the feeder power factor.

Data base interrogation. The SYSRAP package has been designed to display real- and reactive-power injections, line losses, and number of customers for each feeder on the basis of total feeder, line section, or feeder zone. The feeder zone display capability allows an operator to quickly determine the load and customer number between any two points on a feeder or the total load and customer number below any single point. In addition, the package can display or write to a printer or file real-power flow, reactive-power flow, current, loss, voltage, short-circuit current and megavolt-amperes, number of customers, capacity, load margin, node and line section label, and connectivity pointer for each line section of a feeder. The component status and capacity can also be displayed or printed out.

Data base editor. The SYSRAP package scales customer load on the bases of the total single-phase feeder real- and reactive-power injections, single-phase bus voltages at the feeder breaker, billed kilowatt-hours, and connected transformer kilovolt-amperes. The loads can be represented as voltage-sensitive or -insensitive load models (any load composition of constant power, constant current, and constant impedance). The real-power load composition can be specified differently from the reactive-power composition.

A full-screen line section editor allows an operator or planner to change any parameters of a given feeder line section/component or insert/delete line sections/components. The user may access any line section by keying in the first few letters of the line section label; the program then displays the first line section matching the pattern. The user may then edit any data, page through the feeder by line section connectivity pointer, or page through alphabetically by line section label. A displayed connectivity pointer shows the user where the line section is located with respect to the main line or any laterals. After all editing changes have been made to any feeders, the feeder voltage/loss profiles are automatically recalculated as needed. In addition, SYSRAP allows the user to create new feeders and import/export ASCII versions of the feeder data.

Finally, the program has the capability to correlate the program data base with real-time distribution system analog and status data collected by a distribution automation system and written into an ASCII file. Currently, the format of the file consists of (1) the single-phase real- and reactive-power injections and the bus voltage values for each feeder and phase collected at the three substations of the AUB distribution system and (2) the monitored status of capacitors, regulators, circuit breakers, in-line switches, and intertie switches on the twelve AUB feeders.

Feeder Load Model

Experimental observations made on the automated AUB system have shown that the use of a simple load model, such as a constant-power sink, is inadequate to accurately simulate system response to control actions that affect the feeder voltage profile.[2] Such control actions include capacitor switching, regulator tap adjustments, and feeder reconfigurations. For example, a constant-power representation of loads predicts that the real-power injection measured at the feeder breaker will decrease when a capacitor bank deployed on the feeder is switched in to move the feeder power factor from a lagging condition closer to the unity power factor. Because the total power absorbed by the feeder loads remains constant with the constant-power model, the predicted reduction in real power injected at the breaker is exactly equal to the loss reduction associated with the capacitor switching. Experimentally, we have observed that a capacitor switching, as above, results in an increase in total real-power injection at the feeder breaker. The explanation is that while losses are reduced by moving closer to the unity power factor, the feeder voltage profile improves and results in an increase in load that exceeds the amount of loss reduction. To make the SYSRAP simulator as realistic as possible, provision has been made to use highly detailed feeder models, including voltage-sensitive loads, as outlined below.

Feeder load profile. An important part of the feeder model is the distribution of load along the feeder. Even if the feeder line model is completely correct, the voltage profile and losses predicted by the model will not be accurate unless the load is correctly distributed along the feeder. While loss reduction and voltage leveling are important concerns, the consequences of inaccuracy in feeder load distribution will be most severe in attempting to predict the acceptability of load transfers. Unless the distribution of load on both feeders involved in a proposed transfer is accurately known, the ability of a supporting feeder to accept the additional load without overload or serious degradation in voltage profile cannot be predicted with confidence. This problem will be particularly crucial as load factors increase because of delayed facility expansion.

As part of its billing system data base, AUB has, at selected locations along each phase of each feeder, aggregate information on customer number, connected transformer kilovolt-amperes and monthly kilowatt-hours. This information is available at about 40 to 90 electronic data points (EDPs) per feeder per phase. In the absence of extensive load surveys, billed kilowatt-hours and connected transformer kilovolt-amperes are reasonable first cuts at establishing feeder load distribution profiles.

The data base of the SYSRAP program provides for all EDPs in the AUB billing data base resulting in feeder models consisting of approximately 40 to 90 nodes per feeder per phase. This level of detail is desirable from an accuracy perspective, but it increases the data base storage requirements and the computational burden in attempting to execute power flows in near real time. The computational problems are discussed in more detail in a subsequent section.

Billed customer kilowatt-hours are currently used to establish the real feeder load profile, while connected kilovolt-amperes are used to establish the reactive load profile. The profile consists of a specification at each EDP of the amount of real and reactive load at that EDP under nominal voltage conditions. Let $P_{L_i}(V_i)$ and $Q_{L_i}(V_i)$ denote the real and reactive powers drawn by the load at EDP i as functions of node voltage V_i and let V_o denote nominal distribution voltage. The load profile is thus specified by giving $P_{L_i}(V_o)$ and $Q_{L_i}(V_o)$ for each EDP. The basic distribution of load along the feeder is presumed to be constant until a new set of $P_{L_i}(V_o)$ and $Q_{L_i}(V_o)$ values is input to the data base. Increases and decreases in the total feeder load with time, such as the diurnal load cycle, are handled by simply scaling the nominal load distribution profile. To update the data base from an "old" operating condition to a "new" condition, let $P_{T_{new}}$ and $Q_{T_{new}}$ represent the total injections at the substation breaker in the new condition (some specified value for study purposes or the value obtained from the SCADA system) and let $P_{T_{old}}$ and $Q_{T_{old}}$ represent the total substation injections corresponding to the old condition currently represented in the data base. Define load profile scale parameters as

$$\alpha_P = \frac{P_{T_{new}}}{P_{T_{old}}}$$
$$\alpha_Q = \frac{Q_{T_{new}}}{Q_{T_{old}}} . \tag{1}$$

Then, the old load profile is scaled to the new condition by computing

$$P_{L_i}(V_o)_{new} = \alpha_P \, P_{L_i}(V_o)_{old}$$
$$Q_{L_i}(V_o)_{new} = \alpha_Q \, Q_{L_i}(V_o)_{old} . \tag{2}$$

Because of load sensitivity to voltage and the fact that P_T and Q_T include both load and losses, this scaling may have to be done iteratively, converging the voltage profile at each iteration and then checking to see if the total injections given by the model match the specified injections.

Load sensitivity to voltage. In attempting to use SYSRAP to replicate experimental observations on system response to volt/var control actions and feeder reconfigurations, it was necessary to model load sensitivity to voltage. As shown below, modeling each load as a parallel connection of constant-power, constant-current, and constant-impedance components is adequate for this task.

Let $P_L(V)$ be the real power consumed by some load as a function of applied voltage, V. $P_L(V)$ may be a very complex function if the load is an aggregate of many distinct types of electrical loads. With a Taylor series expansion, $P_L(V)$ can be written as

$$P_L(V) = P_L(V_o) + P_L'(V_o)(V - V_o) + \tfrac{1}{2} P_L''(V_o)(V - V_o)^2 + HOT \ , \tag{3}$$

where V_o denotes nominal voltage,

$$\begin{aligned} P_L'(V_o) &= \frac{dP_L(V)}{dV}\bigg|_{V=V_o} \\ P_L''(V_o) &= \frac{d^2P_L(V)}{dV^2}\bigg|_{V=V_o} \ , \end{aligned} \tag{4}$$

and HOT stands for higher-order terms. Because distribution voltages are typically maintained within $\pm 5\%$ of the nominal, an accurate approximation for $P_L(V)$ can be obtained by neglecting the HOT, that is,

$$\begin{aligned} P_L(V) = {} & [P_L(V_o) - V_o P_L'(V_o) + \tfrac{1}{2} V_o^2 P_L''(V_o)] \\ & + [P_L'(V_o) - V_o P_L''(V_o)]V + [\tfrac{1}{2} P_L''(V_o)]V^2 . \end{aligned} \tag{5}$$

This expression shows that if a nominal power, $P_L(V_o)$, and the first and second sensitivities of load with respect to voltage $[P_L'(V_o), P_L''(V_o)]$ can be determined, such as by experimentation with load-tap-changing (LTC) transformers, then $P_L(V)$ can be represented as a quadratic polynomial in voltage.

If we define the coefficients in Eq. (5) as

$$\begin{aligned} P &= P_L(V_o) - V_o P_L'(V_o) + \tfrac{1}{2} V_o^2 P_L''(V_o) \\ I_r &= P_L'(V_o) - V_o P_L''(V_o) \\ R^{-1} &= \tfrac{1}{2} P_L''(V_o) \ , \end{aligned} \tag{6}$$

then Eq. (5) becomes

$$P_L(V) = P + I_r V + R^{-1} V^2 \ , \tag{7}$$

which can be interpreted as the real power consumed by a parallel connection of a constant-power sink (P), constant-current sink (I_r), and a constant resistance (R).

One way of determining the model parameters (P, I_r, R) without knowing the sensitivities is to assume that each load component type; that is, constant power, current, and impedance, contribute a given fraction of the total load at nominal voltage. Define

$$\begin{aligned}
\epsilon_p &= \text{fraction of } P_L(V_o) \text{ contributed by the} \\
&\quad\ \text{constant power component} \\
&= \frac{P}{P_L(V_o)} \\
\epsilon_{I_r} &= \frac{I_r V_o}{P_L(V_o)} \\
\epsilon_R &= \frac{R^{-1} V_o^2}{P_L(V_o)} \ ,
\end{aligned} \tag{8}$$

where

$$\epsilon_p + \epsilon_{I_r} + \epsilon_R = 1 \ . \tag{9}$$

Then in terms of a given nominal total power $P_L(V_o)$, such as is available from the nominal load distribution at each EDP, the model parameters are

$$\begin{aligned}
P &= \epsilon_p P_L(V_o) \\
I_r &= \frac{\epsilon_{I_r} P_L(V_o)}{V_o} \\
R^{-1} &= \frac{\epsilon_R P_L(V_o)}{V_o^2} \ .
\end{aligned} \tag{10}$$

Similar relations can be written for Q, I_x, and X to model reactive power where ϵ_q, ϵ_{I_x}, and ϵ_X represent the fractions of $Q_L(V_o)$ contributed by each component.

The advantage of this approach, particularly in a research environment, is that by varying the component contribution parameters (ϵ_p, ϵ_{I_r}, ϵ_R), the load can be made to assume any voltage dependence between the extremes of a constant-power model ($\epsilon_p = 1$, $\epsilon_{I_r} = \epsilon_R = 0$) and a constant impedance model ($\epsilon_R = 1$, $\epsilon_{I_r} = \epsilon_p = 0$).

On the basis of the above discussion, a decision was made that the familiar constant-power, constant-current, and constant-impedance techniques for load modeling would be adequate for representing load sensitivity to voltage provided provision was made to handle all three types of models simultaneously.

At each EDP, the aggregate load is viewed as a parallel connection of constant-power, constant-current and constant-admittance components. Figure 8-1 shows the structure of the model at some hypothetical node *i*.

Note that six independent parameters are in the model: P_i, I_r, R_i, Q_i, I_x, and X_i. With this model, the total real and reactive powers absorbed by the load at node *i* are quadratic functions of the voltage magnitude at node *i*, that is

$$\begin{aligned} P_{L_i}(V_i) &= P_i + I_{r_i}V_i + R_i^{-1}V_i^2 \\ Q_{L_i}(V_i) &= Q_i + I_{x_i}V_i + X_i^{-1}V_i^2 \ . \end{aligned} \tag{11}$$

All loads except "special loads" are viewed as having the same sensitivity to voltage as specified by a common set of ϵ_p, ϵ_{I_x}, and ϵ_R values for real power and an analogous set of ϵ_q, ϵ_{I_x}, and ϵ_X values for reactive power. The model parameters in terms of the power consumed at nominal voltage and the model type contribution factors are

$$\begin{aligned} P_i &= \epsilon_p P_{L_i}(V_o) & Q_i &= \epsilon_q Q_{L_i}(V_o) \\ I_{r_i} &= \epsilon_{I_r} P_{L_i}(V_o)/V_o & I_{x_i} &= \epsilon_{I_x} Q_{L_i}(V_o)/V_o \\ R_i^{-1} &= \epsilon_R P_{L_i}(V_o)/V_o^2 & X_i^{-1} &= \epsilon_X Q_{L_i}(V_o)/V_o^2 . \end{aligned} \tag{12}$$

Power flow analysis. The method used to calculate power flows heavily influences both the time and space resources used by the computer system and hence must acknowledge the limitations the system imposes. A simple

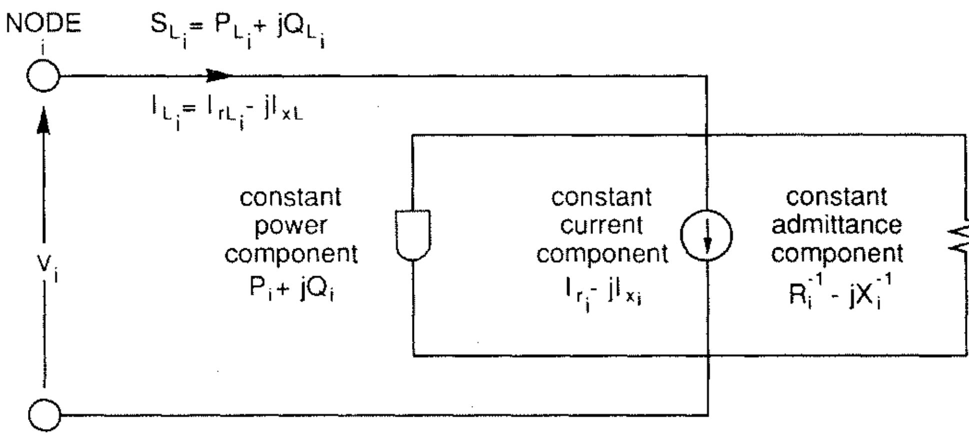

Figure 8-1 Load model at node i.

power-flow calculation approach was used to determine voltages, losses, and power flows on which to base reconfiguration decisions. The algorithm used to calculate feeder voltages and losses consists of the following procedures.

1. Scale the loads by computing load scale factors as the ratio of the specified total breaker power injections to the breaker injections currently in the data base.
2. Convert the per-unit complex load at the last radial bus from its constant-power, constant-current, and constant-impedance load components to an equivalent complex current at the (assumed) bus voltage.
3. Calculate the real voltage drop and losses on the next line section upstream toward the feeder breaker by using the equivalent current in step 2. The program is capable of representing load as a lumped load at the end of the line section or, preferably, as a linear distribution of load over the line section. In the latter representation, losses are integrated over the line section length.
4. Add the calculated losses to the accumulated load and combine this load with the next bus constant-power, constant-current, and constant-impedance load components at the next (assumed) bus voltage to produce a new equivalent current.
5. Repeat steps 3 and 4 up to the breaker, accounting for all circuit branching.
6. At the breaker, assume a bus voltage equal to the specified per-unit substation bus voltage.
7. Calculate the absolute voltage at the next bus downstream from the breaker equal to the previous bus voltage minus the calculated voltage drop.
8. Repeat step 7 to the end of the feeder.
9. Repeat steps 2 through 8 until voltage convergence is obtained.
10. Accumulate the load plus losses up to the substation breaker. If the total power injection agrees with the specified values (within a given tolerance), then terminate; otherwise, return to step 1.

This approach includes approximations that are familiar to many power distribution engineers.[3] First, the reactive portion of the voltage drop over each line section is ignored. No mutual coupling is assumed, and no attempt is made to calculate neutral current. The result is a fast voltage, loss, and radial-power flow calculation that can be implemented in an indexed sequential access-oriented data base management system (DBMS) environment in real time on a microcomputer. Indexing the data records by a line section connectivity pointer allows a list, rather than a sparse matrix, approach to be used. The significant advantages of a list approach is appreciated when other, more DBMS-oriented, as opposed to calculation-oriented, tasks are demanded of the data base.

The results of the above algorithm with a constant-power load model were compared with a fully complex Newton-Raphson power flow on data from an Athens feeder. The feeder was a 25% loaded, 10-MVA, three-phase circuit having 57 buses per phase. The test consisted of switching out all the connected capacitors on the feeder (3600 kvar) and running a load flow. The difference between the Newton-Raphson results and the SYSRAP results were <0.03% for voltage magnitudes, <0.006% for line power flows, and <0.07% for line losses. With a voltage convergence criterion of 0.001 per unit, the SYSRAP algorithm converged 28 times faster than the Newton-Raphson power flow method. Of course, much faster Newton-Raphson codes may be available. The point is that the SYSRAP algorithm proved to be a very simple means of achieving satisfactory accuracy and speed while providing powerful DBMS capabilities in real time to perform a wide variety of other tasks.

Example Applications

Volt/var example. This example will show how a substation LTC transformer test can be used to generate the voltage-sensitive load model parameters for SYSRAP. The parameters are in turn used to show how SYSRAP can represent system response to transformer tap changes.

In a 1986 volt/var experiment, LTC transformers at the South Athens Substation were controlled for 40 seconds to determine the load sensitivity to voltage. A high-speed data acquisition system was used to observe the real- and reactive-power and bus voltage for South Athens circuit No. 9 at the circuit breaker. The LTC transformers were set at tap position −3 (3 positions below nominal setting) when the experiment began. During the experiment, the tap settings of the LTC transformers were raised from position −3 to position 7 in a sequential fashion within 15 seconds, kept at position 7 for approximately 15 seconds, and then lowered from position 7 to position 3 in 10 seconds. As the LTC tap settings were raised from position −3 to 7, the voltage on circuit 9 increased from 7.24 to 7.61 kV and as the LTC tap settings were lowered from position 7 to position 3, the voltage decreased from 7.61 to 7.46 kV. Table 8-1 shows the real- and reactive-power and bus voltage data collected at the circuit breaker of circuit 9 for each LTC tap setting.

The experiment resulted in a $<\pm 5\%$ change in circuit voltage and real power and a $<\pm 20\%$ change in reactive power. Although SYSRAP can accommodate up to a second-order Taylor series expansion of load sensitivity

TABLE B-1 Monitored real- and reactive-power and bus voltage for load-tap-changing transformer test and System Reconfiguration Analysis Program (SYSRAP) simulation results

Monitored B phase data				SYSRAP output results											
				$\epsilon_p = 1.0, \epsilon_{I_r} = 0.0$ $\epsilon_q = 1.0, \epsilon_{I_x} = 0.0$				$\epsilon_p = 0.08, \epsilon_{I_r} = 0.92$ $\epsilon_q = 0.08, \epsilon_{I_x} = 0.92$				$\epsilon_p = 0.08, \epsilon_{I_r} = 0.92$ $\epsilon_q = -2.45, \epsilon_{I_x} = 3.45$			
LTC tap position	Voltage (kV)	Real power (kW)	Reactive power (kvar)	Real power (kW)	% error	Reactive power (kvar)	% error	Real power (kW)	% error	Reactive power (kvar)	% error	Real power (kW)	% error	Reactive power (kvar)	% error
−3	7.24	2988	826	2988.0	0.00	826.0	0.00	2988.0	0.00	826.0	0.00	2988.0	0.00	826.0	0.00
−2	7.31	3015	857	2987.3	0.92	816.6	4.71	3014.7	0.01	828.6	3.31	3014.3	0.02	855.2	0.14
−1	7.33	3028	872	2987.1	1.35	813.9	6.66	3022.5	0.18	829.3	4.00	3021.8	0.21	863.6	0.87
0	7.36	3038	884	2086.9	1.68	809.8	8.39	3034.0	0.13	830.4	6.06	3033.0	0.16	876.1	0.89
1	7.38	3045	893	2986.7	1.91	807.2	9.61	3041.8	0.11	831.1	6.93	3040.6	0.14	884.4	0.96
2	7.41	3050	900	2986.4	2.09	803.1	10.77	3053.3	0.11	832.2	7.53	3051.9	0.06	896.9	0.17
3	7.46	3072	919	2985.9	2.80	706.4	13.34	3072.4	0.01	833.9	9.26	3070.6	0.05	917.6	0.10
4	7.51	3106	958	2985.5	3.88	789.6	17.58	3091.7	0.46	835.6	12.78	3089.4	0.54	938.5	1.75
5	7.54	3113	966	2985.2	4.11	785.6	18.67	3103.2	0.31	836.6	13.40	3100.7	0.40	951.0	1.55
6	7.57	3125	980	2985.0	4.48	781.5	20.26	3114.8	0.33	837.6	14.53	3112.0	0.42	963.3	1.70
7	7.61	3133	991	2984.7	4.73	766.0	21.70	3130.0	0.10	838.9	15.35	3127.0	0.19	980.0	0.74
7	7.61	3163	991	3163.0	0.00	991.0	0.00	3163.0	0.00	991.0	0.00	3163.0	0.00	991.0	0.00
6	7.57	3150	980	3163.4	0.43	996.6	1.69	3147.6	0.08	989.0	0.92	3147.9	o.07	972.0	0.82
5	7.54	3136	955	3163.7	0.88	1000.8	4.80	3136.0	0.00	987.5	3.40	3136.6	0.02	957.6	0.27
4	7.51	3113	946	3164.0	1.64	1005.0	6.24	3124.4	0.37	986.0	4.23	3125.3	0.40	943.3	0.29
3	7.46	3106	927	3164.5	1.88	1012.0	9.17	3105.0	0.03	983.4	6.08	3106.4	0.01	919.4	0.82

Note: LTC = load tap changing.

to voltage, only a first-order expansion is considered here; consequently, the constant impedance contribution factors ϵ_R and ϵ_X are zero. A first-order Taylor series expansion of the real and reactive power consumed by the circuit loads was used to model the load sensitivity to voltage because there was a $<\pm 5\%$ change in voltage. The coefficients for the polynominal representation of $P_L(V)$ and $Q_L(V)$ were determined by using the monitored real- and reactive-power data for 7.24, 7.36, 7.46, 7.54, and 7.61 kV to calculate the first-order sensitivities of load with respect to voltage [$P_L'(V_o)$ and $Q_L'(V_o)$] for 7.36, 7.46, and 7.54 kV. The polynominal coefficients determined for real power (Table 8-2) were $\epsilon_p = 0.08$ and $\epsilon_{I_r} = 0.92$, and the coefficients determined for reactive power (Table 8-3) were $\epsilon_q = -2.45$ and $\epsilon_{I_x} = 3.45$. These coefficients and the real- and reactive-power data for the bus voltage of 7.24 kV were used to determine the initial load scaling for SYSRAP when the voltage was raised from 7.24 to 7.61 kV. The real- and reactive-power data (3163 kW, 991 kvar) for the bus voltage of 7.61 kV were used to determine the initial load scaling for SYSRAP when the voltage was lowered from 7.61 to 7.46 kV. In SYSRAP, the bus voltage at the circuit breaker of circuit 9 was increased from 7.24 to 7.61 kV and decreased from 7.61 to 7.46 kV in a sequential fashion exactly like the LTC experiment to reproduce the real- and reactive-power injections generated from the

TABLE 8-2 Polynominal coefficients for first-order Taylor series expansion of $P_L(V)$, the real power consumed by the load on South Athens circuit No. 9

LTC tap position	Monitored B phase voltage (kV)	$P(V_o)$	$P'(V_o)$	Polynominal coefficients		Contribution factors	
				P	I_r	ϵ_p	ϵ_{I_r}
−3	7.24	2988					
0	7.36	3038	381.8181	228.9636	381.8181	0.075366	0.924633
3	7.46	3072	380.0000	238.3400	380.0000	0.077584	0.922415
7	7.61	3133					
7	7.61	3163					
5	7.54	3136	380.0000	270.8000	380.0000	0.086352	0.913647
3	7.46	3106					
					Average	0.079767	0.920232

Note:
$P(V_o)$ is the monitored real power flow at a given voltage.
$P'(V_o) = [P(V_o + \Delta v) - P(V_o - \Delta v)]/[(V_o + \Delta v) - (V_o - \Delta v)]$.
$P = P(V_o) - V_o' P'(V_o)$.
$I_r = P'(V_o)$.
$\epsilon_p = P/P(V_o)$.
$\epsilon_{I_r} = I_r V_o / P(V_o)$.

TABLE 8-3 Polynominal coefficients for first order Taylor series expansion of $Q_L(V)$, the reactive power consumed by the load on South Athens circuit No. 9

LTC tap position	Monitored B phase voltage (kV)	$Q(V_o)$	$Q'(V_o)$	Polynominal coefficients		Contribution factors	
				Q	I_x	ϵ_q	ϵ_{I_x}
−3	7.24	826					
0	7.36	884	422.7272	−2226.00	422.7272	−2.51810	3.518104
3	7.46	919	428.0000	−2272.59	428.0000	−2.47290	3.472900
7	7.61	991					
7	7.61	991					
5	7.54	955	426.6666	−2262.06	426.6666	−2.36865	3.368656
3	7.46	3106					
					Average	−2.45322	3.453220

Note:
$Q(V_o)$ is the monitored reactive power flow at a given voltage.
$Q'(V_o) = [Q(V_o + \Delta v) - Q(V_o - \Delta v)]/[(V_o + \Delta v) - (V_o - \Delta v)]$.
$Q = Q(V_o) - V_o' Q'(V_o)$.
$I_x = Q'(V_o)$.
$\epsilon_q = Q/Q(V_o)$.
$\epsilon_{I_x} = I_x V_o / Q(V_o)$.

experiment. Table 8-1 shows the comparison of the monitored data and the results generated from SYSRAP with a voltage-insensitive model (100% constant real and reactive power) and a voltage-sensitive model using the above polynominal coefficients. The results show that not only is the error for the voltage-insensitive model (constant power) higher than the errors for the two voltage-sensitive models but that the trend of decreasing real and reactive power with increasing voltage and increasing power with decreasing voltage is different from that of the monitored power values. The first voltage-sensitive model ($\epsilon_p = \epsilon_q = 0.08$ and $\epsilon_{I_r} = \epsilon_{I_x} = 0.92$) used only the coefficients calculated for real power to model both real and reactive power and resulted in a much lower error for real power and a correct increasing trend with increasing voltage and decreasing trend with decreasing voltage similar to the monitored values. However, the error in the reactive power was decreased further in the second voltage-sensitive model ($\epsilon_q = -2.45$ and $\epsilon_{I_x} = 3.45$) that incorporated a set of coefficients for the reactive power independent from that of the real power.

Fault example. This example will show the use of SYSRAP in developing switch orders for service restoration around a faulted feeder zone. The circuit involved is AUB circuit No. 7 on the South Athens substation

(SA-7). A simplified one-line diagram of this feeder is given in Figure 8-2. Note that there are three automated in-line switches: SW70, SW14, and SW207; and three tie switches: SW126 to North Athens substation circuit No. 5 (NA-5), SW15 to South Athens circuit No. 8 (SA-8), and SW43 to North Athens circuit No. 1 (NA-1).

If a permanent fault occurs at EDP 702 near the feeder breaker of SA-7, such a fault would be cleared by the lockout of the SA-7 circuit breaker (BRS07), leaving all 1099 customers on this feeder out of service. Under fairly typical load conditions, this would correspond to a 5-MW outage. The automation system would alarm the breaker lockout and automated fault detectors located at SW14, and SW70 would not report high

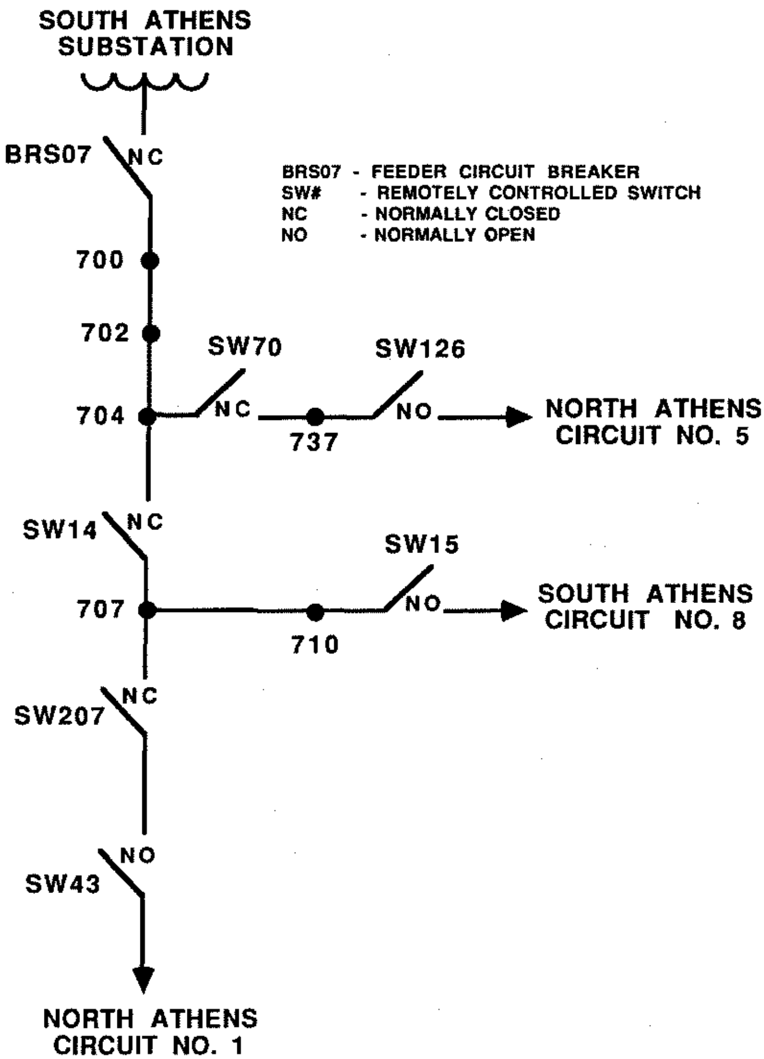

Figure 8-2 One-line diagram for South Athens circuit No. 7.

current. The operator would know that the fault was rather close to the substation.

Entering the postfault load transfer study of SYSRAP and entering the fault location as EDP 702 yields the display shown in Table 8-4. As shown in the table, SYSRAP recommends to the operator that in-line SW70 be opened and tie SW126 to NA-5 be closed. This transfer restores 310 customers and 1.06 MW of load to service. It is also recommended that in-line SW14 be opened and tie SW43 to NA-1 be closed, restoring an additional 403 customers and 1.68 MW to service. After these two transfers, 386 of the original 1099 customers remain out of service awaiting a line crew to pinpoint and repair the problem.

The section of SA-7 below SW14 could also be restored to SA-8 by using tie SW15; or the section could be sectionalized into two zones by opening SW207 and using tie SW15 and SW43. These possibilities are shown as "alternates" by SYSRAP.

In the above scenario, the load on supporting feeder SA-8 was only 2.5 MW, which is not high enough to preclude picking up all of the load below SW14 on SA-7. However, if the load on SA-8 is increased to 12 MW (an overload condition for SA-8), then the load transfer recommendations by SYSRAP corresponding to the fault at EDP 702 on SA-7 are as shown in Table 8-5. Note that no transfers involving SA-8 are recommended, because SA-8 does not have adequate margin to pick up any additional load.

TABLE 8-4 Postfault load transfer recommendations for a fault at electronic data point 702 on South Athens circuit No. 7: normal load conditions

Location	Open	Close	Restored		Total unserviced	
			Number of customers	kW	Number of customers	kW
Above the faulted line section	BRS07				1099	5310
Below the faulted line section	SW70	SW126	310	1062	789	4248
	SW14	SW43	403	1680	386	2568
(alternate)	SW14	SW15	403	1680		
(alternate)	SW207	SW43	260	636		

Note:

BR = Switch circuit breaker.

SW = Switch.

TABLE 8-5 Postfault load transfer recommendations for a fault at electronic data point 02 on South Athens circuit No. 7: 12-MW load on South Athens circuit No. 8

Location	Open	Close	Restored		Total unserviced	
			Number of customers	kW	Number of customers	kW
Above the faulted line section	BRS07				1099	5310
Below the faulted line section	SW70	SW126	310	1062	789	4248
	SW14	SW43	403	1680	386	2568
(alternate)	SW207	SW43	260	636		

Note:
BR = Circuit breaker.
SW = Switch.

Large-scale automation systems have become standard components in modern industrial plants. Many industries such as petrochemical, paper, and steel have used automation for many years to improve plant efficiency and produce higher quality products. Electric distribution utilities are viewing this technology for similar reasons. In general, the benefits that can be achieved with automation are bounded by only the limits of the overall system or its application. One effective mechanism employed to maximize the use of automation systems is the development system, which is used to develop control concepts and the software for implementation on the larger scale system. The development system may also serve to verify and validate the software before it is installed on utility automation systems. The development system used at AUB is the AACETS.

Description of the System

The structure of the AACETS is similar to that of the Athens automation system in that it consists of two major subsystems. The first is the minicomputer-based SCADA system, which features the same software and peripheral equipment as the Athens control system (Figure 8-3). The second subsystem, the smart test panel, is a distribution system simulator that provides hardware-compatible signals for monitoring by the SCADA

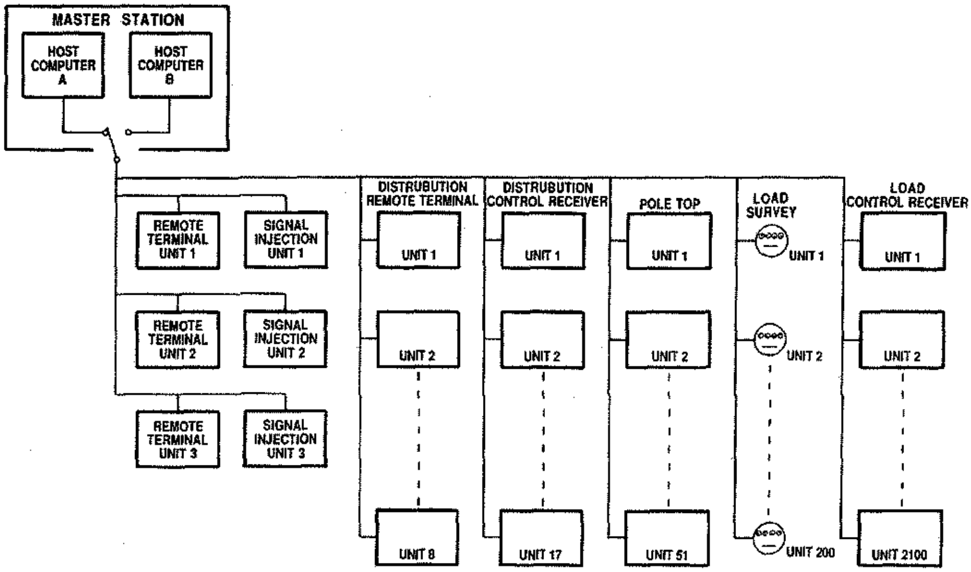

Figure 8-3 Major components of the Athens Automation and Control Experiment Test System (AACETS).

subsystem. The smart test panel is implemented with a programmable controller, a commercially available industrial device. In the AACETS configuration, the programmable controller, instead of being used to control a process or system, is used as the process to be controlled. That is, the programmable controller is programmed to present signal levels and equipment states that represent simple models of the Athens distribution system. This application is illustrated in Figure 8-4, where characterization data are tabularized in the programmable controller's memory. These data are sequentially accessed and transferred to hardware output modules that convert the numeric data into analog voltage signals wired into the SCADA

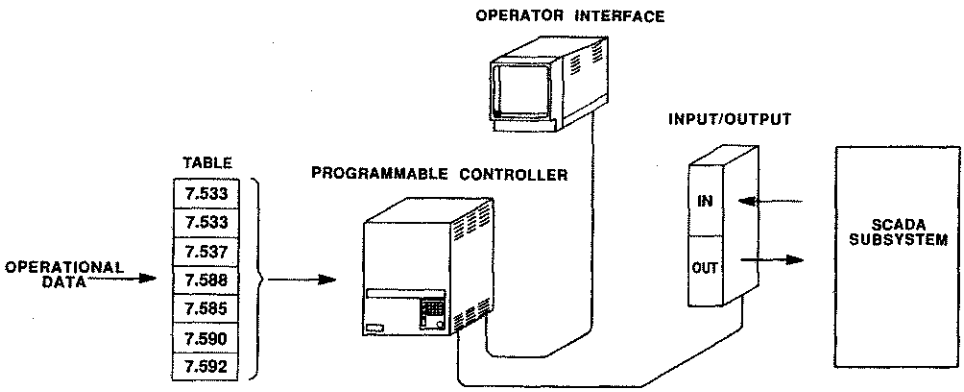

Figure 8-4 Use of operational data in the smart test panel.

subsystem for appropriate action. Because simulated information from the smart test panel interfaces to the SCADA subsystem through feeder-level monitoring hardware, the simulation of residential load models is accomplished by software.

The smart test panel features a color cathode-ray tube (CRT) and touch-screen-based operator interface that graphically displays simulation information to the experimenter in a manner similar to that of the SCADA subsystem. The smart test panel is configured to provide 40 analog output signals (representing feeder kilovolts, kilowatts, and kilovars), 24 relay outputs (representing switch position, fault-detector status, etc.), and 16 status inputs (representing commanded switch position, capacitor state, etc.). The smart test panel hardware has a total capacity of over 2000 input and output states (bits) configured as discrete state data or multibit information (analog/numeric). In addition, the smart test panel features a total of 16 Kwords of read/write memory in the programmable controller and 700 Kbytes in the operator interface. Programming of the smart test panel is accomplished in "relay-ladder logic" and a PASCAL-derived graphic language called VEUCALC.

A block diagram of the SCADA subsystem, shown in Figure 8-5, is based on a Digital Equipment Corporation PDP-11/44 minicomputer with 1-Mword of memory. Two fixed-disk drives and a single removable hard disk provide a total mass storage capacity of 498 Mbytes. A magnetic tape drive provides a means to transfer programs and data between the AACETS and other computer systems. High-speed program listings are printed on a 600-line per minute printer, while two slower hard-copy printers provide alarm and event logging for the SCADA software package. Twenty-four data lines are supported for user access and data acquisition, and a graphic display system provides color CRT-based operator screens. Two remote terminal units interfaced to the smart test panel are used as field monitoring devices.

Software Development Procedure

The development of on-line, real-time software off line of the Athens control system is a primary mission of the AACETS. The AACETS provides this capability in a SCADA subsystem that features MODSCAN, the same system software used in the Athens control system; a hands-on approach to its use; and facilities for testing the software being developed.

Software developed on the AACETS generally falls into two categories, the first of which is support programs of general importance to all experimental areas. Examples are data-conversion programs that translate archived MODSCAN data into a form that is readable by mainframe computers at ORNL and a reverse compiler that "captures" any data base changes entered from the operator console, thereby providing a cost-effective

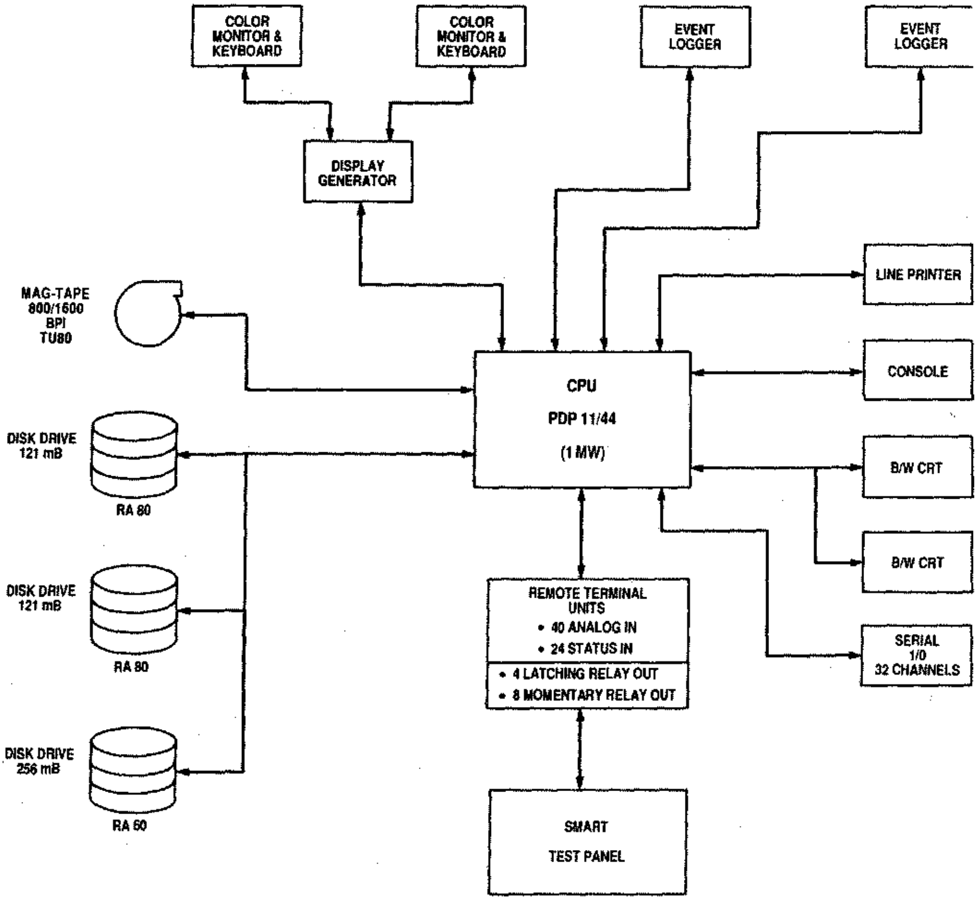

Figure 8-5 Supervisory Control and Data Acquisition subsystem block diagram.

method of maintaining the data base as the Athens control system evolves to meet changing experimental needs.

The second software category consists of application programs to support the system experiments. The discussion of these programs includes some analysis tools used to support experiments at the SCADA system level. It should be noted that the AACE approach is to automate the experiment to the maximum extent possible, thus reducing the dependency on and responsibilities of the operators.

Once a particular software package is developed, it is tested on the AACETS. The testing of any software package is approached with a "mission success" philosophy. That is, all software must meet established requirements prior to use on the Athens control system: the software (1) must meet the functional requirements of its intended purpose, (2) must meet electrical system and personnel safety requirements, (3) must operate in a homogeneous manner with the rest of the control systems' activities, (4) must interface with the operator or experimenter or both in an effective and consistent way, and (5) must be written in a structured and well-documented manner. Once these requirements are met, the software package is ready for use on the Athens control system.

System Support

A considerable amount of engineering effort is expended in system support. System support encompasses such activities as data base maintenance, isolation and correction of system errors (software bugs), training and support of system users, and feature enhancement. Normally, a control system user expects a certain amount of vendor-supplied support for a period of time following installation. However, when advanced application of the system is planned, the control system owner is required to supply this level of support. For the Athens experiment, AACETS was assembled and operational one year before acceptance testing of the actual control system. This lead time allowed ORNL staff members to become well acquainted with system operation and support, precluding the need for vendor support.

Data Acquisition

In the application of any automation system, personnel must understand the process and its characteristics before control of the process can be attempted. This understanding is commonly accomplished by analyzing process data gathered under similar operating conditions. In the case of the Athens experiment, there was a need to acquire several types of system data for personnel to understand the operational characteristics of the distribution system before installation of the main controls. Two major types of data were gathered on the AACETS: distribution feeder and weather condition data from the three main Athens substations and remote submetering of residential appliance loads.

Acquisition of remote distribution feeder and weather data is by hardware commercially available from Acurex Corp. (Figure 8-6). Software developed by ORNL is used to command the remote units (NETPACS) to scan their input channels and to transmit data to the AACETS minicomputer every 5–10 minutes. These actions are accomplished over a standard telephone line with an auto-dial modem on the AACETS end and an autoanswer modem on the remote end. The software allows a 16-digit telephone number, thereby accommodating government, commercial, and direct-dialed long distance as well as local and foreign exchange calls. Configuration options for the remote data acquisition hardware include intermixable voltage, thermocouple, current, and contact inputs that can be added in groups of 20 points.

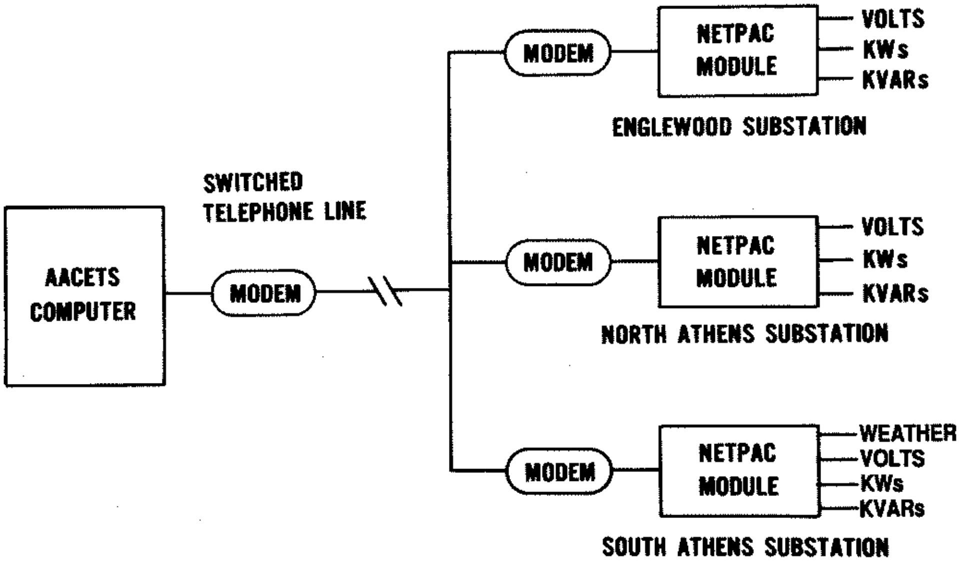

Figure 8-6 Configuration of the distribution feeder and weather data acquisition package.

The data from the EPRI-furnished ARMS units are also stored and processed by the AACETS minicomputer (Figure 8-7). The ARMS units are described in Chapter 6. These units allow up to four selected residential appliances (such as water heaters and heat pumps) plus the internal residential temperature and whole-household load level at each of 200 selected residences to be monitored by a load profile recorder. Each load profile recorder includes a modem connected to a standard residential telephone line and a local memory capable of storing 6 days of data collected at 5-minute intervals on each of the four appliances. The minicomputer software acquires the load profile recorder information each day and stores the appliance energy-use data in memory. Because the load profile recorders use customers' telephone lines, data are transmitted within a preset time window (such as between midnight and 5 a.m.). The data collected are later transferred to magnetic tape for subsequent analysis and long-term storage.

Distribution Feeder and Weather Condition Data Acquisition Software

Distribution feeder and weather data acquisition was used to provide early system characterization for designing experiments. The data acquisition system was developed for use with NETPAC remote terminal equipment manufactured by Acurex Corporation, Autodata Division. This generic data acquisition program was developed on the AACETS with communication subroutines purchased from the hardware vendor. A NETPAC remote terminal unit was located in each of the three AUB substations. Real power, reactive power, and voltage were monitored on each feeder phase at the

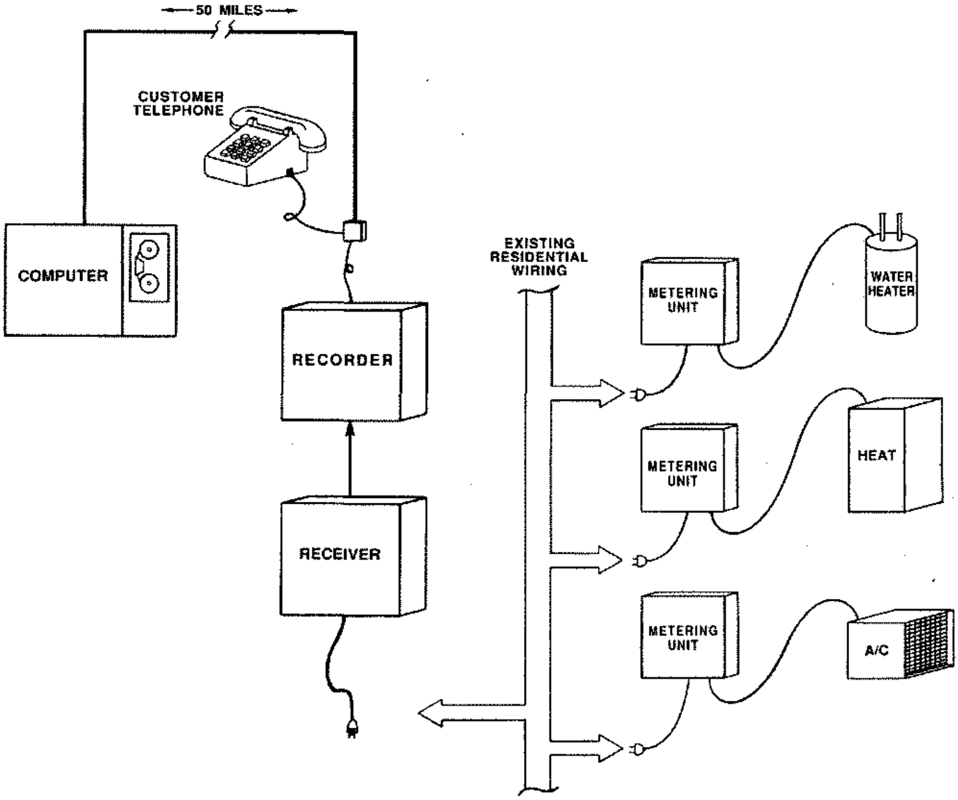

Figure 8-7 Residential appliance monitoring system.

substations, and weather was monitored at the South Athens substation. As a check on hardware integrity, internal power supply voltage and internal temperature were monitored in each NETPAC unit as well. The NETPAC units allowed current, voltage, and thermocouple input types to be mixed on the same interface card, and all three input types were used in this application. Transducers used to interface to the power distribution grid were also used for the primary SCADA system described in Chapter 2. Hardware features of the NETPAC units allowed parallel connection of this equipment with the SCADA system.

The developed data acquisition software was generic in that all application- and location-specific information was contained in a data file and could be modified with an editor. The program code contained no input type or location-specific information. Placing location-specific information in a data file enabled the same program to be used for all three substations even though the number of input channels and the point types were different. Input channel changes were accomplished by editing a data file, and new applications could be configured by simply creating a new data file.

Data were gathered by standard voice-grade, dial-up telephone lines between a 1200-baud auto-dial modem on the AACETS computer end and 1200-baud auto-answer modems at each remote terminal site. An interface converter was used at each remote site to convert the RS 422 output signal from the NETPAC unit to an RS 232 signal for modem input. Data were retrieved every 10 minutes from each substation by a single modem and telephone line for calls to all three substations. The maximum data rate was approximately one scan every 7 seconds on a remote unit with 40 channels. The maximum rate was achieved by placing a call to the remote unit and repeatedly scanning the remote channels until a message was received to stop scanning.

The acquired data could be plotted on a per-day and per-substation basis on the AACETS computer, as shown in Figure 8-8. However, more detailed analysis was performed on a main-frame computer. Data were transferred to the mainframe computer via magnetic tape.

Load Control Software

Load control for air conditioning, space heating, and water heaters was implemented with strategies described in Chapter 6. The appropriate daily strategies were entered into the automation system data base by the utility dispatcher. Software written to implement these strategies was also enabled or disabled in the data base by the utility dispatcher. The software programs determined load shed and restore times to implement the specified strategies. The automation system was then sent the appropriate command at the required time for each load control action. These commands were sent via the

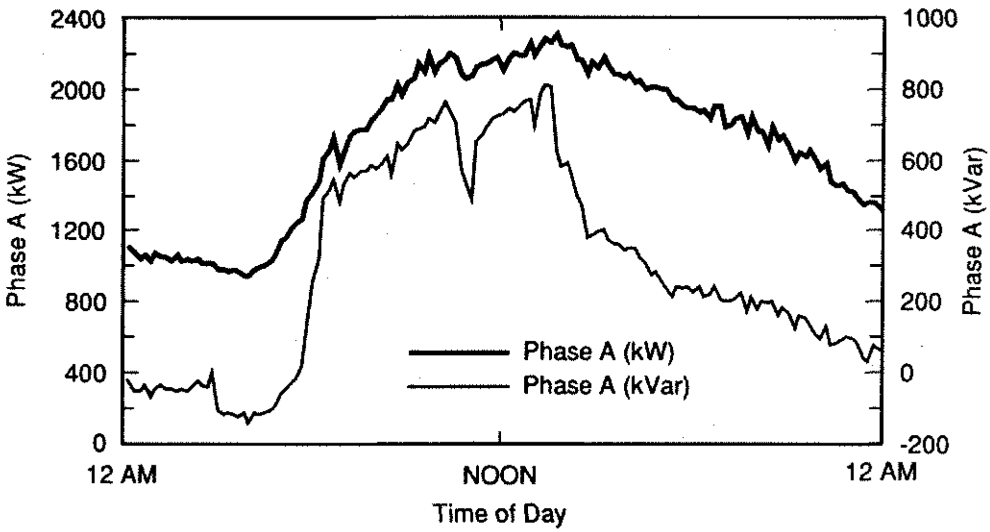

Figure 8-8 South Athens monitored real and reactive power.

automation data base to the signal injection units in the substations, and the signal injection units injected the appropriate bit patterns on the power line for control of the appliances by the load control receivers. When necessary, "re"-sheds were used to shed loads for periods longer than the automatic restore time. A restore command was sent after the load shed time interval elapsed if this interval was less than the normal automatic restore time interval.

An 80-character event description message was logged into a common message file on the SCADA host computer each time a control action occurred. This file allowed detailed reconstruction of all activities on the system and provided a permanent time-stamped record of all load control activities.

These programs were developed on the AACETS. The tests used a smart test panel with two scale-model houses wired to represent actual customer loads.

Capacitor Control Software

Capacitor bank switching to reduce system var loading can be readily automated. An algorithm was developed to determine when to switch capacitors to maintain the lowest possible lagging reactive power for a particular feeder as measured at the substation. A lagging power factor was maintained because the utility is penalized for leading power factor under the TVA billing system.

The software can be activated at timed intervals or in response to an alarm condition for reactive power. Alarm values for reactive power are set on each feeder according to the size of the feeder's capacitor banks. Switching is determined by examining the end of the radial feeder and working back toward the substation, switching in or out capacitors as the total reactive load dictates. Monitored kilovar values at sites away from the substation are used whenever they are available. In addition, a file is updated each time a capacitor bank is switched, and the elapsed time is checked before the capacitor bank is again switched (to prevent excessive switching). Frequent switching of capacitor banks can decrease their functional life. The neutral current is also checked at the substation, because it was observed that the switching in capacitor banks can increase the neutral current and possibly trip a neutral overcurrent relay, resulting in the interruption of power at the substation.

Capacitor bank sizes and locations are contained in separate data files for each feeder, allowing the same program to be used for any feeder and simplifying capacitor bank size and location changes.

All software development was performed on AACETS. Software testing was performed with the smart test panel to simulate distribution system performance.

The software was implemented incrementally to ensure reliability and to gain the utility dispatcher's confidence. First, the software recommended capacitor-switching operations via a special screen on the color CRT of the automation system. The capacitor bank was switched if the operator chose to do so. The software was then extended to actually perform the capacitor-switching operation by initiating control commands to the capacitor bank.

SUMMARY

The introduction of distribution automation systems promises significant improvements in reliability and efficiency of distribution system operation. It will not be possible for operators to rely purely on judgment and experience to operate the system if feeder reconfiguration and volt/var control adjustments become routine daily operations. Rather, analysis software that can assist the operator in selecting appropriate control actions on the basis of actual operating conditions and in accurately predicting the consequences of those actions will be needed.The computer programs written for AACE are a start in this direction.

The functional requirements for the SYSRAP system were derived from the iterative process of planning automation experiments, deciding what tools were necessary to design and execute the experiments, and performing the experiments. This process is acceptable in a research environment where the software functional requirements are driven by experimental observations, but it may not be acceptable in an actual utility planning environment.

Every feature in the SYSRAP package was prompted by a need to either explain data gathered by a high-speed data acquisition system or to facilitate a DBMS task considered burdensome with a conventional distribution analysis package. To achieve the rapid computer response needed for a real-time system, rough calculation approximations were first implemented and then gradually refined until acceptable agreement was reached between the physical system data and calculated data. The result is a fast man-machine interface, unburdened by restrictive engineering calculations, yet sufficiently accurate for distribution automation analysis and control purposes.

The initially adopted DBMS approach facilitated the development of additional applications and enhancements to the system as originally conceived. The DBMS emphasis makes this reconfiguration analysis software unique compared with conventional distribution load-flow and voltage calculation methods commonly used in the past.

To enable portability, the microcomputer was targeted as the application vehicle for maximum transferability. Utilities may use this system directly, or they may experiment with it to help define their own systems. SYSRAP uses a highly detailed feeder model that includes voltage-sensitive loads.

Comparison of experimental observations and SYSRAP results has proven the adequacy of the program for simulating system response to system reconfiguration and volt/var control, which affect the feeder voltage profile.

The AACETS proved to be an invaluable support tool in the activities of the AACE. It provided an optimum environment for the development of experimental control software by permitting the development and debugging of programs off line of the main automation system in Athens. Conditions are well suited for the development of the software because a scaled-down version of the Athens control system and a distribution simulator are employed in an effort to duplicate actual system conditions. Experience gained from the use of the AACETS has allowed more effective use of the Athens control system as well as independence from the vendor for system support. Besides the development of software, AACETS provided the capability to acquire two types of characterization data before the main control system was installed, thus allowing an early determination of the operating characteristics of the new automation system.

REFERENCES

1. "Power Delivery Software: What's Out There?" *Electr. World,* **200**(7), 61–65 (July 1986).
2. D. T. Rizy, J. S. Lawler, J. B. Patton, and W. R. Nelson, "Measuring and Analyzing the Impact of Voltage and Capacitor Control with High Speed Data Acquisition," IEEE Paper No. 88 WM 098-6, presented at the IEEE PES Winter Meeting, New York, February 1988; published in *IEEE Trans. Power Delivery,* **4**(1), 704–14 (January 1989).
3. *Electric Transmission and Distribution Reference Book,* 4th ed., Westinghouse Electric Corporation, East Pittsburgh, Pa., 1964.

9

EXPERIENCES WITH THE EQUIPMENT

E. R. Broadaway, N. Fortson, L. D. Monteen,
J. P. Stovall, and G. R. Wetherington

The AACE Integrated Distribution Control System (IDCS) is described in Chapter 2. The IDCS can be divided into three subsystems: (1) substation control and monitoring, (2) distribution feeder control and monitoring, and (3) customer load control and monitoring. The communication and control center, or central control computer, provides the link that integrates the three subsystems and provides the intelligence required for operating the IDCS. In addition, the AACE Test System described in Chapter 8 was used for the appliance research metering system (ARMS).

This chapter documents the experiences with the hardware and indicates potential problem areas to designers of new automation systems. The equipment installed for the system includes

- communication and control center,
- color cathode-ray tube (CRT),
- remote terminal units (RTUs),
- signal injection units (SIUs),
- interface equipment,
- weather station equipment,
- pole-top units (PTUs),
- distribution control receiver (DCR) units,

- load control receivers (LCRs),
- smart meters (SMs),
- AACE test system (AACETS), and
- appliance research metering system.

A decision was made early in the conceptual phase of the project to use state-of-the-art, off the shelf equipment whenever possible. A unique feature of the AACE system is that the automation system combines supervisory control and data acquisition (SCADA), distribution automation, load management, load research, load planning, load monitoring, and data gathering into one system, which is centrally controlled by a minicomputer.[1]

COMMUNICATION AND CONTROL CENTER

The communication and control center, which consists of dual minicomputers with associated peripheral equipment, provides the data collection and organization required for system operation. One computer operates as the on-line system and handles all data acquisition and control actions; the other computer functions as the standby system with identical software and updates its data base from the on-line computer once per minute. The man-machine interface consists of two color graphic displays, terminals, and printers. Auto-answer modems are used for remote access. Vendor-supplied data acquisition and control software monitors and controls all field devices while specific application software developed on the AACETS provides support for the data acquisition and control effort for the experiments.

A few computer failures or shutdowns have occurred. Because the dual computer configuration provides redundancy, a single computer failure will result in failover to the standby computer, with system functionality restored within 1 minute. System failover can be caused by either hardware or software failure.

Correcting software failures was the responsibility of ORNL engineering personnel after the warranty period of the equipment expired. The ORNL personnel had a strong working knowledge of the computer hardware and software acquired through the use of similar systems and the AACETS. The availability of these personnel greatly reduced reliance on vendors when problems were encountered.

The hardware failures of the computer system were primarily associated with the disk drives. Some of these occurred during the warranty period, and service was provided by the vendor. After the warranty period, computer hardware failures were diagnosed and serviced by ORNL technical service personnel. This type of service is not normally available within most utilities.

When using a system such as this, consideration must be given to whether service will be supplied in-house, by vendor contract, or by third-party service personnel.

COLOR CATHODE-RAY TUBE

The color CRTs used as the dispatcher's monitors generally performed well. Display and control actions could be initiated using the keyboard and/or the light pen. Because the light pens were fragile and easily broken, the dispatchers eventually discarded them and used the keyboard to initiate the actions. This procedure is slightly inconvenient but does not reduce functionality.

REMOTE TERMINAL UNITS

A substation remote terminal unit (RTU) is located in each of the three substations to monitor real power, reactive power, voltage, transformer tap position, air temperature, humidity, breaker position, relay status, and capacitor status. A weather station was monitored with one of the substation RTUs. The RTU also initiates control actions to breakers, transformer tap changers, and capacitor switches as directed from the communication and control center.

The distribution RTU is a smaller version of the substation RTU and is part of the feeder automation subsystem. It monitors local three-phase real power, reactive power, and voltage on all three phases and can detect the status of relays and fault sensors on distribution feeders. These RTUs can control several switches or voltage regulators at each distribution location.

Both types of RTUs are connected to the communication and control center computers by a 1200-baud, 4-wire leased telephone line with continuous two-way communication.

Problems encountered with the RTUs were primarily lightning related—one of the distribution RTUs was totally destroyed by a direct lightning strike. Very little can be done to prevent this type of damage. Most of the other failures were at one particular substation and were of a transient, low-voltage type with no visible component damage. This RTU was originally powered from the substation batteries located about 100 feet away. The power supply cable was run underground next to the substation ground grid. After this configuration was suspected to be the cause of the failures, a battery backed-up power supply was installed and used to power the RTU. Additional investigation of the problem was delayed by the end of the lightning season, although the change in power supply appears to have reduced (if not eliminated) these failures.

Problems were encountered in the input/output (I/O) cards for these units. Commercially available equipment with a level of sophistication that allows remote determination of the causes of problems was not available on the Athens equipment. Initially, during the warranty period and afterward, the failed I/O cards were returned to the vendor for repair. AUB in-house personnel later began repairing these cards, and a supply of electronic components was maintained. Although redundancy of key RTUs may be desirable, the cost effectiveness of this redundancy has not been determined.

SIGNAL INJECTION UNITS

The signal injection units (SIUs) modulate the power system voltage signal by injecting a 340-Hz voltage waveform onto the 60-Hz voltage wave. This "ripple" signal is detected by receivers located downstream of the injection location, which are used to control capacitor banks and residential loads.

It is necessary to tune the SIUs to ensure proper coupling of the device to the power system. If the impedance is not properly matched to the feeder, significant deterioration of the coupled signal will occur. Low-level signal drift on some feeders may be attributed to impedance changes after lines were reconfigured or reconductored. Initial tuning of the SIUs was performed by the vendor, but subsequent tuning was done by AUB personnel.

One SIU was originally a three-phase unit since that substation received power in a delta configuration. However, signals from this unit were fed back through 13.2/69-kV transformer connections to the 69-kV subtransmission system and then to other parts of the distribution system. The signal from this unit interfered with signals from another SIU, as all three substations are supplied from the one with the delta configuration. Converting the three-phase unit to a single-phase unit, with the signal injected on each phase separately, alleviated the problem. As a result of this conversion, however, some signal strength was lost. This attenuation effect is characteristic of carrier communication systems and is very difficult to remedy. The other two substations are supplied in a wye configuration, and the ripple signal is injected on the neutral conductor.

A certain amount of signal induction is evident on the telephone circuits. Ripple signals travel beyond their intended path and are induced into areas where they may create problems. Telephone company equipment is grounded wherever possible. Frequently, the telephone equipment was connected to AUB pole grounds, which are connected directly to the system neutral.

Most of the expertise needed to address these issues at AUB was provided by the manufacturer. This technology and equipment was not new and has been used for several years in both Europe and the United States.

Operation of circuit breakers, capacitor banks, or disconnect switches can create signal disturbances on the line. These disturbances may distort the injected signal and delay or prevent devices from receiving the complete message. Some problems associated with signal distortion can be alleviated if the device must receive its entire command sequence before it can operate. This was not the case with the devices at AUB and did result in some problems.

INTERFACE EQUIPMENT

Signal transducers were used at locations where real power, reactive power, and voltage measurements were taken. The purpose of these transducers was to convert standard ac signals from the metering class instrument transformers into signals of the appropriate level for input to the RTUs and PTUs. The signal transducers performed well. Calibration of these instruments was checked by plotting a range of points from minimum to maximum to ensure linearity. Normally, routine recalibration is required at 6- or 12-month intervals.

WEATHER STATION EQUIPMENT

One major and two smaller weather stations were provided. The two small stations measured only temperature and humidity. The major weather station capability included temperature, humidity, wind speed, wind direction, barometric pressure, and solar radiation. Some difficulty was encountered in getting the stations operational because AUB installation personnel were not familiar with the equipment and the documentation provided by the manufacturer was inaccurate.

Weather station interfacing was complicated by incorrect impedance matching between the output and the RTU. This problem was corrected by bypassing part of the output circuitry on the weather station electronics module. The consensus is that the manufacturer should have been requested to install the weather station. Maintenance of the sensors is difficult, and AUB did not have the facilities necessary for proper calibration. In particular, the humidity sensors performed very poorly. Spider webs on the temperature and humidity sensors were an additional cause of inaccurate readings. The electronic modules that interface the sensors to the RTUs were calibrated after the modifications for this installation were noted.

POLE TOP UNITS

The pole top units (PTUs) are similar to the RTUs with the exception of the communication method and the number of control and monitoring connections. The unit receives its control signal from the signal injection unit and conveys information to the central computer via a dial-up, 300-baud, voice-grade telephone line. If the computer telephone lines are busy, the PTU will periodically reinitiate a call. Also, the PTU has backup telephone communications capability; if a power outage interrupts communication between the signal injection unit and the DCR in the PTU, the computer can send a control signal to the PTU over the telephone line.

When the system was purchased, the PTU was newly designed and no field experience was available. Many of the problems encountered with the PTU operation were the result of communication collisions associated with the call-in feature on the telephone circuit. The use of off-premises extension lines (with a number of PTUs on the same line) instead of dedicated lines also created problems. Because the PTUs report by exception, a problem developed when several PTUs needed to report problems over a large area at the same time. To help alleviate this call-in collision, the units were staged so that each unit on the party line would attempt to call at 20-second intervals. This feature improved the operation but did not completely eliminate the problem.

Installation of the PTUs along the feeder also created some difficulties. For telephone extension-line operation, the spacing is typically hundreds of feet, but PTU spacing along the feeder can be several miles. The PTUs sense voltage drop along the line to determine if the line is in use, and this voltage drop was significantly different for the various units. This resulted in several PTUs on the same line attempting to communicate simultaneously; consequently, no communication was possible. A diode in the unit was replaced to alleviate this problem; however, the problem can recur if the local telephone company significantly changes the impedance of the communications circuit. The telephone company does not issue specifications for voltage drop. Instead, the specifications relate to changes in the current traveling on the line.

Some problems unique to the PTU controller card were encountered. The vendor solved these problems by a series of diagnostic tests, culminating in a field acceptance test at AUB. The controller card and the PTU were manufactured by two different companies, and both underwent a series of factory tests to ensure proper operation; however, operational problems were encountered during the field acceptance test. Although the 7-month field acceptance testing procedure was time consuming, it significantly reduced the number of problems encountered in the field. Three modifications to the controller card were made. A change in the firmware necessitated returning the cards to the manufacturer for correction. One of the electronic chips on the PTU controller card did not meet temperature specifications. The manufacturer subsequently checked all components on the controller cards and found two additional components that did not meet the specification. All of the out-of-specification components were replaced by the manufacturer.

DISTRIBUTION CONTROL RECEIVERS

The DCR is a one-way control device that was installed at most capacitor locations. It receives its control signal from the communication and control system via the signal injection unit and connects or disconnects a capacitor bank. Control verification is most often received by the central computer indirectly by observing a change in reactive power flow for the feeder at the substation RTU.

Distribution control receivers were installed on 17 capacitor banks. At times, the capacitor banks are not switchable, but this is seldom the result of DCR failure. Most of these failures can be attributed to oil switch, capacitor bank, and/or fuse failures.

The capacitor banks sometimes fail to switch even though all components, including the DCR, are functional. This occurs because of the method of communication with the DCR. There is no error checking on the received signal and the entire signal is not required for the device to operate. This allows the capacitor bank to switch while the message is still being sent, and the resulting transient distorts the rest of the message. This is further compounded in the DCR by the use of latching relays that get a "close" and then "open" in the same command so that they operate like a momentary relay. The relay can get the "close" part of the message, switch the bank, and the resulting transient can eliminate the "open" part of the message. This situation results in the DCR relay "hanging" in an inappropriate state and may result in undesired capacitor bank operation. This problem occurs most often in the DCRs associated with PTUs and can be alleviated by sending a "demand scan" command to the PTU prior to sending the capacitor switching command.

The DCRs, which are a variation of the LCR used for residential load control, have been deemed inappropriate for distribution device control because of the lack of error checking or delayed operation and the use of one-way communication.

LOAD CONTROL RECEIVERS

The LCRs located in the homes of consumers decode the ripple signals from the SIUs to create a control message. The LCR has three internal relays to control individual loads such as water heaters, space heaters, and air conditioners. Normally, three different controllable loads are connected to each LCR. The LCRs use the same communication scheme as the DCRs. This is appropriate for residential load control because a missed command by one or even a few LCRs will not cause distribution system problems. The loads controlled by the LCRs will automatically restore after a period of time if no other command is sent to the unit.

SMART METERS

The SMs were installed in the homes of 190 residential consumers who were identified by the customer load surveys. The SM integrates a standard kilowatt-hour meter with an electronics package that counts the revolutions of the electric meter disk. The revolution counts are stored in SM memory and are transferred to the communication and control center computer using the customer's telephone line. All SMs call in to a four-line rotary telephone system connected to the communication and control center computer. When the call is placed, the meter identifies itself, transmits all data, and records the time. The computer then selects the proper time for the SM to call back. Although there is two-way communication between the SM and the computer during a call in, all calls must be initiated by the SM. Failure to call in at the designated time results in a late-call alarm being logged at the communication and control center.

Failure rates of the SMs have been unusually high. The SMs were designed for automatic daily, weekly, or monthly meter reading. However, the AACE project used them for load research, which sometimes required readings every 15 minutes, and the increased frequency of transmission placed an unusually high stress on the device. Investigation of the failures has revealed that many were caused by a bad battery, which draws down the dc voltage. Replacement of the nickel cadmium battery restored the unit to service.

Initially, there was a minor problem with the callback feature as a result of a design error in the integrated circuit. The design error allowed noise on the telephone to interfere with the error-checking procedure for the data being transmitted and recorded, which resulted in the callback time being incorrectly received and the smart meter not calling back to the communication and control center. The problem was detected during the field acceptance test, and the SMs were returned to the manufacturer for modifications. These meters were tested several times before they were placed in operation and had performed well at other locations. The meters apparently operate well under ideal test conditions, but minor problems occur under field conditions.

APPLIANCE RESEARCH METERING SYSTEM

The ARMS units were installed in the homes of 74 customers. Two hundred of these units were furnished by the EPRI under a separate agreement with AUB for the purpose of load control studies; however, because of problems in keeping the ARMS operating, only 74 were installed. The AACETS computer at ORNL was used for data retrieval and storage of the ARMS data. The ARMS units monitor the electricity used by individual water heaters, central heating units, and air-conditioning units at 5-minute intervals. The units also measure the total household power usage and the inside-house ambient air temperature. Load profile recorders were used at the residence for storage and transmission of the data to AACETS at a specified time. The data were transmitted to AACETS via the customer's telephone line.

When first received by AUB, the ARMS units were designed with a "call-out" type feature and required dedicated (additional) telephone service to each home in which an ARMS unit was installed. Communications to the ARMS were to be by the AACETS computer, which would initiate a telephone call to the ARM unit to transfer stored data. Because of the estimated high costs of installing dedicated telephone service in 200 homes, the cost and monthly service charges for a 2-year data collection period, a modification was made to the ARM units. The modification added the "call-in" feature which allowed the ARM unit to share the customers existing telephone line. Communications were made by the ARM unit initiating a local telephone to call in to the AACETS computer to transfer stored data. The calls were made between 2 a.m. and 4 a.m. to minimize interference with customer telephone service.

Several problems were encountered when the first few ARMS units were installed. Apparently, the manufacturer did not provide a high degree of quality assurance before shipping the devices. After discussions with EPRI, factory and field acceptance tests were conducted by ORNL and AUB personnel. Additional problems encountered later appeared to be component failures resulting from insufficient quality assurance during manufacturing. A review of repair reports for a several month period failed to indicate any common component failure even when failure symptoms were similar. All repairs were performed by the manufacturer under contract with EPRI.

SUMMARY

The project personnel concluded that, with the exception of the appliance research meters, the smart meters, and the distribution control receivers, the equipment performed satisfactorily. Problems with the smart meters probably resulted from the units being overstressed and their being used in an experimental mode. Problems experienced with the distribution control receivers were caused by the application of new or inappropriate technology to new control procedures.

Some suggestions are offered for designers of new, centrally controlled automation projects. The project management team should require a detailed and effective test procedure that includes both factory and field (site) acceptance tests. Adequate diagnostics (both on-site and remote) are essential to the success of the operation. The diagnostic procedures should be user friendly and should not involve complicated conversion processes and interpretations. Often the equipment is sophisticated, and in many cases different manufacturers may furnish separate devices for a particular application. Personnel with proper skills to maintain and operate the equipment must be available. To fully exploit the benefits of the automation system, unique skills and expertise may be required.

REFERENCE

1. Purucker, S. L., et al., "The Design of an Integrated Distribution Control System," *IEEE Trans. Power Appar. Syst.* **PAS-104**(3), 745–52 (March 1985).

10

IMPROVEMENTS, ACCOMPLISHMENTS, AND RESULTS

P. A. Gnadt, J. S. Lawler, D. T. Rizy, and J. P. Stovall

The Athens automation system is the first fully integrated distribution system in the United States and probably in the world. The accomplishments of the Athens experiment have advanced distribution automation technology in utility systems far beyond expectations. The experiments performed from 1985 through 1987 have set the stage for advancing from the demonstration phase to full operational status. Further, the Athens experiment should be applicable and of interest to electric power distributors everywhere, particularly to those in the Tennessee Valley.

Operating and maintenance improvements in the distribution system at Athens have been demonstrated in several key areas. AUB reports that the AACE system has improved reliability of service; improved maintenance and lowered maintenance costs of the system; improved system safety; improved the power factor, which has resulted in reduced power delivery costs; improved customer relationships; improved system planning; and improved capacity utilization.

Load control experiments have shown that it is possible to accurately measure changes in load to control actions and use high-speed data acquisition at the feeder level as an alternative to monitoring equipment located at each customer home under control.

System reconfiguration experiments have demonstrated that load can be transferred more quickly and more economically than before the system was automated; load transfers do not necessarily result in loss reduction as normally expected because of the sensitivity of customer load to voltage.

Volt/var experiments indicate that customer load is sensitive to the voltage profile of the system and that the load must be modeled accurately to quantify loss reduction. An improvement in voltage profile because of the switching in of capacitors can result in a load increase that exceeds loss reduction. Conventional constant power load models do not accurately model changes in system operating parameters resulting from capacitor switching.

For the first time, measurement of system operating parameters in real time allows study of the results of control actions, and new measurement system techniques allow more accurate analysis of system response to control actions.

Computer programs developed to control and analyze distribution automation functions make it possible to estimate the effects of planned control actions on the distribution system prior to taking action, control feeder capacitors to improve power factor and to reduce losses and power delivery costs, control customer loads to gather data for load research and to shift load to off-peak times, and calculate losses on the system.

IMPROVEMENTS

Improved Reliability of Service

Distribution automation has improved AUB's ability to restore service to customers following an abnormal condition such as a fault. Before automation, AUB relied on customers to call the system operator's office to report loss of electric service. As part of the automation system, fault detectors are placed at various locations on the distribution system to identify and locate faults and report the location to the system operators at the dispatch office. The ability to control feeder breakers and switches from a central location enables AUB to transfer loads from one substation or feeder to another during an abnormal system occurrence. AUB can now restore service to critical loads, such as the area hospital, in a few minutes when it previously took one-half hour.

In a panel discussion (Recent Experiences in Feeder Acquisition and Control) at the 1987 Summer Meeting of the IEEE Power Engineering Society, AUB pointed out to other utility representatives that the cost of a distribution automation system is justified by system reliability improvements. AUB has several small commercial customers in the 3- to 4-MVA-capacity range for whom three or four outages a year would cause financial hardships as a result of lost time, lost production, restart costs, and damaged goods.

Improved Maintenance of the System

Distribution automation provides AUB with the ability to control feeder breakers and feeder switches to deenergize an entire substation, feeder, or feeder section for maintenance. This ability has greatly simplified and reduced the personnel and time needed to service or repair distribution equipment. The system operator simply opens the feeder breaker and/or feeder load break switches to isolate the feeder or feeder section. While the system operator is deenergizing part of the system, the line crew is dispatched to the work site and services or repairs the system after confirming that the work site is deenergized. The ability to transfer load from one substation or feeder has enabled AUB to ensure continuous service to customers during maintenance operations.

The capability to locate faults has greatly improved AUB's ability to dispatch line crews during abnormal conditions. Before automation, AUB sent several line crews to drive along distribution feeders to look for blown fuses or open cutouts. In most cases, the automation system eliminates the need to dispatch more than one crew to look for the fault site. System operators use the automation system to determine the approximate location of the service outage, normally within several utility pole spans, and to dispatch a line crew to the site without having to send extra crews or spend extra time to locate the fault.

Improved Voltage Control

At one substation, the automation system controls two load-tap-changing (LTC) transformers; at another substation, the automation system controls voltage regulators located at various points on the feeders. The automation system continuously provides the system operators with information on the system voltage provided by TVA and the voltage at various points on the feeders. TVA provides the voltage to the main substation for the AUB system; however, the voltage along each of the feeders varies with customer load demand. The system operators can closely regulate the feeder voltage profile as the load changes during the day. Before automation, local controllers adjusted the settings of the LTC transformers and feeder voltage regulators. AUB has found that a better voltage profile can be maintained with automation. Maintaining a level voltage profile ensures quality power to AUB's customers.

Improved Power Factor Control

TVA implements a rate charge for poor power factor correction and charges distributors a higher delivery rate when the power factor of the distributor's system is leading during off-peak times and more than 0.95 lagging during on-peak times. The new rate does not present a problem for AUB because the automation system allows the system operators to remotely control feeder capacitors on the AUB system to correct the power factor as load varies on the system. Before automation, some capacitors were controlled by local var controllers and the others were fixed. Typically, the locally controlled and fixed capacitors resulted in sufficient power factor correction during peak load conditions but overcorrected during low load conditions.

The automation system can now determine when capacitor banks have failed to operate. When a capacitor bank is switched, a change in the reactive power at the substation is observed if the switching is successful. When a change in reactive power is not observed, AUB dispatches a line crew to determine the source of the problem. The correct operation of the capacitor banks is critical to maintaining AUB's power factor correction level.

Improved Customer Relations

The improvement in system reliability and system performance has improved AUB's relationship with its customers. Since the installation of the new automated system, several consumers have called to ask the utility how they have been able to restore electric service so quickly during a storm.

Improved System Planning and Capacity Utilization

AUB has found the automated system to be helpful in planning changes to its system. In 1987, AUB reconfigured half of its system to relieve two feeders that were heavily loaded and to move the load to three feeders with surplus capacity. The two feeders were becoming overloaded, and one feeder was close to tripping out because of overload. The automation system is similar to a real-time load flow program. The system shows the real and reactive power needed by each feeder and substation and the voltage at the substation and along the feeder. The real-time information indicates when a reconfiguration of the system is needed to more equally load the distribution feeders.

The automated system has enabled AUB to optimize capacitors location. Before installation of capacitors on the system, AUB and ORNL performed load flow analyses to determine where to place the controllable capacitors on the AUB system for the AACE experiment. The results of the automation system later helped determine that some of the capacitor placements were not needed and that capacitors were needed in other locations. Results of the experiments showed that larger capacitor banks were needed in some locations.

ACCOMPLISHMENTS AND RESULTS

High-Speed Data Acquisition System

A high-speed data-gathering system was developed to measure millisecond-duration phenomena at the distribution system level. The system is portable and features an aggregate data scan rate of 250 to 10,000 samples per second over 10 channels of input signals. Data may be gathered over variable time periods ranging from several seconds to 5.5 hours. A specially designed cabling configuration allows easy connections to distribution level equipment (watt/var and voltage transducers) and quick installation of the equipment. Sophisticated filtering of power system signals is needed to properly measure system parameters. The acquisition system graphically presents acquired data for in-the-field interpretation of results. Off-line data analysis is performed with mainframe computers after transferring data from the high-speed system by magnetic tape. The application of this system allows examination and interpretation of events typical of an electrical distribution system, such as capacitor switching, voltage regulation, load transfer, and load control, in a manner not possible with conventional substation or feeder level monitoring.

Analysis Software for Implementing and Analyzing Distribution System Automation

An innovative distribution automation application software package called SYSRAP (System Reconfiguration Analysis Program) was developed for and is used for assessing system configuration and volt/var control on interconnected radial distribution feeder conditions. SYSRAP provides off-line and on-line analysis of reconfigured distribution feeders. The software package combines power flow analysis, short-circuit analysis, and data base management. Feeder loads are modeled as voltage sensitive or insensitive (any load composition of constant power, constant current, and constant impedance). The loads are scaled according to total feeder real- and reactive-power flow, bus voltage, and connected transformer kilovolt-amperes and/or billed kilowatt-hours. The package provides the capability to study load transfers, capacitor switching, voltage control, and faults under various loading and temperature conditions. SYSRAP has been developed into a personal computer program and has been used to determine load transfers on the AUB system and to simulate load transfers that were believed to be too risky for experimentation.

The on-line use of SYSRAP includes a feature to update the data base with system values and status of switches and circuit breakers collected by supervisory control and data acquisition (SCADA) and feeder-monitoring equipment. The use of voltage-sensitive load models shows close agreement between the actual and computer voltages and power flows applied on the AUB system.

Automated Control of Capacitor

A computer program was developed to control feeder capacitors using the SCADA and feeder automation hardware, and the program has been implemented on the AUB system. In 1987, the procedure was used to advise the system operators on optimal use of capacitors to maintain a slightly lagging power factor. Later, the program was modified to automatically switch capacitors in and out to control the feeder power factor.

Automated Control of Customer Loads

A computer program was developed to control residential customer loads (water heaters, air conditioners, and space heating) using the SCADA and load control receivers placed at customers' homes. The program can vary the length of the off times (duty cycles) for the loads. The program automatically turns customer load off by load group and back on by feeder section. Currently, 1000 load control receivers are being controlled.

Load Control Experimental Results

The experiments show that it is possible to directly observe changes in load and to attribute these changes to load control actions. The sampling rates used for the experiments were of sufficient resolution to observe the switching of subgroups with as few as three air conditioners.

A cluster analysis of monthly billing was used to identify and recruit customers who have and use electric space-conditioning appliances and/or electric water heaters for the load control experiments. Customers were recruited from four user classifications: super users, heavy users, moderate summer users, and moderate winter users. Most of the participants were from the super-user and heavy-user classification groups. Recruiting was accomplished through personal contacts, and incentives were not used.

Direct control of water heaters effectively shifts load from peak times to off-peak times. Water heaters were controlled for 2-, 3-, and 4-hour periods in the mornings or evenings, depending on the season. The typical expected demand deferred was between 800 and 900 W per unit.

The current design of space heating systems makes peak shifting difficult and impractical. Existing control circuitry in heat pumps is designed to ensure that internal temperatures do not get cool when compressors lose efficiency at low external temperatures or when a 3 or 4°F differential exists between air temperature and thermostat setting. This design can result in the use of more power during control periods. Control of resistive heating is effective if the heating can be centrally controlled. The use of special control circuits and special relays to control the power to these circuits may not be economical.

Control of air conditioners is effective in reducing peak loads without causing discomfort to the household being controlled. Between 200 and 250 kW of air conditioner load was dropped on the experimental circuit each time a control action was initiated. In every case, the total amount of load restored after the control action was less than the amount originally dropped.

These experiments have several implications. First, they suggest that it may be possible to reliably determine the controllable load two to four hours before load control actions are scheduled, which will make load control a dispatchable option. Second, the results suggest that high-speed data acquisition coupled with programmable load control receivers can provide an alternative to current methods of load research for major appliances. Third, the experimental results suggest that load control can be accomplished with equipment that is much less expensive, more reliable, and more accessible to utility personnel than end-use monitoring equipment.

System Reconfiguration

Automated fault detectors, feeder monitoring, and automated load transfers between distribution feeders by remotely controlled switches have the potential to reduce equipment capacity requirements, reduce network losses, simplify maintenance operations and decrease maintenance costs, and increase service reliability.

Experimental results show that there is no significant diversity in the time of occurrence of the daily peak load on the various AUB feeders. Consequently, a load transfer to reduce the daily peak on one feeder results in a similar increase in the peak load on another feeder.

Loss reduction is possible under some circumstances; however, most load transfers result in increased losses. One reason is that when tie switch locations are selected to minimize losses under typical load conditions, a transfer will generally result in a greater network impedance between the transferred section and the source. Another reason for the increased losses is the fact that the AUB feeders are "telescoped," with conductor size on the feeder decreasing with distance from the substation. A reconfiguration may often involve rerouting power to a line section through a smaller conductor than in the normal configuration.

Significant voltage effects were observed following load transfers. In general, the voltage profile rises on the feeder being relieved of load and decreases on the feeder that accepts additional load. These changes in voltage alter customer load because the loads are voltage sensitive. As a consequence of the voltage effects, load transfers were not conservative; more load is shed from the feeder being relieved than is picked up by the supporting feeder.

Automated fault detectors, combined with remote control of distribution circuit breakers, power reclosers, and load break switches, can significantly reduce the time required to detect and locate faults, increase the speed of isolating faulted equipment, and provide faster load restoration. The Predictive Reliability Assessment Model (PRAM), an EPRI-sponsored computer program, was used to quantify the effect of varying degrees of automated switching capability of the distribution system. The value of automation was found to be highly sensitive to the historical outage data used to establish component failure rates and to the economic worth of reliability assigned by the utility.

Operating experience with the automation system has shown that there are significant intangible reliability benefits and tangible cost savings associated with automation that are outside the scope of conventional distribution reliability indices. There are actual cases where the automation system resulted in significant cost savings and reliability benefits that are not captured by conventional reliability indices. The automation system has prevented outages or greatly reduced the outage area, provided a cost savings through the use of the automation system during daily and routine events that were normally performed manually, improved system safety, or detected failing equipment before a catastrophic failure of the equipment and subsequent outage. The cases resulted in a direct benefit of $256,384 (1986 dollars) over a period of 30 months. These savings could not have been predicted by analytical studies, and as time goes on, other cost savings will add to the total. Many of the major benefits of an automation system resulted from the diagnostic ability to prevent small problems and outages from escalating into large outages.

Volt/Var Experimental Results

The effects of capacitor switching on feeder operating variables were measured in the substation by the high-speed data acquisition system. Consistent with the modelling of feeder loads as constant power, the switching in of a capacitor bank to improve the power factor results in decreased var injection and increased phase voltages. However, contrary to constant power load modelling, a reduction in real-power (kilowatts) injection reflecting reduced line losses was not observed. In fact, the measured real power injection increases. Similarly, the switching out of a capacitor bank results in increased reactive power injection (kilovars), decreased phase voltages, and decreased real power injection. Analysis of experimental results, using voltage-sensitive load models and SYSRAP, shows that while feeder losses are reduced following feeder power factor correction, the attendant improvement in the voltage profile results in an increase in load that exceeds the amount of loss reduction. Consequently, distribution system operators employing SCADA systems will not be able to observe the loss reduction associated with capacitor switching to improve the power factor. System planners will need to know the exact nature of load sensitivity to voltage in order to quantify the economic benefits of installing and switching capacitor banks. Fortunately, the development of the high-speed data acquisition system provides a convenient means of obtaining the data necessary to determine the load sensitivity to voltage. The development of SYSRAP allows accurate modeling of changes in system parameters due to volt/var control.

Automation Systems of the Future

The fact that the results from the Athens experiment are available to the public and to industry is significant. The fully integrated system has shown that it is feasible to measure how every part of the distribution system responds to control actions and to diagnose and remedy problems quickly and efficiently. The willingness of customers and operations and maintenance personnel of the Athens Utilities Board to accept changes has significantly benefited both customers and AUB.

The knowledge gained at Athens points the way to the introduction of expert systems applications to distribution system operations. The technology developed during the experiments along with the information provided by the monitoring system will allow expert knowledge to be programmed into the computer so the computer can help diagnose problems, identify and locate problems, and suggest solutions to the problems. Eventually, the computer should be capable of taking the necessary actions to alleviate problems.

As we learn more about the operation of distribution systems and how they react to changes in supply conditions and load conditions and to operator controls, we can operate the distribution system much more efficiently, reliably, and easily. The technology application learned on the distribution system should be applicable to operation of transmission systems, and these systems can also be operated more reliably, efficiently, and easily.

11

ABOUT THE AUTHORS

P. A. Gnadt retired in 1988 as Manager of the Power Systems Technology Program at the Oak Ridge National Laboratory. The major goal of the program is research and development in concert with electric utilities and manufacturers. The objectives of the program are higher-efficiency operation of electric power delivery systems. The Athens Automation and Control Experiment was part of the Power Systems Technology Program. Mr. Gnadt was employed with Union Carbide Corporation–Nuclear Division, Martin Marietta Energy Systems, Inc., and Oak Ridge National Laboratory since 1954. During that time, he was project engineer and principal investigator for experimental test facilities for Aircraft Nuclear Propulsion, Pressurized Water Reactor, Molten Salt Reactor, Gas-Cooled Reactor, and Liquid-Metal Fast Breeder Reactor nuclear projects.

Before going to Oak Ridge, Mr. Gnadt spent three years with Empire District Electric Company, Joplin, Missouri, as relay and substation engineer and one year as testing engineer at a steam electric generating plant at Electric Energy, Inc., Joppa, Illinois.

He has authored and coauthored 50 technical reports and publications. Mr. Gnadt received his education in Electrical Engineering at Pittsburg (Kansas) State University.

J. S. Lawler is a Professor of electrical engineering, specializing in electric power systems. He received his Ph.D. degree in systems science from Michigan State University, East Lansing, in 1979 and has been with The University of Tennessee, Knoxville, since graduation. His active research interests include automation of electric distribution systems and power electronics circuits and controls. Dr. Lawler is a member of IEEE, Phi Kappa Phi, and Sigma Xi.

D. Bargiotas received a B.S. degree in electrical engineering from the Polytechnic School of Patras, Greece, in 1981, and an M.S. degree in electrical engineering from The University of Tennessee, Knoxville, in 1986. He is currently pursuing a Ph.D. degree in electrical engineering at The University of Tennessee, Knoxville. Since 1983 he has been a research assistant at the Electrical Engineering Department, The University of Tennessee, Knoxville. His research interests include electric power systems, transient stability analysis, large-scale systems, and estimation theory.

J. D. Birdwell is a Professor of electrical engineering, specializing in systems and control theory and applications of computers and artificial intelligence principles to electrical engineering design. He obtained his Ph.D. degree in electrical engineering from the Massachusetts Institute of Technology, Cambridge, in 1978 and has been with The University of Tennessee since graduation. Dr. Birdwell's areas of active research are the development of prototype expert system environments for control system analysis and design, the application of advanced concepts from systems theory to electric power systems, and the application of knowledge representation methods from artificial intelligence to estimation and control theory. Other areas of research and development experience include the theory of reliable control systems, nonlinear distributed estimation theory, and decision network performance analysis. Dr. Birdwell is a member of Tau Beta Pi, Eta Kappa Nu, and Sigma Xi, and is a senior member of the Institute of Electrical and Electronics Engineers, Inc.

E. R. Broadaway received a B.S. degree from Mississippi University for Women, Columbus, Mississippi, in 1977 and a B.S. degree in electrical engineering from Memphis State University in 1983. Ms. Broadaway is employed by Martin Marietta Energy Systems as a development staff member in the Instrumentation and Controls Division of the Oak Ridge National Laboratory. She has 4 years' experience in advanced computer system development and integration. Her special interests include real-time data acquisition and control system development, management, and applications and biomedical computer instrumentation applications. Ms. Broadaway has (co)authored three technical publications.

Robert P. Broadwater is an Associate Professor of electrical engineering at Virginia Polytechnic Institute and State University at Blacksburg, Va. He received his B.S., M.S., and Ph.D. degrees in electrical engineering from Virginia Polytechnic Institute. Dr. Broadwater is interested in simulation and control in nuclear power generation and electrical power distribution. He has worked for the Tennessee Valley Authority, Tennessee Valley Public Power Association, Oak Ridge National Laboratory, Babcock and Wilcox, and General Electric. He is a member of the American Society of Engineering

Education, the Society for Computer Simulation, and the Power Engineering Society and Automatic Control Society of IEEE.

A. Chandrasekaran received a B.E. degree from the University of Madras, India, in 1961, an M.E. degree from the Indian Institute of Science, Bangalore, India, in 1963, and a Ph.D. degree from the Indian Institute of Technology, Madras, India, in 1973. He was on the faculty of the Electrical Engineering Department at the Indian Institute of Technology, Madras, from 1963–84. Dr. Chandrasekaran was visiting faculty at the Rochester Institute of Technology and University of North Carolina at Charlotte. He is currently on the faculty of the Center of Excellence for Electric Power at Tennessee Technological University, Cookeville, Tennessee. Dr. Chandrasekaran was awarded the German Academic Exchange (DAAD) Fellowship during 1969–70 and the Alexander von Humboldt Senior Fellowship during 1975–77. He worked at the R&D department of Siemens, Erlangen, W. Germany, for four years. His current areas of interest are computer-aided analysis of transmission and distribution systems and power electronic circuits.

N. H. Fortson obtained his Bachelor of Electrical Engineering Technology degree from Southern Technical Institute, Marietta, Georgia. Mr. Fortson has worked for municipal, rural electric, and generation and transmission utilities and is currently employed by Athens Utilities Board as superintendent of power. His work has been in SCADA, load management research, system reconfiguration, electrical distribution engineering, and system operations management for the past 15 years. Mr. Fortson has been on several statewide and national association committees dealing with electrical power distribution problems and innovations and has co-authored several reports on these issues.

Jih-Sheng Lai received a B.Ed. and an M.Ed. from National Taiwan Normal University and an M.S. degree in electrical engineering from The University of Tennessee, Knoxville, in 1975, 1980, and 1985, respectively. He is currently working on a Ph.D. at The University of Tennessee, Knoxville. From 1980 to 1983, he was Instructor and Chairman of the Department of Electrical Engineering at Ming-Chi Institute of Technology, Taipei, Taiwan. He served as an Instructor in the Department of Electrical and Computer Engineering at The University of Tennessee, Knoxville, from 1986 to 1987. He is now a research assistant in a joint program established by The University of Tennessee and the Power Electronics Applications Center. His research interests are computer applications in modern control systems, power systems, and power electronics motor drives. Mr. Lai is a student member of IEEE and a member of Phi Kappa Phi.

L. D. Monteen received a B.S. degree in electrical engineering in 1973 and an M.S. in electrical engineering in 1977 from Tennessee Technological University. He completed course work for a doctorate degree at The University of Tennessee, Knoxville, in 1980. Mr. Monteen has over 45 continuing education units in various areas. He has worked as an industrial engineer for the American Motors Corporation (1970–71), a graduate assistant for Tennessee Technological University (1973–77) and The University of Tennessee (1977–80), a project engineer for the Naval Air Systems Command Mine Hunting Branch (1971–75), and project manager for the Athens Utilities Board Athens Automation and Control Experiment (1980 to present). He is a member of the IEEE Distribution Automation Working Group and the APPA Communications and Control Committee.

William R. Nelson received an A.S. degree in computer science technology from the State Technical Institute at Memphis, Tennessee. He has worked at the Oak Ridge National Laboratory for the past ten years as an engineering assistant. From 1977 to 1985, he worked on the Liquid Metal Fast Breeder Reactor Safety program. He currently works on data processing and analysis for the Athens Automation and Control Experiment.

J. B. Patton received a B.S. degree from the University of Colorado, Boulder, in 1975 and an M.S. degree from Rensselaer Polytechnic Institute, Troy, New York, in 1976. He worked as a field engineer for General Electric before joining Systems Control of Palo Alto, California, in 1979. While at Systems Control, Mr. Patton investigated dispersed generation interconnection protection and distribution automation benefits. In 1982, he became an independent consultant, working primarily on the Athens Automation and Control Experiment. He is the author of the SYSRAP distribution automation application software.

John H. Reed received his Ph.D. in sociology from Cornell University. He is currently a research staff member and group leader of the Information Technologies and Human Behavior Group, Energy Division, Oak Ridge National Laboratory, Oak Ridge, Tennessee. Dr. Reed has done considerable work in the evaluation of energy conservation programs for the State and Local Programs Branch of the U.S. Department of Energy. He helped to design and conduct a series of workshops on program evaluation for state energy offices. In recent years, he worked on the load management portion of the Athens Automation and Control Experiment, Athens, Tennessee, a project sponsored by the Office of Energy Storage and Distribution, Electric Energy Systems Program, U.S. Department of Energy. Most recently, Dr. Reed has been involved in the design of microcomputer-based decision support systems. He has given talks at the IEEE Power Meetings and at numerous utility and program evaluation gatherings.

D. Thomas Rizy received a B.S. degree in electrical engineering from the University of Virginia, Charlottesville, in 1976 and an M.S. degree in electrical engineering power systems from Virginia Polytechnic Institute, Blacksburg, in 1977. He has worked for the Oak Ridge National Laboratory located in Oak Ridge, Tennessee, in the Energy Division since 1978, and his research activities have involved load management, distribution system protection, and distribution system automation. He is a member of the

Institute of Electrical and Electronics Engineers (IEEE) Working Group on Distribution System Design and the IEEE Standards Coordinating Committee on Dispersed Storage and Generation. He is a senior member of the IEEE Power Engineering Society.

J. P. Stovall received a B.S. degree in electrical engineering in 1974 from the Rose-Hulman Institute of Technology in Terre Haute, Indiana, and an M.S. degree in electric power systems from The Ohio State University in 1975. He previously worked as an engineer in the engineering computer applications group at Public Service Company of Indiana, an investor-owned electric utility.

Mr. Stovall joined the Energy Division at Oak Ridge National Laboratory in April 1978 and has since gained extensive experience in load management, distribution system design, power system reliability, and distribution system automation through in-house research and project management of subcontracts. He is currently working in the Power Systems Technology Program and is the project manager for the Athens Automation and Control Experiment. Mr. Stovall has authored or coauthored 12 technical reports and publications. He is a registered professional engineer in the state of Tennessee and a member of the electrical engineering honorary society, Eta Kappa Nu.

G. R. Wetherington, Jr., received a B.S. degree in electrical engineering from the Georgia Institute of Technology in 1977 and received an M.S. degree in electrical engineering from The University of Tennessee in 1983. Mr. Wetherington is employed by Martin Marietta Energy Systems as a development staff member in the Instrumentation and Controls Division of the Oak Ridge National Laboratory. He possesses 10 years' experience in advanced system design, integration, and development. His particular specialties include the development of high-speed data acquisition systems, signal processing systems, and specialized application of measurement and automation technologies. He is the acting project manager for the development of several such systems. Mr. Wetherington has (co)authored eight technical publications and holds one patent.

E. W. Whitfield received a B.A. degree in English from The University of Tennessee, Knoxville. Mr. Whitfield is employed by Martin Marietta Energy Systems as a technical editor in the Publications Division at Oak Ridge National Laboratory. He has 9 years' experience as an editor. He previously worked for Science Applications International Corporation in Oak Ridge, Tennessee.

Appendix A. ADVISORY COMMITTEE— ATHENS AUTOMATION AND CONTROL EXPERIMENT

K. W. Clinard
Carolina Power & Light
Raleigh, NC 27602

E. C. Dawson
Baltimore Gas and Electric
Baltimore, MD 21203

G. C. Gellings and S. Braithwaite
Electric Power Research Center
Palo Alto, CA 94303

C. L. Carter and D. W. Hilson
Tennessee Valley Authority
Chattanooga, TN 37402

L. McCall
Ontario Hydro
Toronto, Ontario
Canada M5G 1X6

W. Prichett
Tennessee Valley Public Power Association
Chattanooga, TN 37402

C. Gentz/T. E. Sharp
Public Service Electric and Gas
Newark, NJ 07101

G. M. Sloan
Sulphur Springs Valley Electric
Wilcox, AR 85643

W. M. Warwick
Bonneville Power Administration
Portland, OR 97208

Appendix B. PUBLICATIONS LIST

1. J. H. Reed, J. C. Thompson, R. P. Broadwater, and A. Chandrasekaran, "Analysis of Water Heater Data from Athens Load Control Experiment," IEEE Paper No. 88 SM 596-9, presented at IEEE PES Summer Meeting, Portland, Oregon, July 1988; published in *IEEE Trans. Power Delivery,* 4(2), 1232–38 (April 1989).
2. J. S. Lawler, J. S. Lai, L. D. Monteen, J. B. Patton, and D. T. Rizy, "Impact of Automation on the Reliability of the Athens Utilities Board's Distribution System," IEEE Paper No. 88 WM 087-9, presented at IEEE PES Winter Meeting, New York, February 1988; published in *IEEE Trans. Power Delivery,* 4(1), 770–80 (January 1989).
3. D. T. Rizy, J. S. Lawler, J. B. Patton, and N. H. Fortson, "Distribution Automation Applications Software for the Athens Utilities Board," IEEE Paper No. 88 WM 097-8, presented at IEEE PES Winter Meeting, New York, February 1988; published in *IEEE Trans. Power Delivery,* 4(1), 715–24 (January 1989).
4. D. T. Rizy, W. R. Nelson, J. S. Lawler, and J. B. Patton, "Measuring and Analyzing the Impact of Voltage and Capacitor Control with High-Speed Data Acquisition," IEEE Paper No. 88 WM 098-6, presented at IEEE PES Winter Meeting, New York, February 1988; published in *IEEE Trans. Power Delivery,* 4(1), 704–14 (January 1989).
5. J. H. Reed, W. R. Nelson, G. R. Wetherington, and E. R. Broadaway, "Monitoring Load Control at the Feeder Level Using High-Speed Monitoring Equipment," IEEE Paper No. 88 WM 095-2, presented at IEEE PES Winter Meeting, New York, February 1988; published in *IEEE Trans. Power Delivery,* 4(1), 694–703 (January 1989).

6. J. H. Reed, R. P. Broadwater, and A. Chandrasekaran, "Load Control Experiments with Heat Pumps During the Winter," IEEE Paper No. 88 WM 094-5, presented at IEEE PES Winter Meeting, New York, February 1988; published in *IEEE Trans. Power Delivery,* 4(1), 646–52 (January 1989).
7. D. Bargiotas and J. D. Birdwell, "Residential Air Conditioner Dynamic Model for Direct Load Control," IEEE Paper No. 88 WM 066-3, presented at IEEE PES Winter Meeting, New York, February 1988; published in *IEEE Trans. Power Delivery,* 3(4), 2119–26 (October 1988).
8. D. T. Rizy, E. W. Gunther, and F. McGranaghan. "Transient and Harmonic Voltages Associated with Capacitor Switching on Distribution Systems," Paper No. 86 T&D 594-6, presented at IEEE PES Transmission and Distribution Conference and Exposition, September 1986; published in *IEEE Trans. Power Systems,* **PWRS**(3), 713–23 (August 1987).
9. S. L. Purucker, R. J. Thomas, N. H. Fortson, and L. D. Monteen, *Athens Automation and Control Experiment: Substation and Distribution System Automation Designs and Costs,* ORNL/TM-9596, Oak Ridge National Laboratory, June 1986.
10. S. D. Braithwait et al., *Athens Automation and Control Experiment Project Review Meeting, Knoxville, Tennessee, December 3–5, 1985,* ORNL/TM-10021, Oak Ridge National Laboratory, August 1986.
11. K. F. McKinley, "Economics of Distribution Automation," pp. 211–15 in *Proceedings: The Eighteenth Southeastern Symposium on System Theory, University of Tennessee, Knoxville, April 7–8, 1986.*
12. G. R. Wetherington, Jr., E. R. Broadaway, and R. R. Bentz, "The Role a Development System Plays on Electrical Distribution Automation Experiments," pp. 206–10 in *Proceedings: The Eighteenth Southeastern Symposium on System Theory, University of Tennessee, Knoxville, April 7–8, 1986.*
13. J. B. Patton, J. S. Lawler, and K. F. McKinley, "Designing Distribution Automation Application Software," pp. 201–5 in *Proceedings: The Eighteenth Southeastern Symposium on System Theory, University of Tennessee, Knoxville, April 7–8, 1986.*
14. R. A. Stevens, D. T. Rizy, and S. L. Purucker, "Performance of Conventional Power Flow Routines for Real-Time Distribution Automation Applications," pp. 196–200 in *Proceedings: The Eighteenth Southeastern Symposium on System Theory, University of Tennessee, Knoxville, April 7–8, 1986.*
15. J. Zrida, F. C. Chow, and J. D. Birdwell, "Utility Substation Data Modeling," pp. 176–79 in *Proceedings: The Eighteenth Southeastern Symposium on System Theory, University of Tennessee, Knoxville, April 7–8, 1986.*

16. J. Zrida, F. C. Chow, and J. D. Birdwell, "Analysis of Household Load Data," pp. 170–75 in *Proceedings: The Eighteenth Southeastern Symposium on System Theory, University of Tennessee, Knoxville, April 7–8, 1986.*
17. D. T. Rizy, "Implementation of Real-Time Regulator and Capacitor Control on the Athens Utilities Board System," pp. 79–87 in *Proceedings of IEEE Southeastcon,* Richmond, Va., March 1986; IEEE Publication 86-CH-2306-9.
18. S. L. Purucker, "The Athens Automation and Control Experiment Distribution Automation Project," published in *Transactions of the 1986 Rural Electric Power Conference, Charleston, South Carolina, April 20–22, 1986;* IEEE Catalog No. 86-CH-2316-8.
19. J. P. Detwiler, J. Lawler, L. Markel, J. McIntyre, K. McKinley, L. Monteen, S. Purucker, J. Reed, T. Rizy, B .Smith, R. Sullivan, and R. Wetherington, *Athens Automation and Control Experiment Project Review Meeting,* ORNL/TM-9758, Oak Ridge National Laboratory, December 1985.
20. G. R. Wetherington, E. R. Broadaway, R. R. Bentz, and S. L. Purucker, "Use of a General-Purpose Development System in Support of a Large-Scale Electrical Distribution Control System," published in *Proceedings of the International Load Management Conference and Exposition, Chicago, Illinois, Dec. 9, 1985.*
21. S. L. Purucker, R. J. Thomas, and L. D. Monteen, "Feeder Automation Designs for Installing an Integrated Distribution Control System," *IEEE Trans. Power Appar. Systems,* **PAS-104**(10), 2929–34 (October 1985).
22. S. L. Purucker, D. T. Rizy, and J. H. Reed, "Automation and Control of a Distribution Power System," pp. 54–59 in *Proceedings of the IEEE Control of Power Systems (COPS) Conference, Oklahoma City, March 20–21, 1984;* IEEE Catalog No. 84-CH-2027-1.
23. S. L. Purucker, T. W. Reddoch, J. S. Detwiler, and L. D. Monteen, "The Design of an Integrated Distribution Control System," *IEEE Trans. Power Appar. Systems,* **PAS-104**(3), 745–52 (March 1985).
24. B. W. McConnell, T. W. Reddoch, S. L. Purucker, and L. D. Monteen, "Distribution Energy Control Center Experiment," *IEEE Trans. Power Appar. Systems,* **PAS-102**(6), 1582–89 (June 1983).
25. K. D. Van Liere, D. R. Ploch, M. S. Kuhn, C. M. Hand, B. W. McConnell, and B. H. Bronfman, *Public Reactions to Load Management: A Summary of Baseline Community Data for the Athens Automation and Control Experiment,* ORNL/TM-7961, Oak Ridge National Laboratory, June 1982.

INDEX